ISSN — 0132 — 1447

BULLETIN

OF THE GEORGIAN ACADEMY OF SCIENCES

საქართველოს მეცნიერებათა აკადემიის

მოამბე

158

№ 1

1998

TBILISI • თბილისი

The Journal is founded in 1940

BULLETIN

OF THE GEORGIAN ACADEMY OF SCIENCES

is a scientific journal, issued bimonthly in
Georgian and English languages

Editorial Office:
Georgian Academy of Sciences
52, Rustaveli Avenue,
Tbilisi, 380008,
Republic of Georgia

Telephone : + 995 32 99.75.93
Fax : + 995 32 99.88.23
E-mail : **BULLETIN@PRESID.ACNET.GE**

CONTENTS

საქართველოს მეცნიერებათა აკადემიის მოამბე, 158, №1, 1998
BULLETIN OF THE GEORGIAN ACADEMY OF SCIENCES, 158, №1, 1998

MATHEMATICS

R.Gachechiladze, O.Maisaia

Signorini's Problem in the Couple-Stress Elasticity and its Reduction to the Boundary Variational Inequalities

Presented by Academician T.Burchuladze, October 23, 1997

ABSTRACT. **The first part of the present paper is the realization of the general theory of abstract, one-sided problems for systems of equations of statics of the couple-stress elasticity for inhomogeneous, anisotropic elastic media. In the second part by using the method of boundary variational inequalities we study Signorini's problem, which allows one to investigate these problems for outer regions in the case of homogeneous anisotropic media.**

Key words: Signorini's problem, couple-stress elasticity, variational inequalities.

Let R^3 be a three-dimensional Euclidean space, $x = (x_1, x_2, x_3)$, $y = (y_1, y_2, y_3)$, ... be the points of this space and let $\Omega \subset R^3$ be a bounded region with sufficiently smooth $\partial\Omega$ boundary [1].

The basic equations of statics of the couple-stress elasticity for inhomogeneous anisotropic media has the form [2]:

$$M(x, \partial)U(x) + \rho(x)\mathcal{F}(x) = 0, \tag{1}$$

where $U = (u, \omega)$, $u = (u_1, u_2, u_3)$ is a displacement vector, $\omega = (\omega_1, \omega_2, \omega_3)$ is a rotation vector, ρ is a medium density, $\mathcal{F} = (F, G)$, $F = (F_1, F_2, F_3)$ is a mass force, $G = (G_1, G_2, G_3)$ is a mass moment and $M(x, \partial)$ is a matrix differential operator of statics of the couple-stress elasticity.

Elastic constants a_{ijlk}, b_{ijlk}, c_{ijlk} $(i, j, l, k = 1, 2, 3)$ appearing in the definition of the operator $M(x, \partial)$, are the functions of the class C^∞ satisfying the conditions

$$a_{ijlk} = a_{lkij}, \; c_{ijlk} = c_{lkij},$$

there exists $M > 0$ such that $\forall x \in \overline{\Omega}$ and $\forall \xi_{ij}, \eta_{ij} \in R$:

$$a_{ijlk}\xi_{ij}\xi_{lk} + 2b_{ijlk}\xi_{ij}\eta_{lk} + c_{ijlk}\eta_{ij}\eta_{lk} \geq M(\xi_{ij}\xi_{ij} + \eta_{ij}\eta_{ij}). \tag{2}$$

It is known that the complete energy of deformation in the couple-stress elasticity is of the form

$$\mathcal{E}(U, V) = \int_\Omega \{a_{ijlk}\xi_{ij}(U)\xi_{lk}(V) + c_{ijlk}\eta_{ij}(U)\eta_{lk}(V) + b_{ijlk}\xi_{ij}(U)\eta_{lk}(V) + b_{ijlk}\xi_{ij}(V)\eta_{lk}(U)\}dx,$$

where

$$\xi_{ij}(U) = \frac{\partial u_i}{\partial x_j} - \varepsilon_{ijk}\omega_k, \; \eta_{ij}(U) = \frac{\partial \omega_i}{\partial x_j}, \; \varepsilon_{ijk} \text{ is the Levy-Civita's symbol.}$$

Here and in what follows, repetition of the index means summation with respect to this index from 1 to 3

Let

$$\mathcal{N}(x, \partial, \nu) = \begin{Vmatrix} \mathcal{N}^{(1)} & \mathcal{N}^{(2)} \\ \mathcal{N}^{(3)} & \mathcal{N}^{(4)} \end{Vmatrix}_{6\times 6}$$

be a matrix differential stress operator and assume that $\partial\Omega = \Gamma_1 \cup \Gamma_2$, $\Gamma_1 \cap \Gamma_2 = \varnothing$. Consider the following

Problem *K* (K = I, II, III, IV). Find $U = (u, \omega)$ such that in Ω equation (1) be satisfied;

$$\text{on } \Gamma_2\text{: } (u)_\nu \geq 0,\ (\mathcal{N}^{(1)}u + \mathcal{N}^{(2)}\omega)_\nu \geq \xi,$$
$$(\mathcal{N}^{(1)}u + \mathcal{N}^{(2)}\omega)_\sigma = \eta, \quad (u)_\nu[(\mathcal{N}^{(1)}u + \mathcal{N}^{(2)}\omega)_\nu - \xi] = 0,$$
$$\omega = \varphi \quad \text{for } K = \text{I} \quad \text{or} \quad K = \text{II};$$
$$\mathcal{N}^{(3)}u + \mathcal{N}^{(4)}\omega = \psi \quad \text{for} \quad K = \text{III} \quad \text{or} \quad K = \text{IV};$$
$$\text{on } \Gamma_1\text{: } \mathcal{N}U = \Psi \quad \text{for} \quad K = \text{I} \quad \text{or} \quad K = \text{III};$$
$$U = \Phi \quad \text{for} \quad K = \text{II} \quad \text{or} \quad K = \text{IV},$$

where the symbols $(\cdot)_\nu$ and $(\cdot)_\sigma$ denote respectively the normal and the tangent components of the vector $(\cdot)$, $\xi\colon \Gamma_2 \to \mathbb{R}$, $\varphi, \psi, \eta\colon \Gamma_2 \to \mathbb{R}^3$, $\Phi, \Psi\colon \Gamma_1 \to \mathbb{R}^6$ (note that this problem is posed formally).

Consider the case K = III. For the sake of simplicity we assume that $\xi = \eta = \psi = 0$.

To formulate Problem III variationally, it is necessary to introduce into consideration a closed convex set $V_{(\text{III})}$ and a functional $F_{(\text{III})}$:

$$V_{(\text{III})} = \{U \in (H_1(\Omega))^6 : (u)_\nu\big|_{\Gamma_2} \geq 0\},$$

$$F_{(\text{III})}(U) = \int_\Omega \rho\mathcal{F}U dx + \int_{\Gamma_1} \Psi U dS,$$

where $\rho\mathcal{F} \in (H_0(\Omega))^6$ and $\Psi \in (H_0(\Gamma_1))^6$ (for the spaces $H_s(\Omega)$ and $H_s(\Gamma)$, see [3]).

Consider the following variational problem: find $U \in V_{(\text{III})}$ such that

$$\forall V \in V_{(\text{III})}\colon \mathcal{B}(U, V - U) \geq F_{(\text{III})}(V - U). \tag{3}$$

For the investigation of the solvability of the variational inequality (3) we have to define semi-coerciveness of the form $\mathcal{B}$ in order to make application of the general theory of abstract one-sided problems possible [1].

Condition (2) and the second Cauchy's inequality [1, 4] allow one to prove the existence of $c > 0$ such that

$$\mathcal{B}(U,U) \geq c\left\|PU\right\|_1^2, \quad \forall U \in (H_1(\Omega))^6,$$

where I-P is the operator of orthogonal projection of the space $(H_1(\Omega))^6$ onto a set of solution of the equation $\mathcal{B}(U,U) = 0$. It is known that the set of solutions of this equation in the space $(H_1(\Omega))^6$ is

$$\mathcal{R} = \{([a \times x] + b, a)\},$$

where a and b are arbitrary constant vectors.

Denote $\mathcal{R}' = \mathcal{R} \cap V_{(\text{III})}$ and $\mathcal{R}^* = \{(\rho, a) \in \mathcal{R}' : (\rho)_\nu\big|_{\Gamma_2} \geq 0\}$. The following theorem is valid.

Theorem 1. *For the variational inequality (3) to be solvable it is necessary that the conditions*

$$F_{(\text{III})}(V) \leq 0, \ \forall V \in \mathcal{R} \tag{4}$$

be fulfilled. If condition (4) is fulfilled in a strong sense, i.e., the equality sign takes place if and only if $V \in \mathcal{R}^*$, then inequality (3) is solvable.

Moreover, if $\mathcal{F}$ and Ψ are the sufficiently smooth functions, then the solution of the variational inequality (3) satisfies as well the conditions of Problem III.

Let $\{B\}_{\Gamma_2}$ be a σ-ring of the Borel subsets of the set Γ_2 and assume $\Gamma_2 = \bigcup_{k=1} S_k$, where S_k, $k = 1, \ldots, q$ is non-overlapping two dimensional cells of the class C^∞ [1]. Then the following theorem holds.

Theorem 2. *On the σ-ring $\{B\}_{\Gamma_2}$ of the Borel sets of the set Γ_2 there exists a non-negative real measure γ such that if U is a solution of inequality (3), then $\forall v \in (H_1(\Omega))^3 \cap (C^0(\Omega \cup \Gamma_2))^3$, $\forall \omega \in (H_1(\Omega))^3$:*

$$\int_{\Gamma_2} v_i v_i d\gamma = \mathcal{B}(U, V) - F_{(III)}(V),$$

where $V = (v, \omega)$, a singular set of measure γ is contained in the set $\bigcup_{k=1}^{q} \partial S_k$ and the function $(\mathcal{N}^{(1)}u + \mathcal{N}^{(2)}\omega)_v$ is its Lebesgue derivative.

In the case of one concrete problem when the supporting surface Γ_2 is a bounded region of the plane $x_3 = 0$ and $\overline{\Omega} \setminus \Gamma_2$ lies in a half-space $x_3 > 0$, this theorem allows one to prove that the above fulfilled (in a strong sense) conditions (4) are necessary for the solvability of inequality (3).

For the sake of simplicity, let us investigate Signorini's problem by means of the boundary variational inequalities.

Let $\mathbb{R}^n (n \geq 2)$ be an n-dimensional Euclidean space, and let $D \subset \mathbb{R}^n$ be a bounded region with a boundary $\Gamma \in C^\infty$. Consider the following

Problem. Find $u \in (H_1(D))^n$ such that the following conditions be fulfilled:

$$\begin{aligned} &A(x,\partial)u(x) = 0, \ x \in D; \\ &(u)_\nu\big|_\Gamma \geq 0, \ (Tu)_\nu\big|_\Gamma \geq f, \\ &<(Tu)_\nu - f, (u)_\nu>\big|_\Gamma = 0, \ (Tu)_\sigma\big|_\Gamma = g, \end{aligned} \tag{5}$$

where A is a matrix differential operator of statics of elasticity, T is a stress operator [1], $f \in H_{-\frac{1}{2}}(\Gamma)$, $g \in (H_{-\frac{1}{2}}(\Gamma))^n$, and $<\cdot,\cdot>$ denote the duality relation between the spaces $H_{-\frac{1}{2}}(\Gamma)$ and $H_{\frac{1}{2}}(\Gamma)$.

To investigate this problem let us consider an auxiliary problem: find $u \in (H_1(D))^n$ such that

$$\begin{aligned} &A(x, \partial)u(x) = 0, \ x \in D; \\ &u\big|_\Gamma = h, \ h \in (H_{\frac{1}{2}}(\Gamma))^n. \end{aligned} \tag{6}$$

We prove that the problem has the unique solution.

Let

$$G: (H_{\frac{1}{2}}(\Gamma))^n \to (H_1(D))^n$$

be an operator defined as follows: $\forall h \in (H_{\frac{1}{2}}(\Gamma))^n Gh$ is the unique solution of problem (6). G is called the Green's operator of the first boundary value problem. Define the operator

$$L: (H_{\frac{1}{2}}(\Gamma))^n \to (H_{-\frac{1}{2}}(\Gamma))^n$$

by the equality

$$\forall h \in (H_{\frac{1}{2}}(\Gamma))^n: Lh = T(Gh)\big|_\Gamma .$$

It can be easily verified that the operator L satisfies the following conditions:

1) $\langle Lu, v\rangle = \langle Lv, u\rangle$, $\forall u, v \in (H_{\frac{1}{2}}(\Gamma))^n$;

2) $\langle Lu, u\rangle \geq 0$, $\forall u \in (H_{\frac{1}{2}}(\Gamma))^n$;

3) $\langle Lu, u\rangle \geq \alpha \|Pu\|^2_{\frac{1}{2}}$, $\alpha > 0$,

where $I - P$ is the operator of orthogonal projection of the space $(H_{\frac{1}{2}}(\Gamma))^n$ onto a set of solutions of the equation $(H_{\frac{1}{2}}(\Gamma))^n$ (note that this is a set of vectors of rigid displacements).

Consider the variational inequality: find $h_0 \in$ such that

$$\forall h \in K: \langle Lh_0, h - h_0\rangle \geq \langle f, (h - h_0)_v\rangle + \langle g, (h - h_0)_\sigma\rangle, \qquad (7)$$

where

$$K = \{h \in (H_{\frac{1}{2}}(\Gamma))^n: (h)_v\big|_\Gamma \geq 0\}.$$

We can prove that if h_0 is a solution of inequality (7), then Gh_0 is a solution of problem (5), and vice versa, if $u \in (H_1(D))^n$ is a solution of problem (5),then it can be uniquely represented in terms of Gh_0, where h is a solution of inequality (7). This equivalence permits to establish the sufficient conditions for the solvability of problem (5). Using this method, we can study Signorini's problem for outer regions in the case of homogeneous, anisotropic elastic media.

A.Razmadze Mathematical Institute
Georgian Academy of Sciences

REFERENCES

1. *G.Fichera*. Handb d. Physic, Bd. VI/2,No. 3, Springer-Verlag, Heidelberg, 1972.
2. *B.D.Kupradze, T.G.Gegelia, M.O.Basheleishvili, T.B.Burchuladze*. Trekhmernie zadachi matematicheskoi teorii uprugosti i termouprugosti. M., 1997 (Russian).
3. *J.-L.Lions, E.Magenes*. Neodn. granichnye zadachi i ikh prilozh. M., T.I. 1971 (Russian).
4. *O.I.Maisaia*. Bull. Acad. Sc. Georgia, 75, 2, 1974 (Russian).

M.Bitsadze

Uniform Convergence and Summability of Multiple Trigonometric Series

Presented by Academician L.Zhizhiashvili, May 5, 1998

ABSTRACT. **The paper presents the results on the uniform convergence and summability of the negative order of special trigonometric series by the method of Cesaro.**

Key words: convergence, summability, trigonometric, sequence.

1. By symbol E^n we denote a n-dimensional Euclidean space with well-known linear operations. We denote points of the space E^n by $x = (x_1, x_2, ..., x_n)$, $y = (y_1, y_2, ..., y_n)$, ... We assume that

$$\|x\| = \left\{\sum_{i=1}^{n} x_i^2\right\}^{\frac{1}{2}}, \quad T^n = [-\pi, \pi]^n.$$

We give the notations, some of which were introduced in the papers [1,2] and [3,4].

Assume that $P = (P_1, P_2, ..., P_n)$ ($P_i = 0, 1, ..., i = \overline{1,n}$). By $(a_p)_{p \geq 0}$ we denote a n-fold sequence of real numbers; $\lambda(P)$ is the number of the vector P coordinates which are equal to zero. Let $M = \{1, 2, ..., n\}$ and B be an arbitrary subset of the set M and $B' = C_M B$ ($B' = \varnothing$ if $B = M$, $B' = M$ if $B = \varnothing$). By symbol $P(B)$ we denote the set of the coordinates of the vector P whose indexes form the set B. $\|P(B)\|$ denotes the sum of all P_i which form P. Furthermore if $(I_j)_{i=1}^{n}$ are basic vectors of the space E^n then we assume

$$\Delta(a_p, \{i\}) = a_p - a_{p+I_i},$$

i.e. it is a Δ operation with respect to the coordinate P_i of the vector P. By the symbol $\Delta(a_p, B)$ we denote the expression which is obtained by successive application of the operation Δ to the coordinates of the vector P whose indexes form the set B.

We consider the n-fold trigonometric series of the form

$$\sum_{p \geq 0} 2^{-\lambda(p)} a_p \prod_{i \in B} \cos p_i x_i \prod_{j \in B'} \sin p_j x_j, \tag{1}$$

where $(a_p)_{p \geq 0}$ is a sequence decreasing in the Hardy [5] sense, i.e. for each $B \subset M$ the condition $\Delta(a_p, B) \geq 0$ is satisfied.

If $B = \varnothing$ the series (1) is n-fold (if $n \geq 2$) sine-series and if $B = M$ cosine-series. We note that all functions under consideration are assumed to be 2π periodic with respect to each coordinate of the point X. In the assertions below the convergence is always used in Schtolz-Pringsheim sense.

Let $f \in L(T^n)$. Following [1] we denoted n-fold trigonometrically Fourier series of function f by the symbol $\sigma_n[f]$, i. e.

$$\sigma_n[f] = \sum_{p \geq 0} 2^{-\lambda(p)} \sum_{B \subset M} a_p^{(B)}(f) \prod_{i \in B} \cos p_i x_i \prod_{j \in B'} \sin p_j x_j, \tag{2}$$

where

$$a_p^{(B)}(f) = \frac{1}{T^n} \int_{T^n} f(x) \prod_{i \in B} \cos p_i x_i \prod_{j \in B'} \sin p_j x_j dx.$$

The expression

$$t_m^{\alpha}(x, f) = \frac{1}{\prod_{i=1}^{n} A_{m_i}^{\alpha_i}} \sum_{p=0}^{m} \prod_{i=0}^{p} A_{m_i - p_i}^{\alpha_i - 1} S_p(x, f)$$

denotes n-fold Cesaro means of the series $\sigma_n[f]$, where

$$\alpha = (\alpha_1, \ldots, \alpha_n) \ (\alpha_i > -1, \ i = \overline{1,n}),$$

$$A_i^{\beta} = \frac{(\beta+1)\ldots(\beta+i)}{i!} \quad (\beta = > -1)$$

and $S_p(x, f)$ is a rectangular partial sum of the series $\sigma_n[f]$.

2. In one-dimensional case for sine and cosine series fundamental results are obtained which are given in different monographs and articles [5-9]. Relatively little has been done in the case of $n \geq 2$. This is indicated in [10] and [1].

In the present paper the assertions concern uniform convergence and Cesaro summability of negative order of the series (1) and (2).

Theorem 1. Let $(a_p)_{p \geq 0}$ be a sequence decreasing in the Hardy sense and $B \neq \varnothing$, $B \neq M$ in the series (1). Assume that

$$b_{p(B')} \equiv \sum_{p(B) \geq 0} a_p .$$

Satisfaction of the following condition is the necessary and sufficient condition for uniform convergence of series (1) on $T^{(n)}$

$$\lim_{\|p(B')\| \to \infty} \prod_{j \in B'} P_j b_{p(B')} = 0$$

Theorem 2. Let $B \neq \varnothing$. The necessary and sufficient condition of uniform convergence of the n-fold sine-series of a function $f \in C(T^n)$ is satisfaction of the following condition

$$\lim_{\|p\| \to \infty} \prod_{i=1}^{n} P_i a_p = 0.$$

Theorem 3. Let a function $f \in C(T^n)$ and its Fourier coefficients satisfy the condition

$$\overline{\lim_{\|p\| \to \infty}} a_p^B(f) \|P\|^n = 0,$$

for each $B \subset M$. If $\alpha = (\alpha_1, \ldots, \alpha_n)$ with $\alpha_i \in (-1,0]$. $(i = \overline{1,n})$ then

$$\lim_{m \to \infty} \left\| t_m^{\alpha}(f) - f \right\|_{C(T^n)} = 0$$

Finally we note that I.E.Zhak and A.A.Shneider [11] investigated the question of uniform convergence of sine-series for $n = 2$.

Tbilisi I.Javakhishvili State University

REFERENCES

1. *L.V.Zhizhiashvili.* UMN, 28, v p. 2, 1973, 65-119 (Russian).
2. *L.V.Zhizhiashvili.* Nekotorye voprosy mnogomernogo garmonicheskogo analiza. Tbilisi, 1983, 113 (Russian).
3. *M.C.Bitsadze.* Soobsh. AN Gruz. SSR, **138**, 1, 1990, 21-23 (Russian).
4. *M.C.Bitsadze.* Nekotorye voprosy teorii funktsii. TTU, III, 1986, 3-29. (Russian)
5. *G.H.Hardy.* Quart J. Mathem. vol. 39, 1905, 53-79.
6. *N.K.Bari.* Trigonometricheskie ryady. M. 1961, 936 (Russian)
7. *R.P.Bois.* Integrability theorems for trigonometric transforms. Merlin; New York, 1967.
8. *A.Zygmund.* Trigonometric series, vol. I, Cambridge University press., Cambridge, 1959.
9. *I.N.Pak.* UMN, 35, vyp. 2, 1980, 91-144 (Russian).
10. *M.I.Diachenko.* UMN, **47**, 5, 1992, 97-162 (Russian).
11. *I.E.Zhak, A.A.Shneider.* Izv. vyssh. ucheb. zavedenii, Matematica, 4, 1966, 44-52. (Russian).

საქართველოს მეცნიერებათა აკადემიის მოამბე, 158, №1, 1998
BULLETIN OF THE GEORGIAN ACADEMY OF SCIENCES, 158, №1, 1998
MATHEMATICS

U.Goginava

Convergence and Summability of Multiple Fourier-Walsh Series in $L^P([0,1]^N)$, $P \in [1, +\infty]$ Metrics

Presented by Academician L.Zhizhiashvili, September 15, 1997

ABSTRACT. **In this paper we study the convergence and summability of N-multiple Fourier-Walsh series in $L^P([0,1]^N)$, $P \in [1, +\infty]$ metrics. In case $P = \infty$ by L^P, we mean C_ρ to be the collection of uniformly ρ - continuous function endowed with the supremum norm and the convergence is defined in Pringsheim sense.**

Key words: Walsh Paley system, ρ - continuity, rectangular partial sum, convergence in L^P - norm, uniform convergence

We consider the Walsh orthonormal system $\{\omega_j(x): j \geq 0\}$ defined on the unit interval $[0,1)$ in the Paley enumeration [1]. To be more specific, let

$$r_0(x) = \begin{cases} 1, & if \quad x \in [0,\ 1/2), \\ -1, & if \quad x \in [1/2,\ 1), \end{cases} \qquad r_0(x+1) = r_0(x),$$

$$r_j(x) = r_0(2^j x), \ j \geq 1 \text{ and } x \in [0,1)$$

be the well-known Rademaxer functions. For $j = 0$ set $w_0(x) = 1$, and if $j \geq 1$,

$$j = \sum_{i=0}^{\infty} j_i\, 2^i, \ j_i = 0 \vee 1$$

is the dyadic representation of an integer $j \geq 1$, the set

$$\omega_j(x) = \prod_{i=0}^{\infty} [r_i(x)]^{j_i}.$$

Denote by $C_\rho(Q_N)$ space of uniformly ρ-continuos [2] on $Q_N = [0,\ 1)^N$ periodical relative to each variable functions with the norm

$$\|f\|_{C_\rho(Q_N)} := \sup_{x \in Q_N} |f(x)|.$$

We write L^∞ instead of C_ρ and set $\|f\|_p := \left(\int_{[0,1]^N} |f(x)|^p dx \right)^{1/p}$, $1 \leq p < \infty$

Let us assume $M = \{1, \ldots, N\}$, $B = \{l_1, \ldots, l_r\}$, $l_k \leq l_{k+1}$, $k = \overline{1, r-1}$, $v_B = \{v_{l_1}, \ldots, v_{l_r}\}$, $m_B = \{m_{l_1}, \ldots, m_{l_r}\}$, $\alpha = \{\alpha_1, \ldots, \alpha_N\}$, $\alpha_i \in]-1, 0]$, $i \in M$.

For integer m we shall denote vector $(m, \ldots, m)$ of space E_N by the symbol $\widetilde{m}$. Let $\overline{d}(B)$ be for element number in B, $B' = M \setminus B$,

$$B_0 \equiv \{j: j \in B,\ \alpha_j = 0\},\ B_1 \equiv \{j: j \in B,\ \alpha_j \neq 0\}.$$

For any $x \in E_N$ and $B \subset M$ by $(x_i)_{i \in B}$ symbol we denote a vector of E_N space, the coordinates of which with indexes from B set coincide with x vector coordinates and the coordinates with indexes from B' set are zero.

Later we shall identify symbols $\sum_{\nu_B=\bar{0}_B}^{m_B}$ and $\sum_{\nu_{e_1}=0}^{m_{e_1}} \dots \sum_{\nu_{e_r}=0}^{m_{e_r}}$, du_B and $du_{e_1},\dots,du_{e_r}$.

Given a function $f \in L^1(Q_N)$, we form its N-multiple Fourier-Walsh series

$$\sum_{\nu_M=\bar{0}_M}^{\infty} a_{\nu_M} \prod_{i\in M} \omega_{\nu_i}(x_i) \tag{1}$$

with

$$a_{\nu_M} = a_{\nu_1,\dots,\nu_N}(f) \equiv \int_{[0,1]^N} f(x) \prod_{i\in M} \omega_{\nu_i}(x_i)\,dx_M .$$

The rectangular partial sums of series (1) are defined by

$$s_{m_M}(f,x) = \sum_{\nu_M=\bar{0}_M}^{m_M-\bar{1}_M} a_{\nu_M} \prod_{i\in M} \omega_{\nu_i}(x_i),$$

and

$$s^{\alpha} m_M(f,x) = \frac{1}{\prod_{i\in M} A_{m_i}^{\alpha_i}} \sum_{\nu_M=\bar{0}_M}^{m_M} \prod_{i\in M} A_{m_i-\nu_i}^{\alpha_i-1}\; s_{\nu_M}(f,x)$$

Cesaro (c,α) - means of particular sums s_m.

Let $\Delta^{\{j\}}(f,x,s_j) = f(x \dotplus (s_i)_{i\in\{j\}}) - f(x)$, where $\dotplus$ denotes the operation in the dyadic group, the set of all sequences $(t_1, t_2, \dots)$, $t_n = 0.1$ for $n = 1,2, \dots$ is addition modulo 2 in each coordinate. Expression, which we get by successive application of operations $\Delta^{\{j_1\}}(f,x,s_{t_1}), \dots, \Delta^{\{j_r\}}(f,x,s_{t_r})$ is denoted by the symbol $\Delta^{\{B\}}(f,x,(s_j)_{i\in B})$.

We remind the reader that the total modulus of continuity of a function $f \in L^p$ in L^p norm, $1 \le p \le \infty$, is defined by $\omega(\delta,f)_p := \sup_{\|h\|\le\delta} \|f(\cdot\dotplus h) - f(\cdot)\|_p$.

Let $\omega_B(\delta,f)_p := \sup_{|s_i|\le\delta_i,\ i\in B} \left\|\Delta^{\{B\}}(f,\cdot,(s_i)_{i\in B})\right\|_p$.

We also use the notion of the partial modulus of a function $f \in L^p$ in L^p norm, $1 \le p \le \infty$, defined by $\omega_t(\delta,f)_p := \sup_{|s_t|\le\delta} \left\|\Delta^{\{t\}}(f,\cdot,s_t)\right\|_p$.

We set

$$V_{K_A-\bar{1}_A,K_B}(f,u_M,\alpha) := \sum_{q_A=\bar{0}_A}^{2^{K_A}-\bar{1}_A} \sum_{q_B=\bar{0}_B}^{2^{K_B}-\bar{1}_B} \prod_{j\in A\cup B} \lambda_{q_j}^{\alpha_j-1} \times$$

$$\left| \Delta^{A\cup B}\left(f, u_M \dotplus \left(\frac{2q_i}{2^{K_i}}\right)_{i\in A} \dotplus \left(\frac{2q_i}{2^{K_i+1}}\right)_{i\in B}, \left(\frac{1}{2^{K_i}}\right)_{i\in A} + \left(\frac{1}{2^{K_i+1}}\right)_{i\in B} \right) \right|$$

where $A \subset M$, $B \subset M$, $A \cap B = \{\varnothing\}$, $\lambda_0 = 1$ and $\lambda_{q_j} = q_j$, $q_j \ge 1$.

We prove the following theorems.

Theorem. If $f \in L^p([0,1]^N)$, $p \in [1, +\infty]$, $m_i = 2^{K_i} + m'_i$, $0 \le m'_i < 2^{K_i}$
$\forall B: B \subset M$, $B \ne \{\varnothing\}$, $\forall A: A \subset B$, $\alpha_i \in [0,1)$, $i \in M$,

$$\left\| t^{\cdot}_{K_{A_1}-1_{A_1}, K_{B\setminus A}}(f;\cdot,\alpha) \right\|_p \to 0, \ (m_i \to \infty, i \in A_1 \cup (B \setminus A)), \text{ then } \lim_{m_M \to \infty} \left\| S^{-\alpha}_{m_M}(f) - f \right\|_p = 0$$

Consequence 1. Let $f \in L^p(Q_N)$, $p \in [1, +\infty]$, $\alpha_i \in [0,1[$, $\forall i: i \in M$, $\forall B: B \subset M$

$$\prod_{i \in B} \lambda(m_i, \alpha_i)\, \omega_b(1/m, f)_p = o(1) \ (m_i \to \infty, i \in B), \text{ then } \lim_{m_M \to \infty} \left\| S^{-\alpha}_{m_M}(f) - f \right\|_p = 0, \text{ where}$$

$$\lambda(m_i, \alpha_i) = \begin{cases} m_j^{\alpha_j}, & \alpha_j \in]0,1[, \\ \log m_j, & \alpha_j = 0. \end{cases}$$

Consequence 2. ([3,4]) Let $f \in L^p(Q_N)$, $p = 1$ or $p = \infty$, $\forall B: B \subset M$, $B \ne \{\varnothing\}$, $\omega_b(\delta, f)_p \prod_{i \in B} \log(1/\delta_i) = o(1)$, $\delta_i \to 0+$, $i \in B$, then $\lim_{m_M \to \infty} \left\| S_{m_M}(f) - f \right\|_p = 0$.

Consequence 3. ([3,4]) Let $f \in L^p(Q_N)$, $p = 1$ or $p = \infty$ and there exists i_0 for which the following condition is fulfilled $\omega_{i_0}(\delta, f)_p = o\left(\left(\log \frac{1}{\delta}\right)^{-N}\right)$, $\delta \to 0+$, and

$\omega_i(\delta, f)_p = O\left(\left(\log \frac{1}{\delta}\right)^{-N}\right)$, $(i = \overline{1, N}, \ i \ne i_0)$ then $\lim_{m_M \to \infty} \left\| S_{m_M}(f) - f \right\|_p = 0$.

Consequence 4. Let $\beta \in [0,1[$, $K \in [0, N]$, $\overline{d}(M_1) = K$, $f \in L^p(Q_N)$, $p = 1$ or $p = \infty$, $\alpha_1 + \ldots + \alpha_N = \beta$, $\alpha_i > 0$, $i \in M_1$, $\omega_i(\delta, f)_p \cdot \delta^{-\beta}\left(\log \frac{1}{\delta}\right)^{N-K} \to 0$, $(\delta \to 0+)$ then $\lim_{m_M \to \infty} \left\| S^{-\alpha}_{m_M}(f) - f \right\|_p = 0$.

Consequences 1-4 are analogue of Zhizhiashvili's assertion, which was settled for trigonometrical system [5].

The issue of non-strengthening of the consequences 2,3 was studied in the papers [3,6,7].

Tbilisi I.Javakhishvili State University

REFERENCES

1. *A.Paley*. Proc. London Math. Soc., 34, 1932, 241-279.
2. *B.I.Golubov, et al.* Riady i preobrazovania Uolsha. M., 1987 (Russian).
3. *R.D.Getsadze*. Anal. Math. **13**, 1, 1987, 29-36 (Russian).
4. *F.Moricz*. Studia Math. **102**, 3, 1992, 225-237.
5. *L.V.Zhizhiashvili*. Nekotorye problemy teorii trigonometricheskikh riadov Furie i ikh sopriazhonnikh. Tbilisi, 1993 (Russian).
6. *R.D.Getsadze*. Soob. AN GSSR, **106**, 1982, 489-491 (Russian).
7. *R.D.Getsadze*. Soob. AN GSSR, **102**, 3, 1981, 545-548 (Russian).

საქართველოს მეცნიერებათა აკადემიის მოამბე, 158, №1, 1998
BULLETIN OF THE GEORGIAN ACADEMY OF SCIENCES, 158, №1, 1998

MATHEMATICS

S.Kemkhadze, Z.Rostomashvili

General Geometric Lattices

Presented by Corr. Member of the Academy H.Inassaridze, November 30, 1997

ABSTRACT. **According to J.von Neumann one of the main problems of the lattice theory is the axiomatic description of $PG(K, X)$ – the lattice of submodules of the torsion free K-module X. A.A.Lashkhi solved this problem for the principal ideal domain. These ideas are developed and generalised in the present paper.**

Key words: lattice, modular lattice, isomorphism of lattices.

Below everywhere L is a torsion free lattice, i.e. $0 \in L$ and no one element of L covers 0.

Definition 1. (i) In a lattice L we say that b D-covers a and write $\alpha \overset{D}{<} b$ if the interval $[\alpha, b]$ is the infinite distributive lattice with maximum condition and moreover for every $c \in L$ $\alpha < c < b$, one and only one among the following two intervals $[\alpha, c]$ and $[c, b]$ is the torsion free lattice.

(ii) An element $p \in L$ is called a D-point when $0 \overset{D}{<} p$;

(iii) We write $\alpha \overset{D}{<} b$ if $\alpha \overset{D}{<} b$ or $\alpha = b$;

(iv) We say that a lattice L satisfies the upper D-covering condition, if for all $\alpha, b, c \in L$, $\alpha \overset{D}{<} b$ implies $\alpha \vee c \overset{D}{<} b \vee c$.

Proposition 2. *Any modular lattice satisfies the upper and the lower D-covering conditions.*

Note that the inverse statement generally is not true, i.e. there exist non-modular lattices with the upper and the lower D-covering conditions.

Definition 3. *A lattice L is called D-pointwise, when every non-zero element α of L is the join of D-points contained in α.*

Theorem 4. *A lattice L is D-pointwise if and only if L satisfies the following condition:*

If $\alpha < b$ then there exists a D-point p such that $p \not\leq \alpha$ and $p \leq b$.

Theorem 5. *Let L be such lattice that every non-zero element α of L contains a D-point. Then L is D-pointwise if and only if L satisfies the following condition:*

If $\alpha > b$ in L then there exists $c \in L$ such that $0 < c \leq \alpha$ and $c \wedge b = 0$

Definition 6. (i) *A lattice L is called D-semimodular when it satisfies the upper D-covering condition;*

(ii) The set $\{x_1, \ldots, x_n | x_1, \ldots, x_n \in L, x_1 < \ldots < x_n\}$ of L is called D-chain when $x_i \overset{D}{<} x_{i+1}$ for all $i = 1, \ldots, n-1$.

(iii) On the D-semimodular lattice L the height of $\alpha \in L$ is defined as follows: $\tilde{h}[\alpha]$ is the length of the longest maximal D-chain in $[0, \alpha]$, if such D-chain exists. Otherwise we consider that $\tilde{h}[\alpha] = \infty$.

It is evident, that if L is D-pointwise D-semimodular lattice then $\widetilde{h}[\alpha] = \text{rank}(\alpha)$, where rank($\alpha$) is the number of elements of the set of maximal independent D-points in $(\alpha]$.

Proposition 7. *In the finite lattice L the following conditions are equivalent:*

(i) *L is a D-semimodular lattice;*

(ii) *If* $\alpha, b \in L$, $\alpha \neq b$ *and* $\alpha, b > \overset{D}{} \alpha \wedge b$ *then* $\alpha \vee b > \overset{D}{} \alpha, b$;

(iii) *If* $\alpha, b, c \in L$, $\alpha \leq b$ *and C is a maximal D-chain in* $[\alpha, b]$, *then* $\{x \vee c | x \in C\}$ *is the maximal D-chain in* $[\alpha \vee c, b \vee c]$.

(iv) *For every elements* $\alpha, b \in L$

$\widetilde{h}[\alpha] + \widetilde{h}[b] \geq \widetilde{h}[\alpha \vee b] + \widetilde{h}[\alpha \wedge b]$.

In 7 (iv) there's equation if and only if L is a modular lattice.

Lemma 8. *Let p be D-point of a D-semimodular lattice, and* α *– an arbitrary element of the same one. Then there exists a D-point q such that* $q \leq p$ *and* $q \leq \alpha$ *or we have an isomorphism* $[\alpha, \alpha \vee p] \cong [0, p]$.

Corollary 9. *Let p and q be D-points of a D-semimodular lattice and let for some element* α *of this lattice* $\alpha < \alpha \vee q \leq \alpha \vee p$. *Then* $\alpha \vee q \cong \alpha \vee p$.

Corollary 9 is the analogous of an exchange property from the classical case [1].

Lemma 10. *Every D-semimodular lattice has the exchange property (in the science of corollary 9).*

Lemma 11. *In a D-pointwise lattice the following conditions are equivalent:*

(i) *L has the upper D-covering condition;*

(ii) *L has the exchange property;*

(iii) *If* $\alpha \wedge b \overset{D}{<} \alpha$ *then* $b \overset{D}{<} \alpha \vee b$ *in L;*

(iv) *If* $\alpha \wedge b \overset{D}{<} \alpha$ *then* (α, b) *M* in L;*

Definition 12. (i) *Let* α *and b be elements of L. An element* b_1 *is called a left* Δ*-complement within b of* α *in* $(\alpha \vee b)$ *when*

$\alpha \vee b \cong \alpha \vee b_1$, $\alpha \wedge b_1 = 0$, (b_1, α) M and $b_1 \leq b$.

(ii) We call L α left Δ-complemented lattice when for every pair of elements α and b in L there exists such a left Δ-complement.

(iii) A D-pointwise complete lattice L is called compactly D-pointwise when L satisfies the following condition:

If p is a D-point and S is a set of D-points of L such that $p \leq \nu\,(q, q \in S)$ then there exists a finite subset $\{q_1, \ldots, q_n\}$ of S such that $p \leq q_1 \nu \ldots \nu q_n$.

(iv) A complete lattice L is called upper continuous if L satisfies the following condition:

If $\alpha_\delta \uparrow \alpha$ (i.e. D is a directed set and $\delta_1 \leq \delta_2$ implies $\alpha_{\delta 1} \leq \alpha_{\delta 2}$ and $\alpha = \nu\,(\alpha_\delta, \delta \in D)$) then $\alpha_\delta \wedge b \uparrow \alpha \wedge b$ for every $b \in L$.

Lemma 13. *A D-pointwise complete lattice L is upper continuous if and only if L is compactly D-pointwise.*

Theorem 14. *Let L be a compactly D-pointwise lattice. Then the following conditions are equivalent:*

(i) *L has the upper D-covering condition;*

(ii) *L is* $\perp$*-symmetric;*

(iii) *L is M-symmetric;*

(iv) *L is a left Δ-complemented.*

An element α of a complete lattice L is said to be a compact element if for any subset $X \subseteq L$ $\alpha \leq \vee X$ implies $\alpha \leq \vee X_1$ for some finite subset $X_1 \leq X$ [2].

A complete lattice is called an algebraic lattice if every element of it is the lattice join of compact elements [2,3].

We tried to describe a lattice, which is associated with the geometric lattice of all submodules of the module over the principal ideal domain. Such lattice we called the general geometric or D-geometric lattice.

Deffinition 15. [4] A lattice L is called general geometric or D-geometric lattice when L is D-semimodular algebraic lattice, the compact elements of L are the finite units of the D-points and only they and all D-points of L are isomorphic to each other.

It follows from the definition that D-geometric lattice is complete, compactly D-pointwise, $\perp$-symmetric, M-symmetric and left Δ-complemented lattice and it satisfies the upper D-covering condition.

Corollary 16. *Let* $\Omega = \{\alpha \in L \mid \widetilde{h}\,[\alpha] < \omega\}$ *be the set of finite elements of the D-geometric Lattice L. Then*

(i) *If* $\alpha, b \in \Omega$ $\alpha < b$ *then* $\widetilde{h}\,[\alpha] < \widetilde{h}\,[b]$.

(ii) Ω *is an ideal of L.* Ω *is a D-semimodular, M-symmetric and a left Δ-complemented lattice. Every element of* Ω *is the finite join of D-points of L.*

Corollary 17. (i) *An element* $c \in L$ *is a D-point of* $[\alpha, b] \subset L$ *if and only if there exists a D-point* $p \in L$ *such that* $c = \alpha \vee p$, $\alpha \wedge p = 0$ and $p \leq b$.

(ii) *Every interval of D-geometric lattice is a D-geometric lattice too.*

Lemma 18. *Every element* α *of a D-geometric lattice is the join of some independent set of D-points. Moreover, it is the join of any independent set of D-points of* $(\alpha]$.

Definition 19. (i) A lattice L is called a Δ-complemented lattice when for every element $\alpha \in L$ there exists such $d \in L$ that $\alpha \wedge d = 0$ and $[0, \alpha \vee d] \cong [0,1]$.

(ii) L is called a relatively Δ-complemented lattice, when for any $\alpha, x_1, x_2 \in L$ there exists such $s \in L$ that $\alpha \wedge s = x_1$ and $[x_1, \alpha \vee s] \cong [x_1, x_2]$.

It is evident that relatively Δ-complemented lattice of finite rank is also the Δ-complemented.

Theorem 20. *Every D-geometric lattice is a Δ-complemented lattice.*

Proposition 21. [4]. A lattice L is a D-geometric if and only if L is a D-pointwise upper-continuous D-semimodular relatively Δ-complemented lattice.

Definition 22. (i) *Let* α *and b be elements of a lattice L; then we say that* α *and b are Δ-perspective and write* $\alpha \overset{\Delta}{\sim} b$ *when they have a common Δ-complement.*

(ii) We say that α and b are Δ-projective ($\alpha \overset{\Delta}{\approx} b$) when there exist elements $x_1, \ldots, x_n$ such that $\alpha \overset{\Delta}{\sim} x_1 \overset{\Delta}{\sim} x_2 \overset{\Delta}{\sim} \ldots \overset{\Delta}{\sim} x_n \overset{\Delta}{\sim} b$.

Lemma 23. *Let p and q be independent D-points of a modular D-geometric lattice. Then* $p \vee q$ *contains a third independent with p and q D-point if and only if* $p \overset{\Delta}{\sim} q$.

Lemma 24. *Let p and q be independent D-points of a modular D-geometric lattice L and* $p \overset{\Delta}{\sim} q$. *Then there exists a D-point r such that* $p \overset{\Delta}{\sim} r, q$ *and* $r \leq x$.

Lemma 25. *Let p, q and r be independent D-points of a modular D-geometric lattice L. If* $p \vee q$ *and* $q \vee r$ *contain third D-points then* $p \vee r$ *contains a third D-point too.*

Theorem 26. *The Δ-perspectivity is the relation of equivalence on the set of all D-points of the modular D-geometric lattice.*

Corollary 27. *Let p and q be D-points of the modular D-geometric lattice. Then* $p \overset{\Delta}{\approx} q$ *implies* $p \overset{\Delta}{\sim} q$.

Georgian Technical University

REFERENCES

1. *F.Maeda, S.Maeda.* Theory of symmetric lattices, Springer-Verlag, New-York. N.Y. 1970.
2. *G.Gratzer.* General lattice theory. Academie-Verlag,Berlin,1978.
3. *G.Birkhoff.* Lattice theory. Third edition, New-York: Amer. Math. Soc. Colloq. Publ. 1967.
4. *A.A.Lashkhi.* General geometric lattices and projective geometry of modules, modern mathematics and application, Probl. of geom. VINITI, 1995, T.1, 168-203 (Russian).

საქართველოს მეცნიერებათა აკადემიის მოამბე, 158, №1, 1998
BULLETIN OF THE GEORGIAN ACADEMY OF SCIENCES, 158, №1, 1998

MATHEMATICS

D.Chkhatarashvili

K. von Staudt's Theorem over Ore Domains

Presented by Corr. Member of the Academy H.Inassaridze, December 15,1997

ABSTRACT. **Cross-ration, harmonic quadruple and K.von Staudt's theorem for free modules over left Ore domains are studied.**

Key words: harmonic quadruple, Ore domain projective plane.

The first generalization of von Staudt's theorem belongs to G.Ancochea (1942). The classic studies described the theory over division rings. R.Baer and J.von Neumann pointed out a possible extension the theory to the case of ring, generating intense research activity in the area of geometric algebra over rings.

Further contribution in this field (harmonic maps and von Staudt's theorem) was made by B.R.McDonald, N.B.Limaye, H.Schaeffer, W.Benz, V.Havel and others. B.V.Limaye and N.B.Limaye (1971-1977) generalized the theorem to noncommutative local rings by adopting the definition of harmonic maps. However, for commutative principal ideal domains the von Staudt's theorem is invalid (C.Bartolone, 1981).

The first article of noninjective harmonic maps between projective lines was due to F.Buekenhout (1965); after D.G.James got the same result (1982). In 1985 C.Bartolone and F.Bartolozzi extended some of Buekenhout's ideas for the ring case.

Cross-ration, harmonic quadruple and von Staudt's theorem in Moufang planes was studied by V.Havel (1965-1968) and I.C.Ferrar (1985).

Many interesting and fundamental results according to this and boundry problems were obtained by W.Benz and his scholars (1973-1990). For more complete picture of references, evolution and modern state see surveys C.Bartolone and F.Bartolozzi, F.Veldkamp, W.Benz, H.-J.Samaga and H.Schaefer the books B.R.McDonald, W.Benz, F.Buekenhout.

In [1] A.A.Lashkhi calculated more general (non-bijective) harmonic maps with the classical definition of a harmonic quadruple for non-commutative principal ideal domains and obtained the complete analog of the classical case.

Our aim is to prove A.Lashkhi's theorem for left Ore domains.

A non-zero ring R is called a left Ore domain if it has no zero divisors and $Ra \cap Rb \neq \{0\}$ for arbitrary nonzero $a, b \in R$. The R-module over left Ore domain is called torsion-free if $rx = 0$ implies $r = 0$ or $x = 0$ for all $r \in R$ and $x \in X$. It is well known that each left Ore domain R possesses a skew field of left quotients $F \supseteq R$ with

$$F = \{a^{-1}b;\ a, b \in R,\ a \neq 0\}.$$

Let M be a torsion-free module over left Ore domain R and F be the skew field of left quotients of R. According to U.Brehm (1983), consider the tensor product $\overline{X} = F \otimes_R X$, then the canonical mapping

$$i: M \to F \otimes_R M$$

is injective and thus M can be regarded as an R-submodule of F-vector space X. It is obvious that $FX = < FX > = \overline{X}$.

Definition 1. Let R be an integral domain (not necessarily commutative). X is a torsion-free module over R. The projective space $P(X)$ corresponding to X is the set of all R-free submodules of rank 1.

For every R-free submodule $U \hookrightarrow X$ the projective dimension $\dim_p$ will be defined as $\dim_p U = \dim U - 1$. We shall use the terms: "point" "line" "plane" for free submodules of the projective dimensions 0, 1, 2. We shall consider the zero submodule as an "empty element" of the projective space $P(X)$ with projective dimension -1.

Definition 2. The set of points $\{P_\alpha,\ \alpha \in \Lambda\}$ of the projective space $P(X)$ will be called collinear, if there exists a line $U \hookrightarrow X$ such that $P_\alpha \in U$ for every $\alpha \in \Lambda$ and strictly collinear if there exists a line U for which $U = P_\alpha + P_\beta$ for every $\alpha, \beta \in \Lambda$.

In the sequel R is the group of units of the ring R. If $s \in R$ is an arbitrary element, then by $[s]$ we denote the set of all conjugate elements of the form $t^{-1}st$, where $t \in R$.

Let $P_1 = \mathrm{Re}_1$, $P_2 = \mathrm{Re}_2$ be independent points, i.e. $P_1 \cap P_2 = 0$. If $U = P_1 + P_2$ and $P_3 = k(\alpha e_1 + \beta e_2) \hookrightarrow U$ be an arbitrary point. Then it is obvious that the points P_1, P_2, P_3 are strictly collinear if and only if $\alpha, \beta \in R^*$. It's also obvious that if P_1, P_2, P_3, P_4 are strictly collinear points and U is a principal line passing through these points, then there exist the unimodular elements e_1, e_2 of this line U and an invertible element $s \in R^*$ such that

$$P_1 = \mathrm{Re}_1,\ P_2 = \mathrm{Re}_2$$
$$P_3 = R(e_1 + e_2),\ P_4 = R(e_1 + se_2).$$

The element $s \in R^*$ is called cross-ratio of these points. If R is commutative, then s is unique. For the non-commutative situation the cross-ratio is $[s]$.

For the quadruple of strictly collinear points and their cross-ratio we use the notation

$$[P_1, P_2, P_3, P_4] = [s].$$

Remark that the order of the points P_i is essential. The quadruple of the strictly collinear points $P_1, P_2, P_3, P_4 \in P(X)$ is in harmonic relation if $[P_1, P_2, P_3, P_4] = -1$. Note that this definition implies that $1/2 \in R$.

Denote by $\mathfrak{R}(X)$ the lattice of all submodules of R-module X.

Suppose as well that F_1 is some skew field and R_1 is a subring of F_1. Let $\overline{X}_i$ be a F_1-vector space and X_1 be a R_1-submodule of $\overline{X}_1$ such that $\langle F_1 X_1 \rangle = \overline{X}_1$.

Definition 3. The map $f: P(X) \to \mathfrak{R}(X_1)$ will be called harmonic if for each quadruple of harmonic points $P_1, P_2, P_3, P_4 \in P(X)$ and their images $f(P_1), f(P_2), f(P_3), f(P_4)$ there exist $y_1, y_2 \in X_1$ such that

$$Q_1 = k_1 y_1 \hookrightarrow f(P_1)$$
$$Q_2 = k_2 y_2 \hookrightarrow f(P_2)$$
$$Q_3 = k_1(y_1 + y_2) \hookrightarrow f(P_3)$$
$$Q_4 = k_1(y_1 - y_2) \hookrightarrow f(P_4)$$

i.e. the points Q_1, Q_2, Q_3, Q_4 are in harmonic relation.

The map $\sigma: R_2 \to R_1$ will be called anti-isomorphism if it is an isomorphism on abelian groups R_1 and R_2 and $\sigma(xy) = \sigma(y)\sigma(x)$ for arbitrary $x, y \in R_1$. The map σ will be called semi-isomorphism if it is either an isomorphism or antiisomorphism.

Definition 4. Let X_1 and X_2 be vector spaces over the skew fields R_1 and R_2, $\dim X_1 = \dim X_2 = 2$ and $\sigma: R_2 \to R_1$ is anti-isomorphism. The map $\mu: R_2 \to R_1$ will be called a semilinear isomorphism with respect to σ (σ is a semilinear anti-isomorphism),

if μ is defined on the basis B (i.e. for e_1, e_2 the images $\mu(e_1)$ and $\mu(e_2)$ are fixed) and then we continue as follows:

$$\text{(i) } \mu(ae_i) = \sigma(a)\mu(e_i), \quad i = 1, 2;$$

$$\text{(ii) } \mu(a_1e_1 + a_2e_2) = [\sigma(e_2)]^{-1}\mu(e_1) + [\sigma(a_1)]^{-1}\mu(e_2)$$

for each $a, a_1, a_2 \in R$, $aa \neq 0$.

Theorem 1. Let R be left Ore domain, $1/2 \in R$ and X be a torsion-free module over R, $\dim_p X = 1$. If $f : P(X) \to \mathfrak{R}(X_1)$ is a harmonic map, then there exist a semi-isomorphism $\sigma : F \to F_1$, a σ-semilinear (anti)-isomorphism $\mu : \overline{X} \to \overline{X}_1$ and a subring $K_1 \hookrightarrow F_1$ such that $K_1\mu(X) \leq X_1$ and $f(Rx) = K_1\mu(x)$ for all $x \in X$.

Corollary 1. (K. von Staudt's theorem) Let R be a left Ore domain $1/2 \in R$; X be a torsion-free R-module, $\dim_p X = 1$. The bijection $f P(X) \to P(X_1)$ is harmonic if and only if there exist an isomorphism or an anti-isomorphism $\sigma : R \to R_1$ and σ-semilinear $\mu : \overline{X} \to \overline{X}_1$ isomorphism such that $f(Rx) = R_1\mu(x)$ for every $x \in X$.

Georgian Technical University

REFERENCES

1. *A.Lashkhi.* Georgian Mathematical Journal. **4**, 1, 1997, 41-64.

საქართველოს მეცნიერებათა აკადემიის მოამბე, 158, №1, 1998
BULLETIN OF THE GEORGIAN ACADEMY OF SCIENCES, 158, №1, 1998

MATHEMATICS

M.Okropiridze

On the Symmetrically Continuity of Two Variables Functions

Presented by Corr. Member of the Academy V. Kokilashvili, January 5, 1998

ABSTRACT. **We introduce the notions of symmetrically continuity, separately symmetrically continuity in the strong and in the angular senses for functions of two variables. The relation between them is established. Some of the known properties equivalent to continuity with respect to each of the variables are not preserved to symmetrically continuity. We also introduce one more notion of symmetrically continuity that is non-comparable to symmetrically continuity.**

Key words: symmetrically continuity, separately symmetrically continuity in the strong and in the angular senses.

Below, we will mean everywhere that the function to be considered receives only finite values. It is well known that function $f(x)$ of one variable is called symmetrically continuous at an inner point x_0 of the interval (a, b), if the equality

$$\lim_{h\to 0} [f(x_0 + h) - f(x_0 - h)] = 0$$

is fulfilled.

I. Definition 1.1. A function of two variables f (x, y) will be called symmetrically continuous at a point (x_0, y_0), if the equality

$$\lim_{(h,k)\to(0,0)} [f(x_0 + h, y_0 + k) - f(x_0 - h, y_0 - k)] = 0$$

is fulfilled.

Proposition 1.1. *If a function $f(x, y)$ is continuous at a point (x_0, y_0), then $f(x, y)$ is symmetrically continuous at (x_0, y_0). Moreover, there is a symmetrically continuous function at a given point that is discontinuous at the same point.*

Definition 1.2. A function $f(x, y)$ will be called symmetrically continuous with respect to x [with respect to y] if the equality

$$\lim_{h\to 0} [f(x_0 + h, y_0) - f(x_0 - h, y_0)] = 0$$

[correspondingly $\lim_{h\to 0} [f(x_0, y_0 + k) - f(x_0, y_0 - k)] = 0$] is fulfilled.

A function $f(x, y)$ will be called separately symmetrically continuous at a point (x_0, y_0), if $f(x, y)$ is symmetrically continuous at (x_0, y_0) with respect to each of the variables.

Proposition 1.2. *If a function $f(x, y)$ is symmetrically continuous at a point (x_0, y_0), then $f(x, y)$ is separately symmetrically continuous at (x_0, y_0) but not vice versa.*

Definition 1.3. A function $f(x, y)$ will be called symmetrically continuous in the strong sense with respect to x [with respect to y], if the equality.

$$\lim_{(h,k)\to(0,0)} [f(x_0 + h, y_0 + k) - f(x_0 - h, y_0 + k)] = 0$$

[correspondingly $\lim_{(h,k)\to(0,0)} [f(x_0+h, y_0+k) - f(x_0+h, y_0-k)] = 0$] is fulfilled.

A function $f(x, y)$ will be called separately symmetrically continuous in the strong sense at a point (x_0, y_0) if $f(x, y)$ is symmetrically continuous in the strong sense at (x_0, y_0) with respect to each of the variables.

Proposition 1.3. *If a function $f(x, y)$ is symmetrically continuous in the strong sense with respect to one of the two variables at a point (x_0, y_0), then $f(x, y)$ is symmetrically continuous at (x_0, y_0) with respect to the same variable, but not vice versa.*

Theorem 1.1. *If a function $f(x, y)$ is separately symmetrically continuous in the strong sense at a point (x_0, y_0), then $f(x, y)$ is symmetrically continuous at (x_0, y_0), but not vice versa.*

Remark 1.1. Continuity of function of two variables is equivalent to the separately strong continuity of this function (see [1], Theorem 1.1., statement 1)). This property is one sidedly preserved for the symmetrically continuity according to theorem 1.1.

In consequence of theorem 1.1. the following question is natural: can separately symmetrically continuity in the strong sense at a point (x_0, y_0) through parting cause continuity of function $f(x, y)$ at the same point? The answer is negative.

Definition 1.4. A function $f(x, y)$ will be called symmetrically continuous in the angular sense at a point (x_0, y_0) with respect to x [with respect to y], if the equality

$$\lim_{\substack{(h,k)\to(0,0)\\ |k|\le c|h|}} [f(x_0+h, y_0+k) - f(x_0-h, y_0+k)] = 0$$

[correspondingly $\lim_{\substack{(h,k)\to(0,0)\\ |h|\le c|k|}} [f(x_0+h, y_0+k) - f(x_0-h, y_0+k)] = 0$] is fulfilled for any constant $c > 0$.

A function $f(x, y)$ will be called separately symmetrically continuous in the angular sense at a point (x_0, y_0), if $f(x, y)$ is symmetrically continuous in the angular sense with respect to each variables.

Proposition 1.4. *If a function $f(x, y)$ is symmetrically continuous in the strong sense at a point (x_0, y_0) with respect to one of the two variables, then $f(x, y)$ is symmetrically continuous in the angular sense with respect to same variable, but not vice versa.*

Proposition 1.5. *If a function $f(x, y)$ is symmetrically continuous in the angular sense at a point (x_0, y_0) with respect to x [with respect to y], then $f(x, y)$ is symmetrically continuous at (x_0, y_0) with respect to x [correspondingly with respect to y], but not vice versa.*

Such is the relation between separately symmetrically angular continuity and symmetrically continuity:

Theorem 1.2. *Symmetrically continuity and separately symmetrically continuity in the angular sense are non-comparable properties.*

Remark 1.2. It is known that the continuity of function of two variables is equivalent to the separately continuity in the angular sense (see [1], Theorem 1.1 statement 2)). According to theorem 1.2 this property is not preserved for symmetrically continuity.

II. The second mixed symmetric difference is called the expression (see [2])

$$\Delta^{sym} f(x_0, y_0; h, k) = f(x_0 + h, y_0 + k) + f(x_0 - h, y_0 - k) - f(x_0 + h, y_0 - k) - f(x_0 - h, y_0 + k).$$

Definition 2.1. A function $f(x, y)$ will be called symmetrically continuous at a point (x_0, y_0) in the $*-$ sense if the equality

$$\lim_{(h,k)\to(0,0)} \Delta^{sym} f(x_0, y_0; h, k) = 0$$

is fulfilled.

Theorem 2.1. *The symmetrically continuity in the $*-$ sense and the symmetrically continuity are non-comparable properties.*

Remark 2.1. If $\alpha(x)$ and $\beta(y)$ are finite functions of one variables, then the function of two variables $f(x, y) = \alpha(x) + \beta(y)$ is symmetrically continuous in the $*-$ sense.

Theorem 2.2. *If a function $f(x, y)$ is symmetrically continuous in the strong sense at a point (x_0, y_0) with respect to some of the variables, then $f(x, y)$ is symmetrically continuous in the $*-$ sense at a point (x_0, y_0), but not vice versa.*

A.Razmadze Mathematical Institute
Georgian Academy of Sciences

REFERENCES

1. *O.P.Dzagnidze.* Proc. A. Razmadze Math. Inst., **106**, 1993, 7-48.
2. *D.Rinne.* Real Analysis Exchange, **16**, 1990-91, 559-564.

საქართველოს მეცნიერებათა აკადემიის მოამბე, 158, №1, 1998
BULLETIN OF THE GEORGIAN ACADEMY OF SCIENCES, 158, №1, 1998

MATHEMATICS

G.Oniani

On the Integrability of Strong Maximal Functions

Presented by Academician L.Zhizhiashvili, March 5, 1998

ABSTRACT. **In the present paper it is studied if it's possible for the given set of frames E to construct the function f such that 1) $M_\theta(f)$ is non-integrable on $(0,1)^2$ for every $\theta \in E$, and 2) $M_\theta(f)$ is integrable on $\{M_\theta(f) > 1\}$ for every $\theta \notin E$, where M_θ denotes the strong maximal operator corresponding to the frame θ.**

Key words: maximal functions, frame, integrability.

We call a frame in space $\mathbb{R}^2$ a set whose elements are two mutually orthogonal straight lines passing the origin. We denote a frame by $\theta(\theta = \{\theta^1, \theta^2\})$. Under θ_0 we assume the frame $\{Ox^1, Ox^2\}$ where Ox^1 and Ox^2 are the coordinate axes of space $\mathbb{R}^2$. Let's denote the set of all of the frames of $\mathbb{R}^2$ by $\theta(\mathbb{R}^2)$.

Introduce the following metric in $\theta(\mathbb{R}^2)$: let $\theta_1 = \{\theta_1^1, \theta_1^2\}$ and $\theta_2 = \{\theta_1^1, \theta_2^2\}$, then

$$\operatorname{dist}(\theta_1, \theta_2) = \min\{\sphericalangle(\theta_1^i, \theta_2^j): i, j = 1, 2\}, \tag{1}$$

where $\sphericalangle(\cdot,\cdot)$ denotes the angle between two straight lines.

Denote by $V(\theta)$ and $V(E)$, respectively, the collection of all neighbourhoods of the frame $\theta \in \theta(\mathbb{R}^2)$ and set $E \subset (\mathbb{R}^2)$. Further, let $D(\theta, \varepsilon)$ and $D[\theta, \varepsilon]$, respectively, be the open and the closed balls with centre θ and radius ε.

Assume $\alpha(\theta_0)$ to be equal to 0. For $\theta = \{\theta^1, \theta^2\} \neq 0$ consider the line θ^i, $i = 1$ or 2, which lies in the first and third quarter of the coordinate plane and define $\alpha(\theta)$ as the angle between the lines Ox^1 and θ^i.

Consider the space $[0, \pi/2)$ with the following metric: for $\alpha_1, \alpha_2 \in [0, \pi/2)$

$$\operatorname{dist}(\alpha_1, \alpha_2) = \min\{|\alpha_1 - \alpha_2|, \pi/2 - |\alpha_1 - \alpha_2|\}. \tag{2}$$

It is clear that the mapping α: $\theta(\mathbb{R}^2) \to [0, \pi/2)$ is an isometry of the space $\theta(\mathbb{R}^2)$ with metric (1) in the space $[0, \pi/2)$ with metric (2).

Let $|\cdot|$ be Lebesgue measure into $[0, \pi/2)$. The measure $|\cdot|_{\theta(\mathbb{R}^2)}$ is defined in the following way: the set $E \subset \theta(\mathbb{R}^2)$ is said to be $|\cdot|_{\theta(\mathbb{R}^2)}$ measurable if the set $\alpha(E)$ is $|\cdot|$ measurable, assuming that $|E|_{\theta(\mathbb{R}^2)} = |\alpha(E)|$.

Let $I^2 = (0,1)^2$. Denote by $\Phi(L)(I^2)$ the class of all functions $f \in L(\mathbb{R}^2)$ having the following qualities: $\operatorname{supp} f \subset I^2$, $\int_{I^2} \Phi(|f|) < \infty$.

We shall call a frame of a rectangle R the frame θ, for which the sides of R are parallel to respective lines $\theta^j (j = 1,2)$ and we denote it by $\theta(R)$.

Denote by $B(\theta)$ the collection of all rectangles R with $\theta(R) = \theta$.

For a frame $\theta \in \theta(\mathbb{R}^2)$ consider its corresponding strong maximal operator M_θ defined as follows

$$M_\theta(f)(x) = \sup_{R \in B(\theta), R \ni x} \frac{1}{|R|} \int_{|R|} |f| \qquad (f \in L(\mathbb{R}^2), x \in \mathbb{R}^2).$$

For the set $E \subset \theta(\mathbb{R}^2)$, $E \neq \varnothing$, denote

$$M_E(f)(x) = \sup_{\theta \in E} M_\theta(f)(x) \quad (f \in L(\mathbb{R}^2), x \in \mathbb{R}^2).$$

Definition. We call the set $E \subset \theta(\mathbb{R}^2)$ Δ-set if there exists a function $f \in L(I^2)$ such that

$$\int_{I^2} M_\theta(f) = \infty \text{ for every } \theta \in E, \tag{3}$$

$$\int_{\{M_\theta(f)>1\}} M_\theta(f) < \infty \text{ for every } \theta \in \theta(\mathbb{R}^2) \setminus E. \tag{4}$$

For the set $E \subset \theta(\mathbb{R}^2)$ denote by S_E the class of all functions $f \in L \setminus L(I^2)$ which has the properties (3) and (4).

2. Following statements are true:

Theorem 1. Every Δ-set is of G_δ type. Moreover for every $f \in L(I^2)$ the set

$$\{\theta \in \theta(\mathbb{R}^2): \int_{I^2} M_\theta(f) = \infty\}$$

is of G_δ type.

Theorem 2. $\theta(\mathbb{R}^2)$ is Δ-set. Moreover for every $f \in L \setminus L(\ln^+ L)^2(I^2)$ there exists an equimeasurable with f function g from the class $S_{\theta(\mathbb{R}^2)}$.

Theorem 3. [1]. $\varnothing$ is Δ-set. Moreover for every $f \in L\ln^+ L(I^2)$ there exists an equimeasurable with f function g such that

$$\sup_{\theta \in \theta(\mathbb{R}^2)} \int_{\{M_\theta(g)>1\}} M_\theta(g) < \infty.$$

Theorem 4. For every function $f \in L\ln^+ L(I^2)$, $f \notin L(\ln^+ L)^2(I^2)$ there exists a sequence of positive numbers $\alpha_k = \alpha_k(f) < \frac{1}{2^k}$ such that for every sequence of balls $D[\theta_j, \alpha_{k_j}]$ $(j \in \mathbb{N})$, where $k_1 < k_2 < \ldots$, there exists an equimeasurable with f function $g \in L(I^2)$ such that

1) for every $\theta \in \overline{\lim_{j \to \infty}} V[\theta_j, \alpha_{k_j}]$

$$\int_{I^2} M_\theta(g) = \infty$$

2) for every $j \in \mathbb{N}$

$$\int_{\{M_{E_j}(g)>1\}} M_{E_j}(g) < \infty,$$

where $E_j = \theta(\mathbb{R}^2) \setminus \bigcup_{i \geq j} V(\theta_i, 1/2^{k_i})$.

From the Theorems 1 and 4 it follows:

Theorem 5. Let $E \subset \theta(\mathbb{R}^2)$ be no more than countable nonempty set. Then

1) E is Δ-set if and only if it is of G_δ type;

2) if E is of G_δ type, then for every $f \in L\ln^+ L(I^2)$, $f \notin L(\ln^+ L)^2(I^2)$ there exists an equimeasurable with f function g from the class S_E.

The statements given below follow from the Theorem 4.

Theorem 6. For every countable set $E \subset \theta(\mathbf{R}^2)$ there exists a Δ-set of zero measure including it.

Theorem 7. There exist zero measure Δ-sets the additions of which are of the first category.

Theorem 8. There exists zero measure perfect Δ-sets.

Tbilisi I.Javakhishvili State University

REFERENCES

1. *G.Oniani.* Bull. Georg. Acad. Sci., **156**, 1, 1997.

საქართველოს მეცნიერებათა აკადემიის მოამბე, 158, №1, 1998
BULLETIN OF THE GEORGIAN ACADEMY OF SCIENCES, 158, №1, 1998
MATHEMATICS

L.Jijeishvili

On the Order of Decrease of Fourier Coefficients

Presented by Academician L.Zhizhiashvili, November 3, 1997

ABSTRACT. **It is proved that there exists complete double orthonormal system ONS at which Fourier coefficients of functions from $L^p(p \geq 1, l^\infty \equiv C)$ by this system converge to zero faster than Fourier-Haar coefficients.**

Key words: Fourier coefficients, double orthogonal series.

It is well-known [1] that Fourier-Haar coefficients of any continuous function f may be estimated by its modulus of continuity:

$$|C_n(f,\chi)| \leq (2n)^{-\frac{1}{2}}\,\omega\left(\frac{1}{n}, f\right). \qquad (1)$$

For the functions of class $L^p(0,1)$, $1 \leq p < \infty$, the analogous estimate [2] is valid:

$$|C_n(f,\chi)| \leq n^{\frac{1}{p}-\frac{1}{2}}\,\omega_p\left(\frac{1}{n}, f\right), \qquad (2)$$

where $\omega_p(\delta, f)$ is the L^p-modulus of continuity of function f.

So all functions of class L^p, $p > 2$ have guarantied order of decrease of Fourier-Haar coefficients. P.Ul'yanov [3,4] arose the question whether the order of decrease in (1) and (2) is the most possible in the class of all orthonormal systems (ONS).

S.B.Kozyrev [5] answered this question negatively: for any strict monotone tending to zero sequence $\{\gamma_n\}$ with $\sum_{n=1}^{\infty} \gamma_n^2 = \infty$ there exists complete ONS φ such that:

$$C_n(f,\varphi) = o(\gamma_n) \qquad \text{for any } f \in C;$$

$$C_n(g,\varphi) = o(\gamma_n^{1-\frac{2}{p}}) \qquad \text{for any } f \in L^p,\ p > 2.$$

Estimates analogous to (1) and (2) are true in two-dimensional space.

$$|C_{mn}(f)| \leq (4mn)^{-\frac{1}{2}}\,\omega\left(f, \frac{1}{m}, \frac{1}{n}\right) \text{ for any } f \in C([0,1] \times [0,1]), \qquad (3)$$

and

$$|C_{mn}(g)| \leq (mn)^{\frac{1}{p}-\frac{1}{2}}\,\omega_p\left(f, \frac{1}{m}, \frac{1}{n}\right) \text{ for any } g \in L^p([0,1] \times [0,1]), \qquad (4)$$

where C_{mn} are the Fourier-Haar coefficients by double system $\{\chi_n(x)\chi_m(y)\}$ are $\omega(f, \delta_1, \delta_2)$ and $\omega_p(g, \delta_1, \delta_2)$ are module of continuity in C and L^p respectively.

The aim of this paper is to learn P.Ul'yanov's question for two-dimensional space: if (3) and (4) are the best results from the point of view of the order of decrease among all ONS.

The answer is negative and the following double analogous to Kozyrev's theorem [5] is true.

Theorem. Let $\{\gamma_n\}$ and $\{\gamma'_n\}$ be strictly monotone sequences,

$$\{\gamma_n\} \to 0, \ \{\gamma'_n\} \to 0,$$

such that

$$\sum_{n=1}^{\infty} \gamma_n^2 = \infty, \quad \sum_{n=1}^{\infty} (\gamma'_n)^2 = \infty.$$

Then there exists ONS φ such that

$$c_{mn}(f, \varphi) = o(\gamma_m \gamma'_n) \qquad \text{for any } f \in C([0,1] \times [0,1]),$$

$$c_{mn}(g, \varphi) = o\left((\gamma_m \gamma'_n)^{1-\frac{2}{p}} \right) \qquad \text{for any } g \in L^p([0,1] \times [0,1]),\ p > 2.$$

Tbilisi I.Javakhishvili State University

REFERENCES

1. *Z.Ciesielski*. Bull. Acad. Polon. Sci. 7, 1959, 227-232.
2. *P.L.Ul'yanov*. Math. Sb. **63**, 3, 1964, 356-391 (Russian).
3. *P.L.Ul'yanov*. Colloquia Math. Soc. J. Bolayai. 49. A. Haar Mem. Conf. Budapest. 1985, 57-96.
4. *P.L.Ul'yanov*. Zap. Nauchn. Sem. LOMI. 170, 1989, 274-284 (Russian).
5. *S.B.Kozyrev*. Vestnik Mosk. Univ. Mat. Mekh. 2, 1993, 16-20 (Russian).

საქართველოს მეცნიერებათა აკადემიის მოამბე, 158, №1, 1998
BULLETIN OF THE GEORGIAN ACADEMY OF SCIENCES, 158, №1, 1998

MECHANICS

T.Iamanidze

Realization of Optimal Elastic Connections in Contact Zone by Selection of Destructing Instrument Parameters

Presented by Corr. Member of the Academy K.Betaneli, June 4, 1998

ABSTRACT. **Destructing instrument parameters for realization of optimal elastic connections in contact zone are considered in the paper.**

Key words: contact zone.

A contact characteristic of the pair "instrument- rock" depends, as it is known on the configuration and sizes of an instrument cutter which contacts with rock, and also on elastic properties of impact bodies. The dependence between impact force and deformation is established in this case by solving a contact problem of elasticity theorem. The similar problems have been solved for cone and plane, wedge and plane, elliptical punch and plane, etc. [1]. Equations for spherical, conic and prismatic (chisel-shaped` instruments are given in the work [2].

A force characteristic for the spherical configuration of the instrument point is expressed by Hertz function

$$P = K_c \cdot h^{2/3}, \tag{1}$$

where $K_c = \frac{4}{3}\frac{\sqrt{R}}{Q_1 + Q_2}$ is a butt-end rigidity factor; R is a rounding radius $Q_1 = \frac{1-\mu_1^2}{E_1}$; $Q_2 = \frac{1-\mu_2^2}{E_2}$ are elastic constants; E_1, E_2 - modules of the instrument and rock elasticity; μ_1, μ_2 – are Poisson factors.

An instant rigidity of the contact zone may be defined according to the formula:

$$K(h) = \frac{dP}{dh} = 1.5\, K_c h^{1/2} \tag{2}$$

For a conic butt-end

$$p = K_k \cdot h^2, \tag{3}$$

where $K_k = \frac{2}{\pi}\frac{\operatorname{tg}\gamma}{Q_1 + Q_2}$ is the factor of the instrument rigidity; γ is the half of an angle in a cone vertex.

The dependence of contact rigidity on deformation in the case considered is linear:

$$K(h) = 2K_k \cdot h \tag{4}$$

For the chisel-shaped instrument we may write

$$h = \left(\frac{2}{\pi}\frac{Q_1 + Q_2}{l}\ln\frac{4}{d}\right)P, \tag{5}$$

where l is the length of the contact platform area;

$$d = d_0 + \left(2\frac{Q_1 + Q_2}{l}\operatorname{tg}\gamma\right)P \tag{6}$$

d is the width of the contact platform area; γ is the half of a sharpening angle.

If the second summand in the expression (6), characterizing the increment of the contact platform area width while impact, is smaller than its initial value d_0, we accept $d \approx d_0$. But if they are commensurable, the mean increment (Δd) is to be found in the interval of the given P.

Taking into account $d \leftarrow d_0$ or $d = d_0 + (\Delta d)\varphi = \text{const}$, we approach the system with a linear elastic butt-end in which a resistance force is directly proportional to the deformation

$$P = K_g h, \tag{7}$$

where $K_g = \frac{\pi}{2}\frac{l}{Q_1 + Q_2}\frac{1}{\ln\frac{4}{d}}$ is the rigititly of inertia-free spring with a linear characteristic simulating the butt-end of the instrument.

The contact rigitidy in this case is constant and equal to

$$K = K_g. \tag{8}$$

The analysis of the characteristics of conic, spheric and chisel-shaped instruments enables to conclude that they are close to optimal characteristics within the certain limits [3].

A concept of an impact zone has been introduced in the work [4,5], and it has been shown that while contacting the tooth of a rolling cutterbit with rock in deep drilling only the impact zone takes place here and not the whole pipe-column; the length of the zone is evaluated according to the formula

$$l_y = a\frac{T_0}{2} \tag{9}$$

where T_0 is an impact pulse repetition period which is defined by the size and rotational velocity of a chisel, a is propagation velocity of a longitudinal wave.

Analysing the relation of the chisel rotation speed with the length of loaded bottom one may conclude that the best cycle can be achieved when time of random impact, which is estimated by the length of loaded bottom, is equal to the time passing between successive impacts of the chisel teeth when it rolls along the face.

If the given condition is observed which is similar to that of wave reflaction from the impact zone point l_y, then the reflected wave approaches the drilling instrument point at the moment of the following impact; in this case load intensity increases, and as a result, the effectiveness of the rock destruction is achieved when, simultaneously, part of the drilling instrument, which is located above the impact zone, is protected from reflected pulses [3].

The same occurs in percussive drilling [6]. Thus, it may be approved that given the relation impact zone length-destruction jump frequencies some conditions are established for using effectively the reflected wave energy and intensification of dynamic face load.

Wave properties of a drilling instrument, on the one hand, and a discrete character of the rock destruction within a single impact, on the other, resulted in the following hypothesis [7].

As a striker in a design diagram of impact is a rod with a free upper butt-end, its natural frequencies will be correlated as odd numbers

$$\omega_{ci}(2i-1)\frac{a}{2l}=(2i-1)\omega_{c_1}\quad (c=1,2,3...). \tag{10}$$

If the number of a destructing jump within a single impact is also odd, and the frequency of a quick constituent of the shock pulse is expressed by the formula

$$\omega_0=(2i-1)\omega_z\quad (i=1\div4) \tag{11}$$

then the condition $l=l_y$ is reduced to the equality of the frequency of teeth disturbances to the frequency of wave process harmonic which takes place in a striker

$$\omega_z=\omega_{C_1}=\frac{a}{2l}, \tag{12}$$

as well as to the equality of any of abrupt constituent frequencies if there are odd numbers of destructing jumps $n=2i-1$ of one of natural frequencies of the striker ω_C $(i>1)$.

Thus, when taking into account the abruptness of the rock destruction within a single impact, the possibility of achieving high-frequency resonance is considered to be of great importance.

The availability of natural frequencies of the striker in the spectre of disturbances which are generated by the contact zone of a distructing instrument with rock causes a semiresonance cycle creating, thus, conditions for the intensity of the destruction process.

Out of several resonance cycles theoretically possible in each concrete destruction process, only two modes are performed: one with fundamental harmonic $\omega_{0,\,i\,=\,1}=\omega_z$ and the second with one of superharmonics.

If we consider the system of non-linear characteristics "rigidity-deformation", semiresonance modes of oscillation may be available here in certain conditions. This problem is studied in the works [8,9] when applied to the absorber of a drilling instrument. It has been shown that the use of an absorber of the given non-linear characteristic enables to increase dynamic of the chisel effect upon face.

This process is reduced to the following differential equation

$$m\ddot{h}+r\dot{h}+k_0 e^{\frac{\omega_0^2}{g}|h|}\cdot h=P_g(t) \tag{13}$$

Taking into account an extreme complexity of the equation (13) let it reduce to the following equation of the theory of non-linear oscillation

$$\ddot{h}+2\delta\dot{h}+\omega_C^2 h+dh^3=\frac{1}{m}P\delta_0\sin\omega_0 t, \tag{14}$$

where $\delta=\frac{\gamma}{m}$; $\omega_C^2=\frac{k_0}{m}$; $d=\omega_C^2\cdot h$; $b=\left(\frac{\omega_0^2}{g}\right)^2\frac{l^c-1}{c^2}$; $c=\frac{\omega_0^2}{g}h_l$ is an admissible error boundary of approximation of the exponential dependence or rigidity on shifting $K(h)$ by a powered multiterm. The mean error of the approximation is minimum in the range of the values $c=2.5$.

The mean relation error in the interval $c=0+2.85$ doesn't exceed 0.11. The operating range of interpolation by shifting is $h=\pm2.5\frac{g}{\omega_0^2}$, by velocity $v=\pm2.5\frac{g}{\omega_0^2}$, by acceleration $v=\pm2.5g$. The depth of contact rigidity control in this case is equal to $k=(1+12)k_0$.

The equation (14) in the absence of attenuation ($\sigma = 0$) has the following approximate solution

$$h(t) = h_0 \sin\omega_0 t + \frac{dh_0^3}{32\omega_C^2}(\sin\omega_0 t - \sin 3\omega_0 t). \qquad (15)$$

where h_0 is defined by the equation

$$\frac{3}{4} d h_0^3 + (\omega_C^2 - \omega_0^2) h_0 = \frac{1}{m} P_q \qquad (16)$$

The solution obtained is the first approximation only and it is valid provided that distortions caused by the third harmonic are not large. High order corrections would introduce the highest odd harmonics of the frequency of effect ω_0.

Taking into consideration a dissipative term, the expression (15) as an approximate solution remains valid, however, the evaluation of h_0 becomes significantly complicated.

Thus, the principal possibility of functional substitution of wave reflector by the equivalent oscillation system with concentrated parameters is based on the capability of non-linear oscillation system with one degree of freedom to generate semi-harmonic oscillation non-linear elastic connection with a given rigid characteristic in one-frequency harmonic effect conditions causes disturbance of the highest odd harmonics, redistribution of the oscillation energy into a higher frequency range.

G.Tsulukidze Institute of Mining Mechanics
Georgian Academy of Sciences

REFERENCES

1. *I.Shtaerman.* A contact problem of elasticity theory. M., 1949 (Russian).
2. *E.Aleksandrov, V.Sokolinski.* Analysis of rock instrument shock interaction. M., 1965 (Russian).
3. *E.Aleksandrov, V.Sorolinski.* Applied theory and calculation of shock systems. M., 1969 (Russian).
4. *P.Balitski.* Interaction of a drilling column with bottom-hole face. M., 1975 (Russian).
5. *P.Eigeles.* Calculation and optimization of bottom-hole processes. M., 1977 (Russian).
6. Rock destruction instrument. Kiev, 1969.
7. *A.Dzidziguri, A.Sepiashvili, T.Iamanidze.* Problem of control processes of shok impact of an instrument with rock within the range of abrupt destruction frequencies. Sience for Industry. Tbilisi, 1983.
8. *A.Sepiashvili.* Methods of analyses and calculation of the system drilling instrument-rock dynamics, Tbilisi, 1986.
9. *T.Iamanidze.* Estimation of vibrodamper rigidity of rolary-impact boring machine body. Bull. Georg. Acad. Sci., **74**, 2, 1974

L.Mgaloblishvili, A.Tsomaia

New Mathematical Basis for General Theory of Electromechanical System Needed

Presented by Academician R.Salukvadze, December 31, 1997

ABSTRACT. **New types of electric machines with forward and back forward motion of machine working elements put the question of necessity of development of general theory of electromechanical systems, adding it with new more general methods.**

Key words: electromechanical systems.

Electromechanical systems take root from 1821 when the first in the world electric motor was created by M.Faraday. The basic principles of electromechanical systems dynamics were developed by D.Maxwell, who proposed to use Lagrange equations of the second order for processes description in electric chains. Maxwell's follower E.Bernully generalized Dalamber's principle and derived the Lagrange-Maxwell equations for electromechanic systems. However, later, these equations were marked to be inapplicable to the systems with volume conductors.

In the 30-40s of the XX century the basic directions of general theory of electric machines started to form. Three basic directions, which are developed in [1-3] can be marked.

A.Kaplianskii suggested to use Lagrange-Maxwell equation for description of electric machines, which gives good results when applied to noncollector machines. However while describing collector machines the use of suggested equations is connected with certain difficulties.

In G.Kron's works later generalized in [4,5] while describing rotary electric machines the real winding of rotor is substituted by two interperpendicular rotors, machine equations are recorded as Lagrange-Maxwell equations followed by transition to other coordinate axes (to the currents of imaginable static coils). Current distribution in each coil is supposed to be sinusoidal. Actually the condition of ideal connections is used, although the question of ideal isn't analyzed.

A.V.Gapunov suggested two ways of description of collector rotary electric machine on the basis of two different models. The first model has various number of degrees of freedom and it is described by Lagrange-Maxwell equations. Stagely integration for real machines is connected with difficulties, caused by small relative length of each of these stages and the necessity of approximation of various active resistance under the brush edges.

Therefore, differential equations on each of these stages are substituded by equations in finite differences. The condition of process cycle makes it possible to record the solution of such equations as recurrent correlations giving discrete chain of parameters values of the process instead of continuous solution. The solution of equations in finite differences in some conditions can be changed by averaged solution, which neglects currents pulsations caused by commutation existence.

The second model with fixed current distribution represents an electromechanical system consisting of two infinitely long co-axial cylinders. Each of them has some distribution of current density of axial direction. The description of the mentioned model is available by S.A.Chaplygin's equations.

The equations of the second model are simultaneously approximated equations of the first model in condition when the number of anchor rotation sections is rather great.

The main goal of general theory of electric machines is not the summing of different methods of calculation, but general dynamic formulation and the study of motion laws of wider class of electric machines. Such general approach not only unifies the composition of equations of motion of different electric machines, but makes possible to perform comparative analyses of dynamic properties of these machines.

The above-mentioned works concerning electric machines of constant current basically touch only upon rotary collector machines.

The creation of new types of electric machines for the last three decades causes the appearance of new works, e.g. [6] in which the equation of Lipel is applied and [7] in which there is an attempt to apply Lagrange equation of the second order to the derivation of conduction MHD machine dependencies. There are works using Gamol equation.

Just the appearance of a new type electric machines with forward and back forward motion of machine working elements puts the question of necessity of development of general theory of electromechanical systems, adding it with new general methods.

Georgian Technical University

REFERENCES

1. *A.E.Kaplianskii*. Elektromekhanicheskie analogii i ich razvitie. Izvestia LETI, 1937 (Russian).
2. *G.Kron*. Primenenie tenzornogo analiza v elektrotekhnike. M.-L., 1975 (Russian).
3. *A.E.Gaponov*. DAN SSSR, **82**, 1952 (Russian).
4. *L.N.Gruzov*. Metody matematicheskogo issledovanija elektricheskikh mashin. M.-L., 1953 (Russian).
5. *O.White, G.Vydson*. Elektromekhanicheskie preobrazovateli energii. M.-L., 1964 (Russian).
6. *V.V.Khrushchev*. Elektricheskie mikromashiny peremennogo toka dlia ustroistv avtomatiki. L., 1969 (Russian).
7. *B.L.Alievskii*. Magnitnaia gidrodinamika, 3, 1971 (Russian).

PHYSICS

L.Akhvlediani, N.Kekelidze, V.Gogiashvili, N.Macharadze, C.Laitadze

Studies of Some Electrical Properties of Homogenous and Uniform InP-InAs Systems Solid Solutions

Presented by Academician R.Salukvadze, October 6, 1997

ABSTRACT. **Electrical properties of pure and doped InP-InAs systems solid solutions in the temperature interval 4.2-300 K were considered.**

For definition impurity atoms concentration by theoretical calculation of mobility foreign atoms concentration caused by components were calculated.

Key words: mobility, solid solution, homogeneity, disorder.

It is known that semiconductors principal properties are defined by the number of impurity atoms existing in crystals. The difference between impurity concentrations in the volume materials used for semiconductor devices production bring about a difference of devices parameters. Therefore growing the crystals with homogeneous distribution of outside and doping impurities is very important for semiconductor materials technology.

It is also important to make liquid semiconductor phase with homogenous distribution in the volume of impurity atoms, and also to make components because heterogeneity of solid solution compositions influences on crystal lattice properties and on its main characteristics, forbidden zone width. Therefore growing of doped or pure homogenous solid solutions is more difficult than growing of uniform doped simple or alloyed semiconductors.

We have worked out the method of growing of evaporative component $A^{III}B^{V}$ semiconductor solid solutions that makes possible to get high quality InP-InAs homogenous solid solutions [1].

Solid solutions of InP-InAs systems have some unique properties because of which they are applied in electronic technique. With the help of these solutions it is possible to create semiconductor devices with continuously variable parameters .They have high electron mobility, pointed absorption, little lifetime of minority carriers, high probability of radioactive recombination, radiation stability because of which solid solutions of InP_xAs_{1-x} will be applied in quantum and microelectronics, in IR spectroscopy, in space radio engineering and in other fields of science and technology.

We have created samples both pure and doped InP_xAs_{1-x} ($x = 0,1; 0,2; 0,3; \ldots, 0,9$) continuous solid solutions with $n = 10^{16} - 10^{18}$ cm. Homogeneity of these samples was examined by a roentgenoscopic method [2] and also by studying their electrical and optical properties.

It is known that the existence of considerable non-homogeneity in crystals makes it impossible to have clear and monotonic curves of charge carriers, effective masses, mobility, forbidden zone width, characteristic frequency of crystal lattices oscillation

dependence on the solid solution composition. It is also impossible to have satisfactory agreement between the calculated and experimental data.

In the present work we have dealt with the electric properties of $InP_{0.7}As_{0.3}$ ($n = 2.5 \cdot 10^{16}$ cm^{-3}) pure solid solution and of doped $InP_{0.5}As_{0.5}$ ($n = 1.25 \cdot 10^{17}$ cm^{-3}) solid solution in a wide temperature interval. Doping was done by tellurium in the process of crystal growth.

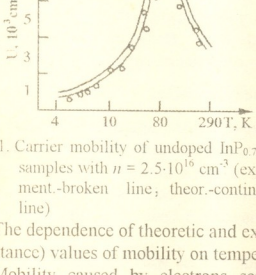

Fig. 1. Carrier mobility of undoped $InP_{0.7}As_{0.3}$ samples with $n = 2.5 \cdot 10^{16}$ cm^{-3} (experiment.-broken line; theor.-continuous line)

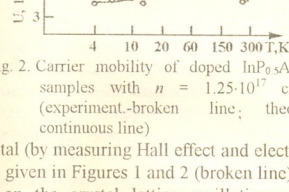

Fig. 2. Carrier mobility of doped $InP_{0.5}As_{0.5}$ samples with $n = 1.25 \cdot 10^{17}$ cm^{-3} (experiment.-broken line; theor.-continuous line)

The dependence of theoretic and experimental (by measuring Hall effect and electric resistance) values of mobility on temperature is given in Figures 1 and 2 (broken line).

Mobility caused by electrons scattering on the crystal lattice oscillation was calculated by the Ehrenreich formula and on the ionized impurities by the Brooks-Herring formula. But mobility caused by scattering on the neutral impurities and on the alloy disorder was calculated by the Erginsoy and Brooks formulae respectively. The calculations have shown that the scattering on the neutral impurities is inconsiderable.

Table 1.

Solid solution InP_xAs_{1-x}	Concentration n, cm^{-3}	Mobility U.cm/v.sec. experimental		Mobility U cm^2/v.sec. theoretical	
		300 K	77 K	300 K	77 K
$InP_{0.1}As_{0.9}$	$1.8 \cdot 10^{16}$	$1.0 \cdot 10^4$	$2.5 \cdot 10^4$	$2.26 \cdot 10^4$	$4.52 \cdot 10^5$
$InP_{0.2}As_{0.8}$	$1.6 \cdot 10^{16}$	$7.3 \cdot 10^3$	$18.3 \cdot 10^3$	$77.9 \cdot 10^4$	$15.6 \cdot 10^4$
$InP_{0.3}As_{0.7}$	$2.3 \cdot 10^{17}$	$7.5 \cdot 10^3$	$10.1 \cdot 10^3$	$3.9 \cdot 10^4$	$7.8 \cdot 10^4$
$InP_{0.4}As_{0.6}$	$7.5 \cdot 10^{17}$	$4.5 \cdot 10^3$	$5.5 \cdot 10^3$	$2.3 \cdot 10^4$	$4.6 \cdot 10^4$
$InP_{0.5}As_{0.5}$	$6.9 \cdot 10^{18}$	$3.1 \cdot 10^3$	$3.7 \cdot 10^3$	$1.1 \cdot 10^4$	$2.2 \cdot 10^4$
$InP_{0.6}As_{0.4}$	$2.2 \cdot 10^{18}$	$2.1 \cdot 10^3$	$2.6 \cdot 10^3$	$1.16 \cdot 10^4$	$2.32 \cdot 10^4$
$InP_{0.7}As_{0.3}$	$2.5 \cdot 10^{16}$	$3.9 \cdot 10^3$	$8.5 \cdot 10^3$	$1.75 \cdot 10^4$	$3.50 \cdot 10^4$
$InP_{0.8}As_{0.2}$	$3.7 \cdot 10^{16}$	$2.9 \cdot 10^3$	$8.1 \cdot 10^3$	$2.48 \cdot 10^4$	$4.96 \cdot 10^4$

During the mobility calculation for the definition of the main parameter, impurity centres concentration (N_i), we took into consideration the fact that our solid solution components were exclusively pure. So we were given the opportunity to calculate outside atom concentrations. In our samples it was 10^{17} at/cm^3, therefore for the mobility calculation we use the value $N = 3.8 \cdot 10^{17}$ at/cm^3 for undoped samples and the

value $N = 5.26 \cdot 10^{17}$ at/cm^3 for doped samples (Fig.1, 2. full line). As is seen from Figures 1 and 2 the theoretical values of mobility are in good correspondence with experimental values.

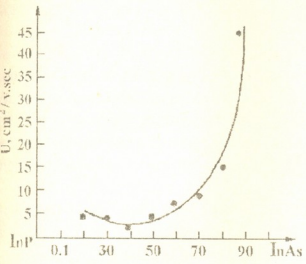

Fig. 3. The dependence of mobility (because of alloys disordering) on the composition for InP_xAs_{1-x} solid solutions at nitrogen temperature.

The electro-physical properties of doped and undoped samples at room temperature and at the nitrogen temperature have been studied. In particular we have studied the alloy disorder influence over the carrier mobility. By the use of corresponding theory [3] we have measured the mobility of alloy disorder. The results are given in Table 1. As this Table shows, the values of mobility which is the result of scattering on the alloy disorder are a degree higher than the experimental values.

The dependence of this mobility on the composition at nitrogen temperature is given in Figure 3. Corresponding curve at room temperature is considered in other works [4,5]. As seen from the comparison our results are different from the results of [4,5]. This research gives us the chance to conclude that undoped and doped InP-InAs solid solutions obtained by us are of higher quality, homogenous and they have uniform distribution of components and doping impurities. They have not any other phases and clusters.

Tbilisi I.Javakhishvili State University

REFERENCES

1. *N.Kekelidze, L.Akhvlediani.* Bull. Acad. Sci. Georg. SSR, **88**, 3, 1977, 574 (Russian).
2. *N.Kekelidze, G.Kekelidze, et al.* In Probl. svarki, metallurgii i smezhnikh tekhn. (mezhd. nauchno-prak. konf.) Tbilisi, 1996, 278-286 (Russian)
3. *L.Makowski, M.Gliksman.* J. Phys. Chem. Solids., **34**, 1973, 487.
4. *A.Levitas.* Phys. Rev, **99**, 1955, 1810.
5. *H.Weiss,* Z.Naturforsh. 10a, 1956, 430.

საქართველოს მეცნიერებათა აკადემიის მოამბე, 158, №1, 1998
BULLETIN OF THE GEORGIAN ACADEMY OF SCIENCES, 158, №1, 1998

PHYSICS

G.Gamtsemlidze, K.Gamkrelidze, M.Mirzoeva, G.Shonia

High Temperature Superconductor Ceramic $YBa_2Cu_3O_{7-x}$ Magnetisation at Rising Magnetic Field

Presented by Corr. Member of the Academy T.Sanadze, October 30, 1997

ABSTRACT. **High temperature superconductor (HTSC) $YBa_2Cu_3O_{7-x}$ ceramic sample was made using the solid state reaction method. Magnetization dependence on the rising outer magnetic field was established by the ballistic method.**

Based on the modified Bean critical model, the analytical expressions for the along-field directed HTSC sample magnetization was obtained within different field ranges.

The quantitative comparison between experimental and theoretical data was made. On the basis of a good coincidence within the error limits it was concluded that the Bean critical state model may be used for HTSC magnetic investigations.

Key words: high temperature superconductor, magnetisation, critical state model, ballistic method.

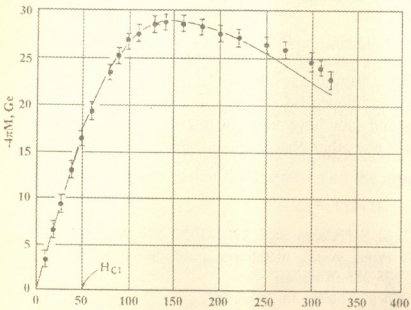

• experimental data.
—— theoretical calculations

Fig. 1. The $4\pi M(H_0)$ magnetization dependence on the outer magnetic field

The cylindrically-shaped $YBa_2Cu_3O_{7-x}$ HTSC ceramic $4\pi M$ magnetisation dependence on the outer magnetic field variation within the 1 ÷ 320 Oe interval is shown in Fig.1.

Measurements were performed using the ballistic method by measuring a charge passed through the galvanometer circuit being excited by the displacement of the along-field directed superconductor from one inductance coil into the other.

$$-4\pi M(H_0) = \frac{CR}{2nS_0(1-k)}L, \quad (1)$$

where C, R, L are the ballistic galvanometer constant ($C = 2\cdot10^{-9}$ K/mm.m), the circuit total resistance ($R = 2\cdot10^3$ Ω) and a galvanometer reading, correspondingly. $n = 3\cdot10^3$ is the number of turns per inductance coil. $S_0 = 0.2$ cm^2 is a sample cross-section area, and $k = 0.14$ is the demagnetisation factor of the sample [1] obtained by taking into account our sample surface $l = 12$ mm length and $R = 0.5$ mm radius values.

It follows from the experimental curve that up to the first critical magnetic field ($H_0 \le H_c = 50$ Oe) $\chi_{ex} = \dfrac{4\pi M(H_0)}{H_0}$ is different from the unity pointing out that an incomplete Meissner effect takes place.

This situation is probably caused by a porosity of the sample and also by such factors as the existence of a nonsuperconductive phase, weak superconductive links between granules and others.

To compare the theory with an experiment quantitatively basing on the modified Bean critical state model, in the frames of which it is not possible to account above mentioned factors, the correction factor

$$\eta = \frac{\chi_{ex}}{\chi_{1d}} = 0.33 \tag{2}$$

was introduced.

The Beam model modification implicates an accounting of the critical current density J_c dependence on a magnetic field taken in our case in the following form:

$$\frac{dB}{dr} = \frac{4\pi}{c} J_c = \frac{\alpha}{B_0^n}\ , \tag{3}$$

where $\dfrac{dB}{dr}$ is the sample induction variation to r coordinate counted along the radius of the centre to the outer surface, α and n are the phenomenological parameters. Integrating of (3) and taking into account the boundary condition:

$$B(R) = H_0 \tag{4}$$

the induction dependence on outer magnetic field H_0 was established in the form:

$$B(r) = [\, H_0^{n+1} - (n+1)\alpha\,(R-r)\,]^{\frac{1}{n+1}} = (a+br)^{\frac{1}{n+1}}, \tag{5}$$

where $a = [\, H_0^{n+1} - \alpha(n+1)]$ and $b = \alpha(n+1)$.

Using (5), sample induction mean value

$$< B > = \frac{2}{R^2} \int \frac{R}{r} B(r) r dr \tag{6}$$

was calculated for different intervals of the outer magnetic field (Fig. 2 a, b) and, correspondingly, $-4\pi M_0 = -(B - H_0)$ magnetization dependence on the outer field:

$$4\pi M_0(H_0) = \eta \begin{cases} \dfrac{2}{R^2}\dfrac{1}{\alpha^2(n+1)}\left[\dfrac{-(n+1)H_0^{2n+3}}{(2n+3)(n+2)} + \dfrac{\alpha(n+1)RH_0^{n+2}}{n+2} + \dfrac{H_{c1}^{n+1}H_0^{n+1}}{n+2} \right. \\ \left. - \dfrac{H_{c_1}^{2n+3}}{2n+3} - \dfrac{\alpha(n+1)RH_{0c_1}^{n+2}}{n+2}\right] - H_0, \quad H_{c1} < H_0 < H_0^* \\ \dfrac{2}{R^2\alpha^2}\left[-\dfrac{H_0^{2n+3}}{(2n+3)(n+2)} + \dfrac{\alpha RH_0^{n+2}}{n+2} + \dfrac{\left[H_0^{n+1} - \alpha(n+1)R\right]^{\frac{2n+3}{n+1}}}{(2n+3)(n+2)}\right] - H_0 \end{cases} \tag{7}$$

$$H_0 > H_0^* \qquad (8)$$

H_0 is the rising magnetic field value at which the vortex front reaches the sample centre for the first time (Fig. 2c)

$$H_0^* = [H_{c_1}^{n+1} + (n+1)\alpha R]^{\frac{1}{n+1}} = 270 \text{ Oe}. \qquad (9)$$

For the evaluation of parameter αR from expressions (7) and (8), the extremum of equation (7) at different n values was found out and corresponding value $H_0 = 150$ Oe for the observed magnetization maximum (29Gs) was taken the extremum point.

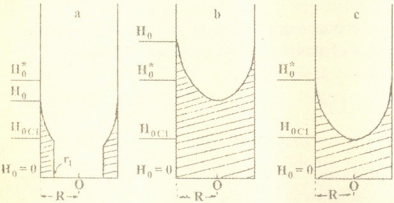

Fig. 2. The vortex distribution profile corresponding to the critical state model:

a) $H_0^* > H_0 > H_{c1}$

b) $H_0 > H_0^*$

c) $H_0 = H_0^*$

By this method for n and αR parameters the optimal values of $n = 0.5$ and $\alpha R = 2750$ Gs$^{1.5}$ (10) were found out.

The $4\pi M(H_0)$ dependence obtained by (7) and (8) taking into account (10) is given by the curve in Fig.1.

A good coincidence of experimental and theoretical results within the error limits (see Fig. 1) show the possibility of using the Bean model for HTSC investigations in the case of rising magnetic fields.

Tbilisi I.Javakhishvili State University

REFERENCES

1. *K.Kikoin.* Tablitsi fizicheskikh velichin, Spravochnik, Moscow, 1976, 1006 (Russian).
2. *C.P.Bean.* Rev. Mod. Phys. **36**, 1964, 31-39.

საქართველოს მეცნიერებათა აკადემიის მოამბე, 158, №1, 1998
BULLETIN OF THE GEORGIAN ACADEMY OF SCIENCES, 158, №1, 1998

PHYSICS

A.Akhalkatsi, G.Mamniashvili

Investigation of NMR Signal Nature in Lithium Ferrite by the Method of Low-Frequency Excitation

Presented by Corr. Member of the Academy T.Sanadze, October 6, 1997

ABSTRACT. **The low-frequency magnetic field excitation method using a modulation of the spin-echo decay envelope as a result of the domain walls oscillation at the sample remagnetization was applied for the multicomponent ^{57}Fe spectrum identification in lithium ferrite. It was experimentally shown that the observed NMR spectrum in lithium ferrite was stipulated by the nuclei located in different magnetically non-equivalent sites.**

Key words: LF magnetic field, NMR, spin-echo.

Observations of the nuclear spin-echo in magnetically ordered crystals in the presence of additional pulsed and low-frequency (LF) magnetic fields of relatively low (considerably less than the demagnetizing field) intensities have revealed effects associated with the anisotropy of hyperfine fields and have made it possible to estimate quantitatively local inhomogeneities as well as the domain wall mobility and have also given a valuable information for the NMR spectrum identification.

In this communication results of the application of the LF magnetic field excitation method for the NMR spectrum nature investigation in lithium ferrite are presented.

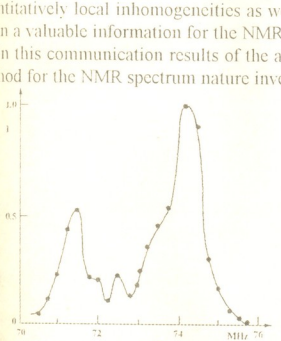

Fig. 1. NMR spectrum of ^{57}Fe in polycrystalline lithium ferrite at T=77 K.

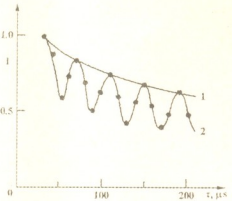

Fig. 2. Decay envelope of spin-echo on the frequency ν_{NMR}=74.4 MHz without (1) and at presence (2) of modulating LF magnetic field with H_m=0.2 Oe and ν_m=27 KHz.

For the first time the LF magnetic field excitation method was applied for the NMR spectrum identification in manganese ferrite [1] to eliminate ambiguities in previous interpretations of the two-component NMR spectrum in manganese ferrite and to separate NMR signals of the nuclei arranged in domain walls (DW) of crystals. The results of this work were lately supported by usual NMR methods [2].

In this method the modulation of the NMR spin-echo decay envelope was used appearing below some threshold value of the exciting radio-frequency (RF) pulses powers as a result of the application of a small demagnetising LF magnetic field to the magnetic material. In this work the methods of [1,3] are used for the investigation of the multicomponent NMR spectrum in lithium ferrite. The work was made by the spin-echo spectrometer described in [4], at T = 77 K.

The spin-echo spectrum of the investigated polycrystalline sample is shown in Fig. 1. As in [5] the spectrum is also multicomponent. In Fig. 2 the spin-echo decay envelope is adduced without and in the presence of modulating LF magnetic field with amplitude $H_m = 0.6$ Oe and frequency $\nu_m = 27$ kHz. Spin-echo amplitude is modulated with period $1/\nu_m$ and has maxima at $\tau_{12} = n/\nu_m$ and minima - at $\tau_{12} = (n + 1/2)/\nu_m$, where n is integer and τ_{12} is a pulse separation.

Fig. 3 represents $A_{min}(H_m)/A_0$ dependence on frequency, where $A_{min}(H_m)$ is minimum of the modulated echo intensity and A_0 is the non-modulated one, measured at the same distance τ_{12} between pulses. H_m and ν_m were maintained constant over the all frequency range and equal to accordingly 0.6 Oe and 27 kHz.

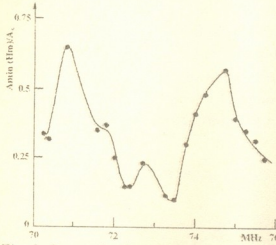

Fig. 3. Spectral dependence of modulation depth $A_{min}(H_m)/A_0$ at H_m=0.6 Oe and ν_m=27 kHz.

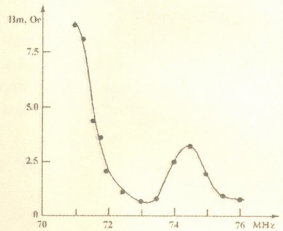

Fig. 4. Spectral distribution of Hm corresponding to the modulation depth ~0.1.

Maximal modulation in lithium ferrite was being observed at NMR frequency 73.5 mHz. In contrast to the modulation spectrum of hexagonal Co [3], the modulation spectrum in lithium ferrite, as it is obvious from Fig. 3, shows an additional structure, connected with presence of 4 magneto-nonequivalent positions of ^{57}Fe nuclei. The echo amplitude modulation, in contrast to work [1], is being over all the experimentally available range of RF powers in the whole of NMR spectrum. Moreover, selecting H_m, it is easy to obtain 100%-modulation of echo amplitude. The frequency distribution H_m, corresponding to the modulation depth ~ 0.1, is shown in Fig. 4.

The presence of 100%-modulation in the whole of NMR spectrum over the all experimentally available range of RF powers allows to suppose, that the echo signal is formed by nuclei, located in the domain walls. This conclusion coincides with analogous one [6] drawn on the basis of the investigation of RF field gain η in lithium ferrite.

It should be pointed out that accordingly to the interpretation of [1] the minimal modulation effect (maxima of the spectrum in Fig.3) corresponds to the DW centers

and the maximal one to the DW edges (minima in Fig.3).

This conclusion is in accordance with the echo signal dependence for the two NMR spectrum maxima on the external static magnetic field, which was similar to the corresponding dependencies for the DW nuclei in manganese ferrite [2].

As it is seen from results of work [4], the reduction effect of the echo signal in lithium ferrite at the LF excitation is considerably stronger than the similar one for cobalt. Besides this, the effective spin-echo decay constant measurement in the presence of the LF field shows a considerable decrease of the effective transverse relaxation time T_2 in lithium ferrite, in the difference to cobalt.

Apparently, the observed effect is similar to the one of [7], where the effective transverse relaxation time decrease was found with increasing amplitude of the LF field H_m in magnetic media. There was shown, that this effect was due to the motion of the micromagnetic structure of the specimen and to a nonuniform variation in the nuclear spin precession frequency. In cobalt similar effect is considerably less manifested in the range of H_m amplitudes used by us.

In connection with this, we may expect that in lithium ferrite the additional echo decay envelope modulation mechanisms related with the domain wall motion may be important. One of these contributions is connected with the situation, when a significant part of nuclei, excited by the first RF pulse, is removed from the domain wall during time τ_{12} before the second RF pulse, and the other one is caused by the RF field enhancement factor η variation over the DW.

Really, an assessment of the lithium ferrite hyperfine field anisotropic component H_a in frames of the model [3], where the main contribution in the modulation effect was connected with the LF field enhancement effect caused by the anisotropic contribution to the hyperfine field as the DW motion shifts the effective position of the nuclei is not in agreement with the available H_a data for lithium ferrite.

Finally, on the basis of the experimental results, it is possible to make the conclusion that the observed NMR spectrum of lithium ferrite is stipulated by the nuclei arranged in the domain walls and located in different magnetically non-equivalent sites.

Besides this, for a correct evaluation of the spin-echo decay envelope modulation effect it is necessary to take into account the additional modulation effects caused by the domain walls motion in addition to the contribution related with the hyperfine field anisotropic component.

This work was supported by the Georgian Academy of Sciences, Grant #2.12.

Institute of Physics
Georgian Academy of Sciences

Tbilisi I.Javakhishvili State University

REFERENCES

1. *G.I.Mamniashvili, V.P.Chekmarev*. Bull. Acad. Sci. GSSR, **100**, 3, 1980, 573-576 (Georgian).
2. *V.P.Chekmarev, I.S.Barash*. FTT, **29**, 1, 1987, 3479-3484 (Russian).
3. *C.V.Searle, H.P.Kunkel, S.Kupca, I.Maartense*. Phys. Rev. B, **15**, 3, 1977, 3303-3308.
4. *A.M.Akhalkatsi, G.I.Mamniashvili*. FMM, **81**, 6, 1996, 79-83 (Russian).
5. *V.D.Doroshev, N.M.Kovtun, V.H.Seleznev*. FTT, **13**, 3, 1971, 1098-1100 (Georgian).
6. *T.V.Gvalia*. Avtor. kand. diss. Tbilisi, 1988, 150 (Georgian).
7. *N.V.Baksheev, V.M.Loginov, E.S.Mushailov, V.I.Tsifrinovich*. JETP, **58**, 3, 1983, 559-561 (Russian).

საქართველოს მეცნიერებათა აკადემიის მოამბე, 158, №1, 1998
BULLETIN OF THE GEORGIAN ACADEMY OF SCIENCES, 158, №1, 1998

PHYSICS

Academician N.Amaglobeli, L.Abesalashvili, B.Chiladze, V.Kartvelishvili, M.Kopadze, R.Kvatadze, N.Lomidze, G.Nikobadze, T.Pitskhelauri, R.Shanidze

Study of $K_S^0 K_S^0$ Interference Correlations in Neutron-Carbon Interactions

Presented June 18, 1998

ABSTRACT. **Bose-Einstein correlations in $K_S^0 K_S^0$ pairs have been studied in neutron-carbon interactions measured with the EXCHARM detector. The measured values for the strength of the correlations and the radius of the K_S^0 emitting source are: $\lambda = 1.13 \pm 0.34 \pm 0.34$ and $R = 1.01 \pm 0.13 \pm 0.18$ fm.**

Key words: correlations, particle.

The Bose-Einstein effect corresponds to an enhancement in the production probability of identical bosons to be emitted with small relative moment, as compared to non-identical particles under otherwise similar conditions. Experimental data are usually analysed in terms of the correlation function defined as the ratio of the two-particle probability density to the product of the corresponding single particle quantities:

$$C(p_1, p_2) = \frac{P(p_1, p_2)}{P(p_1)P(p_2)}, \qquad (1)$$

where p_i is the four-momentum of particle i. For a Gaussian space-time distribution of the particle source, the correlation function takes the form:

$$C(Q) = N(1 + \lambda \exp(-R^2Q^2)), \qquad (2)$$

where Q is the four-momentum difference, $Q^2 = -(p_1 - p_2)^2$ and N is the normalization factor. The parameter λ, known as the incoherence parameter, takes into account the fact that for various reasons, the strength of the correlations can be reduced and R is the radius of the source.

Bose-Einstein correlations have been observed in like-sign charged pion-pairs for reactions with different types of initial state and over a wide energy range [1]. However, only few studies have been reported on interference effects in charged [2-5] and neutral kaon-pairs [6-10]. For charged pion or kaon final states the identical boson-pair system is guaranteed by the requirement of the same charge sign. $K_S^0 K_S^0$ pairs may come either from identical $K^0K^0, \overline{K}^0\ \overline{K}^0$ pairs or from non-identical $K^0\overline{K}^0$ boson-antiboson systems.

In the case of K^0K^0 and $\overline{K}^0\ \overline{K}^0$ decays, the $K_S^0 K_S^0$ pair is originated from an identical boson pair which should show the Bose-Einstein correlation effect. This is not the case when $K_S^0 K_S^0$ pair comes from $K^0\overline{K}^0$ system. However, the $K^0\overline{K}^0$ system is an eigenstate of the charge conjugation operator C with two possible eigenvalues $C = +1$ and $C = -1$. The probability amplitude for a given eigenstate C can be written [11] as follows:

$$\left|K^0;\overline{K}^0\right\rangle_{C=\pm 1} = \frac{1}{\sqrt{2}}\left(\left|K^0(\vec{p});\overline{K}^0(-\vec{p})\right\rangle \pm \left|\overline{K}^0(\vec{p});K^0(-\vec{p})\right\rangle\right) \qquad (3)$$

where $\vec{p}$ is the three momentum of the kaon defined in the $K^0\overline{K}^0$ centre of mass system. In the limit of $|\vec{p}| = 0$ ($Q = 0$), the probability amplitude for the $K_S^0 K_L^0$ pair ($C = -1$ state) disappears and for the $K_S^0 K_S^0$ or $K_L^0 K_L^0$ pair ($C = +1$ state) is maximal. This should lead to a Bose-Einstein correlations like enhancement in the probability to detect $K_S^0 K_S^0$ and $K_L^0 K_L^0$ pairs at low Q values, however this enhancement is exactly compensated by the depletion of $K_S^0 K_L^0$ pairs in the same range of Q. Hence, if all the possible final states of the $K^0\overline{K}^0$ system were detected no Bose-Einstein correlation effects would be observed, as expected for boson-antiboson system.

This study is based on the sample of neutron-carbon interactions collected with the EXCHARM detector. The detailed description of the EXCHARM detector can be found elsewhere [12]. The neutron beam energy was ranged from 20 to 70 GeV with the mean value of about 50 GeV. Contribution from $\bar{n}$, γ and K_L^0 was less than 1%.

The present analysis was carried out with $1.8 \cdot 10^8$ neutron-carbon interaction events with charged particle multiplicity greater than four. The K_S^0 mesons are detected by their decay into $\pi^+\pi^-$ pair. Such decays are normally separated in space from primary vertex. Candidates for secondary decays were found by pairing all tracks of opposite charge. The vertex of each pair was determined by minimizing the χ^2 obtained from the distance of the vertex to the extrapolated tracks. In order to reduce background from secondary interactions in the target region the distance along the beam direction between the edge of the target and the decay vertex of K_S^0 candidate had to be larger than 12 cm. These cuts reject also K_S^0 candidates with common tracks. Additional cuts were made to reduce background from misidentified Λ hyperons and photon conversions.

On the basis of these criteria about 9500 events of two K_S^0 or more were selected for the further analysis. The mass distribution of the reconstructed K_S^0 decays for events with two or more K_S^0 candidates is shown in Fig. 1a. The distribution was fitted with a curve of Gaussian shape plus a polynomial expression for the background. The obtained value of the K^0 mass is 497.56 ± 0.04 MeV/c^2. The quoted error is statistical only. The small difference between the measured K^0 mass and the world average value [13] can be explained by the uncertainty in the magnetic field of EXCHARM detector. The obtained width of $\sigma = 3.71 \pm 0.05$ MeV/c^2, corresponds to the experimental mass resolution. The background in an interval ± 10 MeV/c^2 around the peak mass is 13%.

In order to take into account the background in the invariant mass distribution of $K_S^0 K_S^0$ pairs the following procedure was used. For each $K_S^0 K_S^0$ pair the absolute values of the differences between the invariant mass of the K_S^0 candidate and the world ave-

rage value of the mass (Δm_1, Δm_2) were computed. The invariant mass distribution of $K_S^0 K_S^0$ pairs from the signal region Δm_1, $\Delta m_2 < 10$ MeV/c^2 can be originated from four different sources:

$$(S_1 + B_1)(S_2 + B_2) = S_1S_2 + S_1B_2 + B_1S_2 + B_1B_2; \quad (4)$$

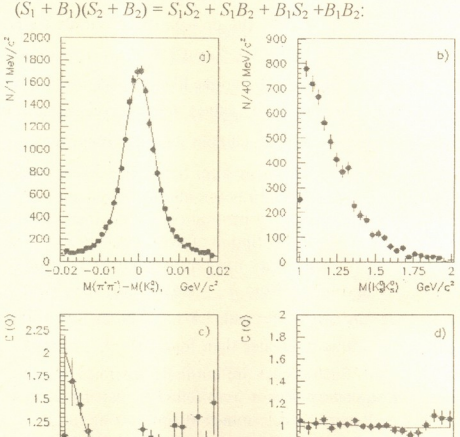

Fig. **a)** The $\pi^+\pi^-$ invariant mass distribution of the K_S^0 candidates; **b)** The invariant mass distribution of the $K_S^0 K_S^0$ pairs; **c)** The measured correlation function for $K_S^0 K_S^0$ pairs. The solid line represents the fit to the data using eq.(2); **d)** The correlation function $C(Q)$ for ΛK_S^0 pairs. The results of the fit is shown by solid line

To estimate the S_1B_2 and B_1S_2 contributions we have used the invariant mass distributions of kaon pairs, when one of K_S^0 candidate is from the signal and another from the background 10 MeV/c^2 < Δm_1, Δm_2 < 20 MeV/c^2 region $(S_1 + B_1)B_2'$ and $B_1'(S_2 + B_2)$. The $B_1'B_2'$ distribution was constructed by using both K_S^0 candidates from the background region. In our case the distributions $(S_1 + B_1)B_2'$ and $B_1'(S_2 + B_2)$ are the same and the invariant mass distribution for $K_S^0 K_S^0$ pairs was obtained

$$S_1S_2 = (S_1 + B_1)(S_2 + B_2) + \alpha_1(S_1 + B_1)B_2' + \alpha_2B_1'B_2', \quad (5)$$

where the values of the parameters α_1 and α_2 are evaluated from the fit of the invariant mass spectra of $\pi^+\pi^-$ pairs of K_S^0 candidates.

Figure 1b shows the invariant mass distribution of $K_S^0 K_S^0$ pairs. This distribution reaches maximum near the threshold and decreases smoothly as mass increases. No indication is seen for the presence of the resonance decays into the $K^0\overline{K}^0$ pairs. It should be mentioned, that there are two low mass resonances $f_0(980)$ and $a_0(980)$ below the $K^0\overline{K}^0$ threshold. To estimate this contribution one requires the knowledge of their production cross-sections in neutron-carbon interactions, decay branching fraction of these states to $K^0\overline{K}^0$ and the $K_S^0 K_S^0$ mass spectra from these decays above the threshold. Unfortunately, these factors are not known with sufficient accuracy. However, it was shown, that in e^+e^- annihilation at Z peak the strength of correlation effect λ is reduced only by about 15% and the radius of emitting source R is less than 10%, when $f_0(980)$ decays are included in the analysis [9].

To construct the correlation function it is necessary to obtain reference sample, which should simulate all aspects of the data except Bose-Einstein effects. For these reasons the reference sample has been obtained using the event mixing method.

The correlation function $C(Q)$ for the $K_S^0 K_S^0$ pairs is shown in Fig. 1c. The clear enhancement is seen in low Q region. The resolution in Q is of the order of 20 MeV and much less than the chosen bin size. The correlation function was fitted by the expression (2) in the range of $0 \le Q \le 1.6$ GeV. The reference sample was normalized to the number of $K_S^0 K_S^0$ pairs in the data within the interval of $0.5 \le Q \le 1.6$ GeV. The obtained results are presented in Table 1. To examine the method of reference sample construction, the same procedure was used for ΛK_S^0 pairs. The correlation function for these pairs is equal to one, as expected for non-identical pairs (Fig. 1d).

Table 1

The fitted values of the correlation function $C(Q)$ parameters λ and R for different selection criteria and fit conditions.

Conditions	λ	R fm	χ^2/DOF
reference fit	1.13 ± 0.34	1.01 ± 0.13	24/17
ΛK_S^0 pairs	0.05 ± 0.03	0.30 ± 0.12	19/17
2 parameter fit	1.12 ± 0.35	1.05 ± 0.13	26/17
4 parameter fit	1.36 ± 0.36	0.85 ± 0.12	18/16
$Q < 1.1$ Mev	1.13 ± 0.34	0.99 ± 0.13	15/11
K_S^0 mass range $\pm$ 15 MeV/c^2	1.05 ± 0.38	0.98 ± 0.13	24/17
K_S^0 selection +10%	1.31 ± 0.30	1.00 ± 0.10	32/17
K_S^0 selection -10%	1.01 ± 0.47	0.99 ± 0.15	17/17

To evaluate the systematic errors connected with the choice of fitted function and the range of normalization, the normalization parameter N in eq. (2) was set to one and

the range of influence of the $f_2'(1525)$ resonance production was excluded from the fit. To take into account the rise of the correlation function at large Q values due to long range two-particle correlations $C(Q)$ distribution was fitted with the function $C(Q) = N(1 + \lambda \exp(-R^2Q^2))(1 + \delta Q)$. Finally, the dependence of our results on the choice of signal and background intervals for K_S^0 candidates has been estimated. The results of these fits are presented in Table 1.

We have estimated the systematic uncertainties connected with the K_S^0 selection criteria. The analysis was repeated with modified selection criteria within the range ±10%. The total systematic error, connected with the choice of reference sample, with variation of the fit conditions and selection criteria, was found by adding in quadrature the deviations from the reference fit.

Table 2

Values of strength of correlations λ and emitting source radius R for neutral kaons obtained in different experiments.

Reaction	ref	variable	λ	R fm
$p\bar{p}$	[7]	q_t, q_0		0,9 ± 0,2
e^+e	[8]	Q	1.14 ± 0.23 ± 0.32	0.76 ± 0.10 ± 0.11
e^+e	[9]	Q	0.61 ± 0.16 ± 0.16	0.55 ± 0.08 ± 0.12
e^+e	[10]	Q	0.96 ± 0.21 ± 0.40	0.65 ± 0.07 ± 0.15
$n-C$	this study	Q	1.13 ± 0.34 ± 0.34	1.01 ± 0.13 ± 0.18

Table 2 presents our values of λ and R parameters together with the results obtained in $p\bar{p}$ and e^+e^- interactions. It should be mentioned that results in $p\bar{p}$ collisions are obtained using the variables q_t, q_0 (q_t is the component of momentum difference $\vec{p}_1 - \vec{p}_2$ perpendicular to $\vec{p}_1 + \vec{p}_2$ and q_0 is the difference of energies [14]) which yields to the higher values of R compared to Q variable analysis. In this experiment the value of the strength of correlation function was not extracted. In e^+e^- annihilation at Z peak the Bose-Einstein correlations of neutral kaons were studied in three experiments using reference sample derived from JETSET Monte Carlo events. This makes comparison of results obtained in different experiments difficult, however all data are consistent with the assumption that Bose-Einstein like correlation exists not only for $K_S^0 K_S^0$ pairs coming from identical K^0K^0 or $\bar{K}^0\bar{K}^0$ systems, but also for ones from non-identical $K^0\bar{K}^0$ systems.

We would like to thank EXCHARM Collaboration for providing experimental data. It is a pleasure to thank R.Müller for useful discussions.

High Energy Physics Institute,
Tbilisi I.Javakhisvvili State University

REFERENCES

1. *B.Lorstad.* Int. J. Mod. Phys. A4, 1989, 2891.
2. *T.Akesson et al.* Phys. Lett., B155, 1985, 128.
3. *M.Aguilar-Benitez et al.* Z. Phys., C54, 1992, 21.

4. *Y.Akiba et al.* Phys. Rev. Lett., 70, 1993, 1057.
5. *H.Beker et al.* Z. Phys., C64, 1994, 209.
6. *D.Bertrand et al.* Nucl. Phys., B128, 1977, 365.
7. *A.M.Cooper et al.* Nucl. Phys., B139, 1978, 45.
8. *P.D.Acton et al.* Phys. Lett., B298, 1993, 456;
9. *P.Abreu et al.* Phys. Lett., B323, 1994, 242; CERN-PPE/96-54.
10. *D.Buskulic et al.* Z. Phys., C64, 1994, 361.
11. *H.Lipkin.* Phys. Lett., B219, 1989, 474; Phys. Rev. Lett., 69, 1992, 3700.
12. *A.N.Aleev et al.* JINR rapid communication 3, [77], 1996, 32.
13. *R.M.Barnett et al.* Review of Particle Physics, Phys. Rev., D54, 1996, 1.
14. *G.I.Kopylov, M.I.Podgoretskii.* Sov. J. Nucl. Phys., 18, 1973, 336; 15, 1974, 219.

N.Dolidze, G.Eristavi, Z.Jibuti, G.Narsia, K.Kasparyan, L.Koptonashvili

Investigation of Small Dose Radiation Stimulated Processes in Semiconductor Materials and Structures

Presented by Corr. Member of the Academy T.Sanadze, February 16, 1998

ABSTRACT. **The paper presents the results of investigations of influence of radiation-thermal treatment (RTT) on the properties of semiconductors and structures based on them (Si, GaAs, GaAlAs, GaP). After RTT the crystal is cleaned of native ("genetic") defects, the degree of homogeneity of lattice increases and electrophysical and optical properties of the semiconductor materials and structures improve ("small dose effect"). The processes taking place during the RTT are discussed and the perspectivity of the method in practice is shown.**

Key words: radiation, annealing, homogeneity, healing of native defects.

As early as 1970's, in investigation of the radiation influence on semiconductors and structures it was revealed that after irradiation with relatively small radiation doses (accelerated electrons, γ-quantum) followed by thermal annealing return radiation degradation effect takes place: lifetime, mobility and concentration of free carriers, crystal lattice homogeneity are increased, parameters of semiconductor devices are improved ("small dose effect") [1-5]. However, this effect is poorly investigated since it depends on many factors, such as type, energy and intensity of irradiating particles, irradiation and annealing temperature, initial defectivity of a semiconductor, etc.

This paper presents the results of experimental investigations of radiation-thermal treatment (RTT) influence on the properties of semiconductors and structures based on them (Si, GaAs, GaAlAs, GaP). Irradiation by $2 \div 4$ MeV electrons was carried out at room temperature, the fluence being $10^{12} \div 10^{14}$ cm^{-2}. The irradiated samples were annealed thermally ($T = 400 \div 670$ K).

For studying the influence of "small dose effect" on silicon epitaxial structures used in semiconductor electronics (КЭФ-0.7) the maps of sheet resistivity distribution throughout the surface before and after RTT were taken (33 points). The sheet resistivity value across the area on the starting wafer varied within the range 0.56÷0.80 Ohm·cm, i.e. 0.68 ± 0.12 Ohm·cm, which means deviation from the average value by 18%. After the RTT process was carried out, there occurred value equalization of the given parameter across the wafer and the deviation from the average value was ~ 5% (0.64 ± 0.03 Ohm·cm). On the basis of this investigation the regimes of the RTT process were determined for epitaxial Si and tested in the production of a pilot lot of various types of integrated circuits (ICs) of the K555/533 series (STTL). The RTT application resulted in an increase of ICs percentage yield by $4 \div 6$ % (then the factual ICs percentage yield under production conditions depending on type was $35 \div 55$%).

The cause of the positive influence of RTT was clearly shown during the visual observation on the dislocation wells on the surface of the wafer epitaxial structures Si and GaAs (thickness 10÷16μm). As is seen from Fig.(a), before RTT areas with strong

accumulation of different size disturbances are revealed on the surface of the GaAs wafer. After RTT most of the disturbances disappear. Exclusion makes big disturbances only which might be drains for simple defects forming small disturbances. Similar picture is obtain in Si.

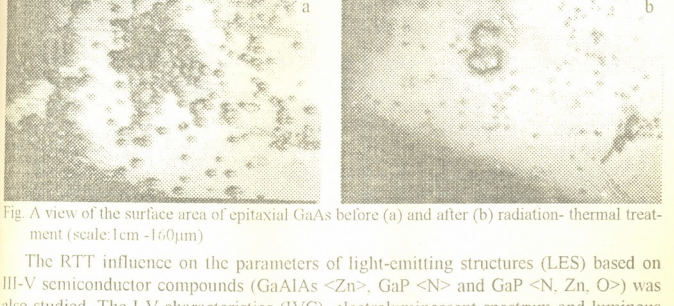

Fig. A view of the surface area of epitaxial GaAs before (a) and after (b) radiation- thermal treatment (scale:1cm -160μm)

The RTT influence on the parameters of light-emitting structures (LES) based on III-V semiconductor compounds (GaAlAs <Zn>, GaP <N> and GaP <N, Zn, O>) was also studied. The I-V characteristics (IVC), electroluminescent spectrum and luminous intensity at a given value of direct forward current (10mA) of light-emitting diodes (LED's) made of this structures have been measured before and after irradiation and after consequent annealing. Two groups of each chip type (20-25 diodes), the first with a luminous intensity twice different from the second, were selected.

The investigations have shown that after RTT only the band intensity changed. Its shape and position (or location) on the spectrum remain unchanged. The IVC's are also unchanged i.e. injection coefficients. A marked increase in the luminous intensity is observed directly after irradiation (Table). Here this effect is more pronounced in the first group of samples. The Table lists the optimal annealing temperatures, further increase of which decreases the luminous intensity.

To explain the above-mentioned experiments we will deal with light-emission mechanisms in particular structures: red emission in GaAlAs<Zn> is a result of electrons transition from the conduction band on the valence band and level of zinc. GaP <N> green emission is formed during the exciton annihilation which is created on the nitrogen isoelectronic captures (N_P), but yellow emission in GaP<N, Zn, O> is formed by definite proportion blend of green and red emission ,where the red emission is result of the exciton annihilation on the captured the isoelectronic molecules (Zn_{Ga}-O_P). The concentration of emission recombination centers in active sections of LED's is ~ 10^{18} cm^{-3} [5]. If one even assumes that radiation defects (RD) play a role of emission centers, the integrated fluxes and thus the RD concentrations are so small that they are incapable to change significantly the concentration of emission recombination centers of the crystals under investigation. Hence, it could be suggested that the effect observed is due to a decrease of the concentration of nonemission recombination centers. It is well-known [5] that the nonemission or infrared emission recombination centers with

deep-levels in the structures under investigation (dislocations, precipitates of impurity atoms, complexes involving vacancies) have capture sections that exceed the section of main emission centers with shallow-levels by several orders of magnitude. Therefore low integral radiation fluxes turned out to be effective.

Table

The results of the investigation of the RTT effect on LED's

Emission structure type	I_0,mcd	Φ,cm^{-2}	$\Delta I_\Phi/I_0$,%	T,K	$\Delta I_T/I_0$, %
GaAlAs<Zn>	0.6	$4\cdot10^{12}$	43	420	30
	0.7	$8\cdot10^{12}$	15	520	55
(RED)	1.2	$4\cdot10^{12}$	12	520	37
	1.3	$1\cdot10^{13}$	-10	420	0
GaP<N>	0.15	$4\cdot10^{12}$	50	420	70
	0.15	$1\cdot10^{13}$	15	420	7
(GREEN)	0.30	$4\cdot10^{12}$	10	420	33
	0.30	$8\cdot10^{12}$	-30	420	-20
GaP<N, Zn, O>	0.15	$4\cdot10^{12}$	42	420	65
	0.15	$1\cdot10^{13}$	20	420	0
(YELLOW)	0.30	$4\cdot10^{12}$	10	420	35
	0.30	$8\cdot10^{12}$	-25	420	-20

I_0,I_Φ,I_T are LED's emission intensities before and after irradiation and after annealing.

Under irradiation of the crystal with high-energy particles two processes take place: accumulation of RD (the crystal transfer into more inequilibrium state) and a stimulation of the reaction of healing the native ("genetic") defects (the crystal tend to equilibrium). At the beginning of small-dose irradiation when the concentration of created radiation defects is small and interaction with native defects prevails over the interaction with each other healing crystal native defects takes place. At RTT this process proceeds in two stages: the first stage takes place during irradiation when the mobile components of Frenkel pairs, in the radiation stimulated diffusion process meeting and healing of native defects of the crystal. The second stage occurs at subsequent annealing when diffusion takes place and simultaneously with healing (annihilation) the accumulation of elementary defects forming native disturbances takes place on the drains. Since temperatures at RTT ($T \leq 670K$) are much lower than those in the crystal growth technology, the crystal remains in a more ordered state after RTT.

Thus, we have shown that by relatively low temperature radiation stimulated processes the homogeneity of crystal lattice can be increased and successfully applied in the technology of semiconductor materials, devices and ICs.

Tbilisi I.Javakhishvili State University

REFERENCES

1. *M.N.Abuladze, et al.* Fiz. Tekh. Poluprov., **8**, 4, 1974, 792 (Russian).
2. *N.P.Chernov, A.P.Mamontov.* Fiz. Tekh. Poluprov., **14**, 11, 1980, 2271 (Russian).
3. *V.V.Bolotov, V.A.Korotchenko.* Fiz. Tekh. Poluprov., **14**, 11, 1980, 2257 (Russian).
4. *R.V.Konakova, et al.* El. tekh., ser. 2. Poluprov. prib., **193**, 2, 1988, 47 (Russian).
5. *A.A.Bergh, P.J.Dean.* Light-emitting diodes, Oxford, 1976.

G.Erkomaishvili, I.Shatberashvili, M.Tsitskishvili

Dynamics of the Annual Changes of Atmosphere's Self - Rectification

Presented by Academician B.Balavadze, March 11, 1998

ABSTRACT. **The results of lasting experimental investigations of geoecological, integral parameter, velocities of self-rectification of the lower atmosphere, which were defined as the ratio of the density of the admixture's stream of the ground surface to the pre-ground concentration of the same admixture are considered in the article.**

The analysis of annual changes for 7 different regions with different climatic conditions is given. Annual changes connected with the characteristic of atmosphere's sediments are analysed. The climatic stability of the parameter is presented.

Key words: atmosphere, self-rectification.

The solid or liquid microscopic particles, suspended in atmosphere, differ from pre-ground atmospheric dust, having long "life" time in atmosphere. These particles constitute atmospheric aerosols. Their chemical and dispersive composition has a wide range of changeability. Recently a lot of researches have been dedicated to the study of physico - chemical qualities of atmospheric aerosols. It was conditioned by climatic and ecological great significance. The results of research of atmospheric aerosols are summarized in many well-known monographs. The research results of atmospheric aerosolic component for Transcaucasia are summarized in our work [1-3]. Here, also, was showed the "climatic stability" of atmosphere's lower layer self-rectification's velocity. The methodology of its experimental definition became possible after the determination of simple gauzed manifold catching effectiveness which is used widely in Georgian hydromet. network; i.e. the effectivity of atmospheric sediment collectors [4].

In the process of theoretical analysis, we have found the total index for the atmospheric aerosol-summary and β-radioactivity. That gives us the possibility to learn integrally the dynamics of atmospheric self-rectification for various aerosols, which are different in dispersion and composition. We defined average velocities of self-rectification for the lower troposphere in months for big towns of the Volga region and the Caucasia. Daily data about sediments, which were collected during 10 years by gauzed manifolds on the surface of ground were worked out in approximately fourty thousands of measurements and the same measurement about aerosol's concentration in the pre-ground layer. The simple analysis of the measurement shows, that any relation of the stream's admixture to its concentration is the velocity. The physical essence of this velocity is: in the given unity of time, given corpulence of lower layer of atmosphere is completely cleared from the aerosol.

In the Table, there are given the quantities of atmosphere's lower layer's self-rectification, which we have got of experimental study. The formation of aerosol's sediment is made by its washing by the sedimentation or the atmospheric turbulence. As a result of many theoretical and practical works, the distinctive quantities of self-rectification are evaluated. It is clear, that minimum velocities coincide with "dry sediments", and maximum values with the annual maximum of solid sediments (snow), when atmosphere becomes more clear, than in unsedimentary days.

The measurements of quantities in the Table are obtained through the elementary transformation: if we take the stream of any admixture towards the surface of the ground as the quantity's stream (M) on the area of surface (S) in the time interval (t), as its relation to the concentration of the same stream (M/V, where $V = SL$ is the volume, L - length), we shall get velocity:

$$v = \frac{M}{S \cdot t} : \frac{M}{V} = \frac{L}{t}$$

Table

Velocities of atmosphere's self-rectification (km/24 - hour period)

Months	Towns							Av. annual change
	Volgograd	Astrakhan	Rostov	Sukhumi	Tbilisi	Baku	Yerevan	
January	4.74	3.88	2.48	2.11	0.76	4.80	2.43	3.02
February	1.73	1.94	1.76	2.20	0.68	2.13	1.55	1.00
March	1.97	1.86	2.04	2.64	0.84	1.67	1.73	1.82
April	1.44	2.14	2.00	2.50	0.73	1.52	1.13	1.64
May	1.46	1.48	1.32	1.89	0.63	1.00	1.24	1.29
June	0.83	0.78	1.13	2.19	0.54	0.91	0.75	1.02
July	0.73	1.04	0.74	1.96	0.40	0.59	0.85	0.90
August	1.31	1.01	1.65	2.25	1.01	1.18	1.08	1.36
September	1.70	2.02	1.63	2.32	1.00	1.54	1.17	1.63
October	2.39	3.42	2.67	2.31	0.87	3.74	1.74	2.45
November	3.66	3.54	4.26	1.98	1.02	3.79	2.20	2.92
December	4.22	6.07	3.36	2.50	1.24	4.72	2.59	3.53
Av. lasting	2.18	2.43	2.09	2.24	0.81	2.47	1.54	

The geophysical essence of obtained characteristics is:

- It comes out, that seaside regions are characterized by high velocities of self-rectification, compared with regions, which are far from the sea (Tbilisi, Yerevan, Rostov).
- Conventionally, we can say, that for the given region there are "three types" (groups) of atmosphere's self - rectification according to the following gradation: continental (Tbilisi, Yerevan) with velocities up to 1.5; transitional up to 2.0 (Rostov); and seaside (Volgograd, Astrakhan, Sukhumi, Baku), where velocities exceed 2.4.

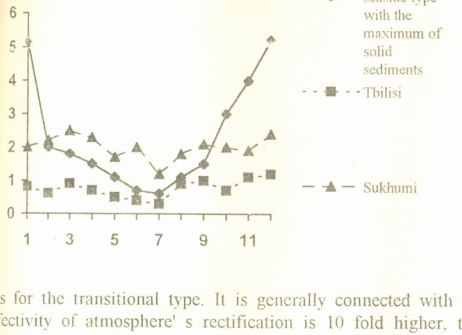

For the real estimation of the results, we analysed the annual changes of these indices. It is interesting, that seaside towns (1 type) are characterized by identical annual changes, with the defined maximum in winter and minimum in summer. Approximately, we have such kind of annual changes for the transitional type. It is generally connected with solid sediments, whose effectivity of atmosphere' s rectification is 10 fold higher, than for unsedimentary weather and it is quite clear. It is supposed for those points where there is a high number of dry sediments, the annual changes should not be so noticeable. Good example for this is Sukhumi (Fig.). The fact of the influence of atmosphere's self - rectification is completely clear on the example of Tbilisi. Here, during the annual change, secondary maximum is noticeable for the warm season, which can be compared with winter's maximum, which is explained by the few number of wintry sediments for Tbilisi and summer maximum of sediments in the annual changes.

The working of huge number of experimental information gave us the possibility to introduce the climatic parameter - the velocity of atmosphere self - rectification. It's noticeable, that this parameter is stable and doesn't change in time [5]. So it is effective for regional regulation and regional division and, in the mean time, it is very important in the sphere of planning measures for the protection the environment from the pollution and establishing a quota and regulating of atmospheric pollution.

Tbilisi I.Javakhishvili State University

REFERENCES

1. *M.Tsitskishvili.* Series Geophysics, **2**, 1987, 52 (Russian).
2. *M.Tsitskishvili, G.Erkomaishvili, M.Nozadze, N.Tsitskishvili.* Atmospheric aerosols in Transcaucasia: dispersive composition and distribution. Tbilisi, 1993, 31, (deposit manuscript).
3. *M.Tsitskishvili, I.Shatberashvili, M.Nozadze, G.Erkomaishvili, R.Diasamidze, L.Kartveli-shvili.* The vertical and horizontal distribution of atmospheric aerosols, influenced by the relief and urbanization. Tbilisi, 1993, 33, (deposit manuscript). (Georgian).
4. *M.Tsitskishvili, I.Shatberashvili, G.Erkomaishvili, M.Nozadze, N.Tsitskishvili, L.Kartveli-shvili.* The effectivity of investigation of gauzed manifolds "catching factor" in Transcaucasia. Tbilisi, 1995, 40 (deposit manuscript) (Georgian).
5. *M.Tsitskishvili.* The investigation of atmosphere's self - rectification with the radioactive aerosols. Abstracts of International Conference. 1975, 150 - 156, (Russian).

საქართველოს მეცნიერებათა აკადემიის მოამბე, 158, №1, 1998
BULLETIN OF THE GEORGIAN ACADEMY OF SCIENCES, 158, №1, 1998

GEOPHYSICS

E.Sakvarelidze, N.Mamulia, A.Goderdzishvili

Estimation of the Radiogenetic Heat Flow for the Trans-Caucasian Territory

Presented by Academician B.Balavadze, October 1, 1997

ABSTRACT. **Radiogenetic heat flow has been calculated for the Trans-Caucasian territory. The maps of radiogenetic heat flow distribution have been drawn up for sedimentary cover, granite and basalt layers and for the whole crust as well (for the given territory).**

Key words: radiogenetic flow, heat generation.

Geothermal flow is a unique energetical characteristic of bowels of the Earth, which is measured experimentally at the Earth's surface. Its variations are caused by global geotectonical factors and a lot of local factors as well [1,2]. Correlation of the heat flow with the other geophysical fields has been established. Investigation of the heat flow distribution is directly connected with the problems of the Earth's heat regime, particularly to the deep temperature distribution in the crust and in the mantle.

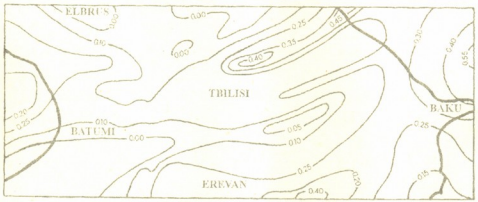

Fig.1. The radiogenetic flow of sedimentary cover

The integrated value of observed heat flow at the Earth's surface has been considered as the sum of the crust and mantle components. The part of the heat flow, formed in the crust is the radiogenetic heat flow, because here the heat generation occurs by radiogenetic heat of existing radioactive elements: ^{238}U, ^{235}U, ^{232}Th, ^{40}K. Calculations of radiogenetic heat flow in the crust have been made for various crust models with assumption that the total heat generation A is a constant in each crust layer. The radiogenetic flow is calculated as AxH product for each layer with thickness H. For three-layer crust, the integrated radiogenetic flow will be

$$q = A_1H_1 + A_2H_2 + A_3H_3,$$

where the indexes 1,2 and 3 correspond to sedimentary, granite and basalt layer respectively.

In the paper, the results of calculations of radiogenetic flow in crust and in its consisting layers are given for the Trans-Caucasian ter-

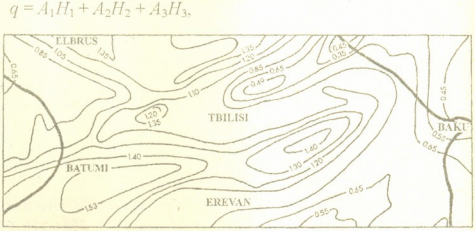

Fig.2. The radiogenetic flow of the granite layer

ritory. In our calculations, the value of heat generation for each layer has been taken from [3] and the construction of investigating crust territory has been taken from [4].

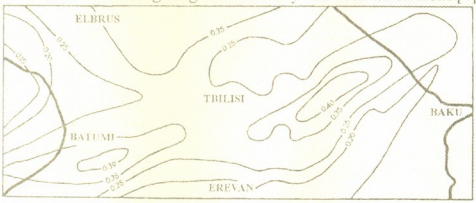

Fig.3. The radiogenetic flow of the basalt layer

The results of calculations are given in Figs. 1-4 as the maps of isolines of heat generation (values of flow are given in cal/cm^2.sec), which give good information about radiogenetic flow distribution for the territory under investigation in the crust. The obtained results can be used in calculation of the deep temperature in the crust.

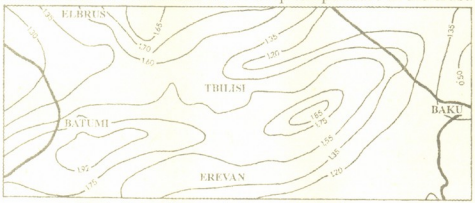

Fig.4. The radiogenetic flow of the Earth's crust

Tbilisi I.Javakhishvili State University

REFERENCES

1. *E.A.Lubimova.* Termika Zemli i Luny. Moskva, 1968 (Russian).
2. *E.A.Sakvarelidze.* Geotermia. Tbilisi, 1993 (Georgian).
3. *A.A.Smyslov.* Geologicheskaia struktura SSSR. 5, 1969 (Russian).
4. *B.K.Balavadze, et. al.* Grav. model Zemnoi kory i werkhnei mantii Zemli. Kiev, 1979 (Russian).

საქართველოს მეცნიერებათა აკადემიის მოამბე, 158, №1, 1998
BULLETIN OF THE GEORGIAN ACADEMY OF SCIENCES, 158, №1, 1998

GEOPHYSICS

G.Gabrichidze

One Inequality of Elastokinetics and its Application in Seismology

Presented by Corr. Member of the Academy T.Chelidze, October 10, 1997

ABSTRACT. **There is obtained an inequality that can connect the parameters of the motion of the earth surface with the energy released at the earthquake focus. On the basis of the obtained inequality a possibility application of special experimental-analytical technique is being discussed.**

Key words: elastokinetics, reciprocity theorem, Laplace transformation, hölder inequality.

Let's consider an arbitrary elastic body, which is pinched on the A_u part of the surface and free from loading on the surface A_σ. Let's consider two systems of mass forces that induce the motion of that body. The first system of causes and effects is denoted by the index (1), while the other one by the index (2). Correspondingly, in the first state we have mass forces $x_i^{(1)}$, caused by the displacements of $u_i^{(1)}$ inside the body, related to the strains $\varepsilon_{ij}^{(1)}$, stresses $\sigma_{ij}^{(1)}$ and volume expansion $e^{(1)}$. In the second state we have the same parameters but with index (2). Besides the above mentioned, there are also given the values of ρ - density of material, λ, μ - Lame constants.

In elastokinetics there is known a reciprocity theorem that connects stress and strain of these two states. Using Laplace transformation

$$L[\sigma_{ij}(x,t)] = \overline{\sigma}_{ij}(x,p) = \int_0^\infty \sigma_{ij}(x,t)\, e^{-pt} dt,$$

reciprocity theorem is written as [1]:

$$\int_v \overline{\sigma}_{ij}^{(1)} \overline{\varepsilon}_{ij}^{(2)}\, dv = \int_v \overline{\sigma}_{ij}^{(2)} \overline{\varepsilon}_{ij}^{(1)}\, dv. \tag{1}$$

By presenting the left-hand side of the equation (1) in the form

$$\int_v \overline{\sigma}_{ij}^{(1)} \overline{\varepsilon}_{ij}^{(2)}\, dv \equiv \int_v \left[(\overline{\sigma}_{ij}^{(1)} \overline{u}_i^{(2)})_{,j} - \overline{\sigma}_{ij,j}^{(1)} \overline{u}_i^{(2)} \right] dv,$$

employing equation of equilibrium, general ratios connecting stresses and strains and considering the boundary conditions along with zero initial conditions, after using the Ostrogradski-Gauss formula, a tensor equation (1) in the open form can be written as:

$$\overline{A}^{(1)(2)}(p) = \int_v \left[\overline{x}_1^{(1)} \overline{u}_1^{(2)} + \overline{x}_2^{(1)} \overline{u}_2^{(2)} + \overline{x}_3^{(1)} \overline{u}_3^{(2)} \right] dv =$$

$$\int_v \left\{ 2\mu \left[\overline{\varepsilon}_{11}^{(1)} \overline{\varepsilon}_{11}^{(2)} + \overline{\varepsilon}_{12}^{(1)} \overline{\varepsilon}_{12}^{(2)} + \overline{\varepsilon}_{13}^{(1)} \overline{\varepsilon}_{13}^{(2)} + \overline{\varepsilon}_{22}^{(1)} \overline{\varepsilon}_{22}^{(2)} + \overline{\varepsilon}_{23}^{(1)} \overline{\varepsilon}_{23}^{(2)} + \overline{\varepsilon}_{33}^{(1)} \overline{\varepsilon}_{33}^{(2)} \right] + \lambda \overline{e}^{(1)} \overline{e}^{(2)} \right\} dv +$$

$$\int_v \rho p^2 \left[\overline{u}_1^{(1)} \overline{u}_1^{(2)} + \overline{u}_2^{(1)} \overline{u}_2^{(2)} + \overline{u}_3^{(1)} \overline{u}_3^{(2)} \right] dv. \tag{2}$$

Formula (2) shows the work of the external forces of the first system on the displacements of the second system, thus it is designated as $\overline{A}^{(1)(2)}(p)$. On the basis of (2), one can also write an expression for the work $\overline{A}^{(1)(1)}(p)$ and $\overline{A}^{(2)(2)}(p)$

$$\overline{A}^{(1)(1)}(p) = \int_v \left[\overline{x}_1^{(1)}\overline{u}_1^{(2)} + \overline{x}_2^{(1)}\overline{u}_2^{(2)} + \overline{x}_3^{(1)}\overline{u}_3^{(2)}\right] dv =$$

$$\int_v \left\{2\mu\left[\overline{\varepsilon}_{11}^{(1)}\overline{\varepsilon}_{11}^{(1)} + \overline{\varepsilon}_{12}^{(1)}\overline{\varepsilon}_{12}^{(1)} + \overline{\varepsilon}_{13}^{(1)}\overline{\varepsilon}_{13}^{(1)} + \overline{\varepsilon}_{22}^{(1)}\overline{\varepsilon}_{22}^{(1)} + \overline{\varepsilon}_{23}^{(1)}\overline{\varepsilon}_{23}^{(1)} + \overline{\varepsilon}_{33}^{(1)}\overline{\varepsilon}_{33}^{(1)}\right] + \lambda\overline{e}^{(1)}\overline{e}^{(1)}\right. \quad dv +$$

$$\left. \int_v \rho p^2\left[\overline{u}_1^{(1)}\overline{u}_1^{(1)} + \overline{u}_2^{(1)}\overline{u}_2^{(1)} + \overline{u}_3^{(1)}\overline{u}_3^{(1)}\right] dv \right. \tag{3}$$

$$\overline{A}^{(2)(2)}(p) = \int_v \left[\overline{x}_1^{(2)}\overline{u}_1^{(2)} + \overline{x}_2^{(2)}\overline{u}_2^{(2)} + \overline{x}_3^{(2)}\overline{u}_3^{(2)}\right] dv =$$

$$\int_v \left\{2\mu\left[\overline{\varepsilon}_{11}^{(2)}\overline{\varepsilon}_{11}^{(2)} + \overline{\varepsilon}_{12}^{(2)}\overline{\varepsilon}_{12}^{(2)} + \overline{\varepsilon}_{13}^{(2)}\overline{\varepsilon}_{13}^{(2)} + \overline{\varepsilon}_{22}^{(2)}\overline{\varepsilon}_{22}^{(2)} + \overline{\varepsilon}_{23}^{(2)}\overline{\varepsilon}_{23}^{(2)} + \overline{\varepsilon}_{33}^{(2)}\overline{\varepsilon}_{33}^{(2)}\right] + \lambda\overline{e}^{(2)}\overline{e}^{(2)}\right. \quad dv +$$

$$\left. \int_v \rho p^2\left[\overline{u}_1^{(2)}\overline{u}_1^{(2)} + \overline{u}_2^{(2)}\overline{u}_2^{(2)} + \overline{u}_3^{(2)}\overline{u}_3^{(2)}\right] dv. \right. \tag{4}$$

The right-hand parts of the expressions (2), (3) and (4) can be presented as local sums:

$$\overline{A}^{(1)(2)}(p) = \int_v \left[\overline{x}_1^{(1)}\overline{u}_1^{(2)} + \overline{x}_2^{(1)}\overline{u}_2^{(2)} + \overline{x}_3^{(1)}\overline{u}_3^{(2)}\right] dv = \int_v \left[\sum_k a_k(p) b_k(p)\right] dv \tag{5}$$

$$\overline{A}^{(1)(1)}(p) = \int_v \left[\overline{x}_1^{(1)}\overline{u}_1^{(2)} + \overline{x}_2^{(1)}\overline{u}_2^{(2)} + \overline{x}_3^{(1)}\overline{u}_3^{(2)}\right] dv = \int_v \left[\sum_k a_k^2(p)\right] dv \tag{6}$$

$$\overline{A}^{(2)(2)}(p) = \int_v \left[\overline{x}_1^{(2)}\overline{u}_1^{(2)} + \overline{x}_2^{(2)}\overline{u}_2^{(2)} + \overline{x}_3^{(2)}\overline{u}_3^{(2)}\right] dv = \int_v \left[\sum_k b_k^2(p)\right] \tag{7}$$

On the basis of the Hölder's inequality [2]

$$\left|\sum_k a_k b_k\right|^2 \le \left|\sum_k a_k^2\right| \left|\sum_k b_k^2\right| \tag{8}$$

one can write

$$\left|\int_v \left[\overline{x}_1^{(1)}\overline{u}_1^{(2)} + \overline{x}_2^{(1)}\overline{u}_2^{(2)} + \overline{x}_3^{(1)}\overline{u}_3^{(2)}\right] dv\right|^2 \le$$

$$\le \left|\int_v \left[\overline{x}_1^{(1)}\overline{u}_1^{(1)} + \overline{x}_2^{(1)}\overline{u}_2^{(1)} + \overline{x}_3^{(1)}\overline{u}_3^{(1)}\right] dv\right| \left|\int_v \left[\overline{x}_1^{(2)}\overline{u}_1^{(2)} + \overline{x}_2^{(2)}\overline{u}_2^{(2)} + \overline{x}_3^{(2)}\overline{u}_3^{(2)}\right] dv\right| \tag{9}$$

or transferring to the originals, and coming back to tensor form,

$$\left|\int_0^t d\tau \int_v x_i^{(1)}(x,\tau) u_i^{(2)}(x,t-\tau)\, dv\right|^2 = \left|\int_0^t d\tau \int_v x_i^{(2)}(x,\tau) u_i^{(1)}(x,t-\tau)\, dv\right|^2 \le$$

$$\left|\int_0^t d\tau \int_v x_i^{(1)}(x,\tau)u_i^{(1)}(x,t-\tau)dv\right| \cdot \left|\int_0^t d\tau \int_v x_i^{(2)}(x,\tau)u_i^{(2)}(x,t-\tau)dv\right|^2 \qquad (10)$$

or

$$|A^{(1)(2)}(t)|^2 = |A^{(2)(1)}(t)|^2 = |A^{(1)(1)}(t)||A^{(2)(2)}(t)|. \qquad (11)$$

It should be mentioned that the content and structure of the obtained expression won't be altered providing not only mass forces are considered, but also the forces that can be applied to outer and inner boundary surfaces of the body. Taking into account the above-mentioned, inequality (11) can be formulated as:

The work of the first system of dynamic forces on the displacements, caused by the second system of dynamic forces for each period of time is less than or equal to the mean proportional of works done by each system of forces on self-induced displacements.

Let's return to the problem under investigation. One system of causes and effects can be referred to the case of earthquake occurrence and designated by the index (1). Then $A^{(1)(1)}(t)$ will express the work of forces in the focal zone on self-induced displacements, i.e. energy that is released in the focal zone.

The other system of causes and effects that is designated by index (2) can be simulated by carrying out physical experiment. On the surface of the earth at the point x_k an arbitrary dynamic force of $x_1^{(2)}(x_k, t)$ can be applied in the given direction and the law of displacement $u_1^{(2)}(x_k, t)$ of point x_k is recorded.

For the above mentioned two systems of causes and effects the inequalities (10) and (11) can be written as

$$\left|\int_0^t x_1^{(2)}(x_k,\tau)u_1^{(1)}(x_k,t-\tau)d\tau\right|^2 \le \left|\int_0^t x_1^{(2)}(x_k,\tau)u_1^{(2)}(x_k,t-\tau)d\tau\right|^2 \cdot |A^{(1)(1)}(t)| \qquad (12)$$

In these expressions $x_1^{(2)}(x_k, \tau)$ and $u_1^{(2)}(x_k, t-\tau)$ are known functions as a result of experiment. Thus, inequality (12) connects directly the law of displacement of point x_k on the earth surface with the energy release in the focal zone during the earthquake. Inequality (12) may be applied for the investigation of direct and indirect problem - if the law of displacement of the point x_k on the earth surface during the earthquake is known, the energy $A^{(1)(1)}(t)$ that is released in the focal zone may be estimated, and vice versa, if the law of energy release at the earthquake focus zone is assumed, the law of x_k point displacement on the earth surface can be estimated.

K.Zavriev Insitute of Structural Mechanics
and Earthquake Engineering
Georgian Academy of Sciences

REFERENCES

1. *W.Novacki*. Theory of Elasticity. Moscow, 1975 (Russian).
2. *G.Corn, T.Corn*. Mathematical Handbook for Scientists and Engineers. Moscow, 1970 (Russian).

საქართველოს მეცნიერებათა აკადემიის მოამბე, 158, №1, 1998
BULLETIN OF THE GEORGIAN ACADEMY OF SCIENCES, 158, №1, 1998
GEOPHYSICS

T.Toroshelidze, S.Chilingarashvili, M.Chichikoshvili

Monitoring the Content of Nitrogen Dioxide in the Stratosphere According to Observation of Fluorescence in the Twilight in 1957-1990

Presented by Academician E.Kharadze, October 27, 1997

ABSTRACT. **The daily, seasonal and long-term behaviour of NO_2 in the stratosphere has been examined according to regular spectrographic observation of the twilight sky in the 500-700 nm spectral region at the Abastumani Observatory (41.8°N; 42.8°E) in 1957-1990. The mechanism of predissociation of nitrogen dioxide by the solar radiation at 400 nm has been proposed for explanation of the NO_2 emission at 602 nm. Positive trend has been revealed for the annual average content of NO_2, especially discernible in 1960-1970.**

Key words: stratosphere, twilight, fluorescence.

The nitrogen species of NO_x (NO, NO_2) are important natural and antropogenic trace atmospheric compounds. They affect the content of ozone in the stratosphere and the mesosphere and play an important part in temperature changes of the middle atmosphere [1]. In spite of numerous observations of atmospheric nitrogen compounds the question about long-term trend, daily and seasonal variations of NO_2 remains open due to the inconsistency of data [2].

In the given article the question concerns monitoring the NO_2 content at heights of 20-60 km on the basis of molecular fluorescence spectrographic observations, which have been carried out at the Abastumani Observatory.

In 1987, while investigating the structure of the Chapuis absorption band of ozone in the twilight, emission at 602 nm was first manifested in Abastumani [3]. In authors opinion, this diffusion fluorescence must be connected either with the $NO + O \rightarrow NO_2 + h\nu$ reaction or the $NO + O_3 \rightarrow NO_2 + O$ reaction. As a result a very weak fluorescence with the maximum near 600 nm is observed in the nightglow continuous spectrum [4]. But the intensity of emission at 602 nm in the twilight attains a value of few kilorayleighs (1 rayleigh = 10^6 photons/cm^2 sec), that is much more than the intensity of the nightglow continuum (a few rayleighs on 1 nm). This evidence suggests a mechanism of predissociation of NO_2 by solar rays at $\lambda = 400$nm, $NO_2 + h\nu \ \ (\lambda \geq 400\ \text{nm}) \rightarrow NO_2^*$ for explanation of NO_2 fluorescence in the twilight. In consequence NO_2 molecules occur in an intermediate excitation, which energy is released as fluorescence with the maximum near 600 nm [5]. The energy of the solar radiation with $\lambda \geq 400$ nm is insufficient for NO_2 dissociation into NO and oxygen atom [1].

We further estimate the NO_2 predissociation rate for $\lambda = 400$ nm

$$dI(NO_2)/dt = J(NO_2) \cdot n(NO_2),$$

where $J(NO_2)$ is the probability of photodissociation, and $n(NO_2)$ is the concentration of nitrogen dioxide. $J(NO_2) = \varepsilon, \eta, \gamma$, where ε is the quantum yield (0.86) for predissoci-

ation, η is the cross-section for absorbtion ($5 \cdot 10^{-19}$ cm^{-2}), γ is solar photon flux ($1.8 \cdot 10^{16}$ photons/cm^2·sec). For the probability of photodissociation we receive $1.2 \cdot 10^{-4}$cm^{-2}. Taking account of the NO_2 column content of $\sim 10^{12}$ cm^{-2} the intensity of emission at 602 nm is 10^8 photons/cm^{2}sec. It must be born in mind, that in the twilight the optical depth for solar rays increase by a factor of 30-40 in comparison with the day-time. This leads to the observed value of intensity of NO_2 emission in the twilight [3].

The extraction of NO_2 fluorescence from spectrographic observations of the twilight sky is performed as follows. In the spectral region of 500-700 nm the Chapuis band has two peaks near 575 and 602 nm with ratio $I_{602}/I_{575} = 0.96$. With allowance for the scattered light intensity distribution in the twilight and the sensitivity of the used photographic films this ratio attains 1.04. For smaller solar depression ($\alpha < 6$-$7°$) the ratio I_{602}/I_{575}, measured on the microspectrograms, is close to 1.04, and for larger ones ($\alpha > 7°$) it is always in excess of this value. This suggests the presence of emission in the 602 nm band.

It should not be overlooked that during the twilight (α = 1-18°) the scattered light intensity varies by a factor of 10^6 and as emission over the background can only be recognised if it exceeds the background by 15%, that cannot be realized in an earlier twilight, when the scattered light intensity is too high.

Spectrographic observations of the twilight sky have been carried out in Abastumani only on clear and moonless days. This lowered number of observations per annum, but excluded errors in I_{602}/I_{575} caused by clouds and the Moon. However, the measured ratio underwent considerable variations from day to day at fixed moments in the twilight, probably, caused by variations in the stratospheric content of ozone and nitrogen compounds.

The twilight observations in Abastumani have been carried out simultaneously in the northern direction and in the direction of the vertical circle of the Sun at 30° above the horizon (sunwards) with different exposures for α = 7, 7.5-8, 8-9, 9-10, 10-12°. We present the observation data, averaged over a month, in terms of I_{602}/I_{575}, separately in the both directions for solar depressions α = 7-12° (Table 1). The data relate to the years 1957-1990. All root-mean-square deviations do not exceed 20%.

It should be noticed that twilight data about I_{602}/I_{575} depends on content of NO_2 along the path of solar rays, which cross a segment of the atmosphere in the terminator region. The lower limit of emitting layer is estimated by the height of the screening solar rays with λ = 400 nm (about 15 km, [6]) and the upper one with height where the concentration of NO_2 is disappeared (~ 60 km, [1]).

As seen from Table 1, in most cases the morning ratios exceed the evening ones, especially in the winter period. Our results confirm a statement from atmosphere chemistry, that at stratosphere heights the NO_2 content increases in the night-time due to the reaction

$$NO + O_3 \rightarrow NO_2 + O_2.$$

On the other hand, the NO_2 content decreases in the day-time owing to following loss processes:

$$NO_2 + O \rightarrow NO + O_2; \quad NO_2 + h\nu\,(\lambda < 400\ \text{nm}) \rightarrow NO + O.$$

The same chemical processes explain the maximum of I_{602}/I_{575} in the winter-time and the minimum in the summer-time, as follows from Table 1.

Table 1

α (degr.)	I_{602}/I_{575}, the northern direction (*m*-morning, *e*-evening)											
	January		February		March		April		May		June	
	m	e	m	e	m	e	m	e	m	e	m	e
7	1.51	1.33	1.36	1.54	1.30	1.20	1.28	1.15	1.26	1.11	1.20	1.16
7.5-8	1.57	1.46	1.47	1.31	1.30	1.18	1.23	1.17	1.24	1.19	1.25	1.21
8-9	1.57	1.48	1.40	1.26	1.30	1.24	1.22	1.26	1.23	1.22	1.23	1.18
9-10	1.52	1.40	1.32	1.43	1.30	1.22	1.46	1.14	1.35	1.21	1.33	1.21
10-12	1.31	1.34	1.34	1.18	1.22	1.29	1.29	1.30	1.29	1.23	1.31	1.23
	July		August		September		October		November		December	
7	1.22	1.32	1.24	1.35	1.36	1.30	1.50	1.41	1.49	1.39	1.62	1.31
7.5-8	1.24	1.26	1.39	1.33	1.46	1.39	1.49	1.40	1.61	1.34	1.65	1.43
8-9	1.27	1.31	1.44	1.30	1.48	1.45	1.56	1.47	1.64	1.48	1.58	1.36
9-10	1.40	1.33	1.50	1.35	1.50	1.48	1.59	1.41	1.66	1.58	1.56	1.48
10-12	1.54	1.29	1.46	1.30	1.41	1.44	1.49	1.56	1.68	1.33	1.52	1.44
α (degr.)	I_{602}/I_{575}, the vertical circle of the Sun											
	January		February		March		April		May		June	
	m	e	m	e	m	e	m	e	m	e	m	e
7	1.30	1.28	1.26	1.21	1.20	1.23	1.18	1.21	1.17	1.23	1.16	1.18
7.5-8	1.31	1.25	1.28	1.19	1.22	1.20	1.16	1.16	1.18	1.19	1.20	1.18
8-9	1.35	1.25	1.28	1.18	1.22	1.24	1.14	1.14	1.16	1.17	1.21	1.21
9-10	1.52	1.39	1.42	1.33	1.40	1.37	1.34	1.30	1.30	1.27	1.30	1.33
10-12	1.60	1.42	1.60	1.41	1.37	1.30	1.35	1.27	1.27	1.26	1.27	1.30
	July		August		September		October		November		December	
7	1.20	1.24	1.27	1.26	1.33	1.36	1.28	1.42	1.32	1.34	1.27	1.32
7.5-8	1.20	1.20	1.28	1.27	1.30	1.30	1.34	1.33	1.28	1.29	1.30	1.23
8-9	1.20	1.21	1.34	1.31	1.35	1.32	1.31	1.38	1.35	1.32	1.32	1.20
9-10	1.28	1.29	1.35	1.44	1.48	1.53	1.57	1.49	1.47	1.43	1.52	1.46
10-12	1.39	1.37	1.39	1.38	1.56	1.52	1.57	1.50	1.42	1.45	1.54	1.46

Table 2 contains mean annual values of I_{602}/I_{575} averaged overall data and corresponding root-mean-square deviations σ.

Table 2

Years	I_{602}/I_{575}	σ	Years	I_{602}/I_{575}	σ	Years	I_{602}/I_{575}	σ
1957*	1.14	0.12	1968	1.31	0.08	1979	1.43	0.08
1958*	1.15	0.09	1969	1.15	0.05	1980	1.40	0.08
1959	1.19	0.10	1970	1.38	0.09	1981	1.36	0.09
1960	1.33	0.08	1971	1.32	0.08	1982	1.35	0.10
1961	1.31	0.07	1972	1.26	0.07	1983	1.42	0.09
1962	1.23	0.06	1973	1.26	0.09	1984	1.41	0.12
1963	1.30	0.07	1974	1.28	0.08	1985	1.46	0.10
1964	1.36	0.05	1975	1.41	0.10	1986	1.38	0.10
1965	1.48	0.09	1976	1.40	0.09	1987	1.50	0.13
1966	1.38	0.09	1977+	1.32	0.11	1988	1.38	0.11
1967	1.42	0.10	1978	1.40	0.10	1989	1.33	0.10
						1990+	1.45	0.12

Notes: – (*) denotes years when observations have been carried out for $\alpha \neq 5\text{-}9°$.
– (+) denotes years when number of observations of the twilight do not surpass 30.

The data of Table 2 allow to calculate the coefficient of linear regression, which is equal to: +1.7% (1960-1970); +1.35%(1970-1980) and +1.00% (1980-1990) or only 4% for 30 years. Thus the NO_2 content in the Transcaucasus stratosphere has a negligible positive trend. The received result is between the value obtained for the NO_2 total content in 1975-1986, which does not detect a trend for the both Earth hemispheres [2] and the "Nimbus-7" value, according to which in 1979-1984 the NO_2 content increased by 38-75% at altitudes of 20-40 km for middle latitudes of the South hemisphere [7].

In conclusion one can mark that the content of stratospheric NO_2 over the Caucasian region underwent the most noticeable positive trend in the 60ies, which coincides with the period of nuclear weapon tests in the atmosphere. The decreasing of the growth of NO_2 quantity during the next years is connected with the different processes of the stock including the chemical cycle of ozone.

Abastumani Astrophysical Observatory
Georgian Academy of Sciences

REFERENCES

1. Spravochnik. Atmosphere. Leningrad, 1991, 509, (Russian).
2. *M.T.Coffey*. Geophys. Res. Lett., **15**, 4, 1988, 331-334.
3. *T.G.Megrelishvili, L.M.Fishkova*. Geomagnetizm i aeronomia. 4, 1987, 689-690 (Russian).
4. *L.M.Fishkova*. Nochnoe izluchenie sredneshirotnoi verkhnei atmosfery. Tbilisi, 1983, 271 (Russian).
5. *J.McEwan, L.Fillips*. Chemistry of the atmosphere.Wiley, New-York, 1975, 301.
6. *T.I.Toroshelidze*. Analis problem aeronomii po izlucheniu verkhnei atmosfery, 1991, 216 (Russian).
7. *M.Callis, B.Lindwood*. Nature, **329**, 6091, 1986, 772-777.

I.Shatirishvili, Sh.Shatirishvili, N.Chkhartishvili

Gas Chromatography and Qualimetric Models of Wine-Making Products Evaluation

Presented by Corr. Member of the Academy A.Shvelashvili, September 15, 1997.

ABSTRACT. **On the example of Georgian wines by reactive gas chromatographic method, which enables to state the effect of individual factors on wine-making product quality, the qualimetric models have been developed.**

Key words: gas chromatography, qualimetric model, correlation method, additivity rule.

The chromatographic methods of analysis have been widely used recently in every field of national economy and in food industry as well. A new approach to investigate wine-making products taste and bouquet which is expressed by drawing qualimetric models joining both chemical composition data of a sample and its wine tasting rating are observed [1]. At the same time it is available to study the effect of the same individual components and the impact of their features on the total wine-tasting indices.

The study of a big amount of cognac alcohols, brandy, ordinary and collection wines indicates some objectivities characterising each sample group (2). For example, concentrations (X1) of separate components greatly correlate with each other. At the same time a large number of such connections significantly exceeds the connection between Z and taste rating Y. It should be noted that it is impossible to state the effect of different components on beverage organoleptical indices by the data of correlation method. The method of correlation is only the early stage of study. The correlative relationship between different components makes it difficult to conduct regressive analysis.

The dependence of the mathematical expression of beverage organoleptic features is based on the following supposition:

The effect of different components on a panelist's receptors is determined by the component concentration in the mixture and by the limited sensitivity to a given substance.

The total effect of a multi-components system satisfies the additivity rule.

The given results are expressed by polynomialic model:

$$Y = b_0 + \sum_{i=1}^{n} bix_1 ,$$

where Y is beverage quality index shown by wine tasting; $x_1(i = 1, 2, \ldots, n)$ are variables which characterise << i >> component in a mixture; b_1 (i = 1, 2, ..., n) experimental subject investigated coefficients. The searched factors of the regressive model subject to an experimental determination.

A number of qualimetric models have been obtained by the chemical analysis and wine-tasting judgment of the groups under study, which enables us to evaluate the effect

of different factors on wine-making products. At the same time it determines the quality of samples with high accuracy by the results of chemical analysis. The most important is that the technologist is given a chart of treatment with possible technological means for such intermediate products as fermented juice or cognac alcohol distillation.

The rules of correlation analysis of the samples by reactive gas chromatographic method for more than a year aged Georgian white wines are given in Table 1. From nine investigated factors one is the total amount of carbonyl compound, eight of them are concentrations of alcohols and ethers. The aging time is not considered.

Table

Georgian White Wines Correlation Matrix
(Z_{iy}, Z_{xiy})

Name of factor X	X1	X2	X3	X4	X5	X6	X7	X8	X9
Carbonyl Compounds (Total) X1	1.0 0	0.36	0.41	0.51	0.51	0.40	0.68	0.71	0.68
Exhylacetate X2	–	1.00	0.38	0.49	0.42	0.42	0.41	0.45	0.51
Methanol X3	–	–	1.00	0.27	0.68	0.65	0.71	0.66	0.82
1-propanol X4	–	–	–	1.00	0.27	0.24	0.39	0.67	0.68
2-propanol X5	–	–	–	–	1.00	0.90	0.80	0.81	0.83
Amyl alcohol X6	–	–	–	–	–	1.00	0.75	0.70	0.87
Ethyl Caprylene X7	–	–	–	–	–	–	1.00	0.79	0.81
Phenetole X8	–	–	–	–	–	–	–	1.00	0.24
Ethyl palmitate X9	–	–	–	–	–	–	–	–	1.00
Sensory Evaluation Zxiy	0.9	0.19	0.35	0.49	0.56	0.58	0.57	0.68	0.55

For the wine <<Hereti>> the simplified qualimetric model which consists of methylacetate (X2), 1 - propanole (X4), 2 -propanole (X3) and phenethyl alcohol (X8) is obtained:

$$Y' = 8.659 + 3.079x_2 + 5.185x_4 + 1.888x_3 + 5.417x_8.$$

It should be noted that there is a certain contradiction between correlation and regression methods, which is the result of complicated correlative connection with such complex mixtures as wine. Wine components are in dynamic balance. Changing the content of one component changes the concentrations of the rest. The suggested approach to the study of the impact of the separate component and their complexes on the sensory features of wine products undoubtedly deserve great attention and future development.

For commercial scale production the organoleptic improvement could be reached only by adopting new progressive technological processes which might be possible only by means of thorough study of beverage chemical on every step of its processing.

Georgian Agrarian University

REFERENCES

1. *A.Lashkhi, et al.* Materials of Conf. on Cognac Production. Tbilisi, 1977, 32 (Georgian).
2. *B.S.Chernіga.* Autoref. Kand. Diss. M. 1974 (Russian).

საქართველოს მეცნიერებათა აკადემიის მოამბე, 158, №1, 1998
BULLETIN OF THE GEORGIAN ACADEMY OF SCIENCES, 158, №1, 1998

ANALYTICAL CHEMISTRY

R.Gakhokidze, N.Sidamonidze, N.Okujava, N.Itriashvili, L.Tabatadze, L.Topuria

Study of Acidic Isomerization of some Disaccharides by Gas-Liquid Chromatography

Presented by Corr.Member of the Academy L.Khananashvili, May 27, 1998

ABSTRACT. **Products of acidic isomerization of disaccharides (lactose, maltose, cellobiose) have been studied by gas-liquid chromatography. It was established that during reaction the break of glycosidic bonds didn't take place and from the given disaccharides 4-O-(β-D-galactopyranosyl]-α-D-glucosaccharinic, 4-O-(α-D-glucopyranosyl]-α-D-glucosaccharinic and 4-O-[β-D-glucopyranosyl]-α-D-glucosaccharinic acids were obtained.**

Key words: acidic isomerization, disaccharides

As it has been shown in our previous papers [1,2] aldoses containing unsubstituted pseudoaldehyde and neighboring alcohol groups under the action of hydroxides of some heavy metals are transferred into isomeric acids. The reaction mechanism has been studied on several simple compounds.

To study acidic isomerization products of disaccharides (lactose, maltose, cellobiose) gas-liquid chromatography [3-9] was used. As carbohydrates and their derivatives are non-volatile compounds, their derivatization was performed in pyridine area by trimethylchlorosilane and hexamethyldisilazane. Trimethylsilyl derivatives, which are well dissolved in hexane and volatiled at 180°C, have been obtained.

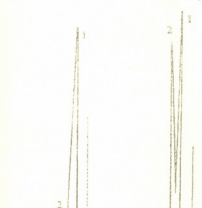

Figs.1,2

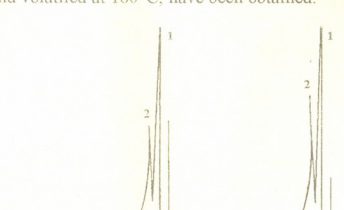

Figs.3,4

It was established that in the course of reaction, breaking of glycosidic bonds didn't take place and from the mentioned disaccharides deoxyaldobionic acids: 4-O-[β-D-galactopyranosyl]-α-D-glucosaccharinic, 4 -O-[α-D-glucopyranosyl]-α-D-glucosaccharinic and 4-O-[β-D-glucopyranosyl]-α-D-glucosaccharinic acids. (Figs. 1,2,4).

While forming of 4-O-[β-D-glucopiranosyl]-α-D-glucosaccharinic acid small amounts of formic acid and acetic acid were found (Fig.3).

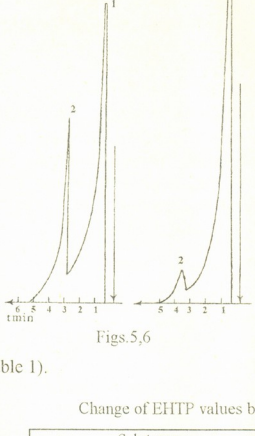

Figs.5,6

The hydrolysis of deoxyaldobionic acids (I) yields α-D-glucosaccharinic acid (II) (Fig.5), which converted into α-D-glucosaccharino-1.4-lactone (III)(Fig.6).

The analysis of substances was carried out on "ΛΧΜ" type chromatograph (column length 2 m, diameter 3 mm). The column was filled by adsorbent Chromaton N-AW-DMCS. It consists of hard packing (Chromaton - N), which is covered by liquid phase SE-30 of 5% (from hard packing weight).

Column temperature was 200°C, vaporizer temperature 250°C. The analyses were carried out at three velocities (20 ml/sec, 40ml/sec, 60 ml/sec). The values of equivalent height of theoretical plate (EHTP) show that the optimal velocity of gas-carriers is 40ml/sec (Table 1).

Table 1

Change of EHTP values by the dependency on gas carriers velocity

Substance	C_1		
	V=20 ml/sec	V=40 ml/sec	V=60 ml/sec
Silyl derivative of 4-O-[β-D-galactopyranosyl]-α-D-glucosaccharinic acid	1.50	1.3	1.38
Silyl derivative of 4-O-[α-D-glucopyranosyl]-α-D-glucosaccharinic acid	0.93	0.78	0.81
Silyl derivative of 4-O-[β-D-glucopyranosyl]-α-D-glucosaccharinic acid	0.28	0.13	0.25
Silyl derivative of α-D-glucosaccharinic acid	5.17	3.4	5.4
Silyl derivative of α-D-glucosaccharino-1,4-lactone	2.5	1.5	3.5

The efficiency of chromatographic column greatly depends on EHTP. The less is the EHTP the more efficient is chromatographic column (Fig.7). From Figure it is seen that EHTP is minimal when gas-carrier velocity equals 40 ml/sec.

EHTP was calculated from formula $V_{EHTP} = \frac{l}{N}$, where l is column length; N is number of theoretical plates, which equals $N = 16\left(\frac{x}{y}\right)^2$, where x is retention time, y is the width of peak at the root.

The coefficient of separation (Cs) is criterion of separation of two-component mixture (hexane-compound) which was calculated at three velocities (20 ml/sec, 40 ml/sec, 60 ml/sec). The highest value was obtained at 40 ml/sec (Table 2)

Table 2

Change of coefficient of separation with dependency on gas-carrier velocity

Binary compounds of substances	C_s		
	V=20 ml/sec	V=40 ml/sec	V=60 ml/sec
Hexane-silyl derivative of 4-O-[β-D-galactopyranosyl]-α-D-glucosaccharinic acid	1.29	1.57	1.32
Hexane-silyl derivative of 4-O-[α-D-glucopyranosyl]-α-D-glucosaccharinic acid	1.36	1.8	1.56
Hexane-silyl derivative of 4-O-[β-D-glucopyranosyl]-α-D-glucosaccharinic acid	2.20	2.68	2.41
Silyl derivative of 4-O-[β-D-glucopyranosyl]-α-D-glucosaccharinic acid – silyl derivative of formic acid	1.5	2.49	2.36
Silyl derivative of formic acid – silyl derivative of acetic acid	1.34	1.87	1.68
Hexane-silyl derivative of α-D-glucosaccharinic acid	3.24	3.48	3.11
Hexane-silyl derivative of α-D-glucosaccharino-1,4-lactone	2.96	3.66	3.35

Coefficient of separation was calculated by the formula

$$K_P = \frac{\Delta X}{\mu_1 + \mu_2}$$

where ΔX is the distance between maxima of two neighboring peaks; μ_1 μ_2 denote the length of line between the first and second peaks.

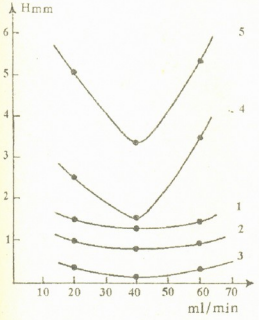

Fig.7. Dependence of EHTP on gas carriers velocity of synthesized compounds

1.Silyl derivative of 4-O-[β-1)-galactopyranosyl]-α-1)-glucosaccharinic acid

2.Silyl derivative of 4-O-[α-1)-glucopyranosyl]-α-1)-glucosaccharinic acid

3.Silyl derivative of 4-O-[β-1)-glucopyranosyl]-α-1)-glucosaccharinic acid

4.Silyl derivative of α-1)-glucosaccharino-1,4-lactone

The given method can be used for control of purity of the obtained compounds and other derivatives of carbohydrates.

Acid isomerization of disaccharides. To a solution of 0.027 mole of disaccharides (lactose, maltose, cellobiose) in water is added 0.042 mole of freshly prepared lead hydroxide and the reaction mixture in oxygen-free media under nitrogen atmosphere was kept 10 days at 25°C. The filtrate is passed through a column of AV-17(oH) anion exchange resin. Acids are eluted by washing the column with 3% solution of NaOH. Then the solution is led through the column with KU-2(H) cation exchange resin to remove sodium ions.

Hydrolysis of deoxyaldobionic acids. A solution of lead salts of deoxyaldobionic acids in 50 ml of 5% sulphuric acid is heated 1 h at 100°C, is neutralized with barium carbonate and is heated again 5 h at 100°C. After filtration the solution is decolorized with activated carbon and barium salt is precipitated from 96% ethanol, crystallized from water and dried over P_2O_5.

Silyl derivatives of deoxyaldobionic acids are prepared from 0.02g of the acids in anhydrous pyridine. 0.5 ml of hexamethyldisilazane and 0.3 ml of trimethylchlorosilane are used as a reagents and the mixture is shaken for 2-5 min. After evaporation in a rotatoryvacuum evaporator at 40°C the residue is dissolved in n-hexane.

Tbilisi I.Javakhishvili State University

REFERENCES

1. *R.A.Gakhokidze*. Doklady AN SSSR, **265**, 3, 1989, 625.
2. *Idem. Ibidem*, 304, 2, 1989, 360.
3. *B.V.Stoliarov, I.M.Savinov, A.G.Vitenberg*. Rukovodstvo k prakticheskim rabotam po gazovoi khromatografii. M., 1984, 280.
4. *P.I.Skhunmakers*. Optimizatsia selektivnosti v khromatografii. M., 1989. 399.
5. *R.A.Gakhokidze*. Uspekhi khimii. M., 1980, 418.
6. *A.B.Kisilieva, V.R.Drevinga*. Eksperimentalnye metody v adsorbtsii i molekuljarnoy khromatografii. M., 1985, 283.
7. *E.Kheftman*. Khromatografia. M., 1986. 422.
8. *G.Petersson, H.Riedl, O.Samuelson*. Svensk Papperstidning, 70, 1967, 371, 11-15.
9. *G.Petersson*. Jour. of Chromatographic Sciences, 15, 1977, 245.

საქართველოს მეცნიერებათა აკადემიის მოამბე, 158, №1, 1998
BULLETIN OF THE GEORGIAN ACADEMY OF SCIENCES, 158, №1, 1998

M.Gverdtsiteli, N.Kobakhidze

Algebraic Investigation of Monohalogenmethanes in Terms of MBL-Matrices Method

Presented by Corr. Member of the Academy L. Khananashvili, September 20, 1997

ABSTRACT. **Algebraic investigation of monohalogenmethanes was carried out in terms of MBL-matrices method. Their diagonal elements represent mass numbers of chemical elements, whereas nondiagonal ones – the lengths of the chemical bonds. Some correlation equations were constructed.**

Key words: monohalogenmethanes, MBL-matrices, correlation.

Contiguity matrices of molecular graphs and their various modifications are efficiently used in algebraic chemistry [1-4]. One type of such matrices are MBL matrices; their diagonal element represents mass numbers of chemical elements bonds (r). MBL-matrix for monohalogenmethane /CH_3X is brought below:

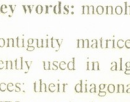

$$\begin{Vmatrix} 6 & r_{C-X} & r_{C-H} & r_{C-H} & r_{C-H} \\ r_{C-X} & M_X & 0 & 0 & 0 \\ r_{C-H} & 0 & 1 & 0 & 0 \\ r_{C-H} & 0 & 0 & 1 & 0 \\ r_{C-H} & 0 & 0 & 0 & 1 \end{Vmatrix}, \qquad (1)$$

where: M_x is mass number of halogen; r_{c-x} is the length of $C - X$ bond; r_{C-H} is the length of $C - H$ bond.

The determinant of (1) matrix can be calculated by formula:

$$\Delta_{MBL} = 12 \cdot M_X - r_{C-X}^2 - 3 \cdot r_{C-H}^2 \cdot M_X. \qquad (2)$$

The decimal logarithm of determinant of MBL matrices for monohalogenmethanes and some of their physico-chemical properties [5] are listed in Table.

Table

The values of lg (Δ_{MBL}) and corresponding physico-chemical properties of monohalogenmethanes

Compound	CH_3F	CH_3Cl	CH_3Br	CH_3I
lg (Δ_{MBL})	2.19	2.46	2.82	3.02
ΔG_0^{298} (ccal/mol)	−53.29	−15.00	−6.70	3.91
ΔH_0^{298} (ccal/mol)	−59.00	−20.60	−8.96	3.50
S_0^{298} e.u.	53.25	56.02	58.76	60.67
$T_{boil.}$ (^{0}C)	−78.4	−23.76	3.56	42.4
$T_{melt.}$ (C)	−141.8	−96.7	−93.6	−66.45
d_4^{20}	0.8428	0.9120	1.6755	2.2790

Some correlation equations are constructed on computer:

$$\Delta G_0^{298} = 62.61 \lg(\Delta_{MBL}) - 182.00 \quad (3)$$

$$\Delta H_0^{298} = 69.38 \lg(\Delta_{MBL}) - 203.25 \quad (4)$$

$$S_0^{298} = 8.75 \lg(\Delta_{MBL}) + 34.23 \quad (5)$$

$$T_{boil.} = 134.86 \lg(\Delta_{MBL}) - 367.81 \quad (6)$$

$$T_{melt.} = 78.29 \lg(\Delta_{MBL}) - 305.00 \quad (7)$$

$$d_4^{20} = 1.7684 \lg(\Delta_{MBL}) - 3.21 \quad (8)$$

Corresponding correlation coefficients r and equal: $r = 0.958$; $r = 0.972$; $r = 1$; $r = 0.983$; $r = 0.995$; $r = 0.994$.

Thus in a case of S_0^{298} ideal correlation is observed; for $T_{melt.}$ and d_4^{20} – excellent correlations; in other cases – approximate correlations.

Thus, we can consider lg (Δ_{MBL}) as the topologic index [6] for "structure – properties" correlations for monohalogenmethanes.

Tbilisi I.Javakhishvili State University

REFERENCES

1. *P.R.Rouvray.* Chemical Application of Topology and Graph Theory. (Ed. A. T. Balaban). Amsterdam, 1983.
2. *G.Gamziani, M.Gverdtsiteli.* Izometriis movlena matematikuri kimiis tvaltaxedvit, Tbilisi, 1992 (Georgian).
3. *M.Gverdtsiteli, G.Gamziani, I.Gverdtsiteli.* The Contiguity Matrices of Molecular Graphs and their Modifications. Tbilisi, 1996.
4. *N.B.Kobakhidze, M.G.Gverdtsiteli, D.S.Tugushi, M.I.Gverdtsiteli.* Correlation "Structure–Properties" in Algebraic Chemistry. Tbilisi, 1997.
5. *M.Kh.Karapetians.* Khimicheskaya termodinamika. Moskva, 1975 (Russian).
6. *G.Gamziani, N.Kobakhidze, M.Gverdtsiteli.* Topologic Indexes. Tbilisi, 1995.

საქართველოს მეცნიერებათა აკადემიის მოამბე, 158, №1, 1998
BULLETIN OF THE GEORGIAN ACADEMY OF SCIENCES, 158, №1, 1998

ORGANIC CHEMISTRY

N.Kobakhidze, M.Gverdtsiteli

Algebraic Investigation of the Reactions of Halogenation of Alkanes

Presented by Corr. Member of the Academy D.Ugrekhelidze, October 20, 1997

ABSTRACT. **The reactions of radical halogenation of alkanes were investigated in terms of ANB matrices method. Diagonal elements of ANB matrices represent atomic number of chemical elements, whereas nondiagonal ones multiplicities of chemical bonds.**

Key words: alkanes, halogenation, ANB-matrices.

The reactions of radical halogenation of alkanes are very interesting multiple-stage processes. One of the stage of these reactions proceeds according to the scheme:

$$RH + X\cdot \longrightarrow R\cdot + HX, \qquad (1)$$

where RH is alkane, X-halogen. The energies of activation of (1) process for different RH and X are listed in Table 1 [1].

Table 1

Energies of activation $E^{\neq}$ for the reactions of radical halogenation of alkanes

X / R	$E^{\neq}$			
	CH3	C2H5	(CH3)2CH	(CH3)3C
Cl	16.0	4.2	2.9	0.4
Br	78.1	58.8	43.7	32.8
I	141	115	102	92

Contiguity matrices of molecular graphs and their various modifications are efficiently used in modern theoretical organic chemistry [2]. One type of such matrices are ANB-matrices [2,3]. Their diagonal elements represent atomic number of chemical elements, whereas nondiagonal elements – the multiplicities of chemical bonds.

The process (1) was studied within the limits of ANB-matrices method – correlations between energies of activation ($E^{\neq}$) and the values of decimal logarithms of ANB-matrices for alkanes (RH) were investigated. For methane ANB-matrix has a form:

$$\begin{Vmatrix} 6 & 1 & 1 & 1 & 1 \\ 1 & 1 & 0 & 0 & 0 \\ 1 & 0 & 1 & 0 & 0 \\ 1 & 0 & 0 & 1 & 0 \\ 1 & 0 & 0 & 0 & 1 \end{Vmatrix} \qquad (2)$$

The values of Δ_{ANB} for 4 alkanes are brought in Table 2.

Table 2

Δ_{ANB} for alkanes

Alkane	ANB	Alkane	ANB
CH_4	2	$CH_3 - CH_2 - CH_3$	30
$CH_3 - CH_3$	8	$CH_3 - \underset{\displaystyle CH_3}{\underset{\vert}{CH}} - CH_3$	108

Three correlation (for chlorination, bromination and iodination) have been constructed on computer:

$$E^{r}_{(Cl)} = -8.40 \lg(\Delta_{ANB}) + 5.78, \quad (3)$$

$$E^{r}_{(Br)} = -42.84 \lg(\Delta_{ANB}) + 95.74, \quad (4)$$

$$E^{r}_{(I)} = -28.28 \lg(\Delta_{ANB}) + 146.11. \quad (5)$$

The coefficient of correlation r for equation (3) is equal $r = 0.932$; for equation (4) - $r = 0.951$; for equation (5) – $r = 0.980$. Thus correlation (3) is approximate, (4) and (5) - satisfactory.

Thus we can consider $\lg(\Delta_{ANB})$ as the topologic index [4] for the processes of radical halogenation of alkanes.

Tbilisi I.Javakhishvili State University

REFERENCES

1. *A.Dneprovski, T.Tiomnikova.* Theoreticheskie osnovy organicheskoi khimii. Leningrad, 1991 (Russian).
2. *P.R.Rouvray.* Chemical Application of Topology and Graph Theory. (Ed. *A.T.Balaban*), Amsterdam, 1983.
3. *N.B.Kobakhidze, M.G.Gverdtsiteli, D.S.Tugushi, M.I.Gverdsiteli.* Correlation Structure - Properties in Algebraic Chemistry. Tbilisi, 1997.
4. *M.Gverdsiteli, G.Gamziani, I.Gverdtsiteli.* The Contiguity Matrices of Molecular Graphs and their Modifications. Tbilisi, 1996.

საქართველოს მეცნიერებათა აკადემიის მოამბე, 158, №1, 1998
BULLETIN OF THE GEORGIAN ACADEMY OF SCIENCES, 158, №1, 1998

ORGANIC CHEMISTRY

M.Karchkhadze, N.Mukbaniani, A.Samsonia, R.Tkeshelashvili, N.Kvelashvili, T.Chogovadze,
Corr. Member of the Academy L.Khananashvili

Carbosiloxane Copolymers with Cyclopentasiloxane Fragments in the Chain

Presented October 20,1997

ABSTRACT. **The reaction of hydrid polyaddition of α, ω dihydriddimethylsiloxanes to 1,5-divinyl-1,5-dimethylhexaphenylcyclopentasiloxane in the presence of platinium chlorhydric acid as a catalyst has been studied and carbosiloxane copolymers with regular arrangement of cyclopentasiloxane fragments in dimethylsiloxane chain have been obtained. The reaction order, activation energies and hydrid polyaddition rate constants have been found. Thermogravimetric, thermomechanical and roentgenographic investigations are carried out.**

Key words: carbosiloxane copolymers, hydrid polyaddition, organocyclopentasiloxanes, thermal-oxidative stability.

It is known from literature that the synthesis of carboorganosiloxane polymers are based on the reaction of hydrid polyaddition of organodihydridsiloxanes to organodialkenylsiloxanes [1]. By using of these reactions it is possible to obtain the copolymers with cyclolinear structure of macromolecules [2]. The carbosiloxane copolymers containing cyclotetrasiloxane fragments in dimethylsiloxane chain have been synthesised by the reaction of hydrid polyaddition of α, ω dihydriddimethylsiloxane to divinylorganocylotetrasiloxane [3].

In literature there is no information about carbosiloxane copolymers with organocyclopentasiloxane fragments in dimethylsiloxane chain.

For synthesis of carbosiloxane copolymers with the regular arrangement of organocyclopentasiloxane fragments in the chain at the first stage 1,5-divinyl-1,5-dimethylhexaphenylcyclopentasiloxane was synthsized. This compound early was synthesized by us with 50% yield [4]. For the increase of the yield of 1,5-divinyl-1,5-dimethylhexaphenylcyclopentasiloxane the reaction of heterofunctional condensation (HFC) has been studied. On the first stage HFC of 1,3-dihydroxytetraphenyldisiloxane with methylvinyldichlorsilane it was carried out with the ratio of initial components 1:3 in anhydrous solution of toluene, in the presence of pyridine. As a result 1,7-dichlor-1,7-dimethyltetraphenyltetrasiloxane with 84% yield was obtained. On the second stage the reaction of HFC of this tetrasiloxane with dihydroxydiphenylsilane in the dilute solution of anhydrous toluene was carried out with 1:1 ratio of initial components in the presence of pyridine at – 5 ÷ 10°C temperature. The reaction proceeds according to the following scheme:

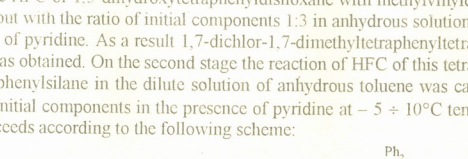

The composition and the structure of synthesized compounds were determined by means of elementary analysis, by finding of molecular mass, by IR and NMR spectra

data, which are in accordance with literature data [4].

For synthesis of carbosiloxane copolymers with organocyclopentasiloxane fragments in dimethylsiloxane chain it was studied the hydrid polyaddition reaction of α, ω dihydriddimethylsiloxanes to 1,5-divinyl-1,5-dimethylhexaphenylcyclopentasiloxane in the presence of platinium chlorhydric acid as a catalyst, at the 75°C, 80°C and 85°C temperature conditions.

The process of the reaction was observed by decrease of amount of active Si-H groups. It was observed, that with the increase of the length of α, ω dihydriddimethylsiloxane chain the rate and depth of the polyaddition reaction decreases. The reaction of hydrid polyaddition proceeds to the following scheme:

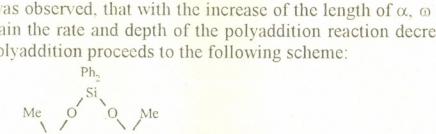

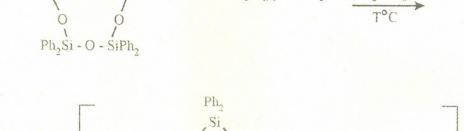

where: n = 2(I), 4(II), 6(III), 12(IV), 23(V).

As a result of the reaction, copolymers are obtained with $\eta_{spec} = 0,09 \div 0,2$, that are liquid or vitreous light yellow products soluble in ordinary organic solvents. Some physico-chemical properties elementary analysis and the yield of copolymers are listed in the Table. As it is seen from the Table in the case of a small values of the length of dimethylsiloxane links *n*, the yield of copolymers is low, which may be explained by intramolecular cyclization, which is in agreement with literature data [5].

By ^{1}H NMR spectra for copolymer I it has been established that catalytic hydrid polyaddition proceeds mainly by the Farmer rule with formation of dimethylenic bridges. In the ^{1}H NMR spectra one can observe a signal for grouping $-CH_2-CH_2-$ with chemical shift of $\delta = 0.34$ ppm, it was established that the hydrid polyaddition partially (about 6÷7%) proceed by Markovnikov rule.

With an increase of the length of dimethylsiloxane links at one and the same temperature, the depth of the reaction of hydrid polyaddition decreases. With an increase of the temperature the depth of the polyaddition reaction increases (at one and the same value of the length of dimethylsiloxane links *n*). It was established that the polyaddition reaction is the reaction of the second order. The reaction rate constants were calculated: $k_{75°C} = 1.4004 \times 10^{-2}$, $k_{80°C} = 1.965 \times 10^{-2}$, $k_{85°C} = 2.559 \times 10^{-2}$ and the activation energy of the hydrid polyaddition reaction has been calculated which is equal to 62.1 KJ/mole.

Table

Some physico-chemical properties of cyclopentasiloxane fragments containing carbosiloxane copolymers

Copolymer N	Yield %	Reaction temperature	η_{spec}*	5 % mass losses	Ressidual mass, %	T_{vitr}	d_1, Å	Elementary analysis, %**			$\overline{M}_w \times 10^{-3}$
								C	H	Si	
II	75	85	0.09	320	28	0÷-2	9.20	61.33 61.02	6.22 5.97	21.77 21.65	189
II	80	85	0.14	–	–	–22	–	57.25 56.95	6.49 6.21	24.05 23.94	
III[1]	92	75	0.15	–	–	–	–	54.18	6.69	25.75	
III[2]	93	80	0.18	–	–	–	–	54.01	6.42	25.44	
III[3]	95	85	0.20	295	24	–53	–				211
IV	95	85	0.24	–	–	–82	–	47.69 47.40	6.95 6.63	29.52 29.44	
V	96	85	0.31	285	19	–123	7.21	42.52 42.35	7.34 7.11	32.32 32.12	236

* in tolune at 25°C

** numerator - calculator values, denominator – experimental values

The thermogravimetric investigation of copolymers has been carried out which shows, that in case of small values of dimethylsiloxane links *n*, the copolymers are characterized with higher thermal-oxidative stability. One can observe 5% mass losses in the temperature region 300-320°C. The main destruction process proceeds over the range 400-640°C and above 700°C, the curves of mass losses do not occur. With an increase of the length of dimethylsiloxane chain the thermal-oxidative stability of copolymers decreases.

X-ray investigations of copolymers show that the copolymers are one phase systems. The maximum value of interchain distances d_1 one can observe at small values of the length of linear dimethylsiloxane links.

Thermomechanical studies of the obtained copolymers have been carried out and it was established that the vitrification temperature of copolymers decreases with an increase of the value *n* of the linear dimethylsiloxane chain. Beginning from the value of n = 12 the influence of carbocyclopentasiloxane fragments is not perceptible. In case of value n = 23 the vitrification temperature of copolymers equalize to the vitrification temperature of the linear polydimethylsiloxane.

So, for the first time we have synthesised and studied the properties of cyclolinear carbosiloxane copolymers with regular arrangement of organocyclopentasiloxane fragments in the main dimethylsiloxane chain.

Tbilisi I.Javakhishvili State University

REFERENCES

1. *K.A.Andrianov, I.Souchek, L.M.Khananashvili.* Uspekhi Khimii, 48, 1979, 233 (Russian).
2. *O.V.Mukbaniani, et al.* Intern. J.Polymeric Mater, 33, 1996, 47.
3. *A.A.Zhdanov et al.* Dokl. Akad. nauk USSR, 211, 1974, 1104 (Russian).
4. *N.A.Koiava, et al.* Zhurn. obshch. khimii, 51, 1981, 130 (Russian).
5. *N.A.Koiava, et al.* Vysokomol. soed., 27, 1985, 2261 (Russian).

G.Kvartskhava, M.Gverdtsiteli, T.Kovziridze, A.Dolidze

Theoretical Study of Bioactivity Using Algebraic Chemistry

Presented by Academician T.Andronikashvili, October 13,1997

ABSTRACT. **Phenoxycarb and bioactive theoretical prognosis of its analogs has been studied using topological indices i.e. contiguity matrices of molecular graphs.**

Key words: matrices, topological indices, phenoxycarb.

Two decades ago L.Poling stated: "Today the investigation of the connection between the structure of compounds and their biological activity being the problem of great significance has been started". Poling's words seems to be more actual nowadays. Along with it a general tendency is observed i.e. the seek by means of trial-and-error method changed into purposeful, theoretically oriented work. Here we mean both empirical generalisation of the existed data and effective action of broad arsenal of contemporary theoretical organic chemistry [1-2]. It should be marked that the use of algebraic chemistry, especially the so-called method of topological indices appeared to be most effective [3-6].

One of the most interesting varieties of topological indices is modernized matrix of molecular graphs, the so-called topological index elaborated on the basis of RNB-matrix.

Generally for ABC molecule, RNB-matrix has a form:

$$\begin{array}{cccc} 1 & 2 & 3 & \\ A & B & C & \end{array} \begin{Vmatrix} Z_A & \Delta_{AB} & \Delta_{AC} \\ \Delta_{AB} & Z_B & \Delta_{BC} \\ \Delta_{AC} & \Delta_{BC} & Z_C \end{Vmatrix} \qquad (1)$$

Its diagonal elements represent ordinal numbers of atoms entering the molecules and nondiagonal ones represent multiplicity of chemical bonds. There are decimal logarithms of RNB-matrix determinant, that represent topological index, on the basis of which "probability - property" of dozen classes of chemical compounds are studied. By means of this way bioactive theoretical prediction becomes possible in case if this last one will be estimated by definite numeric characteristic.

To illustrate the above mentioned let's regard one of the biologically active compound insecticide phenoxycarb:

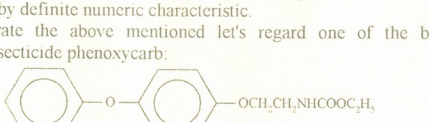

(2)

For this system the record of RNB-matrix, mainly its determinant calculation, is connected with certain difficulties even in case of EGM rapid action. (Number of atoms entering the RNB determinant in our case will be 41). In order to avoid these difficulties the so-called modernised RNB-matrix method has been elaborated, which is based on division of molecules into "unchanged" and "changed" fragments. For instance, if we are interested in dynamics of bioproperty changes while changing C_2H_5 radical by another radical then in this case the "unchanged" fragment will be the whole molecule

with subtraction of C_2H_5 group and "changed" fragment will be C_2H_5 radical itself. So the model may be written as:

$$L - R. \tag{3}$$

Its corresponding modernized matrix rank equals 2. This matrix and calculation formula of its determinant are given beneath:

$$\begin{Vmatrix} Z_L & 1 \\ 1 & Z_R \end{Vmatrix} \quad \Delta = Z_L Z_R - 1 \tag{4}$$

where

$$Z_L = \Sigma Z_l \tag{5}$$

$$ZR = \Sigma Z_r \tag{6}$$

(i.e. Z_L and Z_R are correspondingly the sums of ordinal numbers of atoms entering the L and R fragments). Obviously the simplest model permits to make certain theoretical prognosis.

In case if it is necessary to fix more completely thin structural nuances of R-radical it might be possible to use the model of averaged difficulty:

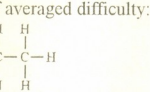

(7)

(in this case it is clear, we'll deal with the solution of 8 order determinant).

Finally by means of necessary calculations and existed bioactive quantitative data of (BA) we'll obtain linear correlation equation:

$$BA = \alpha \lg\Delta + \beta. \tag{8}$$

(As a rule, the construction of Equation (8) i.e. α and β determination occur on EGM) and this last one will help us to regard the examined properties in unity and if it is necessary their inter- and extrapolation. In order to check the efficiency of equation (8) it is necessary to calculate coefficient of r-correlation. The nearer r to the one, the higher order takes place (finally it proves the efficiency of Equation (8)).

P.Melikishvili Institute of Physical and Organic Chemistry
Georgian Academy of Sciences

Tbilisi I.Javakhishvili State University

REFERENCES

1. *C.Idoinsch, A.Leo.* Substituent Constants for Correlation in Chemistry and Biology. N.Y., 1979.
2. *D.Akhobadze.* Zogierti silicium da gogirdorganuli lactomisa da mat bazaze sintezirebuli polimerebis biologiuri aktiuroba. Tbilisi, 1996 (Georgian).
3. *R.Rouvray.* Chemical Application of Topology and Graph Theory (Ed. *A.T.Balaban*), Amsterdam, 1983.
4. *G.Gamziani, M.Gverdtsiteli.* Izomeriis movlena matematikuri kimiis tvaltakhedvit. Tbilisi, 1992 (Georgian).
5. *G.Gamziani et al.* Zogi ram topologiuri indeksebis shesakheb. Tbilisi, 1995 (Georgian).
6. *G.Gamziani, M.Gverdtsiteli.* Graphs, matrixes, determinants and their application. Tbilisi, 1996.
7. Patent 157967, cssr, 1975.
8. *N.B.Kobakhidze, et al.* Correlation "Structure-Properties" in Algebraic Chemistry. Tbilisi, 1997.

საქართველოს მეცნიერებათა აკადემიის მოამბე, 158, №1, 1998
BULLETIN OF THE GEORGIAN ACADEMY OF SCIENCES, 158, №1, 1998

T.Butkhuzi, T.Khulordava, N.Kekelidze, M.Sharvashidze, G.Natsvlishvili, E.Kekelidze

The Inversion of Conductivity Type in Wide Band-Gap Compounds A_2B_6 by Quasi-Epitaxy Method

Presented by Academician R.Salukvadze, November 18, 1997

ABSTRACT. **The possibilities of the control of the self defects concentration in wide band-gap compounds A_2B_6 by quasi-epitaxy method are presented.**

Key words: quasi-epitaxy, cathodoluminescence, ion-beam-etching, photoluminescence.

The peculiarity of the quasi-epitaxy method [1] is that the base crystal is placed in the singlet radicals atmosphere of oxygen. The concentration of radicals near the crystal is:

$$n_0 \approx 10^{14} \div 5 \cdot 10^{14}\ \text{cm}^{-3}.$$

At the first stage of growth, proceeding from the peculiarity of the basic crystals ZnS ZnSe, interstitial components of Zn are coming out on all over the crystal surface. Getting into the environment of active oxygen they are forming the first layers of ZnO. Zn atoms placed in the crystal points, are gradually taking part in creation of the following layers. Therefore in the pre-surface part of the basic crystal surplus concentration of metal vacancies is being created. Thus in the pre-surface part of the basic crystal metal concentration is decreasing.

The thickness of the layer impoverished with metal component can be determined by cathodoluminescence. Cathodoluminescence gives the possibility to study the luminescence of deep layers.

According to [2] penetration length is expressed by the formula:

$$X = 1.1 \cdot 10^{-3} \rho^{-1} [\sqrt{(1 + 2.74\ E_e^3)} - 1],$$

where X is an electron penetration length into solid body; ρ is density of material in g/cm^3; E_e is electron energy in Mev. In the case of ZnS basic crystal after removing $0.5 \div 1$ mc epilayer of ZnO at $X = 60$ mc penetration length, the cathodoluminescence spectrum coincides with the photoluminescence (PL) spectrum of initial basic crystal. Thus we may say, that in formation of $0.5 \div 1$ mc thickness epilayer of ZnO, Zn atoms diffused at least from the depth of 60 mc take part. It must be taken into account that in this case the depth determined by cathodoluminescence is not exact and in the formation of new epilayer deeper layers of basic crystal should take part. When epilayers are growing it is very important for basic crystals to have perfect surface.

It is known that mechanical processing of monocrystals causes structural destructions of surface layer of thickness of several microns. Since the chemical characteristics of A and B components of A_2B_6 binary compounds are sharply different, there is no high quality etchant for them. Besides, A_2B_6 semiconductors are characterized by strong anisotropy of binding energy between the planes. That is why the matter about possibilities of use of ion-beam-etching (IBE) method was used.

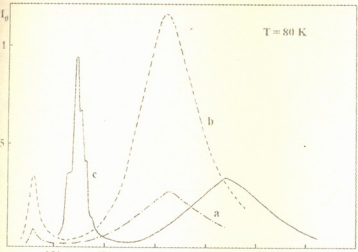

Fig. 1. The PL spectra of **a)** ZnS initial basic crystal; **b)** ZnS basic crystal after removing ZnO epilayers; **c)** epilayers of ZnO.

The PL spectra of ZnS basic crystals after chemical etching in brominemethanol and IBE were investigated. After chemical etching in PL spectrum the exciton part was suppressed, which, in our opinion, must be connected with the existence of uncontrollable impurities. The rate of IBE, unlike chemical etching, practically does not depend on lattice defects.

The electrical and optical properties of ZnS basic crystal, after removing of ZnO new epilayers, were studied. According to thermo e.m.f. measurements the surface part of the basic crystal displays the hole type of conductivity. In the PL spectrum the new bands connected with the acceptor defects appear (Fig.1). These facts are in good agreement with above represented growth mechanism.

As for the new epilayers of ZnO, their electrical and optical properties are controllable in wide limits. Under fixed concentration of oxygen radicals the decrease of growth temperature from 950°C to 350°C causes the transform of conductivity type from *n* to *p*. The decrease of temperature makes Zn extraction from the basic crystal difficult. This leads to decrease of metal concentration and consequently to suppression of electric conductivity and to appearance of hole type conductivity in new epilayers of ZnO. The inversion of conductivity type takes place at 650°C. $\rho > 10^{13}$ Ohm cm for the samples grown at this temperature. Subsequent lowering of growth temperature leads to increase of the intrinsic defect hole conductivity. The samples grown at 350°C are characterized by sharply expressed hole conductivity – $\rho \sim 10^2$ Ohm cm.

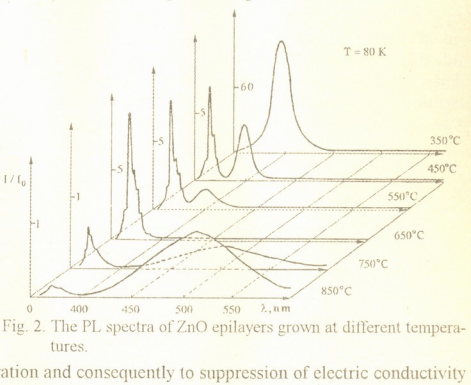

Fig. 2. The PL spectra of ZnO epilayers grown at different temperatures.

The PL spectra of ZnO epilayers grown at different temperatures are given in (Fig.2).

With temperature decrease the intensity of the exciton part of PL spectrum increases and the intensity of visible part decreases. The visible part is completely absent in the

PL spectrum of the sample grown at 650°C .In our opinion this fact speaks about high monocrystalline degree and low concentration of impurities [3].

With temperature decrease the quantity of uncontrollable impurities also decreases and the degree of single crystallinity of the built up layers increases.

Thus, the quasi-epitaxy method enables us to control electrical and optical properties of the building layers.

Tbilisi I.Javakhishvili State University

REFERENCES

1. *T.V.Butkhuzi et al.* Avtorskoe svidetelstvo №1175182, 1985 (Russian).
2. *G.G.Pankov.* Opticheskie protsesy v poluprovodnikakh. M., 1973, 456 (Russian).
3. *M.A.Elango.* FTT 17, 1975, 2356 s. (Russian).

საქართველოს მეცნიერებათა აკადემიის მოამბე, 158, №1, 1998
BULLETIN OF THE GEORGIAN ACADEMY OF SCIENCES, 158, №1, 1998

PHYSICAL CHEMISTRY

N.Kekelidze, I.Davituliani, L.Akhalbedashvili, M.Alapishvili, R.Tabidze, Ts.Sarishvili, G.Karchava

Carbon Dioxide Effect on Y-Ba-Cu-O and Bi-Sr-Ca-Cu-O Ceramics

Presented by Academician T.Andronikashvili, May 15, 1998

ABSTRACT. **The effect of CO_2 on ceramics of Y-Ba-Cu-O(I) and Bi-Sr-Ca-Cu-O(II) types at different temperatures with constant content of carbon dioxide in air phase at microflow system has been studied. It was shown that II samples are more stable to CO_2 to compare with I, but an increase in temperature causes a decrease in the time of full loss of superconductivity. Their degradation may be caused by interaction of migrating over surface alkaline-earth Ca^{2+}, Sr^{2+} and Ba^{2+} cations with water and carbon dioxide. This degradation is of irreversible nature.**

Key words: superconductor, carbon dioxide, sorption, degradation, alkaline-earth cations.

The interaction of CO_2 with ceramic materials is one of the main reasons of high temperature superconductive materials (HTSC) degradation at contact with air. The intensity of the interaction depends on chemical composition, density of samples, air environment composition, in particular the presence of water vapours [1-3], which results in the formation of $BaCO_3$, CuO and $Y(OH)_3$. The investigation of this interaction is very important not only from the point of view of chemical degradation, but also of a wide usage of carbonates as well as organic compounds in HTSC synthesis.

Therefore, it is necessary to minimize the negative effects of the carbon dioxide influence by the selection of methods and regimes of synthesis.

The paper deals with the influence of CO_2 on ceramics of Y-Ba-Cu-O (I) and Bi-Sr-Ca-Cu-O (II) types at different temperatures with the constant content of carbon dioxide in air phase. The studied samples were prepared by a traditional ceramic method with wet grinding. The oxides of the corresponding metals were taken as the initial ones. The stoichiometric mixture was thoroughly ground under the layer of absolute ethanol and calcinated at 930°C for sample I for 8 h and then cooled, pulverized and refired at 930°C resulting in a black material. Sample II was calcinated at 820°C for 30 h at air. Then the powder was pressed into circular disks with the density of 3 to 5.5 g/cm^3, sintered for 2 h at the same temperatures (950°C for I and 820°C for II), cooled to 450°C left for 4 h in flowing oxygen and then cooled slowly up to room temperature with flowing oxygen.

Yttrium samples were obtained with the content of superconductive phase about 80% and lattice parameters, characteristic of rhombic phase: a = 3.82(5); b = 3.88(9); c = 11.67(4). The single phase of Bi-containing samples was no more than 70%. The resistance of ceramics was measured by a four point probe method with the direct current. The measurements of superconductive parameters showed that for Y-samples T_c = = 94.5 K with ΔT_c = 2.2 K and for Bi-containing samples T_c = 82 K with ΔT_c = 3.8 K.

The study of carbon dioxide effect on $YBa_2Cu_3O_{7-x}$ ($x \approx 0,35$-$0,28$ from data of iodometrical titration) and $Bi_2Sr_2Ca_2Cu_3O_x$ (the oxygen content wasn't established) was

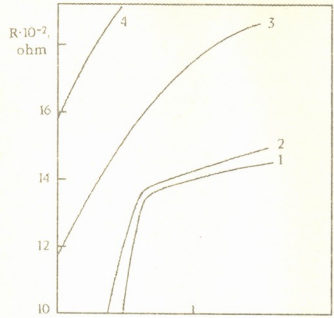

Fig. 1. The temperature dependence of resistance for initial and treated by CO_2 samples: (1)- initial $YBa_2Cu_3O_{7-x}$; (2)- treated at 25°C; (3)- treated at 100°C; (4)- treated at 400°C.

carried out at microflow vertical quartz reactor varying the temperature at a constant velocity of air stream and partial pressure of CO_2 in it. The content of CO_2 in air mixture was about 20 vol. %, but the linear velocity of it – 10 ml/min. The moist carbon dioxide was obtained by missing it through distilled water at room temperature. The change of content of gas mixture before and after reactor was fixed chromatographically using Porapak R. The loss of superconductivity was determined by the disappearance of SC transfer and Meisners effect and by the change of resistance.

The sorption of dry CO_2 (free of water vapor) was not observed, which is in agreement with data of [1]. It is known [3], that water vapor easily interacts with metal ions due to kinetic difficulties and makes their further carbonization easier.

The temperature dependence of the samples resistance practically remained constant after 6 h of treatment by carbon dioxide at 25°C (Fig.1) with the temperature increase up to 100°C. Resistance increases 1.5-2 times more and 3.5 times more for samples treated with CO_2 at 400°C. The transition into superconductive state was absent (measurements were made up to 77 K).

As it is seen from Fig.2 the curves of dependence of nonsorbed carbon dioxide at 25°C coincide for samples I and II specimens and practically don't depend on time. With an increase in temperature to 100°C and so much to 400°C the sorption of CO_2 for sample I sharply increases, while for sample II at 400°C this dependence is minimized. A decrease of carbon dioxide sorption by Bi- containing samples at 400°C may be explained by formation of carbonate layer of $SrCO_3$ and $CaCO_3$ over the surface. These carbonates aggravate further diffusion of CO_2 in the superconductor volume, the process being more difficult for samples with higher density (5.5 g/cm^3) to compare with the less dense samples (3 g/cm^3).

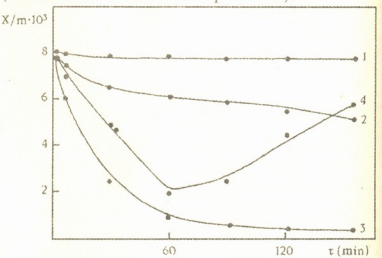

Fig. 2. The dependence of nonsorbed amount of CO_2 on time of exposure: (1)- I at 25°C; (2)-I at 100°C; (3)- I at 400°C; (4)- II at 400°C.

The Bi-containing samples are found to be more stable to carbon dioxide than those of yttrium, but an increase in temperature of CO_2 influence decreases the time of full loss of superconductivity (Fig.3). Sample I practically loses superconductivity in 20-30 min,

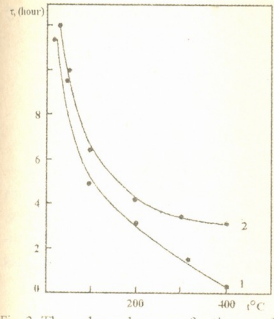

Fig. 3. The dependence of time of superconductivity loss on temperature under influence of CO_2:
1- for $YBa_2Cu_3O_{7-x}$;
2- for $Bi_2Sr_2Ca_2Cu_3O_x$.

but for sample II this time is more than 3 h, which corresponds to the literature data [4,5] on relative stability of bismuth-containing ceramic to atmospheric influence. Its degradation may be caused by the interaction of migrating over the surface alkaline-earth calcium, stroncium and barium cations with water and carbon dioxide.

It should be mentioned that the evolution of oxygen at 400°C was fixed by chromatography, though we failed to observe any regularity in oxygen release.

Thus, the sharp decrease of time of superconductivity loss with the growth of temperature is connected with the enhancement of oxygen vacancy along with the temperature increase. The loss of oxygen makes more easy the diffusion of water molecules into oxygen vacancy, than their interaction with the alkaline-earth cations, resulting in hydroxides formation. These hydroxides are affected by carbon dioxide which causes the formation of corresponding carbonates. The high temperature degradation of Y- and Bi-containing ceramics under influence of CO_2 is of nonreverse nature: further oxidative heating didn't reduce superconductive properties.

Tbilisi I.Javakhishvili State University

REFERENCES

1. *T.E.Oskina, E.D.Soldatov, I.O.Trtiakov.* Superconductivity: Physics, Chemistry, Technique. **4**, 5, 1991, 1032-1039 (Russian).
2. *O.D.Torbova, E.N.Curkin et al.* Ibidem. **4**, 11, 1991, 2242-2245 (Russian).
3. *E.A.Eremina, N.N.Oleinikov, V.I.Nefedov, A.N.Sokolov.* Journal of Union Mendeleev Chemical Sosiety, **34**, 4, 1989, 527-537 (Russian).
4. *M.Garland:* Appl. Phys. Lett. **52**, 22, 1988, 1913.
5. *N.Maeda, Y.Tanaka, M.Fukutomi et.al.* Japan, J.Appl. Phys. **27**,1, 1988, 209.

საქართველოს მეცნიერებათა აკადემიის მოამბე, 158, №1, 1998
BULLETIN OF THE GEORGIAN ACADEMY OF SCIENCES, 158, №1, 1998

N.Jlantiashvili, A.Turuta

Secondary Products of 21-Hydroxylation of 16α, 17α-Epoxy-5α-H-Pregnan-3β-ol-20-one

Presented by Academician E.Kemertelidze, January 20, 1998

ABSTRACT. **In order to get the synthesis scheme of corticosteroid preparations on the basis of local raw material tigogenin the reaction of 21-hydroxylation was carried out. The reaction of 21-hydroxylation of 16α, 17α-epoxy-5α-H-pregnan-3β-ol-20-one by means of diacetoxyiodbenzole and secondary products of this process has been performed.**

Key words: steroid, 21-hydroxylation, secondary product.

For synthesis of steroid preparations one of the main sources are 5α-H steroids. Due to the deficit of steroid raw basis the study of the possibilities of application of 5α-H-sapogenines and obtaining from them 5α-H-pregn-16-en-3β-ol-20-one in synthesis of corticosteroids has been receiving increasing attention and requires the creation of optimal schemes for this group of medical preparations. Our researches have shown that 3β-acetoxy-5α-H-pregn-16-en-20-one (I) obtained by splitting of tigonenin, local raw material at the Institute of Pharmacochemistry of the Georgian Academy of Sciences can be considered as perspective product in synthesis of corticosteroid preparations.

In the process of receiving of 16α, 17α-acetonides [1] and their 17α-thioanalogues syntheses on the basis of pregnenolone acetate (I) one of the main problems was its 21-hydroxylation realization. For this there is suggested earlier aprobated method for Δ^5-3-hydroxy and Δ^4-3-oxoanalogues [3,4], which has not been used yet for 5α-H-steroides.

Particularly, 21-hydroxylation of pregnenolone acetate (I) was realized by means of Moriartry method [5] using oxidation system $PhI(OAc)_2$/KOH/MeOH at 20°C, but this reaction appeared to be less perspective because of methanol connection competing reaction by Michael's method. It proceeds with the formation of compound mixture.

To obtain 16α, 17α-epoxy-5α-H-pregnan-3β-ol-20-one (II) we performed alkali epoxidation of pregnenolone acetate by hydrogen dioxide [6]. Using the above oxidation system epoxide (II) gives 20,20-dimethyl-acetal (III), (72%). Synthesis corticosteroids microbiological activation of A and C rings as a rule is accompanied by 20-oxo group fermentative reduction or corticoid side-chain degradation. It should be noted that by means of this very method the use of 20,20-dimethylacetal protection helped us to get rid of these undesirable processes [7].

Acetyl group [20], separates from 20-dimethylacetal in acetone with p-TsOH. The epoxide (II) transformation into compound (V) can be also realised without dimethyl-acetal (III) separation as well, by reaction mixture treatment with HCl water solution.

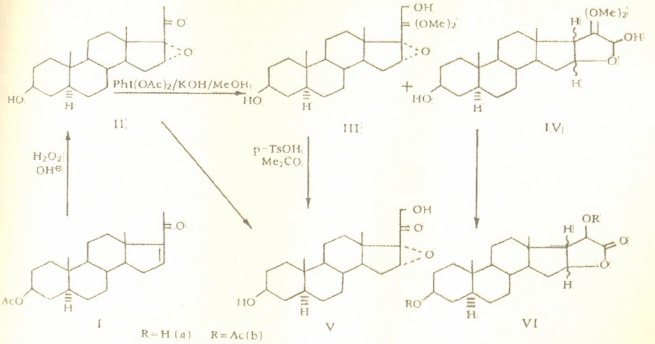

The secondary product of 21-hydroxilation of epoxide (II) is represented by more polar product 20, 20-dimethoxy-16, 21-epoxy-5α-H-pregnan-3β, 21-diol-20-on(IV) (6%). Tm = 173-180°C(MeOH). In conditions of acetal group removal this compound can easily transform into the compound (VIa), by acetilation in the presence of Ac_2O in pyridine of which compound (VIb) can be obtained.

The compound (IV) is rather unstable, which at chromatography on SiO_2 partially loses acetal group (^1H NMR spectroscopic analysis) and transforms into lactone (VIa). For compounds (IV) and (VI) the existence of cyclic structures is proved by the following arguments. The mass-spectra of isomeric products (V) and (VIa) have similar molecular peaks (m/z 348), but they differ essentially by fragmentations, which marks the absence of side-chain in compound (VIa). The same is indicated by ^1H NMR of compound (VIa), which has two interaction (J = 8Hz) protons δ 2.56 m.s (t.C-17) and δ 4.31 m.s (d.C-20). In ^1H NMR spectra of diacetat (VIb) this signal is transmitted into weak field (δ 5.14 m.s). In spectra of the compounds (VIa.b.) the triplet signal of weak field δ 5.08-5.14 m.s belongs to C-16 proton, which is connected with D' lactone cycle. The presence of this proton in the molecule is proved unammbiguously by the existence of high frequency carbonyl bands ν 1765 and 1782 cm^{-1} in IR-spectrum. The stereochemical conjugation of D and D' rings has not been established. The formation of compounds (IV) and (VIa) can be easily explained by Moriartry method of intermolecular cyclization concurrent reaction while 21-hydroxylation (with participation of epoxide cycle oxilation) [5].

The melting temperatures were determined on Kofler block. The ^1H NMR have been obtained on "Bruker WM-250" in $CDCl_3$ solution; IR-spectra are obtained by "Specord-80" by pressure of KBr; the mass-spectra are obtained on mass-spectrometer "Varian MAT CH-6". The silicagel "Silpearl" was used for preparation separating substances.

16.21-epoxy-5α-H-pregnan-3β, 20-diol-20-one (VIa).

T_m = 225-230°C (Et_2O-MeOH). IR-spectrum (ν, cm^{-1}): 1040, 1750, 1765, 3420. ^1H NMR (δ, m.s): 0.82s and 0.85s (18Me, 19Me), 2.56t(H^{17}, J = 8Hz), 3.6m (H^3), 4.31d (H^{20}, J = 20Hz), 5.08t (H^{16}, J=8Hz). Mass-spectrum, m/z: 348M^+, 330(M-H_2O)$^+$, 315(M-H_2O-Me)$^+$, 302 (M-H_2O-CO)$^+$, 289 (M-$COCH_2OH$)$^+$.

3β,20-diacetoxy-16, 21-epoxy-5α-H-pregnan-21-on-(VIb).

T_m = 190-193°C (Et_2O-MeOH). IR-spectrum (ν, cm^{-1}): 1030, 1192, 1225, 1250, 1730, 1755, 1782. ^1H NMR (δ, m.s): 0.8s (18Me, 19Me), 2.03s (3 OAc), 2.16s (20 0Ac), 2.65t (H^{17}, J = 8Hz), 4.7 m (H^3), 5.14t (H^{16}, J = 8Hz), 5.42d (H^{20}, J = 8Hz). Mass-spectrum, m/z: 390 (M-$COCH_2$)$^+$, 372 (M-HOAc)$^+$, 357 (M-HOAc-Me)$^+$, 330 (M-$COCH_2$-HOAc)$^+$, 312 (M-2 HOAc)$^+$.

I.Kutateladze Institute of Pharmacochemistry
Georgian Academy of Sciences

REFERENCES

1. *A.M.Turuta, A.V.Kamernitzky, N.V.Jlantiashvili et al.* Izv. AN SSSR. Ser. Chem., 5, 1991.
2. *N.V.Jlantiashvili, A.M.Turuta et al.* RAS. Ser. Chem., 5, 1992.
3. *A.V.Kamernitzky, A.M.Turuta, Z.I.Istomina.* Izv. AN SSSR. Ser. Chem., 8, 1986.
4. *A.M.Turuta, A.V.Julin, A.V.Kamernitzky.* Izv. AN SSSR. Ser. Chem., 8, 1988.
5. *R.M.Moriarty, L.S.John, P.S.Du.* Chem.Commun., 13, 1981.
6. *H.E.Kenney, S.Serota, E.A.Weaver, M.E.Wall.* J. Am. Chem.Soc., 82, 14, 1960.
7. *A.M.Turuta, A.V.Kamernitzky et al.* Mendel. Commun., 3, 1991.

G.Metreveli, Sh.Kunchulia

Current Cycle of Climate Change and its Influence on the Coastal Zone of Georgia

Presented by Academician Ts.Mirtskhoulava, July 16, 1998

ABSTRACT. **Climatic cycle of the Black Sea seaside zone caused cooling of the sea upper layer by 0.5-1.0°C and rise of its level – eustasy, which is the highest (ΔH = 30-50 cm) in the Poti-Supsa submerging region of Georgia. Sea cooling by the acceleration of its vertical circulation caused the reduction of recreation and vegetation seasons by 6-11 days. In the nearest future activation of the process is expected.**

Key words: climate, eustasy, sea cooling, recreation.

The current cycle of natural change of climate began in the 80s of the last century. Since 50-60s of this century the so-called "greenhouse effect" causing the intensification of warming added to it. An average increment of global air temperature was over 0.5-0.7 and the highest over 2.0°C. Most of climate change prognoses show the "greenhouse effect" activization, due to which Global air temperature in the nearest future (2030-2050) will rise by 1.5-3.0°C. It will cause serious changes in economics, ecology and other spheres of life.

According to global warming separate regions in which air temperature decreased by 0.2-1.0°C during the last decennaries (in the North and Central Atlantic by 0.2-0.5°C, in the North-Western and Southern Pacific Ocean by 0.3-0.7°C, in the Mediterranean and Black Seas by 0.5-1.0°C, etc.)are classified. Because of mosaic character of air temperature global distribution current cycle can be called climate change cycle. Its effect on environment and world economics is different [1].

Climate warming with ≈15-20 years' delay caused the rise of the World Ocean level i.e. current eustasy [3]. This phenomenon was first registered by the instrumental measuring of the sea level in the zone of glacial waters of Greenland (Aberdeen, 1896-1898). Since 1920-1980 this phenomenon spread all over the World Ocean. In the Mediterranean Sea the eustasy takes place since 1915, and in the Black and Azov Seas it does since 1925-1927 [2].

According to the instrumental observation series on the sea level the World Ocean in the process of eustasy presents different expanding cover, the level of which increases with the speed of 1.8 mm/sec in the North Hemisphere and with 1.4 mm/sec in the South.

Eustatic rise of the sea level on this cover ΔH mm/sec is the biggest in the regions where water runs from age-old resource of the Earth humidity (in the seaside zones of the Arctic and Antarctic ice sheets ΔH ≈ 4.0-7.0 mm/sec and in the mouths of the rivers the source of which is glacial, snow and rain waters ΔH ≈ 2.0-4.0 mm/sec).

The current eustasy makes serious danger for the coast of Georgia, especially for its central part between the mouths of the rivers Khobi and Supsa. This region is submerging with a speed of 4.0-5.6 mm/sec. The rate of eustatic rise of the sea level reaches ≈2.0

mm/sec. Respectively, the relative eustasy in this part is 6.0-7.6 mm/sec (60-76 cm per century). The abrasive processes rise serious problems for this part of the coast especially in Poti-Supsa region, where due to the sea transgression the seashore of 0.1-0.9 km width has already been washed down. This process will intensively go on in the nearest future (2030-2050) unless the artificial refilling of the plage takes permanent character.

The current eustasy greatly increases the probability of catastrophic flooding of the river Rioni as well, the reason of which will be the increasing eustatic inundation going on together with the general submerging of Poti-Samtredia region (Kolkheti lowland, where in 1930s flood preventive dams were built along r. Rioni. They safely protected Poti and other populated areas until 1980 s. Catastrophic flood in 1987 revealed that the distance between the tops of the dams and the river level decreased greatly due to the geologic and eustatic processes go there. It decreased so that (≈50-60 cm) in case of floods of high frequency ($p \leq 5\%$) the river can go through the dams and cause serious material damage. The danger will be increased for Poti unless the reconstruction of the dams is done and corresponding monitoring system is made.

Table

The influence of climatic current cycle on the water surface temperature on the coast of the Black Sea (1923-1955)

N	Oceanographic station	Water temperature increment, °C						Time increment, per day	
		February	September	Annual	ΔT*	Season			
						Recreation	Vegetation	Recreation	Vegetation
1	Batumi	0.1	−1.6	−0.6	−1.0	−0.4	−0.8	−11	−6
2	Bichvinta	−0.6	−0.6	−0.5	−0.9	−0.5	−0.5	−8	−10
3	Tuapse	0.0	−0.8	−0.5	−0.7	−0.6	−0.8	−13	−3
4	Novorosiisk	1.6	−0.03	0.2	0.3	−0.6	−0.7	−7	13
5	Feodosia	0.7	−0.7	−0.1	0.0	−0.2	−0.3	−9	−4
6	Jalta	−0.2	−0.1	−0.1	−0.01	0.2	0.2	−5	−9
7	Sevastopol	0.4	−0.4	−0.4	−0.9	−0.5	−0.5	−9	−5
8	Odessa	0.1	−1.3	−0.6	−0.6	−0.9	−1.2	−9	−5
average		0.3	−0.7	−0.3	−0.5	−0.4	−0.6	−9	−4

ΔT* - temperature increment is calculated by regression equation

Climate change has an essential effect on the thermal regime of the World Ocean. The result of this effect is decrease of the temperature in some of its regions, among them water surface temperature of the Black Sea which reached 0.5-1.0°C in 1923-1995 (Table).

According to the sea temperature observation series water temperature decrease is the greatest near Batumi, where the sea cooled by 1.0°C in 1924-1995. Sea cooling was especially noticed in the second half of the year ($\Delta T = -1.3$°C) and its warming in spring ($\Delta T = 0.24$°C).

Cooling of the sea surface along the coast is clearly marked during recreation and vegetation seasons. On the coast of the Caucasus, where the recreation season begins in June, i.e. when average temperature of water is over 20°C, the sea cools by ≈0.5°C. On the north coast, where season lasts until the water temperature is over 15°C, sea temperature falls by ≈0.4°C.

Temperature fall is far more intensive during vegetation period which begins in March on the southern coast and in April on the northern. During this season sea water cooled by 0.6°C.

In the coastal regions water temperature decrease caused the reduction of recreation and vegetation seasons by 9 and 4 days respectively. On the coast of Georgia recreation season lasted about 130 days in 1924-1930, it reduced to 120 days in 1975-1995. In the nearest future in case of prognostic development of the process this season will be reduced to 107-110 days.

Respectively, due to decrease of sea recreation resources Georgia will lose 7% (≈US$ 100mln) of seasonal profit per year, compensation of which will require to build a new health resort complex in the region of less ecological loading. Sea cooling in the breezing and seasonal circulation zones caused the air temperature fall. Therefore, in the west Georgia two layer climate is formed, where on the territory below ≈1000-1500 m the climate is colder and humid and it becomes warmer and dryer above. While the air temperature falls by 0.5-1.0°C in the coastal regions, the temperature in the mountain zone increases and intensive degradation of glaciers takes place.

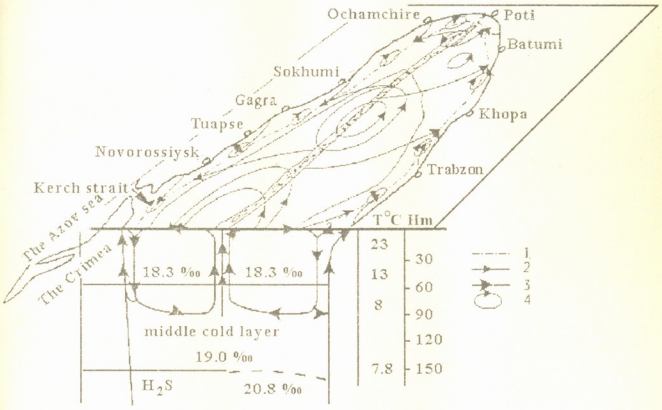

Fig. Horizontal and vertical circulation of the Black Sea:
1)convergence zone; 2)drift currents; 3)vertical circulated currents; 4)convergence rings; 5)divergence zone.

Further climate change prediction is directly connected with the change of the Black Sea thermo and hydrodynamic regimes. The present peculiarity of the sea thermodynamic regime is that the cooling of its surface layer is clearly expressed in summer and autumn, and vice versa in the first half of the year. Permanent cooling of the sea temperature in 1923-1995 shows the acceleration of the sea vertical circulation (Fig.) [4] so that the temperature of the water mass coming from the lower, the so-called middle

layer [5], is constantly less than the temperature of the atmosphere adjacent layers, as the result of which the cooling process of these layers is monotonously progressing. It will maintain this character in the nearest future (2030-2050).

Therefore, by the influence of the current cycle of the climate change in the coastal zone of Georgia there will always exist the sea thermohydrodynamic and eustatic problems of progressive character that may lead the country to serious damages. These problems are more or less acute for all the Black Sea countries. Therefore they have to solve some of them together. It especially concerns those countries, whose economy is oriented on the wide use of sea recreation resources and development of subtropical agriculture.

Tbilisi I.Javakhishvili State University Batumi State Marine Academy

REFERENCES

1. Climate change. Technical summary of the Working Group I Report. WMO, UNEP, 1995, 31-35.
2. *G.Metreveli.* In: Nato Tu-Black sea project. Ukraine, 1997, 24.
3. *R.K.Klige.* Izmenenie globalnogo vodoobmena. M., 1985, 187-195 (Russian).
4. Prakticheskaya ekologiya morskikh regionov, 1990, 25-33, 84-86 (Russian).
5. *O.I.Mamaev.* Priroda, 1996, 12, 70-78 (Russian).

საქართველოს მეცნიერებათა აკადემიის მოამბე, 158, №1, 1998
BULLETIN OF THE GEORGIAN ACADEMY OF SCIENCES, 158, №1, 1998

GEOLOGY

Academician I.Gamkrelidze, D.Shengelia

New Data on the Interrelation and Age of the Dzirula Crystalline Massif Constituting Rocks

Presented December 29, 1997

ABSTRACT. **Dzirula crystalline massif is built up of Precambrian and Paleozoic metamorphic rocks and of Precambrian and Early and Late Herzynian granitoids. New data about the interrelation and age of Dzirula massif pre-Jurassic rocks indicate polycyclical character of regional metamorphism and existence of its three stages: Precambrian and pre-Hercynian (Caledonian?) progressive and Late Hercynian regressive.**

Key words: gneiss-migmatitic complex, precambrian metabasites, polycyclical metamorphism.

Dzirula crystalline massif is mainly built up of Precambrian gneiss-migmatitic complex, metabasites and quartz-dioritic gneisses, of pre-Herzynian metabasites, of Early and Late Herzynian granitoids, of Lower-Middle Paleozoic metavolcanogenic-sedimentary (so-called Chorchana-Utslevi) complex and of closely associated with it rocks of ophiolite association(serpentinites, amphibolites,gabbros and gabbro-diabases)[1].

Mineral paragenesises of gneiss-migmatitic complex rocks correspond to facies of biotite-muscovite gneisses and low-temperature part of biotite-sillimanite-potassium feldspathic facies(here and farther the classification of metamorphic rocks is given after S.Korikovski [2]). It should be noted that by zircons from migmatites with the help of U/Pb method Early Ordovician age – 491^{+91}_{-36} Ma was obtained [3]. After some investigators [4] these data do not reflect real geological interrelation between migmatites and quartz-dioritic gneisses(see below). We think that age of migmatites-491Ma is the age of zircon which arose on later stage of regional metamorphism after forming quartz-dioritic gneisses(see below).In connection with that it should be noted that in migmatites, plagiogneisses and schists of Dzirula massif as a result of superimposed regional metamorphism the change of early high-temperature cordierite ($Cor+Bt_{Fe\text{-}Mg}$+ Sill + +Ksp+Pl±Qtz±Spi) paragenesis with more low temperature garnet ($Grt_{Fe\text{-}Mg}$+ $Bt_{Mg\text{-}Fe}$+ +Andl + Mu + Pl + Q) paragenesis is observed. At the same time collective recrystallization and neomineralization of biotite ($Bt_{Fe\text{-}Mg} \rightarrow Bt_{Mg\text{-}Fe}$) is observed. That is accompanied by appearance of numerous zircons grains inclusions in scales of neogenic biotite.

Besides in gneiss-migmatitic complex the earliest (Precambrian) manifestation of regional metamorphism in Dzirula massif is established as the rocks of this complex are intruded by Precambrian quartz –dioritic gneisses(orthogneisses) which contain xeno-

liths already metamorphozed rocks of this complex including strongly deformed plagiomigmatites and schists[5].

Almost all previous investigators attribute quartz-dioritic gneissis to Early Hercynian formations. They usually were named gneissose quartz diorites and their gnessic structure was considered primary. But in our opinion they are evidently pre-Hercynian because they have undergone metamorphism and obtained a gneissic structure before intrusion of massive quartz diorites which have indeed Early Hercynian age. Lately for zircons from melanocratic quartz diorites by U/Pb method clearly Precambrian age of these rocks – 747^{+100}_{-70} Ma was obtained[3]. To our mind it is true age of zircon of the quartz diorite premetamorphic protolith. Proceeding from these data and from above mentioned geologic considerations we can suppose that quartz-dioritic gneisses have Precambrian (Baikalian?) age and consequently gneiss-migmatitic complex is even older.

Thus in composition of the Dzirula crystalline massif two structural varieties of quartz diorites are identified: with the gneissic structure and massive ones. They are of similar mineral composition and consist mainly of quartz, plagioclase (from oligoclase to basic andesine) and biotite.Amphibole, noncharacteristic mineral of the rock, is established as a relics preserved after biotitization or as a neogenic mineral in the contact aureole of metabasites.

Quartz-dioritic gneisses are featured by extreme heterogeneity of quantitative mineral composition and abundance of inclusions. More often inclusions of metamorphosed massive gabbroids and diorites of greatly different outlines and numerous spheroidal formations(autoliths) are found.

After our observations massive quartz diorites are homogeneous rocks and heterogeneous parts occur in them comparatively seldom; autoliths are absent and are typical zonal plagioclases which are alien to pre-Hercynian complex of Dzirula massif. Massive quartz diorites often have intrusive contacts with quartz-dioritic gneisses and, what is remarkable, with metabasites of second generation. Equalizing of mineral composition of quartz-dioritic gneisses and massive quartz diorites takes place as a result of their late Hercynian granitization.

At the same time in Dzirula massif two generations of basites are present. Basites of first generation formerly was considered as Early Hercynian formation. But in our opinion these rocks (metagabbro,amphibolites) have also Precambrian age because they are present as small and large relics and xenoliths in above mentioned pre-Hercynian quartz-dioritic gneisses.It should be also noted that wide spreading of very old granificated basites in Dzirula massif was noted by many scientists. G.Zaridze, N.Tatrishvili [6] supposed that metabasites are components of "simatic basement of Paleozoic geosyncline". Thus one can conclude that the above named metabasites essentially represent relics of Precambrian melanocratic basement.

As regards the second generation of basites (regionally metamorphosed and schistose gabbros and diabases) they have pre-Hercynian (Caledonian?) age because they cut above named Precambrian quartz-dioritic gneisses and in their turn are intruded by Early Hercynian massive quartz diorites.

All the above enumerated rocks, including quartz-dioritic gneisses and Early Hercynian massive quartz diorites all over the Dzirula massif are intruded by Late Hercynian porphyraceous (so-called Rkvia facies) and equigranular potassium feldspathic granites. Argon age of K-feldspathic granites changes from 270-305 to 325-335 ± 10 Ma [3,4].

Among the Late Hercynian microcline granitoids there are distinguished:

1. Granitization products of quartz-dioritic gneisses and other old rocks(crystalline schists, para-plagiogneisses, plagiomigmatites, amphibolites, metabasites). They represent hybrid heterogeneous, microclinized, bimicaceous, porphyroblastic granitoids [6,7].

2. The second group of granites comprises magmatic massive, equigranular, homogeneous(eutectic) granites. Herein the potassium feldspar is mainly represented by lattice microcline.

According to mineral composition the first two groups of granitoids differ only by much more leucocratic composition and also by homogeneity of the second group granites.

3. The third group of the Dzirula massif granites are represented by coarse-grained porphyraceous granites of the so-called Rkvia intrusion. According to R.Manvelidze [7] in Rkvia intrusion granites porphyraceous segregations of potassium feldspar are represented by intermediate orthoclase.

But in the groundmass lattice microclines and also low and intermediate orthoclases are found.

Some investigators bind up granitization of Dzirula massif crysstalline rocks with Rkvia intrusion. To our mind regional granitization of pre-Hercynian crysstalline basement most likely is conditioned by formation of eutectic group of potassium granitoids.

The latest manifestation of regional metamorphism, which coincides with the formation of Late Hercynian granites, had a retrograde character and was accompanied with the generation of greenschist facies low temperature minerals: lattice microcline, albite, muscovite, chlorite, actinolite, tremolite, minerals of epidote group.

Thus the above given considerations about the interrelation and age of Dzirula massif pre-Jurassic rocks indicate polycyclical character of the regional metamorphism and existence of its three stages: Precambrian (Baikalian?) and pre-Hercynian (Caledonian?) progressive and Late Hercynian regressive. The conditions of the oldest (Precambrian) regional metamorphism reached the biotite-sillimanite-potassium feldspathic facies(high temperature part of amphibolite facies) of metamorphism. Second stage of progressive regional metamorphism which touched on Precambrian gneiss-migmatitic complex,quartz-dioritic gneisses and metabasites of first generation, after metamorphism conditions corresponds to facies of biotite –muscovite gneisses (low and middle temperature part of amphibolite facies).

Side by side with the above mentioned pre- Jurassic rocks in Dzirula massif highly peculiar rocks of exotic composition – potassium feldspathic gabbros, which are usually termed as "ricotites", are present.

Some investigators believe that K-feldspathic gabbro are pre-Hercynian basites remade under the influence of Late Hercynian or Jurassic granitoids. Others connect their formation with assimilation of Paleozoic granitoids by ultrabasic magma considering

the latter as Upper Paleozoic rocks. In our opinion the most acceptable is the scheme suggested by I.Khmaladze (unpublished data) which we share with some specifications. According to this scheme K-feldspathic gabbro is formed as a result of deep assimilation and belongs to the Bathonian intrusion group.

It is to be supposed that initial magma of K-feldspathic gabbro was basic magma, crystallization products of which were presented by pyroxene gabbro with mineral composition – labrador- bytownite and clinopiroxene. This magma was generated at the depth more than 30 km significantly later than the formation of Late Hercynian microcline granites. Most likely generation of basic magma preceded the granitic magmatism manifestation which was connected with Bathonian orogenic phase and took place synchronously with activity of Bajocian volcanism.

A.Janelidze Institute of Geology
Georgian Academy of Sciences

REFERENCES

1. *I.Gamkrelidze, G.Dumbadze, M.Kekelia, I.Khmaladze, O.Khutsishvili.* Geotectonica, 5, 1981, 23-33 (Russian).
2. *S.Korikovski.* Petrology of metamorphic complexes of the Greater Caucasus. Moscow, 1991, 232 (Russian).
3. *Ve.Bartnitsky, O.Dudauri, L.Stepanyuk.* Fifth Working Meeting Isotopes in Nature. Proceedings. Leipzig, 1990, 1-10.
4. *O.Dudauri, M.Togonidze, G.Vashacidze, K.Bacuridze.* Theses of anniversary session of Geological Institute of Georg. AS, Tbilisi, 1995, 29-30 (Russian).
5. *I.Gamkrelidze.* Mechanism of tectonic structures formation and some general problems of tectogenesis. Tbilisi, 1976, 225 (Russian).
6. *G.Zaridze, N.Tatrishvili.* Trudy Geol. Instituta AN GSSR, mineral.-petrograph. ser. 3, 1953, 33-79.
7. *R.Manvelidze.* Geologic. – petrographical significance of potassium feldspars from Georgian granitoids. Trudy GIN AN GSSR, 81, 1988, 124.

საქართველოს მეცნიერებათა აკადემიის მოამბე, 158, №1, 1998
BULLETIN OF THE GEORGIAN ACADEMY OF SCIENCES, 158, №1, 1998

STRUCTURAL MECHANICS

T.Batsikadze, V.Tarkhnishvili, D.Tabatadze

Reduction of a Plane Problem to the Integration of Ordinary Differential Equations for the Analysis of Plates Weakened by Holes

Presented by Corr. Member of the Academy I.Ghudushauri, March 16, 1996

ABSTRACT. **An orthogonal analytical method of solving the title problem is proposed which has been developed by using the elasticity theory in differential equations together with the theory of complex variable functions. Unlike the analogous method developed by the authors earlier instead of numerical method of finite elements the elasticity theory in ordinary differential equations has been used.**

Key words: plate, stresses, holes.

The problem of determining the stressed and strained condition of the plates of any contour weakened by several small circular holes is considered. To solve the problem by means of analytical methods developed on the basis of classical theory of elasticity is connected with great mathematical difficulties. Therefore, nowadays it is considered to be reasonable to use numerical methods, in particular, the methods of finite and boundary elements [1-4].

The method of finite elements can be considered ineffective because around the holes, where the increase of gradient of stresses is expected, the net of finite elements narrows and the order of system of algebraic equations increases greatly. Besides, while forming the matrix of global stiffness its singularity may take place, i.e. the system determinant approximates to zero [4] and also precision of the results of calculations will be reduced by replacing the curvilinear contour of the plate with broken contour.

As to the method of boundary elements, it requires to perform a great deal of arithmetical operations, but for its compensation the series of the system of algebraic equations obtained this way is lower than in the case of finite elements method [2].

The problem given in the paper is solved in two stages as it was solved earlier [5], but at the first stage instead of numerical method of finite elements any analytical method, competitive (as regards to mathematical simplicity) with the above mentioned numerical methods, is to be used with account of modern level of computing techniques. And at the second stage around the holes, where the increase of gradient stresses is expected, the methods of complex variable theory has been used [6]. At present the elasticity theory of ordinary differential equations can be considered to be such competitive analytical method [7]. Just this method has been used in the present work.

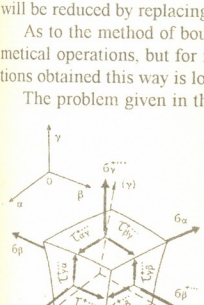

Fig. 1.

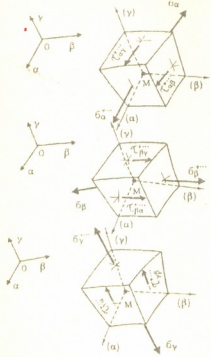

Fig. 2.

Real work of an infinitesimal T body (Fig. 1) is represented in the form of joint action of the similar infinitesimal T_α, T_β, T_γ elements of its geometrically adequate three fictitious system, out of which each can act on tension (compression) and shift only in one direction (Fig. 2). Their interaction is marked by reaction efforts (forces and moments), whose sought functions are preliminarily interpolated in the form of the following infinite series:

$$y^i = \sum_m^\infty \sum_n^\infty \sum_k^\infty A^i_{m,n,k}\, \varphi^i_n(\alpha) f^i_k(\gamma) + \\ + \sum_{j=1} \left[\xi^i_j(\alpha)\eta^i_j(\beta,\gamma) + v^i_j(\beta)\mu^i_j(\alpha,\gamma) + \lambda^i_j(\gamma) g^i_j(\alpha,\beta) \right], \quad (1)$$

where y^i is the i-effort of interaction, $A^i_{m,n,k}$ are the sought constant coefficients, φ'_m, ψ'_n, f'_k are any interpolating functions being continuous together with their derivatives within the area of T body; α, β, γ are orthogonal curvilinear coordinates. As to the single-order series, in every concrete problem out of three addends only one is preserved or all of them are admitted to be equal to zero.

One coordinate dependent function of each addend satisfies the conditions of the above mentioned interpolating functions, and two-coordinate dependent function is defined by means of corresponding boundary condition.

Another important property of the theorem greatly simplifies the problem of correct satisfaction of any boundary conditions for the analysis of shells and plates. In particular, inner tangential stresses belong to the number of T_α, T_β, T_γ interaction efforts of fictious systems, therefore, their sought functions are preliminarily represented in the form of series (1) of the same kind [7].

As to the second stage of analysis determining the concentration of stresses around the holes, it is principally the same as in [5], where only the part of the plate containing the hole is represented. In contrast to the earlier approach [5] any part of the plane of either size and contour can be analyzed, as the displacements of inner stresses acting on the contour can be easily calculated by means of the first stage.

Example. A plane problem for thick circular arch (Fig.3) with fixed abutment points [7] is considered. The arch is affected by uniformly distributed radial loading P = const. The results of solution of this problem for b_r and b_Q inner stresses obtained by means of performing the two above-mentioned stages are given in Fig.4 in the form of their epures. To illustrate the concentration of stresses around the holes the two radial sections are considered. One of these sections passes through the hole and the other, not containing

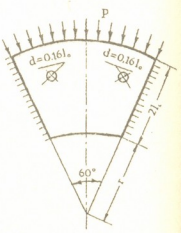

Fig. 3.

a hole, passes symmetrically to it.

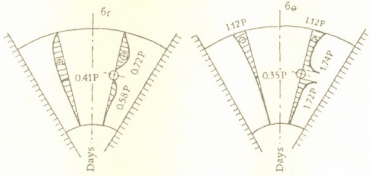

Fig. 4

On the basis of the data obtained it can be concluded that the given analytical method of plane problems represents a real picture of stress-strain state of the plate and it is found to be far more effective than the method proposed in [5].

Georgian Technical University

REFERENCES

1. *L.Berenji, R.Baterfild.* Metody granichnykh elementov v prikladnikh naukakh. M., 1984, 494 (Russian)
2. *K.Berrebiga, C.Uoker.* Prikladnye metody granichnykh elementov v tekhnike. M., 1982, 248 (Russian).
3. *O.Zenkevich.* Metod konechnikh elementov v tekhnike. M., 1975, 541 (Russian).
4. *G.Strench, J. Fiks.* Teoriya metoda konechnykh elementov. M., 1977, 349 (Russian).
5. *V.A.Tarkhnishvili.* Raschet tonkikh uprugikh plastin I obolochek s otverstiyami. Tbilisi, 1990, 222 (Russian).
6. *N.I.Muskhelishvili.* Nekotorye osnovnye zadachi matematicheskoi teorii uprugosti. M.-L., 1949, 635 (Russian).
7. *I.I.Ghudushauri.* Teoriya uprugosti v obyknovennykh differentsialnikh uravneniyakh. Tbilisi, 1990, 448 (Russian).

METALLURGY

A.Bichinashvili, M.Zviadadze, T.Mkhatrishvili, V.Achelashvili.

The Peculiarities of Premartensite Structure Unstability on γ-Mn Basis.

Presented by Corr. Member of the Academy G. Tsagareishvili, December 22, 1998

ABSTRACT. **In the following work the phenomenon of premartensite structure is theoretically studied, particularly, the abnormal behavior of the average importance of the atom substitution, microtensions and Ioung's module are indicated.**

It is supposed that the abnormal behavior of the above-mentioned parameters is caused by the structural and magnetic interaction.

Key words: electrochemical system, electromagnetic radiation, radiowaves, vector-potential.

The martensite transformation close to the second phase transition, proceeds the changes of the initial crystal structure, related with the reduction of steadiness of the crystal polisade to the transformation of the shear in the areas of Ms temperature of the martensite transition [1]. The situation changes if martensite transformation is caused by magnetic regulation, as there can not be observed the structural changes above Tn temperature of this regulation [2].

In the γ-Mn alloys fcc-fct martensite transformation is realized as the result of antipheromagnetic regulation, which is adequate to fcc-fct transition in In-Tl alloys, where in the Ms area [2], the loss of steadiness of cubic structure is evidently observed. That is why we expect the same phenomenon to occur in γ-Mn alloys.

Binar alloys Mn-Cu (Cu ≤ 20%), Mn-N_i (N_i ≤ 20%) and Mn-Fe (Fe ≤ 30%) were examined for this purpose.

Fig.1 presents the dependence of the intensive relativity logarithm

$$\alpha = \ln I(T) / I(T=550k)$$

for difrective ranges on the temperature {800} for the range Mn-Cu (78.6 at. % Mn) from the alloys of γ- phase. As seen from Fig. on the high temperature (T>Ms) the mentioned value increases rectilinearly up to ≈300k temperature. In the ≈100k interval by Ms the deviation occurs in rectilinear dependence because α also depends on the changes of atoms.

$$\alpha=[\langle u^2 (T=550k)\rangle-\langle u^2(T)\rangle]k^2, \qquad (1)$$

where k is the module of difrective vector.

The above-mentioned phenomenon is evidently caused by changes of the average atom deviation indicating the reduction of reciprocity between the atoms. The same reduction occurs in Ms areas by tetragonal disfiguring in cubic polisade which in its turn

gives reason for appearing the microtensions observed during experiment as the expansion of difrective ranges.

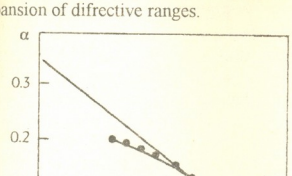

Fig.1

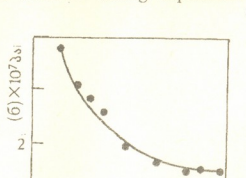

Fig.2

Fig.2 gives the changes of average significance of the microtension $<\sigma>$ caused by temperature when T>Ms is calculated by the following formula [3]

$$<\sigma>=\beta/tg\cdot\theta 0\cdot E/4, \qquad (2)$$

where E is Ioung's module, $\theta 0$ - Breg's angle and

$$\beta=0,5\ [B-b+\sqrt{B(B-b)}]\ . \qquad (3)$$

B and b are breadth of difrective ranges caused by disfiguring of standard specimen taken from semi-heights. The standard specimen are Mn-Cu (39 at. % Mn) alloys, where fcc→fct transformation does not occur. Specimen was Mn-Cu (78,6. at. % Mn) chilled from γ phase in the alloys where tetragonal transformation takes place at the low temperature (Ms ≈ 250K). Microtensions created by the tetragonal areas in cubic structure carries anisotropic character as the maximum disfiguring occurs in <100> direction, that is why the measurements have been carried out at {400} on difrective range. As seen from Fig.2 above Ms temperature, at ≈50K interval $<\sigma>$ changes occur caused by antiferomagnetic regulations in the local areas. The latest caused tetragonal disfigurings, in the mentioned areas, which increased the quantity and value of microtensions in cubic structure.

The magnetic regulations in the local areas have been observed during experiment in Mn-Ni (20.at.% Ni) alloy's by neotronographic method [4] by reflecting areas. These areas cause diffusal maximums. The authors of this work explain local magnetic regulation in γ-Mn alloys by existing of exchanged interaction energy in magnum atoms. This interaction influences the changes in mechanic features.

We have calculated the meaning of the E in Ioung's module at different temperature in Mn-Fe (76 at. % Mn) chilled from γ- phase. We have calculated E by means of the famous formula

$$Ehkl=\nu <\sigma> (\Delta\alpha/\alpha)_{hkl} \qquad (4)$$

where ν is Poison's coefficient.

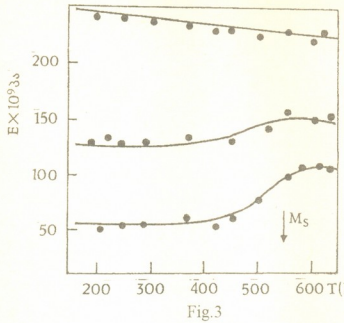

Fig.3

Fig.3 shows the changes of loung's module caused by temperature, in different crystallographic directions, where E changes carry antisotrophic character. E <111> module, the value being twice more that of E <110> at the room temperature and four times more than E <100> at the room temperature, changes normally. E reduces by increasing the temperature. E changes anomalously in Ms area in <110> an<100> directions. E relative anomalous changes in <100> direction is twice more, than in <110> direction. We got the adequate results in Mn-Cu and Mn-Ni alloys. The fact for E being antisotrophic is probably caused by antisotrophic distribution of manganum atoms and also by different directions. Besides the exchanged interaction by Ms in cubic structure causes tetragonal disfiguring, arranged without order, as the value for these areas is not sufficient for fcc→fct transformation. We get general cubic polisade for tension, observed by broadening of difrective ranges. {h00} difrective ranges in comparison with {hko} and {hkl} ranges broaden mostly. Thus, we must take into consideration the structural disfiguring contribution with magnetic contribution in changes of loung's module.

Technical University of Georgia

REFERENCES

1. *E. N.Estrin.* In: Martensitnye prevrashenia. Kiev, 1978, 29-32 (Russian).
2. *P.Makhurane, P.Caunt.* J. ply. C. Solid state phys., **2**, 6, 1969, 959-965.
3. *V. I. Iverinova, G. P. Revkevich.* In:Teorii Rasseyanya rentgenovskikh luchei. M., 1972, 123-127 (Russian).
4. *S. A. Demin.* Fizika metallov i metalovedenia. , **67**, 4, 1989, 775-781 (Russian).

საქართველოს მეცნიერებათა აკადემიის მოამბე, 158, №1, 1998
BULLETIN OF THE GEORGIAN ACADEMY OF SCIENCES, 158, №1, 1998

METALLURGY

D.Jishiashvili, E.Kutelia, B.Eristavi, V.Gobronidze, K.Tskhovrebashvili

Auger Electron Spectroscopy Study of the Amorphous GeO_x Film Structure

Presented by the Academician G.Gvelesiani, October 30, 1997

ABSTRACT. **Ge LMM Auger peak shows relatively large change in chemical shift with change in oxidation state and there are 4 oxidation states observed corresponding to Ge-Ge_yO_{4-y}, y = 1, 2, 3, 4 tetrahedra. A computer analysis was used for curve fitting and finding the constituents of the experimental Ge LMM Auger peaks. Despite the chemical composition the AES results presented in this study yield additional information relative to the homogeneity, local atomic environment and chemical bonding in the germanium suboxides.**

Key words: Auger spectroscopy, structure, amorphous, film, germanium, oxide.

Auger electron spectroscopy was developed as a tool for analyzing the chemical composition of solid materials. During last decade this method was successfully used also to obtain information about the local atomic bonding of constituent elements and phase separation in solids [1]. In such case the method is based on the changes in energies and peak lineshapes for atoms in different chemical environment. This type of analysis is still at the initial stage of development, but it is of significant importance particularly for amorphous materials, as the main characteristic of their structure is the short range order and hence the local atomic structure and the type of chemical bonds.

The purpose of this work was to show the capabilities of AES to determine the local atomic bonding, chemical composition and structure of the amorphous GeO_x films. We have examined the systematic changes in AES spectra, at various stages of oxidation of Ge. The results cover the whole range from Ge to GeO_2.

GeO_x films has attracted our attention as prospective materials for the surface passivation of GaAs. The films where deposited on Si substrate by the reactive ion-plasma technology. The AES spectra were obtained using a Riber LAS-2000 spectrometer operated at 10^{-10} Torr backpreasure . The measurements were performed with the cylindrical mirror analyzer (energy resolution - 0.3%, modulation amplitude - 1 V) at 3 KeV primary beam energy. Ge $L_3M_{45}M_{45}$ Auger transition was studied , which was recorded in the form of the first derivative. The data acquisition sequence will be discussed later. The composition of the films was estimated by the Rutherford backscattering method with the accuracy of 5 at.%.

Like some other 3rd band elements (Ga, Cu, Zn) Ge also preserves the quasiatomic nature of its LMM Auger transition during the oxidation [2]. So the peak lineshape established for pure Ge (Ge-Ge_4 tetrahedrons) will hold true also for GeO_2 (Ge-O_4 tetrahedrons). This result is very useful when modelling the experimental Auger peak and finding its components.

The instrumental distortions were taken into account by measuring and analyzing the LMM peaks for two margin compositions: Ge and GeO_2. Comparison of our data with those available [2] show that the peak parameters (the intensities and energies of ^1S, ^1G, ^3P, ^1D, ^3F terms) are in good agreement with the theoretical data, but slightly differ from them for the value of the full width at half maximum (FWHM). So for the curve fitting the peak lineshape determined on our own instrument was used instead of those published elsewhere.

According to theoretical model [3] in the homogeneous GeO_x the bonds must be chemically ordered i.e. an equilibrium structure must contain only Ge-O and Ge-Ge bonds. The appearance of O-O bonds will be restricted. The structure of film contain only one type of tetrahedron in the following two cases: 1. x = 0, pure Ge with $Ge\text{-}Ge_4$ tetrahedron; 2. $x = 2$, pure GeO_2 with $Ge\text{-}O_4$ tetrahedron. The structures of all other homogenous intermediate compositions can be described as a random network containing 5 types of $Ge\text{-}Ge_yO_{4-y}$, $y = 0, 1, 2, 3, 4$ tetrahedra. For a given composition the concentration of each tetrahedron is determined by its statistical weight factor which depends on x [4].

For the different oxidation states of Ge atom ($y = 1, 2, 3, 4$) the Ge-O bond becomes more and more ionic as the stoichiometric GeO_2 structure is approached. This causes the energy shifts of the Auger peaks from 1147 eV for Ge - Ge_4 to 1139 eV for Ge - O_4. Also the peak broadening is observed in the range of 7.70 - 6.46 eV. It is obvious, that each tetrahedron has its specific energy and FWHM. We assume, that these values are changing linearly with y. The validity of this assumption was proved by all of our following results. The same assumption was proved to be true when analyzing the photoelectron spectra [5]. It is clear that the net experimental Auger peak of homogeneous GeO_x is the superposition of these five peaks.

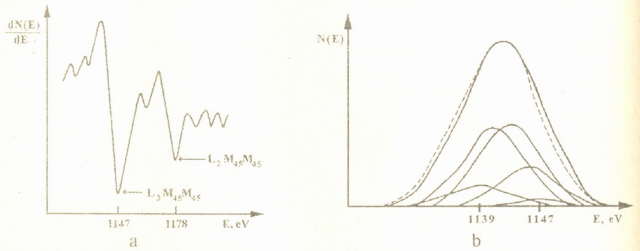

Fig. 1. (a) AES derivative spectrum of Ge $L_3M_{45}M_{45}$ transition obtained from $GeO_{1.3}$ film. (b) The same spectrum after integration and background subtraction (broken line), its five components and their sum (solid line).

GeO_x films with different composition were analyzed. The concentration of Ge and O i.e. x was determined by the Rutherford backscattering method with the accuracy of 5 at.%. The experiments were carried out in a following sequence: for the definite GeO_x film Ge LMM Auger transition spectrum was recorded in the form of the first deriva-

tive EdN/dE. At the following stage 5 peaks, corresponding to Ge-Ge_yO_{4-y}, $y = 0, 1, 2, 3, 4$ tetrahedra, with their characteristic energies and FWHM were found and fitted to the experimental spectra by using a nonlinear least squares method. For each constituent peak the integrated area was estimated which corresponds to the relative concentration of a given tetrahedron in GeO_x. This parameter was compared with the theoretically calculated statistical weight and the deviation was evaluated.

For the film with $x = 1.3$ the germanium $L_3M_{45}M_{45}$ Auger transition peak before and after integration and background subtraction is presented in Fig.1,a,b. The five constituent peaks are also shown and the solid line corresponds to their sum. The calculated peak areas were compared with the statistical weights, estimated by the method described in [4]. Relatively good agreement was found indicating that in $GeO_{1.3}$ the Ge-Ge_yO_{4-y}, $y = 0, 1, 2, 3, 4$ tetrahedral are statistically distributed and its structure is homogeneous . Such a structure is observed for GeO_x films with the compositions in the range of $2 \geq x \geq 1.3$.

For the films with $1.3 \geq x \geq 0$ the decrease of oxygen content leads to the subsequent enrichment of the structure with the overstatistical tetrahedra. Each of the Ge-Ge_yO_{4-y}, $y = 2,3,4$ tetrahedron takes in turn its maximal overstatistical value until the pure Ge is reached but they does not form any new separated phase. These films remain homogeneous as it is evidenced by the X-ray diffraction and transmission electron microscopy data. The pure statistical distribution of tetrahedrons was not observed. We assume that the appearance of overstatistical tetrahedra is due to the nonequilibrium structure which is known to form during the film deposition at low substrate temperatures.

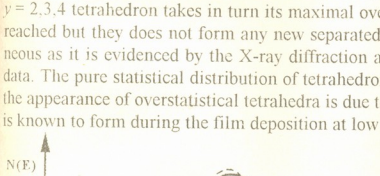

Fig. 2. Experimental AES spectrum of the two phased GeO_x film (broken line), its two component peaks corresponding to Ge - Ge_4 and Ge - O_4 tetrahedra and their sum (solid line).

A total amount of tetrahedra was estimated and then the concentrations of Ge and O atoms were determined. These results were compared with the Rutherford backscattering data. These two values coincide with ±3at.%. As it was mentioned above the accuracy of the Rutherford method was 5at.%, so the accuracy of our approach for quantitative analysis of GeO_x films will be with ~10 at.%. It is worth noting that the concentration of oxygen was deduced in an indirect way by its influence on the Ge LMM Auger transition.

A totally different spectrum was observed for the nonhomogeneous GeO_x film. Fig.2 shows the Ge LMM peak for the two phased film which was deposited pyrolytically at 350°C. The same structure was obtained also for the GeO_2 film after 3 KeV electron bombardment at a fluence level of $3 \cdot 10^{16}$ cm^{-2}. The experimental Auger peak can be resolved into two constituent peaks corresponding to Ge - Ge_4 and Ge - O_4 tetrahedra. Decreasing the oxygen content in the film leads to the decrease of the oxygen related peak intensity but the appearance of the intermediate Ge-Ge_yO_{4-y}, $y = 1,2,3$ tetrahedra

was not observed at any x. It is clear that these films are two phased and contain GeO_2 and Ge phases. This was also proved by the transmission electron microscopy. It was found that films consist of Ge clusters ~ 3-10 nm in size, which are scattered in the amorphous GeO_2 matrix.

On the basis of experimental results the following conclusions can be drawn:

- Auger spectroscopy can be successfully used to study the local chemical environment, deviation from homogeneity and phase composition of GeO_x films;
- Ge LMM Auger peak energy and lineshape is strongly influenced by the presence of the oxygen. Due to this fact the concentration of O can be calculated through the Ge Auger peak without analyzing the oxygen Auger transition.

This work has been supported by Grant G-059 from the International Science and Technology Centre.

Institute of Cybernetics
Georgian Academy of Sciences

Republican Center for Structural Investigations
Georgian Technical University

REFERENCES

1. Practical surface analysis by Auger and X-ray spectroscopy. Edited by *D.Brigs* and *M.P.Seach*. John Wiley & Sons. Chichester. New York. Brisbane. Toronto. Singapure. 1983.
2. *E.Antonides, et al.* Physical Review B, **15**, 4, 1977,669 - 1679.
3. Amorphous semiconductors. Edited by *M.H.Brodsky*. Berlin. Heidelberg. New York. 1979.
4. *L.Schumann, et al.* Physica Status Solidy (b), **110**, 1982, K69 - K73.
5. *D.Schmeisser, et al.* Surface Science, **172**, 1986, 455 - 469.

Z.Mushkudiani, J.Jaliashvili, N.Gvamberia, A.Gabisiani

Gases and Non-Metal Inclusions in Steel Treated by Nitrogen and Hard Slag-Making Mixture

Presented by Corr. Member of the Academy I.Baratashvili, October 20, 1997

ABSTRACT. **It is ascertained that simultaneous treatment of liquid metal in ladle by hard slag-making mixture and gaseous nitrogen blowing through provides a decrease in general quantity of oxygen and non-metal inclusions and a slight increase in nitrogen. The difference between variants of steel treatment by phase analysis of non-metal inclusions is not observed.**

Key words: non-metal inclusions, gas, steel, slag-making mixture.

The treatment of liquid steel in ladle by inert gases and hard slag-making mixture is widely spread at many metallurgical plants [1-3]. But the study of quality of such a tretament requires a complete and thorough research.

The present work reports on the research results of the influence of hard slag-making mixture and nitrogen corning from casting slide gate on the change of gases content in metal, quality of non-metal inclusions and morphology in conditions of steel-making shop of Rustavi Integrated Iron and Steel Works.

Melting, deoxidation and casting of tube steel of brands 20/45 were carried out in the open-hearth furnace in accordance with the technological instructions. Two series of metal melting, control and experimental, were carried out by means of hard slag-making mixture and gaseous nitrogen blowing through.

In the capacity of slag-making mixture were used: quick-burned lime (60%), fluorspar (20%) and the production remainder of secondary aluminium (20%). This mixture weighing 1.5 tonn (or for 7.5 kg/tonn of metal) was placed beforehand on the bottom of ladle and then heated up to 600°C.

The gaseous nitrogen was blown through after metal tapping till slag appearance. The flow rate of nitrogen before filling half of the ladle constituted 30-50 m^3/hour, after filling 100-150 m^3/hour.

In order to research gas and non-metal inclusions, metal samples were taken from ladle and ingot mould by special devices. The samples were taken from the ladle before steel deoxidation (sample N1), after deoxidation (sample N2), at 2/3 height of ladle (sample N3), at 3/4 height of ladle (sample N4), after filling and termination of tapping. Metal samples were also taken from the ingot mould to the third bottom of casting compound (sample N6).

In the above-mentioned samples the quantity of gases (oxygen and nitrogen) was calculated by "Leko TC-136" devices and the non-metal inclusions complex research was carried out by means of metallographic, microchemical, petrographical and spectral methods.

The quality and quantity results of microchemical analysis of melting of the 1st and 2nd series steel 20,45 are given in the Table.

Table

The quantity (%) of gases and non-metal inclusions in metal and their composition

Steel grade	No of samples	Oxygen	Nitrogen	Non-metal inclusions	Silicates	Spinels
20	1	0.0087	0.0060	–	–	–
		0.0081	0.0059			
	2	0.0104	0.0074	0.0189	41.35	58.65
		0.0086	0.0067	0.0164	59.24	40.76
	3	0.0089	0.0064	0.0201	39.67	60.33
		0.0073	0.0061	0.0157	53.13	46.87
	4	0.0078	0.0049	0.0063	36.52	63.48
		0.0062	0.0056	0.0135	49.07	50.93
	5	0.0062	0.0046	0.0122	32.47	67.53
		0.0053	0.0053	0.0104	46.86	53.14
	6	0.0058	0.0044	–	–	–
		0.0041	0.0049			
45	1	0.0081	0.0064	–	–	–
		0.0063	0.0064			
	2	0.0098	0.0070	0.0177	40.54	59.46
		0.0072	0.0072	0.0123	60.34	39.66
	3	0.0087	0.0059	0.0172	38.14	61.86
		0.0095	0.0068	0.0119	57.45	42.55
	4	0.0075	0.0050	0.0144	35.71	64.29
		0.0044	0.0066	0.0096	51.67	48.33
	5	0.0062	0.0045	0.0113	31.53	68.42
		0.0038	0.0059	0.0074	48.89	51.11
	6	0.0052	0.0041	–	–	–
		0.0033	0.0055			

The indicator of control melting is in numerator
The indicator of experimental melting is in denominator

From the results of the analysis it follows that the treatment of tube steel in ladle by slag-making mixture and gaseuos nitrogen enables us to reduce oxygen concentration for steel 20 by 0.0040% and for steel 45 by 0.0030% and provide diffusion annealing with this component (oxygen). The nitrogen quality analysis result shows that the metal of experimental melting is characterized by slight increase in content of nitrogen unlike the metal of control melting. For steel 20 this increase constitutes 0.0003%, whereas for steel 45 it is equal to 0.0009%. The increase of nitrogen till indicated quantity does not entail changes in quality and quantity characteristics of metal [4].

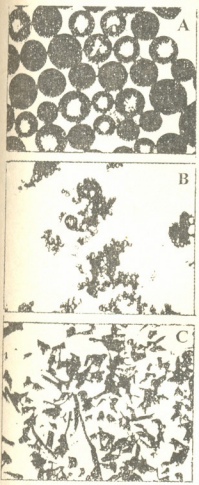

Fig. Non-metal inclusions in metal: silicones (A), spinel (B) and sulphides (C)

In accordance with the results of microchemical analysis of non-metal inclusions it is ascertained that simultaneous treatment of liquid metal in ladle by hard slag-making mixture and gaseous nitrogen decreases the general quantity of non-metal inclusions in tube steel of both grades, in steel 20 by 0.0029% and in steel 45 by 0.0048%. In the 2nd series samples of melting there is an equal distribution of non-metal inclusions in ladle space with a tendency towards decrease whereas in the 1st series metal samples such a distribution is not observed. According to the phase analysis of non-metal inclusions the content of silicate in the metal of the 2nd series samples is increased: in steel 20 approximately up to 15% and in steel 45 approximately up to 18%. Experimental melting of both series is characterized by tendency towards decrease in quality of silicate.

The nature and morphology of non-metal inclusions were studied at the precipitate received by means of anodic dissolution of metal samples and at the metallographic specimens. The main types of non-metal inclusions were ascertained:

Oxides – globule form silicates of large, mediate and small sizes, often of glassy and seldom of crystal structure (Fig. A) and with the dispersive inclusions of crystal form spinel which are optically anisotropical.

Sulphides – small, cornlike species of different shapes (of dendrite, thickened spoke, and round) generally in the form of $FeS \cdot MnS$, often with predominance of MnS (Fig. C).

Therefore, we can make the following conclusion: the treatment of liquid metal by hard slag-making mixture and gaseous nitrogen blowing through provides a decrease in the general quantity of oxygen and non-metal inclusions in metal and a slight increase in nitrogen. The difference between variants of steel treatment by phase analysis of non-metal inclusions is not observed.

F.Tavadze Institute of Metallurgy
Georgian Academy of Sciences

REFERENCES

1. *S.C.Voinov, A.T.Shalimov et al.* Rafinirovanie staly sint. shlakamy. 1970 (Russian).
2. *A.V.Kuklev, U.N.Surovoi et al.* Teoret. osnovy vnepechnoy obrab. staly. 1986 (Russian).
3. *N.O.Gvamberia, A.N.Lomashvili et al.* Stal, **9**, 1986, 36-38 (Russian).
4. *V.V.Averin, A.V.Rivekin et al.* Azot v metallakh. M., 1976 (Russian).

AUTOMATIC CONTROL AND
COMPUTER ENGINEERING

A.Lashkhi, I.Badagadze

Some Aspects of System Analysis for Informative Processes

Presented by Corr. Member of the Academy A.Prangishvili, December 23, 1997

ABSTRACT. **Aspects of influence of the depreciation factor of information on control process giving function of message price approximation and randomization are studied. Volterra's integral equation of coil type is constructed and solved as a mathematical model of random walk of concrete message.**

Key words: information ageing (depreciation), message price function, delay-time.

Strict demands for operativeness, reliability and truth of informative processes arise due to necessity of effective control. If information is not obtained, processed and passed in time, its role is considerably changed. The same is about the truth, and what about reliability, this complicated property correlates with disturbance of correct functioning and capability, and that means full impossibility of conducting the informative process.

The factor of message ageing in informative systems consists its price, expressed by economic indices, which decrease by time. And the moment comes, when this concrete message is useless for control. That means, that its price is zero. The situation can occur, when delayed message is even harmful.

Such circumstances are expressed in Message Price Function (MPF), which is determined by subscriber (respondent) of the message. Let's implicate, that all subscribers can express the price of their message in the same monetary units, e.g. US dollars. That means, that the subscriber can determine the cost of his message in a given moment. So, MPF is a relation between the message delivery price and time. Introduction of MPF makes it possible to determine naturally the criterion of quality of system functioning as income, gained by the system: MPF is given by subscribers and it expresses their interests, the growth of income of system corresponds to improvement of the quality of service.

Let's assume, that MPF is limited from both up and down in such a way that negative meanings are also allowable, and that relates with system taxation for lating a message, or failing it. We consider alternatives: 1) system can refuse to receive the message or delete late messages; 2) system is obliged to receive the message even in those cases, when its transmission in time is impossible and it is to pay tax. In the first case MPF hasn't negative meanings. The fact of throwing out the late message can be interpreted that subscribers lose nothing by deleting the message, but its transmission in time can be rewarded by a "bonus". In the second case MPF has negative meanings, but we can move all functions to the ordinate axes by the value of maximal tax, that instead of any $F(t)$ function we'll consider $F(t) + P\max$, that does not change its character. The result is that we get a number of non-negative MPF-s. Thus, we can consider non-negative functions of price with the top limit, which do not restrict generality [1-3].

Fig. 1 shows MPF, when the message is a telegram of anniversary congratulation. The function has well-expressed maximum, which relates with delivering the message to

the very moment of jubilee. The price of telegram decreases according to increasing the interval between the jubilee time and the moment of delivery.

Let's assume, that keeping the message in the unit of purpose doesn't increase the cost of system. Such assumption often is reasonable. Under these conditions if the message has come earlier than MPF reaches its maximum, it can be detained and delivered to the addressee strictly in time, that will give the maximum income to the system. In such systems the function of price will be non-increasing and non-negative. In case of telegram of congratulation the function of price will be changed as it is shown in Fig. 1 by dotted line.

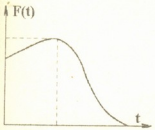

Fig. 1.

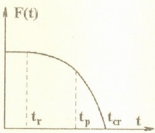

Fig. 2.

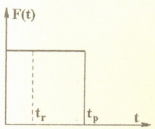

Fig. 3.

According to discussion above the MPF can be expressed, as it is shown in Fig. 2. Some designations are introduced: t_r random time of delivering the message; t_p permissible time; t_{cr} critical time. The regularity shown is established according to the results of experiments held in real systems. The price of the message in interval $[0, t_p]$ is decreasing relatively slowly, and in the interval $[t_p, t_{cr}]$ is quickly falling down to zero. This gives us a chance to approximate the function of price by rectangle rather precisely.

Even after such simplification each MPF analytical modelling of informative systems is quite problematic. Let's analyse the situation. Even when the approximation of function of price by rectangle of all subscribers is held, application of data obtained for system analysis and modelling is impossible. Indeed, the number of subscribers is usually very great and according to their individual needs it's very difficult to make any clever decision. Here, as in all cases like this, the effect of "damned dimension", as it was named by well-known scientist R.Bellman, operates [4, 5].

And here we must consider the set of permissible times, as definite realization of some random vector. The number of components of this vector, of course, must be much less than types of messages, but enough for describing the system "statistically". "Statistics is the skill of saying something about the part of the whole, when the truth is huge for application" [6]. Community of rules for subscribers of the system must be elaborated, and each of these rules must be used for separate subset of subscribers. Each rule will describe this subset statistically, and thus, generality will be reached, or the rule will express distribution of prices of messages. So, random vector of permissible times expresses dividing the multiplicity of messages in classes, and each of them statistically are characterised by one component of the vector. The rank of the class itself determines the index of priority of its service.

There are data of experiments, and also theoretical considerations, according to which components of random vector of permissible times can be considered as exponential random value. It is established, that initial parameters (addresses of the respondent and addressee, the length of the message, the time of essence, permissible time of delivering) in complicated systems are slightly cross-depended. It is known also, that for

some classes of subscribers the permissible time of delivering, measured in some conditional units, is a small quantity in most cases, and the number of messages, the permissible time of which is relatively big, is insignificant. In such circumstances this time must be considered as exponential random quantity [3, 7]. This very situation gives us a chance to describe informative systems, even approximately, by exponential models of queuing theory, where the factor of ageing (depreciation) of information will be taken into account. The last one, according to above mentioned, determines limiting of time of delay by exponential random quantity in different systems.

Exponential queuing systems are well-studied analytically. Likely, if we add to requirement of exponentially of random quantities the principle of Independence of R.Kleinrock and term of randomization, analytical modelling of complicated networks will become possible [2,3,7]. In this attitude the aspect of interpreting results of modelling is very important and we'll dwell on it more detailed. Studying simple system the single-channel tract of delivering message with limited delay time and unbounded queue is enough for illustrating conceptual considerations. Analytical reflection of probability and time characteristics of such systems is well-known [7, 8]. They give us characteristics of system from the position of the observer (System Analyst), who is interested in this whole system from the point of view of its integral abilities. And due to this interest statistical description of the system is needed, e.g., we know the Sojourn-time distribution for the flow of any priority. This distribution characterises delaying "average-statistic" message of a given priority in the system and this characteristic from the point of system analyst is exhaustive. Let's consider the same characteristic from the point of view of a concrete subscriber, who enters the message of concrete length and concrete price into the system. Let the length of message be τ, and the permissible time of delay - T. The subscriber is interested in probability, that under conditions of given priority his message will be delivered to the addressee in time, i.e. less than T. Let's express probability $P(\tau, T)$. To find – this probability we describe the service process in detail.

We imply, that the length of the message is equal to the time of ideal service, which is needed to service channel for delivering the message during non-failure operation. But really channels of delivering are affected by different hindrances – self-regenerating obstacles. Checking the truth of delivering the message happens at the end of delivering and with probability equal to 1 we can establish whether there was an obstacle during delivering or not. If the answer is O.K., the message is delivered once more and the process continues until undisturbed delivering is carried out. Of course, checking the truth needs some time and it must not be neglected, but we can imply, that it is counted in t time. It's easy to understand, that this assumption does not limit generality. Let's imply also, that flow of obstacles is Poissonous with α intensity, the probability of even one obstacle in $[0, \tau]$ interval will be $p = 1 - e^{-\alpha\tau}$. The waiting time considered by us will be the same, as the time of general system waiting. The real delivery time, taking obstacles into account, will differ from general system time. So, if we express the random waiting time with ξ, real delivery time with $\eta = \eta(t)$, the time of informing $\zeta = \zeta(t) = \xi + \eta(t)$.

Let's express

$$G(t) = P\{\xi < t\};\ H(t) = H(\tau, t) = P\{\eta(\tau) < t\};\ \text{then } P(\tau, T) = \int_0^T H(T-u)\, dG(u). \qquad (1)$$

As we have mentioned above, G(t) figure is known from the literature [7,8].

Let's find $H(t)$.

On the basis of standard probability reasoning the Volterra's integral equation of coil type II for $H(t)$ function is written.

$$H(t) = \int_o^t e^{-\alpha u} d_u \sigma(u-\tau) + \int_o^t (1-e^{-\alpha u}) H(t-u) d_u \sigma(u-\tau). \qquad (2)$$

Here $\sigma(\cdot)$ is Heaviside's unit function.

We must applicate Laplace's transformation for (2). Simple manipulation will give

$$\overline{H}(s) = e^{-(s+\alpha)\tau}/(1-pe^{-s\tau}).$$

This function can be expressed as a series

$$\overline{H}(s) = \left[\sum_{k=0}^{\infty} (pe^{-s\tau})^k\right] e^{-(s+\alpha)\tau}. \qquad (3)$$

Such expression is right, as

$$\left|pe^{-s\tau}\right| < 1.$$

Laplace's reinverse transformation gives us

$$H(t) = H(\tau, t) = \begin{cases} 0, & \text{if } t \le \tau \\ \sum_{k=1}^{n} (1-p)p^{k-1}, & \text{if } n\tau < t < (n+1)\tau, \quad n = 1,2\ldots \end{cases} \qquad (4)$$

If we put (4) into (1), calculation of (1) integral for the fixed T will not be difficult. We must take into account the fact, that the number of (4) in real cases decrease rapidly. Because of that we can practically always restrict with sum of several initial members.

We have to notice, that under conditions of the given example (sum) we can find (4) by direct probability discussion without integral equation. Merit of (2) is that if we use it, we can analyse some common cases too. Especially those cases, when instead of $\sigma(\cdot)$ function any function of distribution will be considered, which correlates with the situation when duration of delivering of every message a priori is independent "example" of some random quantities. $\sigma(\cdot)$ function in (2) plays the role of distribution function of delivering time.

Knowing $P(\tau, T)$ will help the subscriber to make argued decision about choosing restricted time of depreciation of the message (if it is not simply determined) or pay more in order to enter his message into class of higher priority messages and keep fixed meaning of $P(\tau, T)$ probability.

Georgian Technical University

REFERENCES

1. Math. Sci., Techn. and Ec. Competitiveness. Ed. by *James G.Glimm*. Washington, D.C. 1991.
2. *R.Disney, D.Konig*. SIAM Reviev **27**, 3, 1985.
3. *G.Ianbykh, B.Stoliarov*. Optimizatsia inf.-vych. setei. M., 1987 (Russian).
4. *N.N.Moiseev*. Matematicheskie zadachi sist. analiza. M., 1981 (Russian).
5. *V.Druzhinin, D.Kontorov*. Sistemotekhnika. M., 1985 (Russian).
6. *M.Ross Eshbi*. Vvedenie v kibernetiku. M., 1959 (Russian).
7. *D.Bertsekas, R.Gallager*. Seti peredachi dannykh. M., 1989 (Russian).
8. *N.Jeicuol*. Ocheredi s prioritetami. M., 1973 (Russian).

საქართველოს მეცნიერებათა აკადემიის მოამბე, 158, №1, 1998
BULLETIN OF THE GEORGIAN ACADEMY OF SCIENCES, 158, №1, 1998

I.Badagadze, R.Kakubava

On the Economic Criterion of Service Effectiveness

Presented by Corr. Member of the Academy A.Prangishvili, March 16, 1998

ABSTRACT. **Economic index of the quality of functioning of the informative system as ranged function of system losses is introduced. The problem of system synthesis is stated as indicated function's minimization problem.**

Key words: service quality, delay-time, system stoppage.

The functioning quality estimation of complex systems is one of the main pre-conditions of its effective control. That means introduction and applying of appropriate criterion. In respect to modern computer and communication systems this is construction of effectiveness criterion of the information flows service (processing, transmission). We will study one of such problems.

Let's consider the service system, the physical analogous of which can be computing system or data transmission path. The information flows service quality to a great extent is stipulated by delay-time of messages. The time is desirable to be little, which requires the high rate of service. In this case idle time increases, that is equivalent to system's discharge. It is natural to demand that in both cases the profit due to the short time of service, must be proportional to the losses caused by demurrage of the equipment. Introducing the economic criterion of effectiveness the optimal balance of both factors can be found in following way.

All messages belong to some i class according to α_1 penalty, which will be paid out by system for delay for a time unit. The number of classes is k. The flow of messages of i class is the simplest with intensity λ_i. It can receive priority service index $j_1 \in J = \{1, 2, \ldots, m\}$. The reflection of classes set I in J determines service discipline, which is vector with r dimension $j = \{j_1 \ldots j_r\}$.

The expression of priority system load coefficient is known, which equals to relative time of system occupancy [1,2]. It has the form

$$\rho = \sum_{i=1}^{k} \lambda_i \tau_{in}^{(j)}(\cdot), \qquad (1)$$

where $\tau_m^{(j)}(\cdot)$ is the average service time of i priority message in case of equality of service channels number to n, its speed equals to $\cdot$ and service discipline class number to j. Correspondingly the idle coefficient will be $1 - \rho$.

Losses of the system in the time unit because of its demurrage are equal to α_0. System's control on the stage of its construction means choosing number of channels n, speed of each channel v and service discipline j, and on the stage of functioning the last parameter's must be chosen according to the above mentioned criteria. Now we determine functions

$$f_n^{(j)}(\cdot) = f_{1n}^{(j)}(\cdot) + f_{2n}^{(j)}(\cdot),$$

$$f_{1n}^{(j)}(\nu) = \sum_{i=1}^{k} \alpha_i \lambda_i \omega_{in}^{(j)}(\nu)$$

where $\omega_{in}^{(j)}(\nu)$ shows average time of staying of i class messages in the system in case of j discipline, and $f_{in}^{(j)}(\nu)$ shows the value of penalty, caused by delaying the messages.

$$f_{2n}^{(j)}(\nu) = \alpha_0 \left(1 - \sum_{j=1}^{k} \lambda_i \tau_{in}^{(j)}(\nu)\right)$$

The problem of synthesis will be set as a problem of mathematical programming: we have to choose n, ν, j in the way, that $f_n^{(j)}(\nu) \to \min$ in conditions of following limitations must be $j \in J$, $n_0 \le n \le n_1$; $\nu_0 < \nu \le \nu_1$.

The essence of the first limitation is clear. Let's consider the second and the third in details.

It is known that one of the most stable principles of the structural and functional organization of informative-computing systems is the principle of integration of resources. The sense is that establishing unique system with joint flow of customers tasks is advisable. The whole resource in such system can be used by that set of customers, which needs it in the given moment of time. If the only one customer needs the service in this moment, he can use the whole capacity of the system, and if there are several customers, the capacity of the system is devided between them according to some rules. Such approach eliminates idle standing of resources in cases, when there exists some work for them and, besides that, customer gains the potential of profit during foreseen lowering prices in conditions, when the whole service of the big system is bought by one customer (here we mean the well-known lowering the prices when wholesale). It is approved, that while the full load of the system is constant, in quite general conditions the optimal number of serving channels is 1. This means, that in order to minimize the average delay time we need to have one resource with big productivity, rather than having the system of several resources with the same sum productivity [2, 3].

Besides that, practical realization of this principle, as a rule, meets great difficulties. On the one hand, maximal fastaction of the single resource on any stage of technical development is always limited, and because of that great need of systems with high productivity creating multichannel systems is necessary. On the other hand, there are some other considerations in favor of creating multichannel systems. One of the important factors is limited reliability of elementary basis. On any level of technology failure of the service channel of the uni-channel system means the failure of the whole system, while failure of one or several channels of the multichannel system does not affect the serviceability of the system. The reasonably projected system keeps the capacity of carrying main functions.

Limitation of the number of serving channels is caused by the above mentioned conditions, in particular, n_0 can show minimal number of channels, which is necessary for keeping obligatory reliability of the system, and n_1 is physically really possible maximal number of channels.

The limitation on speed of channels can be explained in the following way: for existing stationary conditions of the service system under given load minimal producti-

vity of the system is necessary, and this is due to speed of separate channels, V_0 can express exactly minimal possible speed, which is necessary for stability of the system, even in case of maximal possible number of channels.

Here is the particular case. Let's consider, that n and j are fixed. $\in [V_0, V_1]$, then the problem is driven to the mathematical programming with one variable. Dependence of $f_{1n}^{(j)}(\cdot)$, $f_{2n}^{(j)}(\cdot)$ and $f_{in}^{(j)}(\cdot)$ function from v is shown in the Fig.

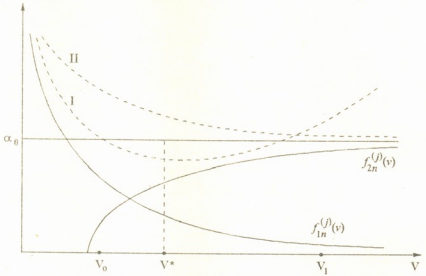

Fig.

Under conditions of free economy organizational and legal preface of functioning of informative systems (aspects of the standardization, reglamentation of usage, tariffs) have such meanings, that $f_n^{(j)}(\cdot)$ function (I), as a rule, has global minimum within $[V_0, V_1]$ segment in V^* point [1, 2]. In some cases this function can have (II) expression, the minimum of which is reached in V_1 point (II).

Georgian Technical University

REFERNCES

1. *R.L.Disney, D.Konig.* Queuing networks a survey of random processes. SIAM Review. 27, 3, 1985.
2. *D.Bertsekas, R.Gallager.* Seti peredachi dannykh. M., 1989 (Russian).
3. L.Kleinrok. Vychislitelnie sistemy s ocherediami. M., 1979 (Russian.)

საქართველოს მეცნიერებათა აკადემიის მოამბე, 158, №1, 1998
BULLETIN OF THE GEORGIAN ACADEMY OF SCIENCES, 158, №1, 1998

SOIL SCIENCE

G.Gogichaishvili

Estimation of Climatic Factor of Potential Erosion Danger of the Lands in Georgia

Presented by Corr. Member of the Academy T.Urushadze, January 13, 1998

ABSTRACT. **For estimation of climatic factor of potential erosion danger the erosion index of precipitation (E.I.P.) was used. In West Georgia E.I.P. changes from 20 to 120 units, in East Georgia it changes from 3.2 to 36.85. Most part of the territory of Georgia is located between 5 - 20 unit isoerodents of E.I.P.**

As a result of specification of lands according to the volumes of E.I.P. 37 erosion regions were grouped.

Key words: erosion, distribution of erosion index.

For estimation of climatic factor of soil erosion a parameter should be introduced, the structure of which contains kinetic energy and amount of rain. The parameter is the erosion index of precipitation (E.I.P.), which is equal to the kinetic energy of precipitation multiplied by 30 min of maximum intensity of rain [1-5]:

$$R = \Sigma(n = 1, \ldots, n)0{,}01\, E_k I_{30}/n\,,$$

where R is erosion index of precipitation (E.I.P.); $t{\cdot}ha{\cdot}h/ha{\cdot}MJ{\cdot}$mm; E_k kinetik energy of rain, $m \cdot t/ha \cdot$ mm; I_{30} is 30 min maximum intensity of rain, mm/min; n is a number of years of observation.

Analysis data of meteorological station in Tbilisi show that E.I.P. for the last 10-15 years period slightly differs (3-5%) from the more longer term.

Different climatic conditions in separate parts of the territory of Georgia have influence on the distribution of E.I.P. At the seaside of Georgia from Batumi till the mouth of the river Enguri E.I.P. exceeds 120 (Fig. 1). In West Georgia within Abkhazia annual E.I.P. falls from 70 till 20 unit. Kolkheti Lowland is located between 120 and 20 units of isoerodents of E.I.P. Upper parts of river gorges of West Georgia are defended from srtaight influence of the Black Sea humid air masses blows by high ranges (Meskheti, Racha, Lechkhumi, Egrisi, Svaneti and others). Because of the r. Enguri gorges (Khaishi-9,06; Mestia-6,20), r. Rioni (Ambrolauri-11,01, Oni-13,64) r. Adjaristskali (Keda-30,35; Khulo- 8,76) E.I.P. sharply decreases. A maximum difference of E.I.P. between seaside and close gorges of rivers is 114.

Between west and east of Georgia the natural border is Likhi Range. It is the basic factor of keeping off the moisture and determining dry climate of East Georgia and all East Transcaucasus. On the east slope of Likhi annual amount of precipitation is 780 mm (Surami), in the east little by little it decreases till 380 mm (Tsiteli Khidi). The most part of East Georgia is located between 5 -20 isoerodent of E.I.P. Extreme edge of East Georgia, Kakheti Caucasian range receives sufficiently high amount of precipitation (more than 1000 mm), therefore E.I.P. here sharply increases and exceeds 30 units (Kvareli - 29.54; Lagodekhi - 35.89).

Volcanic elevation of the South Georgia is high plateau with flat surface and meridional directions of ranges (Samsari and Djavakheti). Annual amount of precipitation here changes from 547 mm (Kartsakhi) to 733 mm (Ninotsminda). Here dominates the lowest

index of E.I.P. which changes from 2.60 (Rodionovka) to 4.20 (Akhalkalaki). In the other part of South Georgia E.I.P. doesn't exceed 7-8. In the Alpine zone of the Great Caucasian Range annual E.I.P. doesn't exceed 5 units (Kazbegi - 4.47).

Erosion danger of precipitation is grouped in the following way: weak till 5.0 E.I.P.; middle from 5.0 to 10.0; strong - from 10.0 to 20.0 and very strong is more than 20.0. This gradation is significantly different from D.Germaniuk's grouping [2]. According to grouping of E.I.P. the most part of the territory of Georgia is located in the area with strong and very strong erosion danger. Only southern part (high plateau of Akhalkalaki) and Alpine zone of the Great Caucasus are distinguished by low erosion danger of E.I.P.

Seaside part of West Georgia is characterized by one maximum of E.I.P. in August and September; hill and mountain forest zones by two maxima of E.I.P., from which first takes place in June-July, second in August-September. All the territory of East Georgia is characterized by two maxima of E.I.P., from which first is found at the end of spring and in the beginning of summer (May-June), second in the beginning of autumn (September).

For estimation of soil protection property of agricultural and natural lands cumulative curve lines of annual distribution of E.I.P., which was joined in 37 groups were made. Each group belongs to separate regions. Complicated structure of the territory of Georgia, circulation of the air masses, directions and exposition of the ranges, hollows between mountains, Alpine plateau and closed gorges caused the division of the territory into many regions. Therefore in a short distance (20 km long) from Borjomi to Bakuriani three regions, 18, 19 and 20 are distinguished (Fig.1).

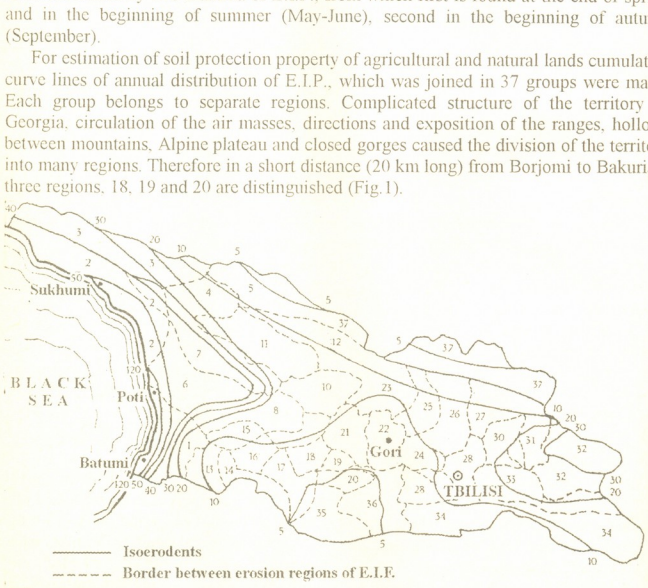

Fig.1. The schematic map of division into districts and distribution of E.I.P.

The map of the erosion index of the precipitation and division of the territory into regions according to annual percentage of distribution of E.I.P. give us the possibility to determine potential soil loss easily using U.S.L.E. It can be used for division of the territory of Georgia into erosion districts and for exposure of erosion danger periods,

choosing agricultural plants, soil conservation systems and the stages of the erosion arrangement control.

M.Sabashvili Institute of Soil Science and
Agricultural Chemistry

REFERENCES

1. *W.Wischmeier, D.D.Smith.* Predicting rainball erosion losses. USDA, 1978, 1- 57.
2. *M.Zaslavsky.* Soil erosion. M., 1979, 275 (Russian).
3. *M.Zaslavsky.* Erosion science. M., 1983, 320 (Russian).
4. *M.Zaslavsky, et al.* In: Soil erosion and processes of river bed. Pub. of MSU, issue 8th., 1981, 17-29 (Russian).
5. *A.Larionov.* In: Estimation and cartographical exposition of erosion and deflation dangers. Pub. of MSU, 1973, 38-46 (Russian).

საქართველოს მეცნიერებათა აკადემიის მოამბე, 158, №1, 1998
BULLETIN OF THE GEORGIAN ACADEMY OF SCIENCES, 158, №1, 1998

BIOPHYSICS

M.Jibladze, S.Uchaneishvili, M.Tsartsidze

Lasertherapy by E Light Field of Radiation

Presented by Academician G.Sanadze, November 28, 1997

ABSTRACT. **It is known that low-intensity laser radiation in orange-red and near infrared area of spectrum leads to activation of biological system of a body.**

In submitted work it is shown, that during therapeutic treatment of patients the laser irradiation may be replaced by non-coherent emission with the respective spectrum of emission, which markedly decreases the cost of treatment and in many cases simplifies the process of treatment.

Key words: phototherapy, non-coherent, field, low-intensity, laser, fibre, catalyse, citochromoxidase, dissipation, adsorption, energetical level.

It is known that low-intensity laser radiation in orange-red and near infrared spectrum area leads to activization of biological system of a body. Marked increase of activity of catalyse and citocromoxidaze has been observed. At the expense of activation of ferments the intensity of metabolism increases too.

As it has been shown by the studies of a degree of coherence while passing emission of He-Ne laser through a 10 cm fibre, complex degree of coherence decreases to 0.7 [1]. It is clear that while passing 1 m length fibre the degree of laser coherence decreases significantly.

On the other side, at the interaction of laser radiation with biological objects, laser beam, due to dissipation-dispersion on the large molecules of media and on the uneven skin surface becomes practically completely non-coherent. It should also be noted that at the absorption of laser emission, light coherency and polarisation do not play any role.

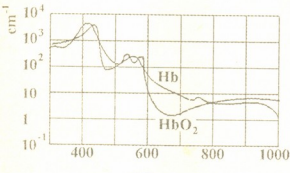

Fig. 1.

Investigations dealing with the study of interaction of emission and blood have shown that the most efficient is the interaction of light waves of 0.6 – 1 μ length corresponding to minimum indices of absorption coefficient of blood (Fig.1). Actually, absorption coefficient value of both arterial and venous blood in this area is three orders lower than in the diapason of the wavelength below 0.6 μ. Hence, if ultraviolet and blue-green beams are practically completely absorbed while passing the blood thickness of some dozens of microns, the yellow-red and especially infrared beams (up to 1 μ) can penetrate several centimetres deeper. This fact conditions the possibility of exposure of maximum volume of blood. Namely, in this zone He-Ne and semiconductor laser of Ga-As crystal emit.

Calculations have shown that interaction of emission with blood increases efficient (electron) temperature of biological media, which leads to sharp increase of a rate of biochemical reactions.

Actually, at a temperature T, distribution of electrons in atoms, according to energetic equations can be determined by the formula

$$n_i = n_0 e^{-E_i/kT}$$

where n_i is for concentration of electrons at the excited level, n_0 – at the basic level, E_i- energy of energetic level, and k- constant of Boltzman. As it is seen, with the increase of temperature the population suffers sharp increase at the excited level. If the light falls on the system of atoms, this distribution changes significantly. The reason of this change is the forced transition of electrons from the basic level to the excited energetic levels with the energy $E_i = h\nu$ (where $h\nu$ is energy of the emission quantum).

The higher the medium temperature is, the more atoms occupy the excited energetic levels and the more active is the biological molecule, i.e. the rate of biological reaction increases. At the exposure to light (irrespective of the fact whether the light is coherent or not), additional population of the excited level occurs, and the Boltzman's distribution now corresponds to another higher temperature, which is called effective temperature of medium T_{ef}. The greater power of electromagnetic wave of the system of absorbed atoms is, the higher the temperature is.

At additional increase of population of the excited E_i level as a result of absorption of photons the picture of Boltzmann distribution suffers significant change and atom system attains the state which corresponds to the relatively higher electron temperature. Namely, this electron temperature conditions the rate of biochemical reaction in biological media.

It should be stated that in the excited state, atoms (molecules) may appear only during the excitation by light. Thus speeding up of biochemical reaction in biological media occurs only during exposure to light though the products of this reaction lead to other biochemical reactions having therapeutic effect.

Undoubtedly, energy of a photon absorbed by atoms is small, but initiated by this absorption, biochemical reactions need relatively higher energetic expenditures of biological system. Therefore, during phototherapy the body loses rather great energy for supporting the cascade of biochemical reactions induced by photon absorption.

Due to the fact that coherency of radiation does not affect the process of photon absorption by the atom system, as well as high directivity and polarisation of laser emission, non-coherent emission may be used in phototherapy.

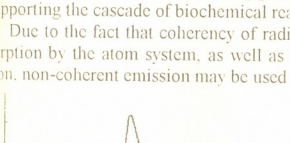

Fig. 2.

Absence of necessity of application of coherent laser emission in laser therapy enables us to create highly efficient non-coherent sources of light on the base of crystals GaAlAr(Zn), emitting with two maximum peaks in the wavelenghts of 0.675 μ and 0.9 μ. Emission spectrum of crystals GaAlAr(Zn) fall to the most favourable zone of absorption spectra of blood (Fig.2). On the other hand, taking into consideration wide bands of absorption of biological molecules, high monochromaticity of laser emission loses its importance. Semiconductor irradiators are simple to be prepared and exploited. They are cheap and characterised by high treatment efficiency. Irradiators

have passed clinical testing in several clinics of Tbilisi (Institute of Urology of the Ministry of Health Care of Georgia, Scientific Practical Centre of Burns, Otorhynolaryngological Centre of the Tbilisi Medical Academy, etc.). Studies have shown that effect of treatment by the use of non-coherent irradiation of GaAlAr(Zn) is analogous to the effect of coherent emission of He-Ne laser.

At the Chair of Otorhynolaryngology of Tbilisi Medical Academy the clinical experiments were conducted dealing with therapeutic effect of He-Ne laser and the emission of non-coherent light on the GaAlAr(Zn) crystals, during treatment of hypertrophic rhynite [2].

Thus, during therapeutic treatment of patients the laser radiation may be replaced by non-coherent emission with the respective spectrum of emission, which markedly decreases the cost of treatment and in many cases simplifies the process of treatment.

Tbilisi I.Javakhishvili State University

REFERENCES

1. *M.Jibladze, M.Perel'man, V.Chaglov, T.Chelidze.* Izv. AN SSSR, ser. Physics., **43**, 2, 1979, 292-295, (Russian).
2. *S.Khechinashvili, M.Jibladze, N.Tvildiani.* Georgian Medical News, 21, Dec., 1996, 28-29.

საქართველოს მეცნიერებათა აკადემიის მოამბე, 158, №1, 1998
BULLETIN OF THE GEORGIAN ACADEMY OF SCIENCES, 158, №1, 1998

BIOPHYSICS

O.Khomeriki, T.Paatashvili, L.Gheonjian, N.Kapanadze, N.Invia

The Influence of 7-day Variations of Interplanetary Magnetic Field on the Frequency of Myocardial Infarctions

Presented by Academician V.Okujava, April 13, 1998

ABSTRACT. **This paper is dedicated to the study of the influence of solar activity on human being. On the basis of statistical investigation of the frequency of myocardial infarctions we discover the 7-day variations and the dependence of their intensity on 11-year solar cycle. We confirm the hypothesis that 7-day variations of interplanetary magnetic field caused by its sector structure synchronize endogenous 7-day rhythms of human beings during the stage of maximum of solar activity, and hypothesize that the probability of infarction is higher on a certain stage of the endogenous rhythm.**

Key words: myocardial infarctions, biorhythms.

At present sufficient amount of statistical data confirming the reality of the influence of solar activity on biosphere is accumulated. The role of geophysical processes and magnetic fields as a transitive link is estimated [1,2] and technical facilities for the protection from negative impact of geomagnetic storms are developed [3,4]. But the manifestation of helio-geophysical activity one observes as exceedingly low changes of physical parameters of environment. Electromagnetic signals and noises generated by industrial and home devices exceed the variations of natural electromagnetic fields. The absence of appropriate explanations, confirmed by experiments, gave rise to generally skeptic attitude towards the reliability of statistical results.

For the discovery and the study of helio-geophysical factors acting on biological objects, it is necessary to carry statistical investigations of biological data. It is expedient to use and examine the hypothesis, which assumes the synchronizing influence of solar activity on the state of biological objects [2]. According to this hypothesis external rhythms - the rhythms of solar events, the rhythms of events in interplanetary medium, in terrestrial atmosphere and magnetosphere, influence on proper endogenous rhythms of biological objects, or biorhythms. Bio-

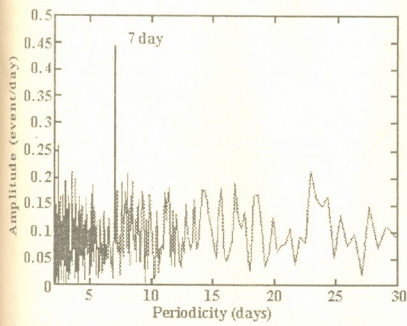

Fig. 1. The dependence between the amplitudes and periods of cycles for the data from 1980 to 1992.

logical objects can be compared with systems in nonequilibrium state, continuously adapting to variations of environmental parameters. Helio-geophysical rhythms can synchronize as well as desynchronize biological processes. The absence of long-time systematic biological observations makes difficult the examination of this attractive hypothesis.

We examined the hypothesis by the use of statistical data concerning the functioning of cardiovascular system of human being. This statistical data reflect the mortality caused by myocardial infarctions in Tbilisi from 1980 to 1992. The series consist of daily values of the frequency of mortality.

The processing procedure included spectral analysis for the discovery of periodicity and the estimation of their reliability [5]. We were looking for the critical, from the point of view of mortality, values of the duration of cycles in the time interval from two days to one month. The periodicities longer than one month we excluded by the use of the method offered in [6]. Fig. 1 represents the result of spectral analysis: the dependence between the amplitudes and the periods of cycles. Further we call the dependence as periodogram. Horizontal axis represents the values of periods or cycles, vertical axis represents corresponding values of amplitudes of cycles. The main peculiarity of this periodogram is well defined peak corresponding to 7-day periodicity of the frequency of mortality. This period is known in chronobiology and is considered as one in a basic set of rhythms [7-9]. It is weighty to mention that such distinct demonstration of 7-day rhythmisity in biological data, as it is represented in Fig. 1, chronobiology receives for the first time.

The same period is typical for interplanetary media. It is caused by the sector structure of interplanetary magnetic field [10]. The initial reason of the origin of the sector structure is the structure of solar magnetic field. Chronobiology assumes that living organisms acquired 7-day rhythm during the evolution of species under the impact of solar activity. The simple and complicated organisms adapted their proper rhythmical structure to the time scale connected to the period of solar rotation. The main rhythms should be equal to the period of rotation of the sun, approximately 27 days, or should be equal to harmonics of it [2].

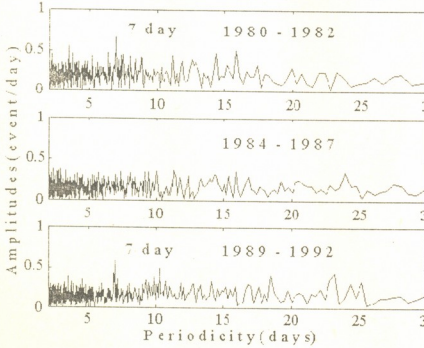

Fig. 2. The dependence between the amplitudes and periods of cycles for the intervals of high level (1980-1982 and 1989-1992) and low level (1984-1987) of solar activity.

The structure of solar magnetic field, and correspondingly the sector structure of interplanetary magnetic field, changes during 11-year cycle of solar acti-

vity. During the periods of low activity the sector structure is not developed. During the periods of high activity one can observe four sectors. In each sector the field is directed toward the sun or from the sun [10]. Neighbor sectors have opposite signs of magnetic field. During one rotation of the sun four times with periodicity about 7 days the sign of interplanetary magnetic field changes. There is the factor, which may synchronize 7-day biorhythms of different organisms. It is clear that synchronizing factor is absent during the period of low solar activity. If we accept the synchronization hypothesis and suppose that the probability of infarction is higher on a certain stage of the endogenous 7-day rhythm, statistical analysis of our data must reveal 7-day periodicity during the years of high activity and the absence of it at years with low activity.

The statistical data cover the time corresponding to two periods of high solar activity and one period of low solar activity. Fig. 2 represents periodograms calculated for three intervals of time. The first interval covers the period from 1980 to 1982, the period of maximum of activity. The interval from 1984 to 1987 corresponds to the minimum of activity. The interval from 1989 to 1992 corresponds to the maximum of the next 11-year cycle of activity. The level of solar activity is estimated by the use of generally accepted statistical index Wolf number (W). This index characterizes the quantity of sunspots. Usually during the years of maximum of activity annual value of W exceeds 100.

Fig. 2 demonstrates that the amplitudes corresponding to 7-day periodicity are well defined at the years of maximum of activity, but during the years of minimum of activity, the amplitude does not exceed the average value. The estimation of statistical reliability of results represented in Fig. 2 confirms high reliability of 7-day periodicity during the years with high activity. For the estimation of reliability we used the procedure described in [11].

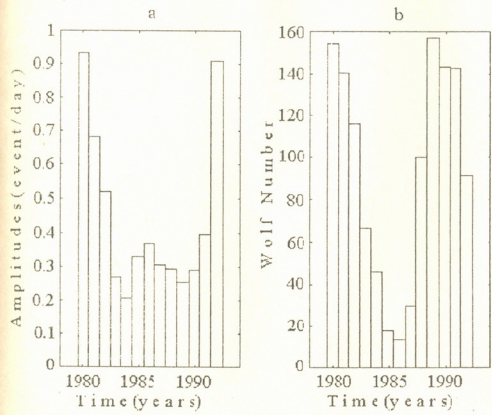

Fig. 3. (**a**.) annual values of the amplitude of 7-day periodicity;
(**b**.) annual values of the index of solar activity.

Fig. 3 represents annual values of Wolf number and amplitudes of 7-day periodicity from periodograms calculated for each year. The dependence of the amplitudes on the state of solar activity is obvious.

The formation of sector structure depends on the structure of solar magnetic field in new cycle and this process lasts approximately two

years. Some geophysical manifestations of solar activity demonstrate two year delay. Our data demonstrate the same phenomenon.

The result of our investigation confirms the conception about the synchronization of biological rhythms with environmental rhythms. We find the confirmation of the assumption we have done and hypothesize that the probability of infarction is higher on a certain stage of the endogenous rhythm. The role of the structure of interplanetary magnetic field and the level of solar activity as an active factors of environment became more clear.

It is necessary to continue the investigation of the role of magnetic fields in synchronization mechanisms and in basic biological processes and rhythms. Present technical facilities open new perspectives for these investigations. The possibility to compensate external magnetic fields and to generate demanded magnetic fields in clinical rooms should be used [3,4].

Georgian Technical University

Abastumani Astrophysical Observatory
Georgian Academy of Sciences

REFERENCES

1. *M.Gnevishev, A.Ol.* The influence of solar activity on terrestrial atmosphere and biosphere. Moscow, 1971 (Russian).
2. *T.Breus, et al.* Ann. Geophysicae, **13**, 1995, 1211-1222.
3. *O.Khomeriki.* Patent of USSR No 1778927, Bulletin of Patents, **44**, 1992 (Russian).
4. *N.Invia, F.Todua, O.Khomeriki.* Transactions of Georgian Technical University, **7**(400), 1993, 131-137 (Russian).
5. *G.Jenkins, D.Watts.* Spectral Analysis. Holden-Day, 1969.
6. *J.Vondrac.* Bull. Astron. Inst. Czech. **20**, 1969, 349-355.
7. *F.Brown.* Cold Spring Harbor Sympos. Quant. Biol., **25**, 1960, 57-71.
8. *G.Cornelissen, F.Halberg.* Introduction to chronobiology. Medtronic Chronobiology Seminar 7, 1994.
9. *F.Halberg.* Cold Spring Harbor Sympos. Quant. Biol., **25**, 1960, 289-310.
10. *J.Wilcox, N.Ness.* J. Geophys. Res., **70**, 1965, 5793-5805.
11. *M.Serebrennikov, A.Pervozvansky.* A search for hidden periodicities. Moscow, 1965 (Russian).

საქართველოს მეცნიერებათა აკადემიის მოამბე, 158, №1, 1998
BULLETIN OF THE GEORGIAN ACADEMY OF SCIENCES, 158, №1, 1998

BIOCHEMISTRY

R.Akhalkatsi, T.Bolotashvili, Corr. Member of the Academy N.Aleksidze

The Nonhistone Proteins of Chromatin as Lectin-Binding Glycoconjugates

Presented October 20, 1997

ABSTRACT. **Rat brain isolated cell nuclei chromatin has affinity to Concanavalin A. The nonhistone proteins display mannoso-(glucoso-), fucoso and galactoso specific lectin-binding ability, which indicates their glycoprotein nature.**

Key words: rat brain, nonhistone proteins, glycoconjugates.

The existence of nuclear glycoproteins had first been suspected by Sevaljevich and Krtolica when some nonhistone chromatin proteins after PAGE-SDS electrophoresis were found to be positive to the periodic acid - Schiff reaction [1]. Glycosylated nonhistone proteins with molecular weight from 10 000 to 190 000 were found in normal [2-4] and in tumoral cells [5-7]. The high mobility group proteins HMG 14 and 17 are the best characterized intracellular glycoproteins [8, 9]. Kinoshita et al. have found that at various stages of embryonal development sea urchin chromatin reveals plant lectin (Con A, WGA, SBA et al.,) binding ability. It was proposed, that such lectin-binding components may play a regulatory role in embryonic chromatin action at early stages of development [10].

Our aim was to investigate plant lectine-binding capacity to rat brain nonhistone chromatin proteins.

White rats of both sexes weighing 100-120 g were used in experiments. Rat brain cell nuclei were isolated by the method of Chauveau [11]. The purity of nuclear fractions was controlled by microscope. Chromatin was prepared by Huang and Huang [12]. The nuclear pellet was washed with 0.075 M NaCl+0.025 M EDTA (pH 8.0) and centrifuged (4 000 g/10 min) three times. The obtained pellet was washed with solutions: 1. 50 mM tris-HCl (pH 7.5), 2. 10 mM tris-HCl (pH 7.5), 3. 5 mM tris-HCl (pH 7.5) and 4. 1 mM tris-HCl (pH 7.5). The pellet, obtained after the last washing, was chromatin. It was resuspended in a small amount of 1 mM tris-HCl (pH 7.5) so that the DNA in chromatin should equal 100 mkg/1 ml.

The isolation of nonhistone proteins of chromatin was performed by Wang [13]. The purified chromatin was dissociated in 1 M NaCl – 0.01 M tris-HCl (pH 8.0) (the final DNA concentration was about 400 mkg/ml) and dialyzed against 6 volume of 0.01 M tris-HCl (pH 8.0). The precipitate was separated by centrifugation 5 000 g/20 min and the supernatant was dialyzed against 0.5 M NaCl – 0.01 M sodium phosphate buffer (pH 7.2). The obtained protein was nonhistone protein. The protein concentration was determined by the method of Lowry et al. [14] and DNA by Dische [15].

The agglutination was studied on trypsinized rabbit erythrocytes by microtitration on U-plates [16]. The lectin activity was measured by the minimal concentration of proteins, still causing clearly expressed agglutination. The lectin-binding activity of chromatin nonhistone proteins was determined by the minimal protein concentration, which inhibited the agglutination of trypsinized rabbit erythrocytes. The lectins with

lectin-binding proteins were preliminarily incubated for 30 min and the quantitative relation of lectin with the amount of lectin-binding proteins (LBP) were expressed in figures [17]. The agglutination was carried out in the solution of 40 mM PBS (pH 7.4) prepared on 0.9% NaCl. In experiments plant lectins from "Diagnosticum Lvov" were used.

In the first series of experiments the lectin activity of rat brain chromatin and nonhistone proteins were studied. It was established that neither chromatin nor nonhistone proteins revealed any lectin activity in our experimental conditions. These results gave us a possibility to investigate the lectin-binding activity of chromatin and nonhistone proteins.

We were preparing a series of double dilution of the investigated proteins in 0.05 ml of 40 mM PBS (pH 7.4). The lectin solution with the titre 1:8, 0.05 ml was added to each loop and preincubation was made at room temperature for 25 min. Then 0.05 ml of 2% suspension of rabbit trypsinized erythrocytes was added to the mixture. After 2 hours in the loops, where erythrocytes agglutination was absent, all the added lectin was bound with lectin-binding protein. The appearance of the agglutination means the presence of the abundant amount of free lectins.

In the following experiments plant lectin-binding capacity of rat brain chromatin nonhistone proteins was studied. In experiments fucosospecific (LAL), galactosospecific (PNA, RCA, SBA, SNA) and mannoso-(glucoso-) specific (Con A, PSL, STA, WGA) plant lectins were employed (Table 1).

Table

The influence of rat brain chromatin nonhistone proteins on hemagglutination activity of plant lectins

The sources of the lectins	Lectins	The carbohydrate specificity	Lectin/lectin-binding protein (nonhistone)
Laburnum anagiroides	LAL	Fucosocpecific α L Fuc	$32 \cdot 10^{-2}$
Arachis hypogeae	PNA	Galactosocpecific β D Gal	$6.2 \cdot 10^{-2}$
Ricinus communis	RCA	α D Gal, D GalNAc	$6.2 \cdot 10^{-2}$
Glicine max	SBA	α D GalNAc	$6.2 \cdot 10^{-2}$
Sambucus nigra	SNA	D Lac, D Gal	$6.2 \cdot 10^{-2}$
Canavalia ensiformis	Con A	Mannoso-(glucoso-)specific α D Man > α D Glc > DGlcNAc	$8 \cdot 10^{-1}$
Pisum sativum	PSL	α D Man > α D Glc > DGlcNAc	$1.2 \cdot 10^{-2}$
Solanum tuberosum	STA	$(D\ GlcNAc)_n$, n = 2, 3, 4	$12 \cdot 10^{-2}$
Triticum vulgaris	WGA	$(D\ GlcNAc)_n$, n = 1, 2, 3; NANA	$1.5 \cdot 10^{-2}$
Lens culinaris	LCL	DMan	$1.5 \cdot 10^{-2}$

As it turned out rat brain chromatin nonhistone proteins display the lectin-binding capacity and cause inhibition of their hemagglutination activity. They display the highest affinity to Concanavalin A (Con A). As it is known Con A is a three-antenal lectin with the specificity to Man, Gluc, GlcNAc with the correlation 100:22:11 accordingly. The

lectins PSL = STA, WGA, LCL have relatively small affinity to the nonhistone proteins. As we know the lectin from Lens culinaris (LCL) is near to Con A and PSL and has specificity to D-mannose. Consequently, nonhistone proteins high affinity to Con A is not caused by the presence of only D-mannose terminal carbohidrates. The fucosospecific lectin LAL is on the second stage by the affinity to nonhistone protein. The nonhistone proteins reveal almost equally feeble binding activity to galactosospecific lectins PNA, RVA, SBA and SNA. Consequently, rat brain chromatin nonhistone proteins contain the following carbohydrate residues:αD Man, α D Glc, D GlcNAc, L Fuc, D Gal, D Lac, D GalNAc.

Proceeding from the received results it can be proposed, that the lectins with analogous specificity should be found in rat brain cellular nuclei. The identification and their isolation is the purpose of our further research.

Tbilisi I.Javakhishvili State University

REFERENCES

1. *L.Sevaljevich, K.Krtolica.* Int. J. Biochem., 4, 1973, 345-348.
2. *G.S.Stein, R.H.Roberts et al.* Nature, 258, 1975, 639-641.
3. *H.Polet, J.Molnar.* J. Cell Physiol., 135, 1988, 47-54.
4. *S.P.Jackson, R.Tjian.* Cell, 55, 1988, 125-133.
5. *D.Tuan, S.Smith et al.* Biochemistry, 12, 1973, 3159-3165.
6. *A.H.Goldberg, L.C.Yeoman, H.Busch.* Cancer Res., 38, 1978, 1052-1056.
7. *R.G.Burrus, W.N.Schmidt et al.* Cancer Res., 48, 1988, 551-555.
8. *R.Reeves, D.Chang, S.C.Chung.* Proc. Natl. Acad. Sci. USA, 78, 1981, 6704-6708.
9. *R.Reeves, D.Chang.* J. Biol. Chem., 25, 1983, 679-687.
10. *S.Kinoshita, K.Yoshii, Y.Tonegawa.* Exptl. Cell. Res., 175, 1988, 148-157.
11. *J.Chauveau, Y.Moule, C.Rouiller.* Exptl. Cell Res. 11, 1956, 317-321.
12. *R.C.Huang, P.C.Huang.* J. Mol. Biol. 39, 1969, 365-378.
13. *T.Y.Wang.* J. Biol. Chem. 242, 1967, 1220-1226.
14. *O.H.Lowry et al.* J. Biol. Chem., 193, 1961, 265-275.
15. *Z.Dische.* In: The Nucleic Acids E. Chargaf and J. N. Davidson Eds, vol 1, Academic Press, New York, 1955, 285-305.
16. *M.D.Lutsik, E.N.Panasjuk, A.D.Lutsik.* Lektiny. Lvov, 1981 (Russian).
17. *R.Akhalkatsi, N.Aleksidze, T.Bolotashvili.* Bull. Georg. Acad. Sci, **153**, 1, 1996, 109-112.

BIOCHEMISTRY

L.Shanshiashvili, D.Mikeladze

Peptide from Myelin Basic Protein as an Inhibitor of the [^{3}H]Diltiazem Binding Sites in Brain

Presented by Academician T.Oniani, October 12, 1997

ABSTRACT. **After the tryptic digestion of myelin basic protein (MBP) a peptide fragment, inhibiting [^{3}H]diltiazem binding to synaptic membranes, has been obtained. The analysis of amino acid composition of this peptide has revealed its similarity to the sequence MBP 95-135. The peptide fragment inhibited [^{3}H]diltiazem binding in a concentration-dependent manner, decreased B_{max}, but did not act on Kd. The inhibition of MBP calcium channels by peptide fragments is supposed to play an important role in the regulation of the activity of nervous cells as well as immune cells.**

Key words: myelin basic protein, [^{3}H]diltiazem, brain.

The study of the structure and function of myelin basic protein (MBP) has been performed intensively in connection with the possibility of its participation in autoimmune diseases. At present it is being cleared up, that the process of myelinolysis occurring during autoimmune diseases of CNS is induced by depletion of MBP[1]. The proteolitic splitting of MBP is catalysed by Ca^{2+} -dependent neutral proteinases, which evidently penetrate through myelin sheath from extra cellular region after the destruction of myelin structure by specific antibodies present in immunoglobulin fractions [2]. In addition, it has been shown, that demyelination is accompanied by the significant increase of brain calcium concentration [3]. The increase of Ca^{2+}-dependent protease activity and intestified breakdown of MBP leads to the appearance of several peptide fragments of this protein in brain, blood and cerebrospinal fluid [4]. However, the degree of proteolysis greatly depends on the degree of posttranslational modification of the MBP and particularly on phosphorylation.

At present it has been revealed that the activation of T lymphocytes as well as their regulation by major histocompatibility antigens are coupled with Ca^{2+}-dependent cell pathways [5]. However, MBP and its fragments do not evidently affect on L-type Ca^{2+} -channel since they do not displace [^{3}H]nitrendipine binding to synaptic membranes[6]. Taking into account the similarity of amino acid sequence of definite MBP fragments with proteins acting on benzothiazepine binding sites [7], the action of MBP fragments on the binding of [^{3}H]diltiazem, a benzothiazepine calcium channel blocker, has been studied in present work.

The MBP was isolated from rat brain according to the method of Chou et al. [8]. Protein kinase C was purified according to the method of Waltonet et al [9]. Crude synaptic membrane fractions of whole brain of Wistar rats, weighing 200-250 g, were homogenized in a buffer containing 50 mM Tris-HCl, pH 7.4 and 0.32 M sucrose (100 mg wet weight\ ml). Synaptosomes were isolated by centrifugation (1.000 g, 10 min), pelleted (20.000 g, 20 min) and resuspended. Suspension was homogenized in buffer containing 5 mM Tris-HCl, pH 7.4,

incubated for 30 min at 4°C, and washed twice by centrifugation (48,000 g, 10 min). The final pellets were suspended in 0.32 M sucrose and frozen at –80°C until use. For the radioligand analysis suspension of membrane (about 100 mg protein) was incubated with 10 nM [^{3}H]diltiazem in 0.5 ml 50 mM Tris- HCl, pH 7.4 at 20°C for 30 min. Incubation was terminated by the addition of 3 ml ice-cold buffer and subsequent filtration through a Whatman GF/C glass fiber filter. After rinsing the filter, radioactivity retained on the filters was measured by a liquid scintillation spectrometer. Nonspecific binding was defined by unlabeled 10 mM diltiazem. For Scatchard analysis the membranes were incubated with a various concentration of [^{3}H]diltiazem (1 nM to 15 nM). Data analysis were performed using the KINETIC binding analysis program [10]. For the tryptic digestion the phosphorylated and nonphosphorylated MBP, 1 mg of each, were suspended separately in 1 ml of 0.1 M ammonium hydrogen carbonate (pH 8.0) containing 10 mM calcium acetate. A solution of trypsin, 0.3 mg/ml in a 0.1 N hydrochloric acid, was added to the protein suspension and the mixture was incubated at 37°C for 15 min. Then the HPLC analysis was performed. The chromatographic separation was achieved on a NOVA-PAK C column and peptides eluted with a solution containing 0.05% TFA and acetonitrile. The concentration of acetonitrile was increased linearly from 0 to 60 % over 30 min. Amino acid composition was determined by HCl hydrolysis and modification with phenylisothiocyanate [11]. Phenylthiocarbamyl derivatives were determined on a Pico Tag analyzer.

It has been found that tryptic digestion of MBP during 15 min allows to obtain 6 fractions of protein fragments, while after its preliminary incubation with protein kinase C additional peptides were obtained (Fig.1). This data indicated that the phosphorylated form of MBP was more sensitive to trypsin than nonphosphorylated forms. The analysis of the fractions obtained after the chromatographic separation of tryptic digest of MBP has shown, that [^{3}H]diltiazem binding to the synaptic membranes is influenced by 2 peptide fractions yielding at acetonytrile concentrations equal to 44-45 % and 55-56 % and having absorption at 214 nm as well as at 280 nm (Fig.1). Taking into consideration the existence of a single residue of tryptophan in MBP with absorption at 280nm (Fig. 1*A*) it can be concluded, that both fractions correspond with peptide fragments containing Trp 118.

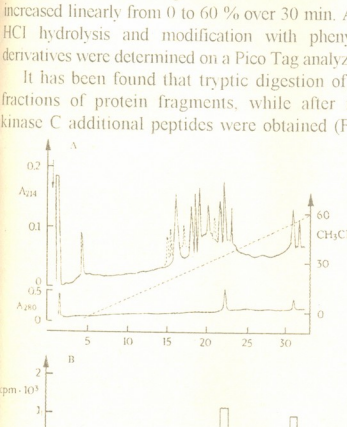

Fig. 1. HPLC of triptych digests from phosphorylated and nonphosphorylated MBP on a NOVA PAK C18 column

A – absorbance at 214 nm and 280 nm. Solid line - nonphosphorylated MBP, dotted line – additional peaks from phosphorylated MBP

B – [^{3}H]diltiazem-displacing activity.

Amino acid analysis of both MBP fragments affecting [^{3}H]diltiazem binding has shown that they

differ in His, Lys, Thr and Gly quantity (Table 1). The comparison of amino acid composition with rat MBP sequence [12,18] has allowed to conclude, that the less hydrophobic peptide fragment yielding at 24.2 min corresponds to MBP sequence 74-140, but the more hydrophobic one to MBP sequence 93-135. They can be formed as a result of incomplete tryptic hydrolysis, or on account of the existence of endogenous phosphate groups in these peptides which may change the intensity of proteolysis [12].

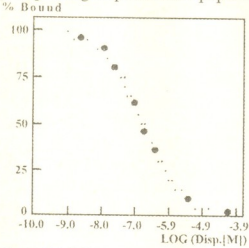

Fig. 2. Inhibition of [3H]diltiazem binding by the fragment 93-135 of MBP.

It has been found out that the peptide 93-135 inhibits [^{3}H]diltiazem binding in higher grade than the peptide 74-140. Inhibition of [^{3}H]diltiazem binding by the peptide 93-135 is concentration dependent (Fig.2) and displaces [^{3}H]diltiazem with high affinities (IC_{50} is equal to 61.5 nM). Only the capacity of [^{3}H]diltiazem binding sites in cerebral membrane homogenates is affected by the inhibitory peptide, whereas Kd does not change. Hill coefficient decreases from 0.94 to 0.79, which indicates the absence of significant cooperative interactions. B_{max} declines from 130 to 76 fmol/mg in the presence of 30nM peptide. It has been supposed that the inhibitory peptide decreases [^{3}H]-diltiazem binding in a noncompetitive manner.

Table 1

Comparison of amino acid composition of the purified inhibitor of [^{3}H]diltiazem binding and rat MBP fragments [a]

Amino acid	Abundance (% total mass)			
	P 24.2[b]	MBP(76-140)	P 32.5	MBP(93-135)
Asp	4.1	3.9	4.5	3.5
Glu	4.2	4.0	6.3	10.7
Ser	8.3	11.2	13.6	17.8
Gly	14.5	18.1	10.1	16.9
His	6.3	4.1	-	-
Arg	4.8	6.0	8.9	10.7
Tyr	4.1	4.1	4.5	3.6
Ala	10.4	6.1	9.0	7.1
Pro	12.1	10.0	13.2	17.8
Val	6.2	6.0	4.5	3.6
Ile	2.0	2.0	4.4	3.5
Leu	4.2	4.1	4.5	3.5
Phe	8.1	8.1	10.2	7.2
Lys	10.4	10.1	6.2	7.1
Thr	2.1	2.0	6.1	7.0

[a] Amino acid composition of rat MBP were calculated from sequence data [12].
[b] P 24.2 and P 32.5 designate the fragments of MBP according to their retention time during HPLC.

Metabolism of MBP in myelin is supposed to be dependent on Ca^{2+} concentration. It has been shown that degradation of MBP is performed by Ca^{2+}-dependent neutral protease [17]. The activity of this enzyme sharply increases in the result of calcium concentration increase in myelin during some autoimmune diseases, such as multiple sclerosis [3]. Ca^{2+} concentration increase has been supposed to be performed endogenously from myelin binding sites by penetration of external Ca^{2+} into the interior side of myelin lamellae. The blocking of synaptic membranes or mitochondrial Ca^{2+}-channels by MBP fragment can have compensatory function of protection from excessively increased Ca^{2+} in myelin.

On the other hand, myelin degradation rate depends on MBP phosphorylation degree. *Turner et al.*[13] have suggested that "excessive" phosphorylation of MBP can cause the collapse of myelin structure. Taking into account that MBP can be phosphorylated by several types of Ca^{2+}-dependent protein kinases (protein kinase C, Ca^{2+} calmodulin dependent protein kinase), the regulation of the concentration of calcium ion in myelin may be important in assembly, reparation or degradation of myelin structure.

MBP contains a number of homologous sequences with GABA-modulin [7], cancer cell basic protein [14], several viral proteins [15]. They can cause autoimmune postinfectious or postvaccinal encephalitis and neuritis mediated by T cells [16]. The immune response of T cells to MBP- like autoantigens is associated with major histocompatibility complex, which in addition to the restriction of cytotoxic activity of T lymphocytes can carry out the receptor-like function [5]. In all given cases Ca-dependent way of regulation of T cell activity and their inhibition by MBP fragment can play an important role in immune cell activation.

I.Beritashvili Institute of Physiology
Georgian Academy of Sciences

REFERENCES

1. *J.F.Hallpike, C.W.M.Adams.* Histochem. J., **1**, 1969, 559.
2. *N.Kerlero de Rosbo, C.C.A.Bernard.* J. Neurochem., **53**, 1989, 513.
3. *W.Craelius, R.Jacobo.* Proc. Soc. Exp. Bbiol. Med., **165**, 1980, 327.
4. *P.Glynn, A.Chantry, N.Groome.* J. Neurochem. **48**, 1987. 752.
5. *J.D.Dasgupta, E.J.Yunis.* J. Immunol., **139**, 1987, 672.
6. *J.S.Nye, S.Voglmaier.* J. Neurochem. **50**, 1988, 1170.
7. *F.Vaccarino, B.M.C.Tronconi.* J. Neurochem., **44**, 1985, 278.
8. *F.C.H.Chou, C.H.J.Chou, R.Shapira.* J. Biol. Chem., **251**, 1976, 2671.
9. *G.M.Walton, P.Bertics, L.Hudson.* Anal. Biochem., **161**, 1987, 425.
10. *G.A.McPerson.* Elsevier Sciences Publishers BV, The Netherlands.
11. *R.L.Heinrickson, S.C.Meredith.* Anal. Biochem., **136**, 1984, 65.
12. *G.L.Stoner.* J. Neurochem. **55**, 1990, 1404.
13. *R.S.Turner, C.H.J.Chou.* J. Neurochem. **43**, 1984, 1257.
14. *W.K.Yong, W.J.Halliday.* J. Cancer, **45**, 1982, 754.
15. *M.J.Weise, P.R.Carnegie.* J. Neurochem., **51**, 1988, 1267.
16. *U.Jahnke, E.H.Fischer, E.C.Jr.Alvord.* Sciences, **229**, 1985, 282.
17. *K.K.Menon, S.J.Piddlesden.* J. Neurochem. **69**, 1997, 214-222.
18. *A.E.Palma, Ph.Own, Ch.Fredric.* Ibidem, 1753-1762.

საქართველოს მეცნიერებათა აკადემიის მოამბე, 158, №1, 1998
BULLETIN OF THE GEORGIAN ACADEMY OF SCIENCES, 158, №1, 1998

BIOCHEMISTRY

N.Koshoridze, Corr. Member of the Academy N.Aleksidze, T.Garishvili, T.Lekishvili

Quantitative Alteration of Galactose and Lactose Specific Lectins at Different Stages of Hen Brain Embryonic Development

Presented October 28,1997

ABSTRACT. **By means of high pressure liquid chromatography membrane protein fractions dissolvable in EDTA-solution have been purified from hen brain embryos of different ages. It has been observed that protein fractions of mol. weight - 12000-19000 Daltons and 24000-45000 Daltons are characterised with lectin activity.**

It is assumed that the protein fraction of 12000-19000 Daltons contains the so-called D-lactose-specific lectin. As for the protein fraction of comparatively high molecular weight that is inhibited also by D-lactose and D-galactose, it is assumed that it belongs to the so-called galaptine-group.

The quantitative changes of the given lectins are studied in the process of the hen brain embryonic development.

Key words: Lectin, embryo, protein, hen's brain, hatched chicken.

According to the literature it is obvious that lectins are assayed as multivalent, mytogene proteins which are able to connect to the free and glycoprotein terminal carbohydrates. Lectins have been discovered in plant, animal and bacterial cells as well. Our attention was drawn by lectin proteins in hen embryos, in different organs of hen embryo, in particular, in retina, spinal cord [1], pectoral muscle [2] and kidney and liver [3,4] lectinally active glycoproteins have been already found; they can easily agglutinate tripsinized erythrocytes of a rabbit.

As for the brain, lectins from nervous matter participate in cell adhesion. It is also well-known that these lectins are of memberane origin connected to the surface and the inner part of the membrane associatingly, ionically [5].

Consequently, the purpose of our research was to purify and characterise free and connected lectins at different stages of brain embryonic development.

Material and methods. The lectins were purified by means of EDTA-solution [6], added to kalium phosphate buffer solution (pH 7.4) in proportion 1:5 and homogenized three times with a minute interval. The homogenate was then filtered in netting and nylon and the filtrate was centrifuged at 16000g during 40 min. According to the supernatant we calculated the lectin specificity activity of proteins dissolved in kalium phosphate buffer solution (pH 7.4). The sediments were treated with EDTA (2mkM) water-solution, homogenized, kept at room temperature for an hour and centrifuged for 16000 g/40 min. The supernatant was dialized against 40 mM kalium phosphate buffer at 0°C, concentrated and estimated the lectin activity on U-like titration table. The sensitivity towards saccharide was calculated by the hapten-inhibitory method [7]. The proteins were fractionated on a high pressure liquid chromatography ("Millipor"), column Protein PAK 300 SW, which was washed in ammonia acetate buffer (pH 6.6). The flow rate 0.8 ml/min. The calculation of the protein quantity was achieved by Lowry method [8].

Results. At the first stage of experiments we studied the distribution of lectin activity throughout the protein fractions, extracted by 2 mM EDTA-water solution at different stages of embryonic development. For this purpose we have used 5-, 8-, 10-, 15- and 20-day old hen embryos. For a better identification of lectin activity we purified the dialized suspension of brain embryo at 20,40,60,80,90 and 100% saturation by ammonia sulphate, and found out that lectin-like proteins can be purified at 80-90% concentration by ammonia sulphate and this reaction enables us to purify them afterwards partially (Table 1).

Table 1

Alteration of protein with lectin activity purified from hen embryo brain of different age at purification by ammonia sulphate

Ammonulia sulphate %	Lectin specific activity (titer-1 x mg/ml-1)				
	5 day	8 day	10 day	15 day	20 day
20	–	–	–	–	–
40	–	–	–	–	–
60	–	–	–	–	–
80	6.6 ± 0.25	4.01 ± 0.11	2.25 ± 0	1.43 ± 0.09	1.08 ± 0.1
90	1.0 ± 0.04	0.94 ± 0	0.65 ± 0	0.43 ± 0.01	0.24 ± 0.02
100	–	–	–	–	–

As it has been discovered, maximum of lectin activity of proteins purified by EDTA solution can be found on the 5th day of embryo development. At coming stages the activity decreases and makes the minimal level in a 1-day old chicken (tab. 1). We can suggest, therefore, that the decrease in lectin activity is brought about not by decrease in their amount, but by increase in the brain volume.

We used the chromatographic method to fractionize the lectins purified by ammonia sulphate and dialized afterwards in order to characterize the purified lectin-like proteins and calculate their molecular weights.

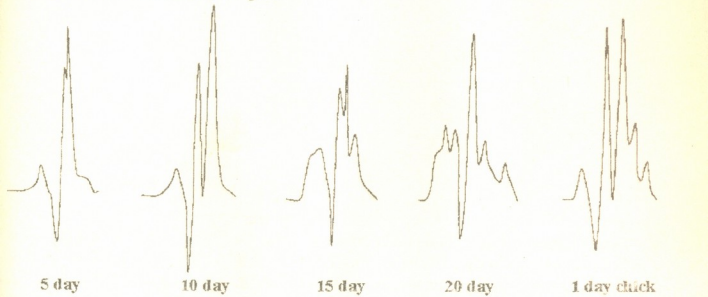

Fig. Chromatograms of different age hen brain embryos membrane proteins in a high pressure liquid chromatography system ("Millipor"). Column-Protein PaK 300 SW. Flow rate-0.8 ml/min. Scale-0.5.

The Figure represents the fractionity of proteins purified at 80% concentration by ammonia sulphate. As we can see from the picture, in embryo the quantity of protein fractions increases and the fraction sight becomes more complicated. From a 5-day old hen embryo brain 2 protein fractions can be purified (mol. weights- 19 and 30 kDa). Lectin activity was discovered in the protein fraction of 19 kDa, which had been chromatographed. As the embryo grows up, the quantity of proteins fraction, purified by the given detergent, increases, e.g. 4 protein fractions of 45,24,19 and 12 kDa can be purified from 15-day old brain embryo. We calculated lectin activity in each of them (Table 2). It is worth noting that lectin activity in the fractions after chromatographing is much higher than that in the brain suspension purified with the help of EDTA solution, e.g. increase in fraction lectin activity when fractionity of the proteins purified by EDTA from a 5-day embryo brain, makes 300% compared with that in the brain suspension.

Table 2

Molecular weights and lectin activity in membrane protein fractions purified by EDTA from hen brain embryos of different ages

Age of the Embryo (days)	Protein fractions purified by EDTA	
	Molecular weights (kDa)	Lectin specific activity
5	30	–
	19	32.66 ± 0.28
10	30	–
	19	29.85 ± 1.03
	5	–
15	45	–
	24	25.85 ± 0.99
	19	26.0 ± 1.97
	12	–
20	45	–
	27	–
	18	20.05 ± 2.03
	11	15.66 ± 1.56
	5	–
1-day old chicken	45	–
	30	–
	20	15.5 ± 0.77
	12	9.58 ± 0.84
	7	–

Very interesting results have been achieved when the carbohydrate specificity of the purified lectins was defined. The lectins purified from a 5-day old embryo brain by EDTA are characterized by sensitivity towards D-lactose, while those from a 15-day old brain, show sensitivity towards D-galactose as well as towards D-lactose. By their presence the ability of agglutination of lectin decreases.

Considering the scientific researches we can suggest that protein fractions of 12-19 kDa mol. weight, which are inhibited, represent the already known, so-called lactose-

lectin which was found in hen embryos, in particular, pectoral muscle, liver and intestines [4] while fractions of 24-45 kDa mol.weight should be lectin-like proteins of galaptine group, the so-called N-CAM, that participate in interconnection of cells in nervous system, exactly in connection of neurones in spinal cord and eye retina. Researches are still going on.

Tbilisi I.Javakhishvili State University

REFERENCES

1. *G.S.Eisenbarth, et al.* Biochem. and Biophys. Res. Commun., **83**, 4, 1978, 1246-1252.
2. *Th.P.Nowak, et al.* J. Biol. Chem., **252**, 7, 1977, 6026-6030.
3. *M.Path, D.Yang.* Biochem. and Biophys. Res. Commun. **95**, 2, 1980, 750-757.
4. *E.C.Beyer, et al.* J. Biol. Chem. **255**, 9, 1980, 4236-4239.
5. *V.A.Beresin.* Contemporary Biol. Successes. **101**, 1, 1986, 56-57.
6. *V.I.Teichberg, et al.* Proc. Nat. Acad. Sci. USA. **72**, 4, 1975, 1383-1387.
7. *H.Lis, N.Sharon.* The Lectins: Properties, Functions and Appl. in Biology and medic. Ac. Press. 1986, 265-285.
8. *M.D.Lutsik, E.N.Panasjuk, A.D.Lutsik.* The Lectins. Lvov; 1981.
9. *O.H.Lowry.* J. Biol. Chem. **105**, 1, 1951, 1-5.

M.Saatashvili, N.Tevzadze, Corr. Member of the Academy D.Jokhadze

The Effect of Biostimulators on Cultivation of Strain *Spirulina platensis* in Laboratory Conditions

Presented October 30, 1997

ABSTRACT. **Cultivation conditions of blue-green algae strain *Spirulina Platensis* on Zaruk media, the effect of phytohormones (Gibberellin A_3, kinetin) and I-ions (KI) on growth of algae culture were studied. Experimental data confirm the presence of biostimulators in strain cultural liquid.**

Key words: *Spirulina*, cultural liquid, biostimulators.

Recently much attention has been paid to the artificial cultivation of green and blue-green microalgae. These organisms are utilised as a source of valuable human and animal food proteins, as well as for the production of important pharmacological preparations. They are rich in various vitamins. Blue-green alga, *Spirulina*, natural dweller of alkaline water reservoirs is of particular interest. *Spirulina* contains large amount of proteins (approx.70%), carbohydrates (18-20%), lipids (4-6%), nucleic acids (4%), vitamins and carotine. *Spirulina* proteins have complete set of amino acids analogously to milk proteins [1,2]. Even a small quantity of *Spirulina* added to fodder considerably increases economic index [3,4]. Therefore, the investigation of the conditions of *Spirulina* cultivation establishment and study of factors responsible for intensive mass growth is considered to be very important. According to literature data the strain was grown in various inorganic media. Among them the medium recommended by Zaruk is considered to be optimal [5].

There are data that algae (including *Spirulina platensis*, *Nostoc calcicola*) secrete biostimulators and some other biologically active compounds into nutrient media affecting the growth of cultivated higher plants, their development and other physiological processes [6]. It's suggested, that these processes are the result of the effect of vitamins and phytohormones.

The mechanism of phytohormone functioning and its influence on gene functioning has been studied at our laboratory. Consequently we are interested in the study of physiological and biochemical effects of growth stimulators synthesized by algae on high plant cells.

Blue-green alga *Spirulina platensis* strain was obtained at the Institute of Botany of the Uzbek Academy of Sciences.

Cultivation conditions, with regard to all required intensive growth factors, were studied [7]. The culture was grown in thermostatic room (25-30°), with constant illumination (5000 lux) and periodic air circulation. Inorganic nutrient media, recommended by Zaruk and Wenkataraman, were used [8]. Media were renewed every 20-25 days, biomass was collected by filtration or centrifugation. Growth intensity of *Spirulina* was estimated by biomass accumulation for a certain period of time (per dry weight) or by microscopic cell calculation in Goryaev Camera.

In selected laboratory conditions the culture intensively grew on Zaruk's medium where biomass increasing in 30 days per dry weight gave 1.6-3 g/1. Though some seasonal dependence in biomass increase was observed: during winter months biomass increase reduced approximately twice (0.8 g/1).

Yellowish powder found in cultural fluid negatively affected culture growth and finally caused culture growth stop and its death. This problem was partially solved by transfer of the contaminated culture to the solid medium and its gradual renewal. Solid medium was prepared by adding of 2% agarose to Zaruk medium. On that medium the culture got completely free from all impurities and continued to grow intensively when placed into liquid medium.

The effect of phytohormones, particularly of *gibberellins* and *cytokinins*, as of stimulators on higher plant growth is well known. In order to choose optimal conditions for *Spirulina Platensis* strain growth in laboratory kinetin and gibberellin effect on algae biomass growth was studied. We also investigated the effect of iodine micro concentrations on algae growth. We observed biomass increase on such iodized medium, whereas high iodine concentrations (100-200 μg) caused growth limitation. The results are presented on the diagram (Fig.1).

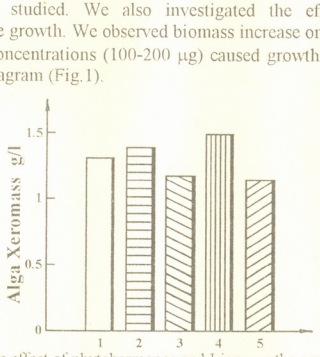

Fig. 1. The effect of phytohormones and I-ions on the growth of strain *Spirulina Platensis*

1. Zaruk medium
2. "-------" + Gibberellin A (10^{-6} M)
3. "-------" + kinetin (10^{-6} M)
4. "-------" + KI (60 μg/L)
5. "-------" + KI (200 μg/L)

These data indicate that physiological concentrations of gibberellin and kinetin (10^{-6} M) don't affect biomass growth. Recently obtained literature data showed that blue-green algae secreted some biologically active compounds into cultural fluid : biotin, thiamin, pyridoxin, indolyl-3-acid, substances similar to gibberellin and kinetin and etc. Because of these peculiarities alga strains are used as biofertilizers to raise the productivity of cultural plant.

Biological methods for phytohormone definition are based on biotesting by means of phytohormone effect determination on growth of the whole plant or plant definite parts.

We carried out series of experiments with higher plants (pea, beans) to study the effect of algae culture on their growth and development, particularly on the growth of

the young stem. Germinated seeds of bean and pea were grown on *Spirulina* strain cultural media. The control plants were grown in the same conditions in water media with gibberellin and kinetin. 15 days old shoots were measured. Our experiments revealed *Spirulina* strain stimulating effect on higher plant stem growth. This effect is equivalent to that of Gibberellin and Kinetin, thus indicating the presence of biostimulators in *Spirulina* strain cultural medium.

Table

The effect of growth stimulators and algae cultural medium on the young plant shoots

Media	Beam (*Phaseolus vulgaris*)		Pea (*Phisum sativum*)	
	stem length (cm)	%	stem length (cm)	%
Water	8.6 + 0.06	100	3.35 + 0.04	100
Spirulina strain	7.8 + 0.05	216	5.0 + 0.06	146
Water + G – A_3 (10^{-5} M)	9.8 + 0.06	272	11.0 + 0.05	328
Water + Kin. (10^{-5} M)	6.5 + 0.04	180	4.0 + 0.06	119

We continue the study of quantitative and qualitative determination of biologically active compounds.

S.Durmishidze Institute of Plant Biochemistry
Georgian Academy of Sciences

REFERENCES

1. *L.Switzer.* Spirulina. Toronto, New-York, 1982.
2. *T.Babaev, J.E.Barashkina, M.A.Kuchkarova, A.T.Tulaganov.* Uzbek. Biol. Zh., **6**, 1981 (Russian).
3. *A.T.Tulaganov, M.A.Kuchkarova.* Ibidem **5**, 1976 (Russian).
4. *Nguen Txi Kui.* Autoref. Kand. diss., Kiev, 1987 (Russian).
5. *Ph.Zaruk.* Thesis Univ. of Paris, 1966.
6. *M.A.Kuchkarova.* Autoref. doct. diss, Tashkent,1990 (Russian).
7. *M.Vladimirova, V.E.Senenco.* Intens. kultura vodoroslei, Moskva,1962 (Russian).
8. *J.Razic, Xaldad.* Autoref. kand. diss., Abovian,1990 (Russian).

BIOCHEMISTRY

F.Kalandarishvili, K.T.Wheeler

Influence of Proliferation on DNA Repair Rates in Regenerating Rat Liver

Presented by Academician T.Oniani, April 2, 1998

ABSTRACT. **This work investigates the influence of cell proliferation on DNA repair rates in regenerating rat liver. We determined the posthepatectomy proliferation kinetics for hepatocytes of the liver. The suspension of cells reacted with both FITC-labeled anti-BrdUrd antibody and propidium iodide, and the particles were analysed by flow cytometry. Liver cells were irradiated with 15.5 Gy γ-rays at various times, from 2 to 144 h after hepatectomy, and their DNA repair kinetics measured by alkaline elution to determine when the faster rate of DNA repair begins and ends relatively to the proliferation kinetics.**

Key words: DNA repair, proliferation, regenerating liver

According to the experimental data it is known that in adult male Fisher-344 rats (4-6 months old) liver cells, stimulated into proliferation by partial hepatectomy, repair their radiation-induced DNA damage faster than quiscent liver cells in unhepatectomized rats. This faster repair at 20-31 h after hepatectomy is accompanied by a change in the accessibility of the DNA to digestion by exogenous endonucleases [1]. Thus, proliferative status appears to be a major determinant of the rate of DNA repair in adult rat liver. This result is in agreement with the previously published Accessibility Hypothesis [2].

The experiments were carried out in the male Fisher 344 rats (4-6 months old), in which ~70% of liver mass was removed as described by Higgins and Anderson [3].

Unhepatectomized rats and rats 2, 12, 20-24, 29-31 or 144 hours after hepatectomy were irradiated with 15.5 Gy Cs-137 γ-rays on a self-shielded irradiator at a dose rate of ~10 Gy/min. Suspensions of single cells or nuclei were prepared as described by Meyn and Jenkins [4].

The percentage of liver cells (primary hepatocytes) in S-phase as a function of the time after hepatectomy was determined by injecting rats i.p. with 100 mg/kg of BrdUrd (5-Bromodeoxyuridine, which is incorporated into DNA in place of thymidine) by multiparametric flow cytometry, which gives detailed information on the kinetics of the cell cycle [5].

The DNA damage and repair was measured by alkaline elution technique modified for unlabeled DNA [6]. The DNA in each fraction was determined fluorometrically using the Cesarone assay [7], which binds Hoechst-33258 to the DNA. According to the method of mathematical estimation we determined the percentage of undamaged DNA remained on the filter; simultaneously we determined the percentage of the damaged DNA remaining in the cell as a function of reparation time [8].

The percentage of liver cells (primary hepatocytes) in S-phase as a function of the time after hepatectomy was determined as described above.

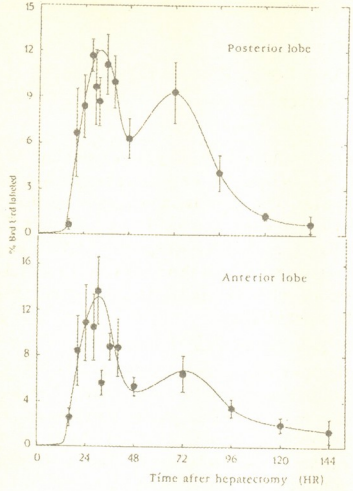

Fig. 1. Percentage of liver cells (primary hepatocytes) in either the posterior or anterior lateral lobes, which were labeled with BrdUrd as a function of the time after hepatectomy. All points are the mean ±S.E.M. of at least 3 rats.

According to the data summarized on Fig.1 the BrdUrd labeled cells did not appear until 14-16 h after hepatectomy. These BrdUrd-labeled cells increased rapidly to a peak at 30-35h. then decreased to a nadir at about 48 h followed by an increase to a second peak at about 72 h. and finally declined to the background levels at 120-144 h after hepatectomy (Fig.1). In our 250-350 g adult rats recruitment and progression of hepatocytes into S-phase is much slower than those in 60-120 g rats where the number of cells in S-phase is maximal at 20-24 h after hepatectomy [9].

The flow cytometry data in our experiments clearly show that the greatest number of liver cells are in S-phase at 30-35 h after hepatectomy.

Once the proliferative kinetics were defined we began a study to determine when the faster rate of radiation-induced DNA damage repair begins and ends relative to the proliferation.

First of all we determined the per centage on unirradiated liver DNA retained on polycarbonate filters after alkaline elution as a function of time after hepatectomy. The summary of data demonstrates that the percentage of DNA retained on the filter is the same, stastistically identical and independent of the proliferative status and time after hepatectomy (88.4%).

The DNA damage measured by the alkaline elution technique includes frank single- and double-strand breaks, alkaline labile bonds [1].

Fig.2 demonstrates DNA repair kinetics for pre- and posthepatectomized liver cells irradiated *in situ* with 15.5 Gy. The DNA repair kinetics at 2 h after hepatectomy were identical to those in unhepatectomized rats.

At 12 h after hepatectomy the DNA repair kinetics appeared to be a mixture of the slower kinetics associated with the unhepatectomized liver cells and the faster kinetics associated with hepatectomized liver cells. Thus, 12 h after hepatectomy come to be the evidence suggesting that the faster DNA repair kinetics were just beginning. By 144 h after hepatectomy the DNA repair rate returned to the repair rate observed in unhepatectomized liver cells.

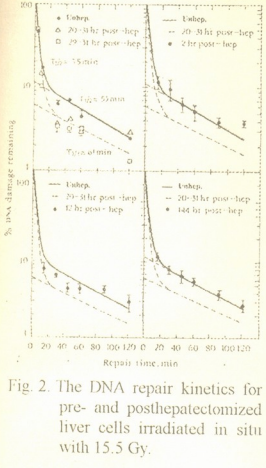

Fig. 2. The DNA repair kinetics for pre- and posthepatectomized liver cells irradiated in situ with 15.5 Gy.

The data at 20-24 and 29-31 h after hepatectomy strongly demonstrate faster repair of their radiation-induced DNA damage, than quiscent liver cells in unhepatectomized rats.

The DNA repair kinetics were biphasic in all cases. Although the early (<45 min) DNA repair in liver cells appeared to be slightly faster at 29-31 h after hepatectomy than at 20-24 h. The percentage of the DNA damage remaining in the cell handled by the slow phase decreased from ~11% in unhepatectomized liver cells to 6% in hepatectomized liver cells. This decrease in the percentage of the DNA damage remaining in the cell handled being the slow phase in unhepatectomized liver cells was accompanied by an increase in the digestibility of the DNA by m. nuclease and DNA-ase I [1] in agreement with Accessibility Hypothesis [2].

Repair of radiation-induced DNA damage in hepatectomized liver is faster than in unhepatectomized liver when the greatest number of liver cells enter the S-phase (20-31 h after hepatectomy). Although elevated levels of c-fos and c-myc in RNA have been reported in liver cells 2 h after hepatectomy and the G_0 to G_1 transition has been initiated [10], the DNA repair kinetics are identical to those found in quiescent unhepatectomized liver cells. Consequently, it is reasonable to hypothesize that the faster DNA repair kinetics are associated with the G_1 to S-phase transition, where activation of the p53, DNA-polymerase-α and polymerase-δ genes occurs [9, 10].

All the data presented support the Accessibility Hypothesis and suggest that proliferative status is a major determinant of the rate of DNA repair in rat liver.

I.Beritashvili Institute of Physiology
Georgian Academy of Sciences

REFERENCES

1. *St.Clair W. H.et al.* Exp. Cell Res., **197**, 1991, 323.
2. *K.T.Wheeler, J.V.Wierowski.* Radiat. Environ. Biophys., 93, 1983, 312.
3. *G.M.Higgins, R.M.Anderson.* Arch. Pathol., **12**, 1931, 186.
4. *R.E.Meyn, W.T.Jenkins.* Cancer Res., **43**, 1983, 5668.
5. Becton Dickenson Immunocytometry Systems Source Book. Section 3.80.1 "Monoclonal Antibodies BrdUrd Detesting Cell Proliferation and Activation, 1988.
6. *K.W.Kohn, et al.* In: A Laboratory Manual of Research Procedures N.Y., 1981, 379.
7. *C.E.Cesarone, C.Bolognesi, L.Santi.* Anal. Biochem., **100**, 1979, 188.
8. *S.G.Swarts, et al.* Radiat. Environ. Biophys., **29**, 1990, 93.
9. *A.W.Murray.* Nature, **359**, 1992, 599-604.
10. *Chun-Li Yang et al.* Biochemistry, **30**, 1991, 7534-7541.

საქართველოს მეცნიერებათა აკადემიის მოამბე, 158, №1, 1998
BULLETIN OF THE GEORGIAN ACADEMY OF SCIENCES, 158, №1, 1998

E.Kirtadze, K.Markozashvili

^{14}C-Proline Assimilation by Yeasts in Secondary Alcoholic Fermentation

Presented by Academician G.Kvesitadze, February 10, 1998

ABSTRACT. **Proline conversion products in yeast and wine were studied. It has been found that the proline carbon skeleton available in fermentation medium is involved in biosynthesis of wine organic acids and amino acids. The proline transformation products are identified in the fractions of yeast proteins and freeamino acids. In the process of secondary alcoholic fermentation proline is partially oxidized to carbon dioxide.**

Key words: proline, yeasts, secondary alcoholic fermentation, organic acids, amino acids.

Detection of peculiarities of energetic and constructive exchange during alcoholic fermentation is closely related with the study of amino acids [1, 2]. The elucidation of the ways of amino acids conversions during wine champaignization tangibly extends the possibilities of studying the chemism of alcoholic fermentation.

The work aimed to reveal the possibilities of ^{14}C-proline conversion in the process of secondary alcoholic fermentation.

For champaignization in bottles the industrial strain of wine yeasts *Saccharomyces vini-39* was used as a fermentation agent. 14.7 mg of ^{14}C-proline per 800 ml of wine was introduced into the tirage mixture, whose radioactivity was 18.5 MBk. Fermentation was carried on in hermetically closed bottles at 14-16°C. Assessment of yeast and wine components was made after the completion of primary fermentation using chemical, chromatographic and autoradiographic methods [2]. Radioactivity of identified compounds was evaluated on LKB-type scintillate spectrometer Rachbeta.

During a normal alcoholic fermentation yeasts rather well assimilate phenolalanine, thyrosin, methionine, serine, leucine. 50-80% of the assimilated amino acids falls on the initial phases [3].

In the secondary fermentation carbon atoms of glycine, serine, alanine, glutaminic acid are actively involved in the yeast biomass 2. Of other amino acids proline is noteworthy, which is contained in large amounts in grape juice, as well as in wine. There is no common view about the possibilities of its conversion in the process of fermentation, though its biological role is rather well known [4].

The results obtained in our conditions indicate that during wine champaignization 6-8% of proline present in the fermentation medium is assimilated and converted by yeast. Proline carbon atoms incorporated in biomass are actively involved in intermediate exchange of amino acids and participate in the synthesis of yeast proteins and free amino acids (Table 1.) The most of radioactivity falls on the overall fraction of yeast protein amino acids. Particularly high radioactivity is possessed by glutaminic acid, aspartic acid, proline and lysine. As a result of proline conversion, on which about 20 % of yeast overall activity falls, free amino acids of various genetic origin are formed. 11 amino acids have been identified. Among them except proline, by high radioactivity are

distinguished glutaminic acid, aspartic acid, alanine and arginine. The pool of free amino acids changes according to the physiological phases of yeast development and their amount is doubled in the exponential phase [5]. At the same time the cultivation conditions also affect the qualitative and quantitative distribution of free amino acids [6]. Distribution of radioactivity among the yeast amino acids seems to be bound with direct proline assimilation that is especially intensive in the exponential phase [5]. Major part

Table 1

Incorporation of ^{14}C-proline carbons in the yeast amino acids

Percentage of radioactivety of identified amino acids in the overall activity of the fraction			
Protein amino acids		Free amino acids	
81.4%		18.6%	
Glutaminic acid	37.2	Proline	39.4
Aspartic acid	18.7	Glutaminic acid	19.2
Proline	16.4	Aspartic acid	13.3
Lysine	14.5	Alanine	11.5
Valine	7.2	Arginine	9.6
Phenylalanine	2.7	Lysine	2.0
Tyrosine	1.5	Tyrosine	1.3
Arginine	1.1	Leucine	1.2
Histidine	0.7	Phenylalanine	1.0
		Serine	0.8
		Histidine	0.7

Table 2

Incorporation of ^{14}C-proline carbons in wine organic acids and amino acids

Percentage of radioactivity of identified compounds in the fraction overall activity			
Amino acids		Organic acids	
91.3%		8.7%	
Proline	51.6	Succinic acid	44.3
Glutaminic acid	15.3	Milic acid	37.2
GABA	11.6	Glyoxylic acid	10.2
Valine	9.2	Fumaric acid	5.4
Leucine	4.2	Glycolic acid	2.9
Threonine	3.1		
Arginine	2.0		
Thyrosine	1.1		
Lysine	0.9		
Phenylalanine	0.6		
Histidine	0.4		

of proline biotransformation products at the end of secondary alcoholic fermentation transfers into wine. Among the isolated fractions the basic ones are amino acids and organic acids. Here too, nearly more than a half of radioactivity of the formed amino

acids falls on proline (Table 2). Among the identified amino acids the basic ones are glutaminic acid, GABA and valine. The qualitative composition of wine amino acids indicate that their synthesis is a result of normal viability of yeast. Under conditions of low pH, in the presence of ethanol autolysis starts after the termination of primary fermentation and proceeds slowly.

Identified in wine were also organic acids, of which by high radioactivity are distinguished succinic and malic acids.

In the process of secondary alcoholic fermentation the proline carbon skeleton takes a complex way of biotransformation . It appears to be closely related to the intermediate exchange of amino acids, as well as the modifications of Krebs cycle, when its significance is fully determined as to provide the carbon skeleton required for the cellular metabolism.

S.Durmishidze Institute of Plant Biochemistry
Georgian Academy of Sciences

REFERENCES

1. *S.V.Durmishidze.* Poblemi evolutsionnoi i tekhnicheskoi biokhimii. Collection of works, M., 1964, 335-341 (Russian).
2. *E.G.Kirtadze, T.M.Kurdoovanidze.* Biochemical peculiarities of secondary alcoholic fermentation. Tbilisi, 1992 (Russian).
3. *Z.N.Kishkovskii, I.M.Skurokhin.* Chemistry of Wine. M., 1976 (Russian).
4. *P.Larher, L.Leport, P.Hervochon.* Physiol. plant, **79**, 2, 1990, 109.
5. *S.A.Konovalov.* Biochemistry of Yeasts. M., 1980 (Russian).
6. *A.M.Bezborodov.* Metabolites of intercellular funds of microorganisms. M., 1974 (Russian).

საქართველოს მეცნიერებათა აკადემიის მოამბე, 158, №1, 1998
BULLETIN OF THE GEORGIAN ACADEMY OF SCIENCES, 158, №1, 1998

CYTOLOGY

N.Beltadze, M.Ukleba

Ultrastructural Changes of Rabbit Eye with Mechanical Damage of Sclera and Posterior Intrascleral Filling

Presented by Corr. Member of the Academy I.Eliava, October 6,1997

ABSTRACT. **The ultrastructural changes of pigment epithelium and photoreceptors of rabbit eye with mechanical damage and posterior intrascleral filling were studied. The close connection between the terminal appendices of pigment cells and outer photoreceptor segments is disturbed on the 4th day after the operation. Mitochondrions are swollen, crysts are disrupted and the phagocytosis of the rejected parts of outer segments are default.**

These changes become normal the month after the operation. Such operations on sclera do not provoke destructive changes in retina.

Key words: photoreceptor, pigment epithelium, outer segment.

Microsurgical technique and in some cases scleraplastic operations are accepted out of surgical methods of scleral wound treatment. At this time the wound is covered with different kinds of transplants. Though only the usage of microsurgical technique cannot disturb the generation surplas and the growth of granuled tissues.

According to the experimental data, the sharp intensification of reparative processes takes place after the filling. The barrier made by filling interferes the growth of sclera deep into the eye and thanks to that stops eye retina layering.

Fig. 1. The rabbit eye pigment epithelium cell. Norm × 40.

Fig. 1. The rabbit eye retina photoreceptors on the 4th day of the operation × 50. Damaged section.

In spite of undamaging the eye pigment epithelium and photoreceptor, they undergo definite changes during the sclera damage. The goal of the present work is to study the ultrastructural changes of eye retina pigment epithelium and photoreceptor cells under the extrascleral filling of sclera wound with xenoderma.

Material and Methods. The object of the research was adult rabbit. The material was taken with the intervals of 4,7 days and a month after the operation (2 rabbits per

term at 12 p.m.). The material from the healthy area and operated eye (on the opposite side of the wound) was taken separately.

Fig. 3. The rabbit eye retina photoreceptor layer on the 4th day of the operation. × 50 damaged section.

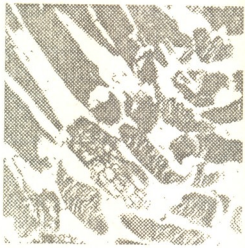

Fig. 4. The rabbit eye retina pigment epithelium layer on the 4th day of the operation, × 20 damaged sections.

As for the operated eye, electrogram got after 4 days showed that clearly expressed changes are revealed near the zones close to the wound, though the damage did not touch directly the retina and pigment epithelium. First of all, the disturbance of close contacts between the external segments of photoreceptors and pigment epithelium cell processes and also forming of free sections between them is necessary to be marked. The intense fragmentation of outer segments is also noticeable. That was probably provoked by the loss of pigment epithelium phagocytosis ability, especially as the material was fixed at 12 p.m. According to the data of most authors, it is known that shedding of the old discs of photoreceptors and the phagocytosis provoked by pigment epithelium must be run intensively in this period of time in animals with the night sight [1-2]. Not any phagosomes were revealed in the layer of pigment epithelium in electronograms obtained by us, whereas this process was coursing in its usual way in normal state on the opposite section of the wound as well and there were a lot of phagosomes of different forms. Number of changes are noticed in the pigment epithelium cells on the 4th day of operation. Namely, the pigment granules are moved in processes and this is natural to the process of phagocytosis in number of animals though as it was also mentioned, the phagosomes were not revealed. The mitochondrion swelling and intensive disruption of crysts were sharply revealed, the increase of vacuolization was also noticeable.

The disks disorientation, their disruption and formation of loop-like structure is revealed in outer segments of photoreceptors. Important changes are not revealed in internal segments. The picture is not almost changed on the 7th day of operation. The reduction of photoreceptors outer segment fragmentation is revealed, though the signs of phagocytosis were not revealed.The disorientation of disks is also reduced. Besides, the renewal of pigment epithelium and photoreceptor contacts were noticed, though this is the single case. The vacuolization and mitochondrions with disrupted crysts are remained in pigment epithelium cells.

As for the opposite side of the wound, here the picture is normal both after the 4th and 7th days of the operation. The close contact between photoreceptors and pigment epithelium cells is restored in the wound area the month after the operation and the outer segment fragmentations are not sparse. The mitochondrion crysts are partially restored and vacuolisation is reduced. And above all, the process of phagocytosis is coursing intensively, which is typical of normal state. There are a lot of external segment disks phagocytized in different periods of time in the pigment cells. The construction of photoreceptors is in norm. The normal structure is restored to the whole lengthwise and there are no disrupted disks.

As for the basic part and Bruch membrane, the changes are not revealed here.

During the mechanical damage of sclera and its posterior filling with xenoderma, the distinct reaction is revealed in the photoreceptor layer of retina and pigment epithelium cells inspite of having direct contact with the damage. First of all, this reaction is expressed in the disturbance of the close contact between the pigment epithelium segment processes and photoreceptor outer segments. It is presumable that this provoked the loss of ability of phagocytosis by the pigment epithelium, though it is not out of question that the reason of this reaction needs extra studies. We can only say that indirect reason is the mechanical damage of retina. The month after the operation the pigment retinitis signs disappear. This phenomenon is natural only for the damaged sections and doesn't spread to the other parts of the eye.

Thus, we can conclude that the above mentioned changes are not deep, that would bring us to the destruction of the eye. However, this problem needs extra studies for the serious damages of the eye cells and the pigment epithelium not to be expected after this kind of operations.

Institute of Zoology
Georgian Academy of Sciences

REFERENCES

1. *M.La Vail*. Science, **194**, 1976.
2. *W.Young*. Ultrastr. Research, **61**, 185, 1977, 1726.

CYTOLOGY

M.Zodelava, Z.Zurabashvili, S.Chuadze, E.Kldiashvili

Peculiarities of Action of Some Leucosis Plasma in Experiment

Presented by Academician T.Chanishvili, December 31, 1997

ABSTRACT. **Formed elements of blood are studied while leucosis. The defence mechanisms of erythrocytes, neutrophils and lymphocytes are described. The material is examined by means of light, luminescent and interference microscopy. Statistical treatment is done.**

Key words: leucosis, formed elements of blood, viruses.

The purpose of the present letter is to study the peculiarities of the action of cerebrospinal fluid (CSF) of patients with leucosis on the central nervous system (CNS) of the experimental animals. The obtained CSF was interperitoneally injected into the experimental animals (rabbits). After this the parts of the CNS have been studied. The plasma of the patient was injected into abdominal cavity of the rabbit at 1.5ml/kg of body weight. The rabbits were sacrificed 2 h later after the beginning of the experiment by the injection of 0.2 ml of ether narcosis into cardiac cavity. The brain pan was opened at once and then the separate parts of it were cut out (cortex, subcortex, brain stem). The material was fixed in spirit, then it was embedded in paraffin. The cross sections were coloured by Andres method. The material was fixed in pyridine by Kakhal method and impregnated by silver.

The study of separate parts of the experimental animals CNS has shown that the "fallout" of basic parts of neurons mainly revealed in the frontal lobe cortex. The greater part of neurons (especially the external complex of the frontal lobe, the cervical and the occipital cortex) was stained hyperchromatically. It mainly concerns the second layer of the mentioned lobes of the cortex.

The dendrites and cell bodies were also hyperchromatically coloured. The dendrites are curved and found at a distance. Perineuronal satellitosis is reduced. Clearly defined adhesion is observed between erythrocytes and glia cells. It is interesting to note that a great number of formed elements of blood (erythrocytes, lymphocytes) has been revealed in different parts of brain lobes of the experimental animals, especially in the brain cortex and adjacent subcortical layer. Very often erythrocytes form adhesion together with glial cells. The same was observed between erythrocytes. The erythrocytes revealed in the brain tissue were mainly of round form. The lymphocytes intensively stained were mostly of round form, very seldom lengthened. As it was mentioned above, very often lymphocytes form adhesion together with erythrocytes and create rosettes. Very often lymphocytes are observed on the surface of the neurons especially on those ones which are not intensively coloured and have a swollen body.

The study of hematoencephalic barrier (HEB) in experimental material (blood plasma of the patient suffering from leucosis) has shown that only erythrocytes in great amount pass the spaces existed between the ependymocytes [1]. As to lymphocytes they penetrate into the brain tissue not by means of HEB, but by penetration of brain tissue capillaries walls.

It should be noted that the penetration of only single erythrocytes and lymphocytes into HEB is observed in control material (the injection of blood plasma of practically healthy person into the experimental animals). There are not found lymphocytes in CSF.

In the experimental material (blood plasma of the patient suffering from leucosis) it has been found out that lymphocytes penetrate into the brain tissue by means of permeability of brain capillaries.

The above mentioned is realized in the cortex, thalamus and hypothalamus. A large discharge of lymphocytes in the brain tissue and their distribution are clearly seen in the cortex and the subcortex. Here erythrocytes assume an elongated form.

Definite structural changes are observed in CNS of the experimental animals after the injection of CSF of patients suffering from leucosis. At the same time a great number of red and white formed elements of blood are thrown into the brain tissue. This factor can be interpreted as a defensive reaction to the penetration of virus agent, which is present in CSF of the patient suffering from leucosis.

The above mentioned phenomenon seems to be connected with changes in blood flow speed, which is reduced in venous plexus covering the brain ventricle and promoting penetration of only single type of formed elements of blood (concretely erythrocytes) into CSF. On the contrary, when it concerns the brain capillaries (especially the cortex and subscortex), the blood flow speed quickens forming the turbulent flow and bringing to the extraction of a great number of only lymphocytes out of the vascular walls which have been widened beforehand. Lymphocytes are discharged as their specific weight is considerably higher than that of erythrocytes. Adhesion of erythrocytes together with the glial cells is connected with potassium metabolism. Potassium is to be introduced into glial cells out of erythrocytes increasing the activity of the latter simultaneously. The increasing activity of glial cells promotes the activity of neurons which are inhibited as a result of a toxical factor.

Adhesion of a number of neurons together with erythrocytes can be connected with the increase of oxygen metabolism in neuron bodies.

Summing up the above said it should be emphasized that the toxical agents presented in the CSF of the patient with leucosis are quite "familiar" agents for the rabbits and that is why the "struggle" against them is expressed by the fact that the formed elements of blood are sent to the brain structure by immune system in absolutely different ways: erythrocytes penetrate into the brain tissue by means of HEB while lymphocytes - by means of brain capillary system.

The existence of virus antigen in the brain structure is proved by irregular distribution of lymphocytes in the nervous system [2,3]. This factor can be considered as the marker of a non-specific infection.

Asatiani Institute of Psychiatry

REFERENCES

1. *V.I.Petrov.* Imunologia. M., 1988 (Russian).
2. *R.Jeffer.* In: Poslednie dostizheniya v klinicheskoi imunologii, M., 1983 (Russian).
3. *A.Bastin, R.Loblet et al.* Ibidem (Russian).

PHYTOPATHOLOGY

Z.Kanchaveli, R.Keshelava

The Role of Phenolic Compounds in the Resistance to Fruit Dryness

Presented by Academician G.Gigauri, April 13, 1998

ABSTRACT. **Different sorts of fruit contain various amounts of phenolic compounds. While infected by fungi causing fruit dryness the amount of phenolic compounds increases in every sort but most of all in resistant sorts. One of the representatives of phenolic compounds hydroquinone inhibits the dryness causing fungi.**

Key words: fruit dryness, phenolic compounds, hydroquinone, steadiness, resistance.

Tracheomycotic dryness of fruit causing great harm is widely spread in Georgia. An effective measure against dryness is the development of fruit resistance.

Phenolics widely spread in the tissues of the plants are very important for the steadiness of the plant. They are significant in the protective reactions of the plant. Many of them have antibiotic nature and prevent the development of the pathogen intruded into the plant. It is determined that the majority of phytoaleksins are phenols, which are developed in response to the infection [1,2]. Apart from that they have toxic features, and in some cases are correlated by phenolic compounds existing in the plant tissues and in the steadiness [3,4]. According to the data the products of phenolics oxidation are more important than the phenolic compounds themselves [5]. Among the products of ferment oxidation of phenolic compounds quinones are characterized as having the highest toxic features, but the importance of self-defence in plant tissues is limited, as they disintegrate easily and stay in tissues for a short period of time. Hydroquinone has been receiving much attention lately. According to the data given in literature it is a chemical immunizator [1].

It is determined that hydroquinone considerably limits malseco spreading in the plant [6]. From the above-mentioned literature data we have studied the total amount of phenols in comparatively steady and susceptible fruit sorts, and the changes during the diseases developed by fungi causing dryness.

Methods of Research. The objects of research were 2–3-year old fruit seedlings diseased by the fungi causing dryness and healthy seedlings of comparatively steady to dryness and succeptible sorts of different stone-cultures (*Verticillium dahliae Kleb., Gliocladium roseum* (*Link*)*Bain., Cephalosporium malorum, Cylindrocarpon destructans Wr.*). The total number of phenolic compounds in the leaves of healthy and diseased plants is determined 40 days later after the disease [7].

The influence of hydroquinone on the growth of fungi, on the secretion of toxic substances and on the activity of pectolytic enzymes is determined on Chapek's liquid area to which different concentrates of hydroquinone were added and the dry weight of fungi was determined. The creation of toxic substances in cultural philtrates was determined according to the percentage of germination of spores taken as bioindicator; the activity of pectolytic enzymes was studied [8].

The results of the research. The total number of phenolic, compounds in the healthy and artificially diseased plants with different steadiness is given in the Table.

Table

The total amount of phenolic compounds in healthy and artificially diseased leaves of different sorts of fruit

Fruit		Sort	Phenols number (in ekst.)				
			healthy	diseased by *V.dahliae*	diseased by *C.malorum*	diseased by *G.roseum*	diseased by *C.destructans*
Peach	steady	Khidistauri tetri	0.21	0.30	0.33	0.35	0.32
	susceptible	Khidistauri vardisperi	0.14	0.18	0.17	0.20	0.19
Plum	steady	Italiuri ungrula	0.22	0.36	0.34	0.37	0.35
	susceptible	Azhanis ungrula	0.16	0.20	0.21	0.19	0.18
Cherry	steady	Kharisgula	0.24	0.37	0.36	0.39	0.35
	susceptible	Droganis kviteli	0.17	0.21	0.20	0.22	0.20
Sweet cherry	steady	Kartuli alubali	0.27	0.42	0.40	0.44	0.41
	susceptible	Andoli	0.19	0.24	0.23	0.26	0.22

As it is shown in the Table the number of phenolic compounds in the comparatively steady sorts of stone-plants is more than in susceptible ones. It should be stated that in stone-cultures the total number of phenolic compounds is comparatively fewer in peaches, the most is in cherry, but plum and sweet-cherry among them have intermediate position.

The above-mentioned cultures are also analogically placed according to their steadiness to dryness: peach is comparatively susceptible and cherry is comparatively steady; plum and sweet cherry have intermediate position.

It is shown in the same Table that as a result of the disease phenolic compounds in every culture are increasing, but it is more obvious in all cultures of comparatively steady sorts than in those of susceptible ones.

We have already studied inhibitory influence of phenolic compounds, in particular hydroquinone, on the growth of fungi causing dryness, on the formation of toxic substances and on the activity of pectolytic ferments.

It is determined that in testing types inhibitory influence of hydroquinone during the low concentrations (10-8 and 10-7) is weak. The germination of spores taken as bioindicator grows insignificantly. With the growth of concentration (10-6, 10-2) the germination of spores decreases gradually and on 10-1 concentration is not pointed out.

The inhibitory effect of hydroquinone on the growth of fungi causing dryness is insignificant at low concentrations (10-8, 10-7). Starting from 10-4 to 10-2 concentration inhibitory effect increases and the growth of fungi stops at 10-1.

Inhibitory effect of high concentration of hydroquinone was marked on secretion of toxic substances by fungi causing dryness.

The addition of certain concentrations of hydroquinone on feeding area causes the limitation of fungi growth and the decrease of secretion of toxic substances. The same happens with the activity of pectolytic ferments (pectinesterase and polygalacturonase), high concentrations of hydroquinone cause the decrease of activity of mentioned ferments.

Thus, it becomes obvious that in response to infection by fungus causing dryness in comparatively steady sorts of fruit, at the first stage of disease significant growth of phenolic compounds occurs and as it is shown, they take an active part in biochemical processes proceeding in plants and the fungus in the process of infection and create a barrier having fungitoxical features to protect the intrusion of parasites and their spreading. One of the representatives of phenolic compounds – hydroquinone causes the limitation of growth of fungi causing dryness, the decrease of secretion of toxic substances and disactivation of pectolytic ferments. Thus, it is obvious that phenolic compounds take an important part in steadiness to dryness and we can consider them as one of the index of steadiness. The obtained results give us the opportunity to suppose that the increase of the phenolics number at the starting stage of the disease represents a significant diagnostic index to determine the steadiness to early dryness of fruit sorts.

L.Kanchaveli Scientific-Research Institute of Plant Protection
Georgian Agrarian Academy

REFERENCES

1. *Yu.T.Diakov*. In: Itogi nauki i tekhniki zaschity rastenii. M., 3, 1983, 217 (Russian).
2. *L.N.Metlitskii, O.L.Ozeretskovskaia*. Biokhimia imuniteta pokoy. M., 1984, 262.
3. *C.M.Jordan et al*. Can. J. Bot., **67**, 11, 1989, 3155-3163.
4. *A.P.Volynets et al*. All-Union conf. of physiologists society. Theses of reports. M., 1973, 176.
5. *L.V.Metlitskii, O.L.Ozeretskovskaya*. Fitoaleksiny, M., 1973, 176.
6. *A.A.Kanchaveli et el*. Collective works of NII ZR. MSX GSSR, XXIII, 1971, 348-351.
7. *E.N.Ksendzova*. Bull. VIZR, 20, 1971, 112-119.
8. *E.G.Salikova, N.N.Gusev*. Doklady AN SSSR, **169**, 2, 1965, 515-518.

საქართველოს მეცნიერებათა აკადემიის მოამბე, 158, №1, 1998
BULLETIN OF THE GEORGIAN ACADEMY OF SCIENCES, 158, №1, 1998

ZOOLOGY

G.Esartia, M.Gergedava

To the Study of Tortricids (*Lepidoptera, Tortricidae*) of Svaneti Fauna

Presented by Corr. Member of the Academy I.Eliava, April 13, 1998

ABSTRACT. **We present the results of the expedition in Svaneti region made in 1990-1991. A certain amount of *Lepidoptera, Tortricidae* have been collected and processed at St. Petersburg Institute of Zoology of the Russian Academy of Sciences. There were obtained 5 species from 10 families. Four species (*Aethes rubidana Tr., Chephasia vargeuriana Tr., Hedya ochroleucana Fröl., Hedya atropunctanaca*) have not been yet registered in Georgian fauna.**

Key words: *Lepidoptera, Tortricidae.*

Lepidoptera, Tortricidae present rather interesting and diverse family of *Insecta* genera. There are no published data of the mentioned family in Georgian flora, except separate publications in which some species of tortricids are regarded as pests of agricultural and forest cultures. The goal of present paper is to establish the structure of tortricids species on the basis of data obtained in Svaneti region in 1990-1991. The authors suppose that the given list is not complete and comparatively much more varieties of species might be found in this region. Common methods and the publications of different authors were used in the research of the mentioned species: Pierce, Metcalfe, (1922); Hanomann, (1961); Danilevsky, Kuznetsov, 1973, 1978; 1994; Bradly, et al. 1979:; Esartia 1988 and materials presented in collections of some Institutes of St. Petersburg of the Russian Academy of Sciences [1-7].

Species revealed by us in Svaneti are listed below.

Aethes rubidana Tr.. Front wings of the moth are yellowish-orange. Transtila is of complete and oval form. Gnathoma is short.

Cnephasia vargeuriana Tr.. Aedeagus is short and big, its length exceeds a little the width of valves. Right wall of aedeagus is comparatively sclerosed, rounded in the end. Worms of first generation winter in diapause. Wintered worms of young age make glasses, then worms of old age twist the leaves of different herbaceous plants (compositae, legiminosae, cruciferous) and develop there.

Archips xylosteanal L.. Individuals of the mentioned species have brownish-yellow wings. Pretornal band is complete and reddish brown, reflection is seen in its costal part on the general background of the wing . As to the genital structures, upper sclerosed part of aedeagus is deepened. Seed worms first grow in the buds of garden, park and forest cultures, then in twisted leaves. The moths fly from June up to the middle of August.

Archips podani meridiana Kozlov et Esartia (*Archips podana* Sc.). Individuals of this subspecies as well as basic species of moths have reddish brown front wings, with vividly expressed brown asymmetric form at the top. The majority of the Caucasian

subspecies individuals has lateral dens on the left wall of the aedeagus, whose head often is divided. Along with it the reduction tendency of the mentioned dens is observed.

Archips lafauriana Rag. The front wings of the moth are of dark orange or yellowish-orange, back wings are dark or dark orange. Sucullus has two appendages: the first one is ventricular long and bend; the second one is distal short, like swellings. The worms grow in wisted leaves and young buds of rose family, as well as in citrus plants and technical cultures.

Archips rosana L. The front wings of this species are greyish-rose, where reticular bands are observed. Individuals of this species have long lateral appendage on the left wall of aedeagus. Seed worms are registered on the plants of 32 families and 130 species. Moths fly in June and August.

Dichelia histrionana Fröl. Front wings are dark grey, on the bottom of which there is light grey waved band. The worms are registered in coniferous plants. Moths fly from July up to the middle of August.

Syndemis musculana Hbn. Front wings of moth are light grey. Pretornal band is dark, brown coloured and widens at the dorsal end. As to the genitals it should be noted that dens row is developed in the left side of aedeagus. The worms are supposed to grow on different kinds of herbaceous plants in Georgian conditions. In Europe the worms are fixed on oak, poplar, willow and other trees. Moths fly in subalpine zone, in July.

Hedya atropunctana Cön. Moths of the mentioned species in discal part of front wings have black points, uncus is thin, not divided at the end as it is in other representatives of this species. The worms are big and wide and grow between the leaves of birch and alder trees glued to each other.

Hedya ochroleucana Fröl. Front wings are yellowish-brown without a black point in the middle part of discal which is characteristic to other species of this genera. Uncus is wide and divided at the end. Their worms are small and thin. They are found on the leaves of dog rose.

Celypha anatoliana Car. Uncus is narrow and it is not divided at the end. Succulus consists of lengthened and needle-shaped seta. Cucullus at the top is slightly widen.

The moth size with streched wings is 14-16 cm.

Phiaris delitana Gn. Front wings of these moths are mainly yellowish-brown and can vary up to dark grey. Wide band in the middle is greyish and it is hardly observed, uncus is narrow and complete. Cucullus is two times thinner than succulus, aedeagus is short, the worms grow on the leaves of herbaceous plants.

Eucosma Hohenwartiana Den. et Schiff. The back wings of these moths are slightly transparent, the length of cucullus is far less as compared to the rest part of valve. The worms grow on different kinds of compositae plants. The moths fly in June and August.

Cydia fagiglandana Z.. The color of front wings is rather unsteady. Generally it is uneven brown grey, the color of back wings is unsteady, often light grey or greyish brown. The size of moths with stretched wings is 10-19 cm. Beneath the succulus basal hole a group of setae is placed. Clearly expressed contours are not observed on postvaginal plates of females, anal papilla are wide and long, its length is about two

times more than width. The worms grow in beech fruit and oak acorn. The moths fly in July, August.

Cydia pomonella L.. Near the valva wall, namely near succulus dens is located. Aedeagus is short. In females ductus is two or three times narrower than copulatory pouch. Anal teats are of ordinary form. At the end they are grown in each other. Worms are developed in apple fruit as well as pear, quince, peach, apricot and others. Three generations are characteristic for them a year.

Thus 15 species from 10 families have been obtained in Svaneti region and four of them are registered for the first time in Georgian fauna.

We would like to thank Corr. Member of the Russian Academy of Sciences, Professor V. Kuznetsov at St. Petersburg Institute of Geology and senior scientific worker A. L'vovski for their help and fruitful discussions.

Zugdidi Teachers Advanced Training Institute

REFERENCES

1. *F.N.Pierce, J.W.Metcalfe.* The Genitals of the British *Tortricaldae-Oundle*. Northants. 1922. 100
2. *A.S.Danilevskii, V.I.Kuznetzov.* Fauna of the USSR. Tortriacidae, Laspeyresiini. L. 1968. 635 (Russian).
3. *V.I.Kuznetsov.* Cheschuekrylye fauny SSSR i sopredel'nykh stran. L. 1973. 44-161.
4. Idem. Opredelitel' nasekomykh evropeiskoi chasti SSSR. L. 1978. 193-686.
5. Idem. Nasekomye, kleschi-vrediteli sel'skokhoziastvenykh kul'tur. St.Peterburg 1994. 144-154.
6. *I. D.Bradly, W.G.Tremewan, et al.* Oletheutinae. London. 1975. 1975, 955.
7. *G.K.Esartia.* Entomologic Review. L. **67**, 1. 1988. 131-141.

EXPERIMENTAL MORPHOLOGY

Zig.Zurabashvili, E.Kldiashvili

Peculiarities of Action of Leukaemic Patients' Blood Serum Upon the CNS of Experimental Animals

Presented by Academician N.Javakhishvili, October 27, 1997

ABSTRACT. **The permeability of the blood-brain barrier (BBB) for blood formed elements under the influence of leukaemic patient serum upon the CNS of experimental animals was studied. The raising of permeability of the brain capillary walls and lymphocytes penetration in the brain tissue is shown. Such phenomena weren't observed in the control group of animals, where donor serum was used.**

Key words: endothelium, leukocyte, neutrophil, monocyte, cortex, brain trunk.

The permeability of the BBB for blood formed elements is still debatable. Usually the blood-brain barrier is practically impenetrable for blood white and red cells. Leukocytes interaction with endothelium has the direct relation to vascular permeability and to lymphocyte entrance in the tissue from bloodstream. In the beginning leukocytes "adhere" to the endothelium and then go through it. There is a dynamic equilibrium between cells of circulable and marginal pools. Normally leukocytes "roll" along vascular wall and are only rarely firmly fixed on the endothelium.

D.N.Majansky [1] notes that neutrophils and monocytes begin their entrance from capillaries simultaneously, but in the beginning migration of neutrophils is much stronger. They perish in infectious nidus, monocytes stay in the zone of damage, where they are transformed into macrophages. Lymphocytes are fixed on the endothelium by microfibers in the presence of calcium ions. They migrate only through intracellular slot. It must be noted that mobility of lymphocytes is less than that of neutrophils and monocytes. In pathological conditions immunocompetent and other cells are intolerable to the brain antigens. They penetrate into the nervous tissue from blood and are accumulated there. They get into the CNS by migration from bloodstream through endotheliocytes and changed cells of capillary. Probably they can pass through endothelium. It is confirmed by electronic microphotos of the brain. Immunocompetent cells of blood are pushed from capillary wall into CSF [2]. The early changes of nervous tissue and its capillary ultrastructures are observed in pathology. They reflect changes of brain bloodstream. Lowering of brain bloodstream is a result of swelling of capillary endothelial cells. It also depends on the developing brain swelling. This results in the following breach of blood circulation on microcirculatory level [3] and also the breach of permeability of the BBB.

Lymphocyte adhesion on endothelium, and consequently microcirculatory breaches, are rather widespread phenomena. H.H.Lypowsky et al. [4] show preferable adhesion of lymphocytes in sufficiently large veinlets (30-50 mkm). The ability of microcirculatory bed to redistribute the bloodstream was also discovered. This mechanism compensates the results of cell adhesion. The result of adhesion of cells in the smallest postcapillary veinlets is the most important haemodynamic breach. Besides, deformation of blood cells makes significant effect in this case. The breaches of function and permeability of

the BBB was found with patients with acute leukaemia or lymphomas with high-grade malignancy [5]. This research aims to study the action of leukaemic patients serum upon the CNS of experimental animals. Serum was injected in experimental animals (rabbits) intraperitoneally. The parts of the CNS were investigated: motor cortex and brain trunk. Serum was injected 1.5 ml/kg of animal weight. Rabbits were killed by injection of 0.2 ml ether in the heart . Box cranium was dissected right away and studied parts of the brain (cortex, brain trunk) were cut out. The material was fixed in alcohol, moulded in paraffin, cut with microtome and tinctured by Andres method. A large amount of blood formed elements (neutrophils) were revealed in different parts of the brain of the experimental animals, especially in the cortex of cerebral hemisphere. They were chiefly roundish. Neutrophils were often placed on the surface of intensively tinctured and swelled neurones. The study of the material showed neutrophil penetration into the brain tissue as a result of raised permeability of the walls of cerebral capillaries. This was clearly apparent in the cortex, ocular protuberance and hypothalamus. Raising of permeability of vascular walls resulted in the rejection of roundish neutrophils in great amounts. Cells were intensively tinctured. It must be noted that neutrophils were not found in the CSF of experimental animals.

Based on our experiments it can be noted that passage of neutrophils through capillary walls is a protective reaction of animal. Probably it may be connected with the change of bloodstream velocity. As bloodstream velocity is increased in cerebral capillaries (especially in cortex capillaries), a turbulent stream was made. It predetermined rejection of neutrophils through walls of dilated blood capillaries. Especially as neutrophils have higher specific weight in comparison with other blood formed elements.

Investigations testify to the role of haemodynamics in the permeability of the BBB for blood formed elements. Changes of permeability of the blood-brain barrier influence upon the functional and structural interactions of different parts of the CNS. This is of special interest in diseases of non-specific genesis. Changes of permeability of the BBB seem to be connected with possibilities of the immune system, as on the basis of data of a range of authors [2, 3, 6-9], the CNS doesn't exist without immunological supervision that is realized by microglia, as well as red and white CSF cells tolerant to brain antigens.

M.Asatiani Institute of Psychiatry
of Georgian Ministry of Health Care

REFERENCES

1. *D.N.Majansky.* Uspekhi sovremennoi biologii, **106**, 2, 1988, 290-295 (Russian).
2. *J.A.Malashchia.* Immunnyi barier mozga, M., 1986, (Russian).
3. *I.V.Gannushkina.* Immunologicheskie aspecty travmy i sosudistykh porazhenyi golovnogo mozga, M., 1974, (Russian).
4. *H.H.Lipowsky et al.* Proc. Satell. Symp. 4th World Congress Microcirc., Taipei, Aug., 5-6, 1987, N-Y, London, 1988, 85-93.
5. *B.Zdziarska, P.Nowacki, B.Millo.* Acta Haematologica Polonica, 26(3), 1995, 299-304.
6. *I.S.Freidlin.* Systema mononucklearnych fagocitov, M., 1984, (Russian).
7. *F.Baldvin.* Eds J. Carr, W. Daems.-New-York, 1, 1980, 635-660.
8. *A.Fontana et al.* J. Immunol., **132**, 4, 1984, 1941-1982.
9. *S.L.Hauser et al.* J. Neuroimmunol., **5**, 2, 1983, 197-205.
10. *D.J.Lange et al.* Arch. neurol. (Chic.), **45**, 10, 1988, 1084-1088.

EXPERIMENTAL MEDICINE

M.Epremashvili

Diabetes Mellitus and Prediabetes Among the Georgian Jews in Tbilisi

Presented by Corr. Member of the Academy T. Dekanosidze, March 2, 1998

ABSTRACT. **According to the obtained data 100 Georgian Jewish families from 700 questioned ones appeared to have diabetes mellitus. Not a single case of its juvenile form of manifestation at the age under 28, and insulin-dependent patients at the moment of manifestation was registered.**

Practically healthy relatives in the families with the hereditary burden of diabetes mellitus must be examined by glucose tolerance test in order to reveal prediabetes or diabete mellitus and take preventive measures in time.

Key words: diabetes mellitus, Georgian jews, prediabetes.

The increased incidence of diabetes mellitus has been revealed thanks to the improvement in the methods of early diagnostics [1, 2].

The aim of diabetes prophylaxis is to reveal its frequency and peculiarities of clinical proceeding in the population of those inhabitants in which according to the existing literature diabetes mellitus is hereditary or heredofamilial disease. According to the same data the main reason of familial diabetes are marriages between relatives. Generally, marriages between relatives have their religious basis. It is known that the Georgian Jews generation is a closed community and it represents the population which members get married to the members of their own community. This phenomena has a great genetic load.

If a certain part of the population is closed, not numerous and isolated from the outside world from the point of view of marriages than marriages between relatives are frequent and two or three centuries are enough for their separate representatives to become blood relatives [2].

Thus, the probability of recessive or dominant gene existence in this population is much bigger and therefore marriages between the close relatives promote the appearance of homozygous phenotype in these families.

According to the same author there are three degrees of family ties: 1) proband's children, parents brother and sister; 2) proband's uncles, aunts, grandchildren; 3) proband's cousins, nieces, nephews and great-grandchildren.

The historical records testify that the Jews live in Georgia for twenty-six centuries and they are known as Georgian Jews. The marriages within Georgian Jews foreseeing religious and other factors occur only between the representatives of their community.

The purpose of the article is to study the Jewish families living in Tbilisi in order to reveal diabetes mellitus or prediabetes in them and initiate prophylactic medical examination and treatment in proper time.

700 Jewish families, living in Tbilisi, were questioned according to the special questionnaire published by WHO. 209 persons from 100 families, appeared to have diabetic disorder. At present 167 patients, from 209 that were registered in these families, are

alive. Two or more persons in each family had diabetes mellitus. 40 persons had insulin-dependent diabetes mellitus (IDDM). Data obtained are demonstrated in Tables 1 and 2. There is only one patient among 25-44 - year old patients that got diabetes at the age of 28, i. e. at the moment of the manifestation of the disorder not a single patient was the age under 28. It should be mentioned that at the moment of diabetes mellitus manifestation all patients in 100 families were insulin-independent and only after some duration of the disease and appearance of various complications a part of them became insulin-dependent.

Table 1

The degrees of family ties in the patients with diabetes mellitus

Degree of family ties	Number of patients IDDM	IDDM	Total
120	100	120	
II	16	49	65
III	4	20	24

Glucose tolerance test was carried out for the early detection of latent diabetes mellitus or prediabete. 52 practically healthy members of the patients' families with the first degree family ties were subjected to the glucose-tolerance test.

Table 2

Ages of patients with diabetes mellitus at the beginning of the disorder

Ages of patients at the moment of disorder beginning	Man	Woman	Total
0-14	0	0	0
15-24	0	0	0
25 44	14	21	35
45-65	52	75	127
65 and more	2	3	5

75g of glucose in 250-300g of water was mixed after taking fasting blood samples. The level of glucose in the peripheral blood from finger is determined by ames-glucosometer 3 in 60,120 min after glucose intake. According to several authors the amount of glucose in blood from finger ranges:

fasting	3.89-6.66 mmol/L
in 60 minutes	9.6-9,99 mmol/L
in 120 minutes	6,66-7.77 mmol/L

The glucose-tolerance test is considered to be disturbed when glucose level in blood was:

fasting	7.49 mmol/L
in 60 minutes	11.37 mmol/L
in 120 minutes	9.6 mmol/L

Thus latent diabetes mellitus is revealed by glucose-tolerance test in 12 cases - 23% (5 men, 7 women), "dubios" glucose was registered in 16 cases - 30.6% (7 men, 9 women), in the other cases normal type of curve was indicated.

The Institute of Therapy

REFERENCES

1. *M.I.Balabolkin.* Endokrinologia M., 1989, 3-5.
2. *A.Mazovetski, V.K.Velikov.* Sakharnyi diabet. 1987, [1], 3-4 (Russian).
3. *K.Stern.* Osnovy genetiki cheloveka. Moskva, 1965, 335-337 (Russian).

R.Otinashvili

Reasons of the Underground Economy in Georgia

Presented by Corr. Member of the Academy L.Chikava, March 12, 1998

ABSTRACT. **The underground economy emerges as one of the major problems in Georgia today. The constituent parts of underground economy are discussed. The necessity of a special organised system against underground economy is offered.**

Key words: underground economy.

The improve of public welfare can be realised only by the development of national economy, which must be ensured by rigid productive potential, corresponding infrastructure and fiscal policy, tight monetary credit system and legal base.

Though Georgia belongs to the developing countries, it has high intellectual potential, original spiritual and material culture, favourable geopolitical position and the best natural and climatic conditions. However the standard of living is very low.

One of the main preventing factors is the underground economy [1], which is a constituent part of any country's economic system in a certain degree. It is a social and economic phenomenon and not occasional, mechanical unity of natural, episodical lawbreaking activities. The mercenary interests and motivations of the individuals and separate social groups form the underground economy. The underground economy includes "fictitious economy", criminal economy and secondary or closed economy [2].

Fictitious economy is uneconomical management and misuse of the fortune, the violation of accounts, departure from accepted standards. (Anything can be written on the paper). According to the data of the World bank's experts the scale of underground economy in many countries, as well as in Georgia reaches 70%. All this is the motive power of corruption and it promotes illegal redistribution of national wealth in favor of separate clans. It neglects the law, paralyses state machinery and causes the social erosion and decay of the population. Under the conditions of centralised economy the corruption is greatly increased. The demonopolisation of the economy, the creation of real market relations considerably lessens its scales.

Criminal or Black Economy is a business undertaking prohibited by the law, e.g. the production and realisation of weapons, poisonous gases, narcobusiness, contraband currency manipulations.

Secondary or closed economy is the secret workshops production without any license. Such kind of activity can take place both in industrial and service spheres. At this time the goods are produced and sold at the market. On the one hand, it has a positive effect on equilibrium goods on market, which lowers the prices, but on the other hand the goods produced by the illegal enterprise are not registered in the national joint manufacture and the calculation of economic indices become difficult. Such establishments do not pay the taxes and the considerable income does not go to the state budget that finally decreases the standard of public welfare [2].

The weaker the legal economy is developed in a country, the larger are the scales of the shadow economy [3]. The shadow economy is a forced reaction on dissatisfaction of demands. People's aspiration for well-being is the same everywhere. If the authorities elected by the people cannot ensure this, men themselves try to obtain the well-being and often use illegal means for it.

The main social and economic reasons of the large scale of the underground economy in Georgia are:

1. The weakness of the civil society and the alienation of the authorities from the society. The civil culture of the authorities, which must bear the responsibility before the nation, is very low. Analogously the self-consciousness of the population who has elected the government and must ask for absence account is also very low.
2. The absence of national ideology. From this point of view the eastern countries such as Japan, South Korea, where the national self-consciousness is very high which plays a great part in economical success, can serve as a model to us.
3. Not very effective economic policy of the authorities i.e. indicative planning which is successfully carried out in many developed states in Georgia, failed to work properly and respond less its demand – to carry recommendatory character.
4. The weakness and serious drawbacks of the judicial bodies, in defencing the laws and other norms, when the law becomes the privilege of those who possess the political and economical power, then those who are lack of it have nothing to do but commit unlawful actions.
5. High indices of unemployment. Today there is a lot of work to do in Georgia but due to the present economic crisis most of the people are unemployed.
6. The average low salaries especially in budgetary organisations where the great part of the population is still employed. It is known that labor productivity is directly proportional to their labor compensation, i.e. the more they are paid the harder they work. In Georgia there is a great disproportion between the minimum wages and the actual wages.
7. High taxation rates. In our opinion in Georgia, where the market relations are being developed and many enterprises have just started working, the taxation rates are high, which reduces the fiscal incomes and the great part of it goes to the shadow economy. For the increasing scales and actuality of the underground economy in Georgia, it is necessary to study the problem and create a special militant organs system against it. This must have a centralised direction not only for the campaign against it. This must have a centralised direction not only for the campaign against the underground economy but it must also study and analyse the causing reasons of the underground economy.

Academy of the Ministry of State Security
of Georgian Republic

REFERENCES

1. Collection of the Academy State Security articles, **138**, 2. Tbilisi, 1997.
2. *E.F.Borisov*. Economical Theory, M., 1996, 478 (Russian)
3. Underground Economy, M., 1991, 160 (Russian).
4. Ernardo de" Soto Inoy put". (translated from English), M., 1995, 320.

G.Molinié, I.Pkhakadze, N.Tsotadze

Verbal Expression of Emotions or Emotion in the Text

Presented by Academician A.Gvakharia, September 15, 1997

ABSTRACT. **Slogans of the advertisement amuse, irritate, frequently obsess us. But, where do the most successful slogans find the power of seduction that makes them insidious? Linguistic resources used by authors stimulate attention, desire, ability to memorise. Establishing formal regularities such as sound repetition, ambiguous terms, different structures and so on we tried to show that slogans obey powerful laws of language.**

Key words: advertisement, slogan, emotion, rhetoric figures, language, tropes.

Advertisement based on the rational axis affects the listener, and this occurs because it contains elements of affect. The advertisement first of all should be attractive, pleasant, exciting. In the given article we will talk only about one component - affective side of the language.

What particular means are used in the advertising language to reach this goal? Rhetoric figures should be mentioned on the first place. Figure is a gap between content and used lexical and syntactic means [1]. The language of advertisement is filled with these ornaments, these affective means of attraction. Which figures does the advertising business use? Based on the considered advertisements we can distinguish both macro-structure and micro-structure figures. In other words, we revealed as word, sense, construction and thought figures. Among the used linguistic means are such real acts of speech as questions or such operational proposition as description and simile. In the list of figures by Bernard Lamy, a figure "doubt" is found. The figure expresses very clearly motion of soul. We can notice this in numerous advertisements. According to Lamy, "exclamation, delight must occupy the first place on this list of figures, because passions are brought to speech by means of these figures. Exclamation is a voice that the inner force makes a delighted, surprised or depressed human being cry out. It is very natural, that speech of the passionate person is full of exclamations" [2]. When reading the following advertising slogans, we hear the voice of delighted author :

- *Un ami c'est génial!*
- *J'ai trouvé l'homme qui va avec la robe de ma vie.*
- *Liberez le top modèle qui est en vous pour 299 francs!* (Elite)
- *Pour plaire, éliminer l'adversaire!* (Payot)

Short verbal or non-verbal phrases, segmented interrogative, antithetical, intense sentences are very characteristic to the emotional advertising language. Interrogative advertising sentences are very impressive. They do not require a reply. The listener does not have to choose answer or not to answer. The trick of the advertisement is, that it does not need quick answers, or, better, a question does not give him the possibility of choice. The speaker says whatever he wants to say by interrogative phrase, which at the

same time signifies something else. Therefore, listener does not analyse these phrases as interrogative and does not fill himself obliged to answer [3]. However, these phrases cause his curiosity, interest, doubt...

- – *Jusqu'à quel âge on est immortel?* (CNP)
- *Pourquoi auriez-vous changé?* (BMW)
- *Aventure : Etes-vous terre ou Esprit?*

The phrases containing denial stimulate curiosity as well as unfinished structures.

- *Ne passons pas à côté des choses simples.*
- *Ne portez rien et vous aurez tout* (Maison du naturalisme)
- *Si votre povoir de séduction repose sur... la singulariré, l'audace, l'impertinence...* (Chanel)
- *Quand un décolleté en Coton rencontre une bretelle en guipure...* (Chantelle).

Such type affective slogans intrigue us, move us by their hidden mystery.

Among the word figures, that only falls on the signifier, we would try to draw your attention to rhythmic and rhymic structures, which makes deep impression on the consumer's psychology. Rhythmic and rhymic slogans are pleasant to hear, seductive, are easy to remember. The below mentioned slogans are characterised by repeating one and the same element. And repetition is one of the basic features of the figure. In the given examples we meet such figures as alliteration, assonance, reprise of the syllable or paronomasia, antanaclase:

- *L'essentiel est dans lactel* (Lactel)
- *Knorr Secret d'Aromes* (Knorr)
- ***Forêts** du monde, **forêt**s des hommes.*
- ***Long**champ et nous c'est pour **long**temps* (Longchamp)

It is simple to conceive interchange on syllable dfour", and sounds [s] and [r] in this well equilibrated and rhythmic phrase :

- *Les fourrures font fourreur. Sensuelles et sophistiquées, elles semblent plus vraies que la réalité. Et pour le rêve... on est cômblées!*

The use of antonyms makes special emotional effect. Their place and number is variable :

- ***Moins** on roule, **plus** on va vite* (Air Inter).
- ***Le mini maxi** ou **le maxi mini*** (Moulinex).

Some advertising agencies not only take special substances, but also use special forms to attract consumer's attention:

Rien que des hites,
Rien que des tops,
Rien que des tubes,
Rien que des succès, rien que tout,
C'est qu'on a aimé,
Rien que tout,
Ce qu'on aimera toujours,
Rien que des trésors,
Rien que de l'or.(RFM)

Among the sense figures, that falls on the **signified**, there are both simple and complex tropes: metonymys, synecdoches, metaphors, hyperboles, oxymorons, similes and etc. Creators of advertisements do not accentuate only this. They play on listeners' narcissistic nature, use all means for the seduction to be maximal. For instance, listeners are often presented as owners of the advertising products. The present time of predicate used in slogans proves this.

- *Votre femme* ***est*** *la plus belle. Vos enfants* ***sont*** *les plus beaux. Vous-même, vous* ***n'êtes*** *pas mal. Voici la voiture qu'il vous* ***faut*** (Citröen Xantia).

- *Le premier mascara créé pour graduer l'intensité de votre regard* (Dior).

- *Saxo. La voiture vous permettra de séduire et d'en assumer les conséquences* (Renault).

- *La gourmandise vous va si bien* (Sveltesse).

For the emotional content or form of advertisement the construction is characteristic, in the first part of which advertising subject and its features are given. In the second part of this construction we become aware of what awaits a listener in case of correct choice. Very often there is no connecting parts (copule) between them :

- *Serenity: la sécurité que vous attendiez* (Serenity).

- *Dior... Fascination* (Dior).

- *Alfa 145. Emotion rare.*

In generally, the first syntax modificator in the advertisement language is a construction figure - ellipsis. It acts on every component of a phrase, and first of all, on determiner.

- *Toute bronzé, dehors, dedans.* Subject and predicate are missing in this sentence. It should be : "elle est".

If we will concentrate on the words used in the advertisement, we will find out, that the choice of the words is not occasional. Most of all, they are epithets of the desired word. In some advertisements the words standing for the feelings and emotions that will be experienced by the listener are directly mentioned:

- *Pour elle, chaque instant est une émotion* (Chaumet).

- *Le plaisir innatendu* (Esté Lauder).

- *C'est si beau d'hésiter* (Kenzo).

- *C'est la folie.*

The language of advertisement is vague, mysterious, interesting, very often, it is ambiguous:

- *Quand il s'enroule, on s'y attache* (Van Der Bauwerde).

- *Attention, ça marche* (Carven).

- *Tu me manques!* (Motorola).

What does "ça", "il", "tu" mean? These pronouns excite our curiosity, which is the first stage of strong emotion.

In order to create emotion, advertisement uses different layers of language : it could be lofty literal language, scientific language, everyday or youth language. Creators of advertisements often use familiar manner to be closer to consumer, pretending to be very intimate and friendly. This fact could not be justified by the literal

norms in phrases, but creators of advertisements estimate this very positively because the aim is reached: word attracts people's attention :

- *Entre le bricolage et vous il faut que ça colle.*

When studying advertisements we have found, that in the advertising language the linguistic means which is known by the name of "mot-valise" is widely used. In this expression two words are connected and partially superimpose on each other. For example, "délicat" and "caresse" break all rules and are united into "délicaresse". This linguistic hybrid causes cheerful mood and interests the listener. At the same time, it is very easy to pronounce and remember. Everything depends on semantic alliance: e.g.: *Cadeaumembert, conforamabilité.*

Between thought figures in advertisement the macro-structure type figure, which is called humour, occupies special place. Emotional reactions, such as fear, humour, facilitate persuasion, as well as erotic messages. In the advertisement the share of linguistic (verbal) or non-linguistic parts are not always similar, they fill each other. Probably humour is a figure, that uses rational mechanism, which causes laugh and which is undoubtedly affective [4]. In one word, this is the technique of laugh, the main idea of which is to create a gap between tone and words, which makes listeners laugh. In the advertisement humour is first of all a tempting, seductive component attracting consumers' attention.

Hence, it can be said, that all mentioned linguistic means play the role of a lever, a lure of a kind. All means, be it stylistic, rhetoric, grammatical or syntactic, serve the only goal: messages, that include these means, act on listeners in the "impressive" way, or, better, their aim is to leave an forgettable trace (impression) on consumer, to excite him/her, that in its turn push him/her to follow an advice of the advertisement. Considering these means, we are persuaded once more by the special nature, inexhaustible possibilities and rules of language.

Tbilisi I.Javakhishvili State University
University Paris Sorbonne Paris IV

REFERENCES

1. *G.Molinié*. Eléments de la stylistique française. PUF. 1991.
2. *Lamy*. La rhetorique ou l'art de parler. Amsterdam: Marret. 1699.
3. *B.Gruning*. Les mots de la publicité. Presse de CNRS. 1990.
4. *P.Fontanier*. Les figures du discours. 1821-1830.

Z.Liluashvili

To the Etymology of Achilles' Name

Presented by Corr.Member of the Academy R.Gordeziani, September 8, 1997

ABSTRACT. **The definition of the etymology of Achilles' name is one of the most problematic questions in scientific literature. We review numerous variants of its origin in our work and at last come to the conclusion that etymology of Achilles name must be generally explained on the background of onomastic principles and it can be regarded as the name of pre-Greek, Pelazgic origin.**

Key words: Achilles.

Achilles became one of the most prominent figures of ancient Greek literature due to the Homeric epos. Homer's skill of transferring the mythological hero into the literary character had played main role in it. There are a number of controversial questions in scientific literature concerning Achilles. First is the problem of his primary connection with the Trojan cycle, then comes the question of his transformation from Pelazgian hero into the Hellenic one and so on. And here can be reviewed the most interesting problem of the etymology of Achilles' name. We must pay our attention to the dual character of the problem: 1)the attitude of Greeks themselves to the above-mentioned question even on the folklore level; 2)the modern approach to this problem.

Evidently the name first appears in Mycenean epoch. As a rule, it is connected with the Nominative case form of Mycenean documents akireu (KNVc106), as for Dative, it is presented by the form - akirewe – 'Aχil(λ)eFε(i) [1]. And if we speak about Homer and after-Homeric traditions, the name here appears in two variants: 'Αχιλεvs and 'Αχιλλευs. Most of the scientists explain the existence of λλ as caused by the metric need, although some authors see in it the typical pre-Greek λλ exchange.

Some alternative etymologies of the name were suggested in antique epoch. The most wide-spread tendency was its connection with αχος, although there were some variations in determining the semantic meaning of the proper name itself, so far as αχος contains a large number of meaningful shades. Due to this fact Αχιλ(λ)ευs was determined as "the Grief of Ilions" (Sch. Il. 1,1 Eustath. Il. 14,18) - because of "the grief and despair of defeated Ilion's population". According to this etymology, Achilles' name consists of two parts: αχος (grief) and "Ιλιευς" (Ilions, the people of Ilion). There is also another etymology of the name, which divides the name into αχος and ιαλλω (appearance) and gives to it the meaning of "griever, the man who brings grief while mourning" (Eust. a.a.G. 14.13). Other interpreters say that alongside with αχος the name consists of λαος (people) and translate it as "people's grief" (Sch.Il.1,1 et. n.).

The other group of etymologists participates the name in α στερητικος (i.e. α of negation) and lexical form χιλος (Eust. Il.14, 18) - "hay, pasture, furage"; but α can have a contrast meaning and in such case αχιλος can be translated as "rich with pasture, furage". There are some attempts of connecting the name with χειλος. Two components are fixed here:

α and χειλος; αχειλος form is explained as "without lips" though the reason, why he was named so isn't quite clear. Tsece in "Lycophros" explains it so: "when Achilles was thrown into fire by his mother Thetis, his lips were burnt". According to Apollodoros "Achilles had never sucked his mothers breasts as he was brought up by Chyron" (Apoll.3.13.6). The same version is given by poet Agamestor of Fersal [2]. So it's clear that the Greek tradition was taken as the background for etymology of Achilles' name by the ancient Greek authors, though they never denied the possibility of pre-Greek or oriental origination of many proper names.

As for modern scientific research in the field of etymology of this name - three main directions can be distinguished here: a)Greek; b)Indo-European; c)Non-Indo-European, pre-Greek.

Some of the supporters of the first theory hold to some ancient etymologies, others are giving us new etymologies of the name on the Greek basis. Some old explanations are still actual in modern classical philology: "the Ilion's griever" - Polt - "the grief giver" - Benseler (he translated the name as "the pain giver"), "without lips" Forchhammer, though he gives different explanation of this name's origination. Kurcius thinks that the word can have several meanings e.g. "subjugator of the people" ('Εχελαος) and "the stone holder" ('Εχελαος) [2]. Krechmer regards that in this case we have 'Αχος and offers us the medieval Greek form 'Αχιλος [3]. K.Tuite points the Greek origination of hero's name, he thinks Achilles is derived from χειλος [4]. Palmer disagrees with wide-spread viewpoint of non-Greek origination of the names of heroes, who belong to earlier generation. He thinks this name to be the abbreviation form of two-member Greek name with characteristic omission of the vowel. According to this 'Αχιλ(λ)ευς can be presented as the shortened form of 'Αχι-λαFος [5].

Number of scientists provide the attempts of explaining the origination of Achilles' name according to Indo-European etymology. Scaliger had the version that the first part of the name presents "aqua" (water) (Lobeck Aglaoph. p.952). V.Georgiev compared the name with Lat. aquila (eagle) [6]. This idea was shared by many modern scientists. Vindecens thought that the name was connected not only with aquila, but with aqua itself [7]. I.Otkupshchikov explains it as the name of Indo-European origin and supposes that the synonymous accordance 'Αχελωος with 'Αχελωος; Italian-Akele. Frig. - Aquilo comes from Indo-European $ak^{w}el$ [8].

Quite a large number of scientists think that the name has an unknown etymology or a pre-Greek one (e.g. Schantron, Merlingen) [7]. In this case the word-building suffix ευ plays the greatest role as it is regarded to be the characteristic suffix of the pre-Greek onomastic. It's also important that Achilles is the Hellenised hero of Pelazgic origin. E.Furnee shares the viewpoint and the interchange λ/λλ in the name non-Indo-European i.e. Pelazgic element [9].

In the recent period R.Gordesiani and E.Furnee suggested the existence of Kartvelian element on pre-Greek linguistic level [10]. They don't deny the possibility of powerful Caucasian migration in Aegeida in III-II mil. B.C. and of mixed autochtonic and migrated population of forming Pelazgic culture and language. The idea of connection the Pelazgic hero Achilles with Caucasian culture was expressed by number of Georgian scientists (S.Kaukhchishvili, R.Miminoshvili) [11]. K.Tuite has presented an interesting

report, concerning the genetic relationships of Caucasian myth of Amirani with two complexes of Greek myths - Achilles (birth and parents) and Prometeus.

According to the above-mentioned facts we think that it's possible to explain Achilles' name with the help of its pre-Greek elements. In such case onomastical suffix ευ must be underlined as an element of pre-Greek origin in Greek proper names:

Besides prefix α could be interpreted as a remain of deictic prefix that is so far characteristic for pre-Greek world. Actually both of these elements are natural part of Kartvelian language world. From our viewpoint the ancient Greek authors and some of modern etymologists do not explain it correctly connecting the Achilles' name with this physical data, or his virtues.

Such interpretation is impossible because of spraying the name already in Mycenean period. Obviously the name includes more general meaning and it is connected with the roots that make the Greek names. Accordingly the etymology of the name can be determined not by myth interpretation but by the onomastical uniforms character is the pre-Greek languages. Because we share the opinion that the pre-Greek origin of Achilles' name is more evident, but the meaning of the forming root (χιλ(λ)) is not quite clear on this level of searching.

Kutaisi State University

REFERENCES

1. *V.Georgiev.* L'importance des toponymes mycenians pour des problems. LB, T.IX, 1, 1978.
2. *W.H.Rosher.* Ausfuhrliches Lexicon der Grichischen und Romischen Mytologie. Leipzig, 1884-1886, 64.
3. *M.Kretschmer.* Die nomina auf -ενς, Gl.4, 1974, 305-308.
4. *K.Tuite.* Achillevsi da Kavkasia. Tbilisi, 1997 (Georgian).
5. *L.R.Palmer.* The interpretation of Mycanean Greek Texts. Oxford, 1963.
6. *V.Georgiev.* Die Trager der Kretish-Mycenishen cultur, ihre Herkunft und ihre sprache. Bdd. Sofia, 1, 1937.
7. *P.Chantraine.* Dictionnarre etymologique de la Langue Greque, t.T, (A.D.), 1968, 150.
8. *Ju.Otkupshikov.* Dogrecheskii substrat. Moskva, 1988, 88 (Russian).
9. *E.J.Furnee.* Die wichtigsten consonantishen erscheinungen des vorgrieshischan. Leipzig, 1972, 387.
10. *R.Gordeziani.* Tsinaberdznuli da Kartveluri. Tbilisi, 1985 (Georgian).
11. *S.Kaukhchishvili.* Berdznuli literaturis Istoria. Tbilisi, 1978 (Georgian).

S.Kasyan

On Musical-Rhetorical Figures in Ockeghem's Creative Works

Presented by Corr. Member of the Academy P. Zakaraia, May 4, 1998

ABSTRACT. **The paper reports on Franco-Flemish composer Johannes Ockeghem, who appears to be one of the pioneers of using musical-rhetorical figures in his creative works.**

Key words: Ockeghem.

Johannes Ockeghem is one of the leading composers in the history of Franco-Flemish polyphonic school. He enjoyed great success and popularity already in his lifetime. The theorist Tinctoris considered him to be the highest authority of musical composition. Many principles of musical development which are widely used in musical arts of the following centuries first appeared in Ockeghem's creations. Among them are musical-rhetorical figures.

In musicology by Adrian Peti Koklin's opinion a pioneer of musical rhetorics is considered to be his teacher Josquin des Prés [1]. At the same time the analysis of Ockeghem's Masses (*Qunti toni, Ecce ancilla Domini, Forsseulement, Mi-mi, Requiem*) reveals that the similar figures have been used by Ockeghem too. It should be also noted that Josquin des Prés might study under Ockeghem and the creative work of these two great composers chronologically went in parallel for a certain period of time. Therefore not putting the question of historical priority we think Ockeghem to be one of the first who used musical rhetorical figures in his creations.

In our opinion the creation of imageable expressive figure is one of the characteristic forms of identical world outlook. The use of the known motif with definite semantic meaning which is strengthened in centuries represents a special form of identical aspect action. From pure technical multiple used means of development it appears in the form of one sound formula-cliché, receiving psycological function of code.

The formation of musical-rhetorical figures in Ockeghem's creative works corresponds to the general tendency of the development of the Renaissance art.

As J.Kheizing points out [2] in his book "Autumn of Middle Ages" it was the epoch when thinking became too dependent on incarnation of images. Visual side, so important for late Middle Ages, became omnipotent. Therefore all thinking was turned into plastic.

It was just that period of European art development when the interest to the antiquity stimulated the approximation of music to rhetorics, when the teaching about affects was attempted also to apply in respect to music. At that time the tendency to reflect the essence of text and its separate words by musical means was revealed very vividly. The composers tried to show how a word "... can be incarnated in music". [3]

All this was a kind of answer to the aesthetical demands of humanism which is concerned with human interests.

Ockeghem is one of those composers who is seeking for the means which help to carry the expressive side of verbal images. He makes the accent on those words of the text which are the most suitable for expressing by musical means. For instance, *mortis* (death), *perpetic* (eternal), *umbrae* (shadow), *Deus* (God), libera (liberate) and so on. For this he used various possibilities of polyphonic facture: canon, imitation, facture – thembre opposition of voices, sequence, repetition and others.

In composer's creations we meet all those basic types of figures which are widely used in XVI especially XVII century music. These are figures of imaginary and expressive class, of repetition, pauses and etc. Along with it in Ockeghem's creative works there is also developed numeral symbolics. The connection between rhetorics and music is also revealed in respect to the structure of compositions. Ockeghem's *Requviem* is of particular interest in this respect, especially the parts *Graduale* and *Kyrie*.

Multiplicity of musical-rhetorical figures revealed by us in Ockegem's creative works testify that they were in the sphere of his special care. That's why we think him to be among one of the first composers using musical-rhetorical figures.

Tbilisi I.Sarajishvili Conservatory

REFERENCES

1. *V.Shestakov*. Muzykal'naia estetika zapadnoevropeiskogo srednevekov'ia i vozrozhdenia. M. 1966 (Russian).
2. *I.Khezing*. Osen' srednevekov'ia. M. 1978 (Russian).
3. J. Problemy muzikal'noi nauki. vyp. 4, M., 1979
4. *I.Mattheson*. Der vollkommene Capellmeister. Kassel. 1954.

EPIGRAPHICS

V.Silogava

The Dated Inscription-Graffiti from Mravaltskaro of Gareji

Presented by Corr. Member of the Academy Z.Aleksidze, August 11, 1998

ABSTRACT. **The dated inscription-graffiti executed in ancient Georgian script *asomtavruli*, found in the recently discovered monastery Mravaltskaro of Gareji is analysed. The text was scratched over the plastered wall of a small church in 851, September 8th on the occasion of the Nativity of Virgin Mary.**

Key words: inscription-graffiti, *asomtavruli*, church.

In summer 1995 a nongovernmental organization Fund "Udabno" discovered an unknown monastery complex Mravaltskaro in the north-west part of Gareji mountains. 6 caves and 5 rock-cut churches, all of them damaged, some buried in earth, others partially filled with silt, have been revealed in a process of monitoring and surveying. A small one nave church (with area of 325x170cm, 285cm in hight) located at the end of the eastern part of the monastery complex was found comparatively well preserved. Fragments of murals have survived on three walls (except the south one) of the church. Numerous (over 50) inscriptions-graffiti dating back to the IX-XIII cc., scratched on plastered walls, as well as graphical images of men, animals, arrow points, spears and various geometrical figures have been found on the church walls. The newly discovered monastery, that lacked close studying, originally was named Tetri Senakebi [1, 2], but later on was renamed into Mravaltskaro [3] based on [4]. Some other authors have also published several preliminary, but rushed and erroneous conclusions; e.g. in one of the newsletters published abroad is noted that more than 10 refined Georgian scratched alphabets have been "carved by barely literate peasants and monks as they learned to read and write" [5]. In another publication is mentioned as if on the church wall is scratched a graffiti with invocation to Christ in which Vicar *(chorepiscopa)* Pavle of Katsareti is mentioned [6]. Actually this is the XII c. graffiti comprising a prayer for the Bishop Khariton of Katsareti on the occasion of St.Peter and St.Paul 's Day. One can also observe fragments of inscriptions written by paint in *asomtavruli* and *nuskhuri*, as well as large fragments (comprising 5 and more verses) of mural inscription; two verses of X c. inscription in *mkhedruli* is found within the niche of the north wall, etc.

Fixing and studying of the graffiti was accomplished in 1996-1998. One of the scratched graffiti was dated from September 8th, 851, and is considered to be one of the most ancient inscriptions not only among Mravaltskaro's graffiti, but among those found in 20 known monastery complexes throughout Gareji as well. And what is more, it is the most ancient *asomtavruli* graffiti among 6 types (lapidary, mosaic, mural, chased metal, embroidery, scratched) of dated inscriptions, and simultaneously is one of the most ancient dated Georgian scripts.

Here follows archeographic discription of the inscription:

asomtavruli; 5 verses scratched by means of alternate bold and fine lines, with use of low and wide letters; fine but clear-cut; located on the west wall of the church, namely at the external (east) side of the inner (small) arch of a niche, below the simple, now crumbled capital. Several examples can be given when text starts on an arch capital of a church; for analogy note two inscriptions of Xc. in Chvabiani (Upper Svaneti) Church of the Saviour [7], and an inscription of the XII c. within the alter-space of Alaverdi Church [8]. Inscription occupies an area of 13x 6 cm. Hight of letters: 1.5-2-2.5 cm. The inscription lacks its beginning - a strip of plaster of the arch capital over the fragment of the text at a hight of approximately two verses crumbled, taking away the lacking letters. The inscription lacks seperation marks. Title of abbreviation: horizontal straight line (in the 2nd and 3rd verses placed along the entire length of a verse). The text of the inscription is as follows:

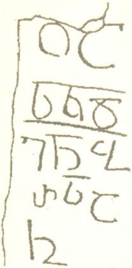

[...]

[...]

ႭႠ

Ⴑ̃ႩႣ [ქრ(ონი)კ|(ო)ნსა]|ოა, ს(ე)კჳ(ე)ნბ(ე)რსა ჱ.

Ⴌ̃ႡႤ

Ⴐ̃ႱႠ

Ⴡ

None of words both in ancient [9] and modern [10] Georgian will end on ႭႠ. Context of the above inscription (with indication of a month and day) implies that the letters stand for the year. Since plaster crumbled at a hight of two lines above these letters, and there was no other text to which the lost verses could belong, the lacking fragment should have read a term denoting a calendar widespread in Georgia - *Khronikoni*. As usual, the term has been written in a shortened form [11,12], therefore, could fit two lacking lines. Hence, the entire text can be restored as given above.

Khronikoni ႭႠ, i.e. 71, according to the modern calendar corresponds to 851 (780+71). So, the inscription states a date: September 8, 851.

Palaeographically the inscription is identical to the dated IX c. manuscript, different lapidaric and mural inscriptions [12-15].

Out of 10 graphemes (a total of 12 graphems are used in the inscription; among them Ⴀ and Ⴑ are used twice) the most ancient one is Ⴍ. Two curves have been scratched by means of two downward strokes on left and right to compose the letter. For this reason, the circle at the bottom is not closed. Of special notice is that Ⴍ lacks a heel. According to Academician G.Tsereteli, initially the outline of Ⴍ matched the given peculiarity: the lower loop has been added later [16]. The analogues Ⴍ is found in Sahadukht's inscription made on a surface of an icon case found in the village of Jvarisa in Racha region, Georgia [16-19]. The same was noted by G.Tsereteli.

Different dates of origination of the monument have been suggested by certain scientists: V c. by Sh.Amiranashvili, VI c. by G.Bochoridze [16-18], around 1000 by

G.Chubinashvili [19]. According to G.Tsereteli "the monument should be dated at the later period than V c. (though the difference should not be too big, as thought G.Chubinashvili)" [16]. Palaeographically the inscription can be dated to the VII-VIII cc. (five letters in it - ⴑ, ⴍ, ⴖ, ⴓ, ⴕ still lack the upper additional horizontal line, that came into existence since IX c.) [11, p.28-29]. Simultaneously ⴁ has the short neck; the horizontal line is slightly seperated from the letter's belly, that is a palaeographic characteristic of the end of the VIII c. and beginning of the IX c. On the one hand, ⴀ from the 851 Mravaltskaro inscription without a heel is very archaic and on the other hand, defines the upper date of Sahadukhti's inscription.

The word "sekdenberi" is written by dissimilation of consonants (mb>nb) [15]. The word is found in two more cases: in the 864 liturgical collection from Sinai [13], and 885 inscription of Mampal Sumbat, son of Ashot from Sioni of Ateni [15]. In the latter case the word has reached us in a form of a fragment. Editors of the book have restored the word as "[sekten]ber[sa] ", but taking into consideration orthography of the IX c. it should have been restored as "[sekden]ber[sa]".

September 8th (by Julian calendar) is the day of Nativity of Virgin Mary. This is the sole celebration mentioned on this day in Palestino-Georgian Church Calendar compiled by Iovanne-Zosime in the X c. [21]. Though one cannot find separate narrative concerning the Virgin in none of liturgical collections - "mravaltavi"(from: Sinai [13], Udabno, Klarjeti), the following comment is found in the most ancient, 864 "mravaltavi" from Sinai: "In the month of September. Nativity of the Saint Virgin. Nativity. narrative about her Nativity to be read, and praise of the Saint Virgin to be leveled, at one's choice" [13, p.216]. "Narration by Bishop Procles of Konstantinopole in the name of Virgin Mary" is included into the Sinai liturgical collection as one of the narrations without stating the day [13, p.40-45]. Entire bibliography in connection with the Nativity of Virgin Mary and the corresponding narration was given by Gerard Garitte in his comments to the calendar of Iovanne-Zosime [21].

Since the inscription states only the date, it must be attributed to finalizing construction of the church and its blessing. The event took place on September 8th, Nativity of Virgin Mary. Probably the church was rock-cut in the Virgin's name. This opinion is supported by the fact of painting the mural with an image of the Virgin and Child in the most notable place - in the center of the north wall; the mural occupies the entire surface within a niche. The same opinion is backed up by several inscriptions found on the Church walls, containing invocation to the Virgin, St. Queen, and St. Mary.

Fixing the date of blessing of a church was widely practiced. One of the examples is the constructional inscription of 777 in Samshvilde church made on *enkenoba*, i.e. September 13th ("In the 3rd year of reigning of King Leon, in the day of *enkenia*, the church was blessed, and populousness lasted for 3 days") [22,23]. Compare with the following: "On September 13th. Blessing of the Holy church, called *Enkenia*". In the latest publication the above inscription was dated to 50s of the X c. [12]. But as a result of recent studies based both on palaeographical peculiarities and historic data, L.Muskhelishvili's viewpoint has been yet again accepted [25, p.234]. Probably the day of blessing is mentioned in the 964 constructional inscription of Kumurdo Church,

since the finilizing of its construction is stated in details (Khronikoni 184, May 1st, Saturday, at the new moon") [24].

If the constructional inscription from Mravaltskaro states the date of ending the construction work, the same date should be applied to the *nuskhuri* inscription of the builder-worker on the north wall, which from palaeographic viewpoint is very archaic and was dated to X c. In this case the latter should also be dated to 851 or closely to it.

The inscription convincingly dates one nave churches of the analogous design found in Gareji monasteries, which have an alter carved out of a rock, and a burial tomb, or niches and a room for keeping skulls in the north. There are several dozens of such examples, and the topic needs special studying.

The inscription dates to the period when Illarion Kartveli (822-875) [26] was carrying out his activities in Gareji, namely in the Laura [27,28]. Hence, curving of churches of the similar design can be attributed to starting of a new style of monastic life in Gareji. The specific date of Mravaltskaro inscription may play the part of a chronological landmark of these new monastic activities.

S.Janashia Georgian State Museum
Georgian Academy of Sciences

REFERENCES

1. *T.Jojua, L.Mirianashvili.* Dzeglis Megobari, 1 (92), 1996, 42,43 (Georgian).
2. *L.Mirianashvili, T.Jojua.* Dzeglis Megobari, 3 (94), 1996, 41, 43 (Georgian).
3. Gareji Mountains and Man, Tb.1997 (Georgian).
4. *Vakhushti Batonishvili.* History of Kartli, v.4; Ed. by *S.Kaukhchishvili*, Tb., 1973, 333 (Georgian).
5. *Antony Eastmond.* Newsletter (The University of Warwick), 223, December, 1997, 1-2.
6. Programme of the National Cultural Heritage. Collection. Tb.,1977 (Georgian).
7. Written Monuments of Svaneti, II. Epigraphic Monuments; Ed. by *V.Silogava*, Tb., 1988 (Georgian).
8. *V.Silogava.* "Matsne", Series of Language and Literature, 4, 1992.
9. *I. Abuladze.* The Inverse Guide to the "Ancient Georgian Language Dictionary", Tb., 1979 (Georgian).
10. Inverse Dictionary, Tb., 1967 (Georgian).
11. Collection of Georgian Inscriptions, I. Ed. by *N.Shoshiashvili*, Tb., 1980. 1 (Georgian).
12. Palaeographic Album. Compiled by I. Abuladze, Tb., 1949, 350, Tables 6,7; (Georgian).
13. Sinai Liturgical Collection of 864. Ed. by *Ak.Shanidze.* Tb., 1959, Tables 4-10 (Georgian).
14. *G.N.Chubinashvili.* "Kartuli Khelovneba", 1, Tb., 1942, Table 2, 1 (Russian).
15. Collection of Georgian Inscriptions, III. Ed. by *G.Abramishvili* and *Z.Alexidze*, Tb., 1989, 91, 93, 132 (Georgian).
16. *G.Tsereteli.* The Most Ancient Georgian Inscriptions from Palestina, Tb., 1960 (Georgian).
17. *G.Bochoidze.* Archive of Georgia, book III, Tb.1927 (Georgian).
18. *Sh.Amiranashvili.* History of the Georgian Art, I, Tb., 1944 (Georgian).
19. *G.N.Chubinashvili.* Art of Georgian Chased Metal, Album, Tb., 1959.
20. *Z.Sarjveladze.* Problems of History of the Georgian Literature Language, Tb., 1975 (Georgian).
21. *G.Garitte.* Le calendrier palestino-georgien du sinaiticus 34 (X^es.), Bruxelles, 1958.
22. *L.Muskhelishvili.* "Enimkis Moambe", XIII, Tb., 1943, 92 (Georgian).
23. *N.Chubinashvili.* Sioni of Samshvilde. Tb., 1963, 28 (Russian).
24. *V.Silogava.* Kumurdo. Epigraphics of the Church, Tb., 1994, 41 (Georgian).
25. *Z.Alexidze.* Mravaltavi, **XVI**, Tb., 1991, 234 (Georgian).
26. *M.Dolakidze.* Illarion Kartveli. Georgian Encyclopedia, 5, Tb., 1980, 105 (Georgian).
27. *K.Kekelidze.* Bulletin of Tiflis University, 1, 1920 (Georgian).
28. *M.Dolakidze.* The Most Ancient Editions of the "Vitae of Illarion Kartveli", Tb.,1975 (Georgian).

Subscription Information

Bulletin of the Georgian Academy of Sciences
is published bimonthly

Correspondence regarding subscriptions, back issues should be sent to:

Georgian Academy of Sciences,
52, Rustaveli Avenue, Tbilisi, 380008, Georgia
Phone : + 995-32 99-75-93;
Fax/Phone : + 995-32 99-88-23
E-mail : BULLETIN@PRESID.ACNET.GE

Annual subscription rate including postage for 1998 is US $ 400

გადაეცა წარმოებას 30.07.1998. ხელმოწერილია დასაბეჭდად 29.09.1998.
ფორმატი 70×108 1/16. აწყობილია კომპიუტერზე. ოფსეტური ბეჭდვა.
პირობითი ნაბ. თ. 11. საღრიცხვო-საგამომცემლო თაბახი 11.
ტირაჟი 400. შეკვ. № 428 ფასი სახელშეკრულებო.

რედაქციის მისამართი: 380008, თბილისი-8, რუსთაველის პრ. 52, ტელ. 99-75-93.
საქართველოს მეცნიერებათა აკადემიის საწარმოო-საგამომცემლო გაერთიანება „მეცნიერება",
380060, თბილისი, დ. გამრეკელის ქ. 19, ტელ. 37-22-97.